

Vegetation Dynamics And Their Relationships With Precipitation in Africa For Drought Monitoring Purposes

PhD Dissertation by
Walther Camilo Andrés Cámara García

**Thesis submitted in fulfillment of the requirements for the degree of
Doctor of Philosophy in Environment and Territory**
Department of Land, Environment and Geo-Engineering,
Faculty of Engineering, Polytechnic University of Turin
Turin, Italy

XXVII Cycle, 2014



Tutor:
Prof. Piero Boccardo

Co-Tutor:
Ing. Francesca Perez

Dedicado a

Mi mamá, que me enseñó a afrontar los desafíos de la vida con una sonrisa...

El recuerdo de su sonrisa me motiva y me inspira todos los días

ACKNOWLEDGEMENTS

I would like to express my sincere gratitude to my supervisor Prof. Piero Boccardo for its support and for giving me the opportunity to development this work during this three years.

I wish to thank all my ITHACA colleagues for sharing their knowledge and for their support during this period. A special thanks goes to Francesca Perez for her patience and for her strong contribution to the realization of this work.

A very special thanks to my dad and my sisters for their continuous support and constant encouragement in the difficult moments. On the same way, I would like to express my gratitude to the rest of my family for their support during this period.

Finally but not less important I want to recognize, and to express my sincere gratitude to my friends in Turin (Especially to the Cuys) for being my family and for their amazing support.

TABLE OF CONTENTS

ACKNOWLEDGEMENTS	ii
TABLE OF CONTENTS	iii
LIST OF TABLES	v
LIST OF FIGURES	viii
1. INTRODUCTION	1
2. DROUGHT AND NATURAL HAZARDS	4
2.1. Natural Hazards and Disaster Risk.....	4
2.2. Drought as a hazard	6
2.3. Types of Drought.....	9
2.4. The role of remote sensing for drought monitoring	11
3. LITERATURE REVIEW	13
3.1. An Overview of drought situation in Africa	13
3.2. Impacts of drought.....	15
3.2.1. Economic impacts	15
3.2.2. Environmental impacts	16
3.2.3. Social impacts	16
3.3. Drought impacts in Africa.....	17
3.3.1. Impact on economic growth and poverty reduction.....	17
3.3.2. Impact on food security	18
3.3.3. Impact on water.....	19
3.3.4. Impact on biodiversity	20
3.3.5. Impact on Energy	21
3.4. Indices for drought monitoring	22
3.4.1. Meteorological drought indices.....	22
3.4.2. Satellite based drought indices for drought characterization.....	25
3.4.3. Water Requirement Satisfaction Index (WRSI).....	27
3.5. Experiences on monitoring drought conditions in Africa	28
4. DATA AND METHODOLOGY	30
4.1. Vegetation Monitoring and ITHACA drought Early Warning System (EWS)	31
4.1.1. Data input and Methodology.....	31
4.1.2. Derived Products.....	37
4.1.3. Drought vulnerability	39
4.2. Precipitation monitoring for drought Early Warning purposes	43
4.2.1. Data.....	43
4.2.2. Standardized Precipitation Index.....	45
4.3. Climate and rainfall analysis.....	49
4.3.1. Additional data used	49

4.3.2.	Climate and rainfall analysis	56
4.4.	Relationship between Vegetation and Rainfall data.....	60
4.4.1.	Correlation Analysis	60
4.4.2.	Test of Statistical Significance.....	64
5.	OUTCOMES AND DISCUSSION	66
5.1.	Land Cover Analysis.....	66
5.2.	Test of Significance Analysis	69
5.2.1.	Open shrublands.....	69
5.2.2.	Woody savannas	74
5.2.3.	Savannas	76
5.2.4.	Grasslands.....	78
5.2.5.	Croplands	82
5.2.6.	Cropland/Natural vegetation mosaic	84
5.3.	Correlation Analysis	88
5.3.1.	Open shrublands.....	88
5.3.2.	Grasslands.....	91
5.3.3.	Cropland/Natural vegetation mosaic	94
5.4.	Integration Analysis	97
5.4.1.	Spatial Correlation Analysis	97
5.4.2.	Vulnerability Analysis.....	100
6.	CONCLUSIONS AND RECOMMENDATION	104
7.	REFERENCES.....	107
8.	APPENDICES	113
8.1.	Test of Significance Analysis	113
8.1.1.	Open shrublands.....	113
8.1.2.	Woody savannas.....	117
8.1.3.	savannas.....	119
8.1.4.	Grasslands.....	121
8.1.5.	Croplands	125
8.1.6.	Cropland Natural Vegetation Mosaic	127
8.2.	Correlation Analysis	131
8.2.1.	Open Shrublands.....	131
8.2.2.	Grasslands.....	133
8.2.3.	Cropland Natural Vegetation Mosaic	135
8.2.4.	Woody savannas	137
8.2.5.	Savannas	139
8.2.6.	Croplands	141
8.3.	Integration Analysis	143
8.3.1.	Spatial Correlation Analysis	143
8.3.2.	Vulnerability Analysis.....	159

LIST OF TABLES

<i>Table 1. Top 10 most important Drought disasters for the period 2006 to 2015 sorted by numbers of killed at the country level. [11].....</i>	<i>7</i>
<i>Table 2. Top 10 most important Drought disasters for the period 2006 to 2015 sorted by numbers of total affected people at the country level. [11].....</i>	<i>8</i>
<i>Table 3. Drought intensity categories defined for values of SPI[38]</i>	<i>23</i>
<i>Table 4. Key to calculate the climate formula of Köppen and Geiger for the main climates and subsequent precipitation conditions, the first two letters of the classification[81]</i>	<i>51</i>
<i>Table 5. Key to calculate the climate formula of Köppen and Geiger, the third letter temperature classification[81]</i>	<i>52</i>
<i>Table 6. MODIS (MCD12C1) IGBP Land Cover Types</i>	<i>54</i>
<i>Table 7. Percentage of the Open Shrublands areas that passed the Student t-test for the correlation between cumulate rainfall and phenological parameters in the first vegetation growing season.</i>	<i>69</i>
<i>Table 8. Percentage of the Open Shrublands areas that passed the Student t-test for the correlation between cumulate rainfall and phenological parameters in the second vegetation growing season.</i>	<i>72</i>
<i>Table 9. Percentage of the Woody Savannas areas that passed the Student t-test for the correlation between cumulate rainfall and phenological parameters in the first vegetation growing season.</i>	<i>74</i>
<i>Table 10. Percentage of the Savannas areas that passed the Student t-test for the correlation between cumulate rainfall and phenological parameters in the first vegetation growing season.....</i>	<i>76</i>
<i>Table 11. Percentage of the Grasslands areas that passed the Student t-test for the correlation between cumulate rainfall and phenological parameters in the first vegetation growing season.....</i>	<i>78</i>
<i>Table 12. Percentage of the Grasslands areas that passed the Student t-test for the correlation between cumulate rainfall and phenological parameters in the second vegetation growing season.....</i>	<i>80</i>
<i>Table 13. Percentage of the Cropland areas that passed the Student t-test for the correlation between cumulate rainfall and phenological parameters in the first vegetation growing season.....</i>	<i>82</i>
<i>Table 14. Percentage of the Cropland/Natural vegetation mosaic areas that passed the Student t-test for the correlation between cumulate rainfall and phenological parameters in the first vegetation growing season.</i>	<i>84</i>
<i>Table 15. Percentage of the Cropland/Natural vegetation mosaic areas that passed the Student t-test for the correlation between cumulate rainfall and phenological parameters in the second vegetation growing season</i>	<i>86</i>
<i>Table 16. Percentages of Open Shrublands areas showing Medium Correlation level between the phenological parameters and cumulated rainfall for the first growing season</i>	<i>88</i>
<i>Table 17. Percentages of Open Shrublands areas showing High Correlation level between the phenological parameters and cumulated rainfall for the first growing season</i>	<i>89</i>
<i>Table 18. Percentages of Open Shrublands areas showing Very High Correlation level between the phenological parameters and cumulated rainfall for the first growing season</i>	<i>90</i>
<i>Table 19. Percentages of Grasslands areas showing Medium Correlation level between the phenological parameters and cumulated rainfall for the first growing season</i>	<i>91</i>
<i>Table 20. High Percentages of Grasslands areas showing High Correlation level between the phenological parameters and cumulated rainfall for the first growing season</i>	<i>92</i>
<i>Table 21. Percentages of Grasslands areas showing Very High Correlation level between the phenological parameters and cumulated rainfall for the first growing season</i>	<i>92</i>
<i>Table 22. Percentages of Cropland/Natural vegetation mosaic areas showing Medium Correlation level between the phenological parameters and cumulated rainfall for the first growing season</i>	<i>94</i>

<i>Table 23. High Percentages of Cropland/Natural vegetation mosaic areas showing High Correlation level between the phenological parameters and cumulated rainfall for the first growing season</i>	<i>95</i>
<i>Table 24. Percentages of Cropland/Natural vegetation mosaic areas showing Very High Correlation level between the phenological parameters and cumulated rainfall for the first growing season</i>	<i>95</i>
<i>Table 25. Vulnerability Index for the phenological parameters using different rainfall cumulating intervals for the Open Shrubland land cover type and for the first growing season.</i>	<i>101</i>
<i>Table 26. Vulnerability Index for the phenological parameters using different rainfall cumulating intervals for the Grasslands Vegetation cover type and for the first growing season.</i>	<i>102</i>
<i>Table 27. Vulnerability Index for the phenological parameters using different rainfall cumulating intervals for the Cropland/Natural vegetation mosaic cover type and for the first growing season.</i>	<i>102</i>
<i>Table 28. Percentages of Open Shrublands areas showing Medium Correlation level between the phenological parameters and cumulated rainfall for the second growing season</i>	<i>131</i>
<i>Table 29. Percentages of Open Shrublands areas showing High Correlation level between the phenological parameters and cumulated rainfall for the second growing season</i>	<i>131</i>
<i>Table 30. Percentages of Open Shrublands areas showing Very High Correlation level between the phenological parameters and cumulated rainfall for the second growing season</i>	<i>131</i>
<i>Table 31. Percentages of Grasslands areas showing Medium Correlation level between the phenological parameters and cumulated rainfall for the second growing season</i>	<i>133</i>
<i>Table 32. Percentages of Grasslands areas showing High Correlation level between the phenological parameters and cumulated rainfall for the second growing season</i>	<i>133</i>
<i>Table 33. Percentages of Cropland/Natural vegetation mosaic areas showing Medium Correlation level between the phenological parameters and cumulated rainfall for the second growing season</i>	<i>135</i>
<i>Table 34. Percentages of Cropland/Natural vegetation mosaic areas showing High Correlation level between the phenological parameters and cumulated rainfall for the second growing season</i>	<i>135</i>
<i>Table 35. Percentages of Cropland/Natural vegetation mosaic areas showing Very High Correlation level between the phenological parameters and cumulated rainfall for the second growing season</i>	<i>135</i>
<i>Table 36. Percentages of Woody Savannas areas showing Medium Correlation level between the phenological parameters and cumulated rainfall for the first growing season</i>	<i>137</i>
<i>Table 37. Percentages of Woody Savannas areas showing High Correlation level between the phenological parameters and cumulated rainfall for the first growing season</i>	<i>137</i>
<i>Table 38. Percentages of Woody Savannas areas showing Very High Correlation level between the phenological parameters and cumulated rainfall for the first growing season</i>	<i>137</i>
<i>Table 39. Percentages of Savannas areas showing Medium Correlation level between the phenological parameters and cumulated rainfall for the first growing season</i>	<i>139</i>
<i>Table 40. Percentages of Savannas areas showing High Correlation level between the phenological parameters and cumulated rainfall for the first growing season</i>	<i>139</i>
<i>Table 41. Very Percentages of Savannas areas showing Very High Correlation level between the phenological parameters and cumulated rainfall for the first growing season</i>	<i>139</i>
<i>Table 42. Percentages of Croplands areas showing Medium Correlation level between the phenological parameters and cumulated rainfall for the first growing season</i>	<i>141</i>
<i>Table 43. Percentages of Croplands areas showing High Correlation level between the phenological parameters and cumulated rainfall for the first growing season</i>	<i>141</i>
<i>Table 44. Percentages of Croplands areas showing Very High Correlation level between the phenological parameters and cumulated rainfall for the first growing season</i>	<i>141</i>

<i>Table 45. Maps showing the Maximum Correlation levels for the Seasonal Small Integral (Smi) on a pixel basis for each cumulating intervals (a) 1 month, b) 3 months, c) 6months) for the Grasslands vegetation land cover type (first growing season)</i>	<i>147</i>
<i>Table 46. a) Maximum Absolute Correlation levels for the Seasonal Small Integral (Smi) on a pixel basis for the Grasslands vegetation cover type for the first growing season, b) rainfall cumulating intervals corresponding to the absolute maximum correlation level for Seasonal Small Integral (Smi) on a pixel basis for the Grasslands vegetation cover type for the first growing season</i>	<i>148</i>
<i>Table 47. Maximum Correlation levels for the Seasonal Small Integral (Smi) on a pixel basis for each cumulative intervals for the Cropland/Natural vegetation mosaic cover type for the first growing season a) 1 month, b) 3 months, c) 6months.</i>	<i>153</i>
<i>Table 48. a) Maximum Absolute Correlation levels for the Seasonal Small Integral (SMI) on a pixel basis for the Cropland/Natural vegetation mosaic cover type for the first growing season, b) rainfall cumulating intervals corresponding to the absolute maximum correlation level for the Seasonal Small Integral (SMI) on a pixel basis for the Cropland/Natural vegetation mosaic cover type for the first growing season</i>	<i>154</i>
<i>Table 49. Vulnerability Index for the phenological parameters using different rainfall cumulating intervals for the Open Shrubland land cover type and for the second growing season.....</i>	<i>159</i>
<i>Table 50. Vulnerability Index for the phenological parameters using different rainfall cumulating intervals for the Woody Savanas land cover type and for the first growing season.....</i>	<i>159</i>
<i>Table 51 Vulnerability Index for the phenological parameters using different rainfall cumulating intervals for the Woody Savanas land cover type and for the second growing season.....</i>	<i>159</i>
<i>Table 52. Vulnerability Index for the phenological parameters using different rainfall cumulating intervals for the Savanas land cover type and for the first growing season.....</i>	<i>160</i>
<i>Table 53. Vulnerability Index for the phenological parameters using different rainfall cumulating intervals for the Savanas land cover type and for the second growing season.....</i>	<i>160</i>
<i>Table 54. Vulnerability Index for the phenological parameters using different rainfall cumulating intervals for the Croplands land cover type and for the first growing season.....</i>	<i>160</i>
<i>Table 55. Vulnerability Index for the phenological parameters using different rainfall cumulating intervals for the Croplands land cover type and for the second growing season</i>	<i>161</i>
<i>Table 56. Vulnerability Index for the phenological parameters using different rainfall cumulating intervals for the Cropland/Natural vegetation mosaic land cover type and for the first growing season.....</i>	<i>161</i>
<i>Table 57. Vulnerability Index for the phenological parameters using different rainfall cumulating intervals for the Cropland/Natural vegetation mosaic land cover type and for the second growing season.</i>	<i>161</i>

LIST OF FIGURES

<i>Figure 1. Trends in occurrence and victims (Death and total affected) [9]</i>	5
<i>Figure 2. Natural disaster summary 1900-2011 (linear-interpolated smoothed lines)[11]</i>	5
<i>Figure 3. Map showing drought potential by the end of the current century.[14]</i>	6
<i>Figure 4. Sequence of Drought Impacts[18]</i>	10
<i>Figure 5. Drought Events per country from 1970 to 2004 within Sub-Saharan Africa [27]</i>	14
<i>Figure 6. Diagram of NDVI/time and derived phenological parameters (A-H) for a vegetation growing season.</i>	32
<i>Figure 7. Pixel based output of the Percent Deviations (PDs) of the phenological parameter Season Small Integral for the 2011 growing season for the Sahel area.</i>	35
<i>Figure 8. Aggregated on the second level administrative boundary output of the Percent Deviations (PDs) of the phenological parameter Seasonal Small Integral for the 2011 growing season for the Sahel area</i>	35
<i>Figure 9. Map showing the Deviations (D) of the phenological parameter Start of the Season date for the 2009 growing season for the Niger and Chad areas; output aggregated on the second level administrative boundary.</i>	36
<i>Figure 10. Map showing the number of negative vegetation productivity deviations between 2006 and 2010 in the Sahel area</i>	38
<i>Figure 11. On the left: agricultural vulnerability and risk surfaces calculated for Niger, on the right: final alert calculated for 2009 season in Niger and distributed over the risk surfaces.</i>	42
<i>Figure 12. TRMM Cumulative Rainfall 16 January 2011. a) 1Month, b) 3Months, c)6Months, d)9Months</i>	44
<i>Figure 13. Evolution of the SPI for 1-month TRMM rainfall accumulations (SPI01)</i>	46
<i>Figure 14. Evolution of the SPI for 3-months TRMM rainfall accumulations (SPI03).</i>	47
<i>Figure 15. Evolution of the SPI for 6-months TRMM rainfall accumulations (SPI06)</i>	48
<i>Figure 16. Africa Köppen-Geiger Map Classification</i>	52
<i>Figure 17. Africa MCD12C1 IGBP Land Cover</i>	55
<i>Figure 18. Geographical Masked Area</i>	56
<i>Figure 19. Behavior of the cumulative monthly precipitation during the solar year distributed in fortnights</i>	58
<i>Figure 20. Behavior of the cumulative three-monthly precipitation during the solar year distributed in fortnights</i>	59
<i>Figure 21. Evolution of the Pearson correlation coefficient (r) between cumulative rainfall for 1 month and the Amplitude in the period between 2000-2013 for the first (In some areas the only one) season of the solar year</i>	62
<i>Figure 22. Evolution of the Pearson correlation coefficient (r) between cumulative rainfall for 3 months and the Amplitude in the period between 2000-2013 for the first (In some areas the only one) season of the solar year</i>	63
<i>Figure 23. a) Pearson correlation coefficient (r) between cumulative rainfall for 3 months and the Small Integral for the period corresponded to 11 November to b) Pearson correlation coefficient (r) between cumulative rainfall for 3 months and the Small Integral for the period corresponded to 11 November with the no significance correlation areas</i>	65
<i>Figure 24. Vegetation Land Cover Distribution in Africa (MCD12C1)</i>	66
<i>Figure 25. Vegetation Land Cover with two growing season at year, Land Cover Distribution in Africa (MCD12C1)</i>	67
<i>Figure 26. Vegetation Land Cover classes used in the analysis. Excluded areas are in white.</i>	68

Figure 27. Outcomes of the Student t-test for the correlation between the Seasonal Small Integral (Sml) and cumulated rainfall (b) 1 month , c) 3 months d) 6 months) for the Open Shrublands vegetation type (a) in the first vegetation season.	71
Figure 28. Outcomes of the Student t-test for the correlation between the Seasonal Small Integral (Sml) and cumulated rainfall (b) 1 month , c) 3 months d) 6 months) for the Open Shrublands vegetation type (a) in the second vegetation season.	73
Figure 29. Outcomes of the Student t-test for the correlation between the Seasonal Small Integral (Sml) and cumulated rainfall (b) 1 month , c) 3 months d) 6 months) for the Woody savannas vegetation type (a) in the second vegetation season	75
Figure 30. Outcomes of the Student t-test for the correlation between the Seasonal Small Integral (Sml) and cumulated rainfall (b) 1 month , c) 3 months d) 6 months) for the Savannas vegetation type (a) in the second vegetation season	77
Figure 31. Outcomes of the Student t-test for the correlation between the Seasonal Small Integral (Sml) and cumulated rainfall (b) 1 month , c) 3 months d) 6 months) for the Grasslands vegetation type (a) in the second vegetation season	79
Figure 32. Outcomes of the Student t-test for the correlation between the Seasonal Small Integral (Sml) and cumulated rainfall (b) 1 month , c) 3 months d) 6 months) for the Grasslands vegetation type (a) in the second vegetation season	81
Figure 33. Outcomes of the Student t-test for the correlation between the Seasonal Small Integral (Sml) and cumulated rainfall (b) 1 month , c) 3 months d) 6 months) for the Cropland vegetation type (a) in the first vegetation season	83
Figure 34. Outcomes of the Student t-test for the correlation between the Seasonal Small Integral (Sml) and cumulated rainfall (b) 1 month , c) 3 months d) 6 months) for the Cropland/Natural vegetation mosaic type (a) in the first vegetation season.....	85
Figure 35. Outcomes of the Student t-test for the correlation between the Seasonal Small Integral (Sml) and cumulated rainfall (b) 1 month , c) 3 months d) 6 months) for the Cropland/Natural vegetation mosaic type (a) in the second vegetation season.....	87
Figure 36. Correlation Analysis for the Open Shrubland land cover type, first growing season.....	90
Figure 37. Correlation Analysis for the Open Shrubland land cover type, first growing season.....	93
Figure 38. Correlation Analysis for the Cropland/Natural vegetation mosaic land cover type, first growing season	96
Figure 39. Maps showing the Maximum Correlation levels for the Seasonal Small Integral (Sml) on a pixel basis for each cumulating intervals (a) 1 month, b) 3 months, c) 6months) for the Open shrublands vegetation land cover type (first growing season)	98
Figure 40.a) Maximum Absolute Correlation levels for the Seasonal Small Integral (Sml) on a pixel basis for the Open shrublands vegetation cover type for the first growing season, b) rainfall cumulating intervals corresponding to the absolute maximum correlation level for the Seasonal Small Integral (Sml) on a pixel basis for the Open shrublands vegetation cover type for the first growing season.....	99
Figure 41. a)Maximum vulnerability Index identified for the whole African continent, for the Seasonal Small Integral (Sml) in the first growing season, and b) corresponding rainfall cumulating interval.....	103
Figure 42. Outcomes of the Student t-test for the correlation between the Amplitude (Amp) and cumulated rainfall (b) 1 month , c) 3 months d) 6 months) for the Open Shrublands vegetation type (a) in the first vegetation season.	113
Figure 43. Outcomes of the Student t-test for the correlation between the Length (Len) and cumulated rainfall (b) 1 month , c) 3 months d) 6 months) for the Open Shrublands vegetation type (a) in the first vegetation season.	114

<i>Figure 44. Outcomes of the Student t-test for the correlation between the Amplitude (Amp) and cumulated rainfall (b) 1 month , c) 3 months d) 6 months) for the Open Shrublands vegetation type (a) in the second vegetation season.</i>	<i>115</i>
<i>Figure 45. Outcomes of the Student t-test for the correlation between the Length (Len) and cumulated rainfall (b) 1 month , c) 3 months d) 6 months) for the Open Shrublands vegetation type (a) in the second vegetation season</i>	<i>116</i>
<i>Figure 46. Outcomes of the Student t-test for the correlation between the Amplitude (Amp) and cumulated rainfall (b) 1 month , c) 3 months d) 6 months) for the Woody Savannas vegetation type (a) in the first vegetation season.</i>	<i>117</i>
<i>Figure 47. Outcomes of the Student t-test for the correlation between the Length (Len) and cumulated rainfall (b) 1 month , c) 3 months d) 6 months) for the Woody Savannas vegetation type (a) in the first vegetation season.</i>	<i>118</i>
<i>Figure 48. Outcomes of the Student t-test for the correlation between the Amplitude (Amp) and cumulated rainfall (b) 1 month , c) 3 months d) 6 months) for the Savannas vegetation type (a) in the first vegetation season.</i>	<i>119</i>
<i>Figure 49. Outcomes of the Student t-test for the correlation between the Length (Len) and cumulated rainfall (b) 1 month , c) 3 months d) 6 months) for the Savannas vegetation type (a) in the first vegetation season</i>	<i>120</i>
<i>Figure 50. Outcomes of the Student t-test for the correlation between the Amplitude (Amp) and cumulated rainfall (b) 1 month , c) 3 months d) 6 months) for the Grasslands vegetation type (a) in the first vegetation season.</i>	<i>121</i>
<i>Figure 51. Outcomes of the Student t-test for the correlation between the Length (Len) and cumulated rainfall (b) 1 month , c) 3 months d) 6 months) for the Grasslands vegetation type (a) in the first vegetation season.</i>	<i>122</i>
<i>Figure 52. Outcomes of the Student t-test for the correlation between the Amplitude (Amp) and cumulated rainfall (b) 1 month , c) 3 months d) 6 months) for the Grasslands vegetation type (a) in the second vegetation season.</i>	<i>123</i>
<i>Figure 53. Outcomes of the Student t-test for the correlation between the Length (Len) and cumulated rainfall (b) 1 month , c) 3 months d) 6 months) for the Grasslands vegetation type (a) in the second vegetation season</i>	<i>124</i>
<i>Figure 54. Outcomes of the Student t-test for the correlation between the Amplitude (Amp) and cumulated rainfall (b) 1 month , c) 3 months d) 6 months) for the Croplands vegetation type (a) in the first vegetation season</i>	<i>125</i>
<i>Figure 55. Outcomes of the Student t-test for the correlation between the Length (Len) and cumulated rainfall (b) 1 month , c) 3 months d) 6 months) for the Croplands vegetation type (a) in the first vegetation season</i>	<i>126</i>
<i>Figure 56. Outcomes of the Student t-test for the correlation between the Amplitude (Amp) and cumulated rainfall (b) 1 month , c) 3 months d) 6 months) for the Croplands/Natural vegetation mosaic type (a) in the first vegetation season</i>	<i>127</i>
<i>Figure 57. Outcomes of the Student t-test for the correlation between the Length (Len) and cumulated rainfall (b) 1 month , c) 3 months d) 6 months) for the Croplands/Natural vegetation mosaic type (a) in the first vegetation season</i>	<i>128</i>
<i>Figure 58. Outcomes of the Student t-test for the correlation between the Amplitude (Amp) and cumulated rainfall (b) 1 month , c) 3 months d) 6 months) for the Croplands/Natural vegetation mosaic type (a) in the second vegetation season</i>	<i>129</i>

<i>Figure 59. Outcomes of the Student t-test for the correlation between the Length (Len) and cumulated rainfall (b) 1 month , c) 3 months d) 6 months) for the Croplands/Natural vegetation mosaic type (a) in the second vegetation season</i>	<i>130</i>
<i>Figure 60. Correlation Analysis for the Open Shrubland land cover type, second growing season.....</i>	<i>132</i>
<i>Figure 61. Percentages of Grasslands areas showing Very High Correlation level between the phenological parameters and cumulated rainfall for the second growing season</i>	<i>133</i>
<i>Figure 62. Correlation Analysis for the Grasslands land cover type, second growing season.....</i>	<i>134</i>
<i>Figure 63. Correlation Analysis for the Cropland/Natural vegetation mosaic land cover type, second growing season</i>	<i>136</i>
<i>Figure 64. Correlation Analysis for the Woody Savannas land cover type, first growing season.....</i>	<i>138</i>
<i>Figure 65. Correlation Analysis for the Savannas land cover type, first growing season</i>	<i>140</i>
<i>Figure 66. Correlation Analysis for the Croplands land cover type, first growing season</i>	<i>142</i>
<i>Figure 67. Maps showing the Maximum Correlation levels for the Amplitude (Amp) on a pixel basis for each cumulating intervals (a) 1 month, b) 3 months, c) 6months) for the Open shrublands vegetation land cover type (first growing season).....</i>	<i>143</i>
<i>Figure 68.a) Maximum Absolute Correlation levels for the Amplitude (Amp) on a pixel basis for the Open shrublands vegetation cover type for the first growing season, b) rainfall cumulating intervals corresponding to the absolute maximum correlation level for the Amplitude (Amp) on a pixel basis for the Open shrublands vegetation cover type for the first growing season</i>	<i>144</i>
<i>Figure 69. Maps showing the Maximum Correlation levels for the Length (Len) on a pixel basis for each cumulating intervals (a) 1 month, b) 3 months, c) 6months) for the Open shrublands vegetation land cover type (first growing season).....</i>	<i>145</i>
<i>Figure 70. a) Maximum Absolute Correlation levels for the Length (Len) on a pixel basis for the Open shrublands vegetation cover type for the first growing season, b) rainfall cumulating intervals corresponding to the absolute maximum correlation level for Length (Len) on a pixel basis for the Open shrublands vegetation cover type for the first growing season</i>	<i>146</i>
<i>Figure 71. Maps showing the Maximum Correlation levels for the Amplitude (Amp) on a pixel basis for each cumulating intervals (a) 1 month, b) 3 months, c) 6months) for the Grasslands vegetation land cover type (first growing season).....</i>	<i>149</i>
<i>Figure 72. a) Maximum Absolute Correlation levels for the Amplitude (Amp) on a pixel basis for the Grasslands vegetation cover type for the first growing season, b) rainfall cumulating intervals corresponding to the absolute maximum correlation level for the Amplitude (Amp) on a pixel basis for the Grasslands vegetation cover type for the first growing season</i>	<i>150</i>
<i>Figure 73. Maximum Correlation levels for the Length of the season (Len) on a pixel basis for each cumulative intervals for the Grasslands vegetation cover type for the first growing season a) 1 month, b) 3 months, c) 6months.</i>	<i>151</i>
<i>Figure 74. a) Maximum Absolute Correlation levels for the Length (Len) on a pixel basis for the Grasslands vegetation cover type for the first growing season, b) rainfall cumulating intervals corresponding to the absolute maximum correlation level for the Length (Len) on a pixel basis for the Grasslands vegetation cover type for the first growing season</i>	<i>152</i>
<i>Figure 75. Maximum Correlation levels for the Amplitude (Len) on a pixel basis for each cumulative intervals for the Cropland/Natural vegetation mosaic cover type for the first growing season a) 1 month, b) 3 months, c) 6months.....</i>	<i>155</i>
<i>Figure 76. a) Maximum Absolute Correlation levels for the Amplitude (Amp) on a pixel basis for the Cropland/Natural vegetation mosaic cover type for the first growing season, b) rainfall cumulating intervals</i>	

<i>corresponding to the absolute maximum correlation level for the Amplitude (Amp) on a pixel basis for the Cropland/Natural vegetation mosaic cover type for the first growing season</i>	<i>156</i>
<i>Figure 77. Maximum Correlation levels for the Length of the season (Len) on a pixel basis for each cumulative intervals for the Cropland/Natural vegetation mosaic cover type for the first growing season a) 1 month, b) 3 months, c) 6months.</i>	<i>157</i>
<i>Figure 78. a) Maximum Absolute Correlation levels for the Length (Len) on a pixel basis for the Cropland/Natural vegetation mosaic cover type for the first growing season, b) rainfall cumulating intervals corresponding to the absolute maximum correlation level for the Length (Len) on a pixel basis for the Cropland/Natural vegetation mosaic cover type for the first growing season</i>	<i>158</i>

1. INTRODUCTION

Drought affects more people than any other natural disaster and results in serious economic, social and environmental costs. The development of effective drought monitoring and early warning has been a significant challenge because of the unique characteristics of drought [1]. In fact, considering the multifaceted nature of drought phenomena (i.e. hydrological, meteorological, and agricultural), a comprehensive and integrated approach is required to define effective Early Warning Systems (EWS), which are thus based on the monitoring of different drought-related parameters and complex drought indicators. In such a context, several studies have shown how temporary changes of vegetation indices and their anomalies are strongly correlated with precipitations, especially in arid and semi-arid environments (see, for instance, [2], [3],[4],[5]). Besides, satellite-derived vegetation indicators and climatic data have been widely used to study and monitoring droughts and included in the main existing EWS developed by the international community (e.g. global systems, such as US-AID FEWSNET, JRC MARS FOODSEC, FAO GIEWS, or designed for a specific area of interest, as in the case of MESA South Africa Drought Monitoring, the US Drought Monitor, and the JRC European Drought Observatory).

In this work, a study aimed at investigating spatial and temporal vegetation dynamics in the whole Africa and their relationships with climate factors, considering as a base data long-term time-series of vegetation-related phenological parameters is proposed. The outcomes of this study have been used in order to define proper drought monitoring procedures to be used by ITHACA (Information Technology for Humanitarian Assistance, Cooperation and Action) for early warning purposes. In fact, in recent years, through its partnership with the World Food Programme (WFP), ITHACA has focused its efforts to develop an automated drought EWS, based on the monitoring of relevant environmental variables that allow the early detection of vegetation stress patterns and agricultural drought phenomena on a global scale, finally providing near real-time alerts about vegetation conditions and productivity. In particular, the fortnightly monitoring of satellite-derived vegetation indexes during growing seasons allows the early detection of water stress conditions of vegetation, and the assessment of derived phenological parameters. These parameters, coupled with the evaluation of precipitation conditions, allow the near real-time assessment of the vegetation productivity which can be expected at the end of the considered growing season. The timely detection of critical conditions in vegetation health and productivity, during a vegetation growing season, leads to the identification of the agricultural areas where crop failures are likely to occur. Finally, the proposed system incorporates a simplified drought vulnerability model, able to show food security conditions starting from the hazard situation evaluated in near real-time [6]. The system outputs and information related to identified alerted areas are updated fortnightly and disseminated using a proper web display application.

The described study has been conducted using time-series of vegetation phenological parameters extracted from satellite-derived NDVI datasets (global 15-day NDVI time-series, available from 2000 to present, at a 5.6 km spatial resolution, derived from the MODIS MOD13C1 Terra CMG dataset), and precipitation time-series obtained from the Tropical Rainfall Measuring Mission TRMM mission (0.25° x 0.25° spatial resolution) Multisatellite Precipitation Analysis estimation, computed at daily intervals (TRMM 3B-42 daily data), for period of 1998-present.

For the purpose of the proposed statistical analysis, ten phenological metrics (the time for the start and the end of the season, the length of the season, the season base level, the time for the mid of the season, the largest NDVI data value during the season, the seasonal amplitude, the rate of increase at the beginning of the season and the rate of decrease at the end of the season, and, finally, the seasonal integral) have been extracted from the yearly NDVI function that best fits the original yearly NDVI time-series and considered for each vegetation growing season [7] in the examined time interval (2000-2014). These metrics are able to describe synthetically the trend of the season in both the time and the integrated NDVI/time domains and are related to the seasonal vegetation productivity.

Different precipitation fortnightly time-series have been used for the study, obtained taking into consideration different cumulating intervals (1-3-6-9-12 months values).

Specific routines have been implemented in order to investigate, on a pixel basis, and to explain the statistical relationship between the considered time-series of phenological parameters and precipitation data. Obtained results have been spatially analyzed and aggregated taking into consideration different vegetation types, and maps showing the areas where the observed vegetation phenological parameters are largely dependent on rainfall patterns have been produced. Moreover, the precipitation cumulative interval and the period, in the year, when precipitation influence on vegetation productivity has proved to be significant, have been identified and discussed, also in relation to the rainfall seasonality and crop calendar in the examined area.

The monitoring of vegetation conditions based on the analysis of phenological metrics, as originally provided in the ITHACA drought EWS, proved to effectively support WFP activities in several cases (i.e. Niger and Chad 2009[8], Sahel 2012, Horn of Africa crisis 2011).

The final aim of conducted statistical study, object of this thesis work, was to correctly define the operational use of precipitation data for drought detection, in support to the vegetation monitoring procedures. The outcomes of the carried out work supported the planning and definition of effective procedures for the integration, where it is meaningful, in the ITHACA vegetation conditions monitoring activities , based on the analysis of phenological parameters, with the near real-time evaluation of precipitation deficits explained, for multiple time scales, using the Standard Precipitation Index (SPI). Indeed, the studied relationships between rainfall and vegetation dynamics allowed to determine the areas where the spatial and the temporal variability in vegetation conditions are closely related to the climate, and the best rainfall cumulating interval to be used for SPI monitoring purposes as well. In these areas, the fortnightly near real-time monitoring of the precipitation permits to earlier identify drought warnings, by considering also climate conditions before the start of the vegetation growing season. Moreover, in the same areas, the near real-time SPI analysis during the vegetation growing season supports the monitoring of phenological parameters in a way to identify very critical events characterized by both vegetation productivity and rainfall anomalies.

2. DROUGHT AND NATURAL HAZARDS

2.1. Natural Hazards and Disaster Risk

According to The World Meteorological Organization (WMO), Natural hazards are severe and extreme weather and climate events that occur naturally in all parts of the world. Apart from that, some regions are more vulnerable to certain hazards than others. Despite of the term “natural”, a natural hazard has an element of human participation. A physical event that does not affect human being is a natural phenomenon but not a natural hazard. A natural phenomenon that occurs in a populated and causes unacceptably large numbers of fatalities or overwhelming property damage is a natural disaster.

Hazards such as droughts, floods, hurricanes, earthquakes, and landslides can have devastating effects on human life and economies. With growing numbers of people living in crowded cities and vulnerable areas, it is really important than ever to improve our understanding of natural disasters and the ways in which humans respond to them.

Each year a number of disasters related to climate change, meteorological and hydrological events, generate significant economic and human losses. As shown by statistics in recent years, in the period between 2003 and 2012 the average annual disaster frequency observed was 388 whilst the annual average of killed people was 106,654 persons and almost 216 million people became victims each year. On the other hand, it was produced economic losses estimated at over US \$ 156.7 billion per year.[9] See Figure 1 and Figure 2.

Regardless of the rising global trend in the occurrence of disasters and associated economic losses, global loss of life related with meteorological, hydrological or climate-related hazards in 2005, decreased to one-tenth of levels in the 1950's. This notable decline is a expression that preparedness and prevention, combined with efficient early warning systems and emergency management, can considerably contribute to reducing impacts of hazards on human life. [10]

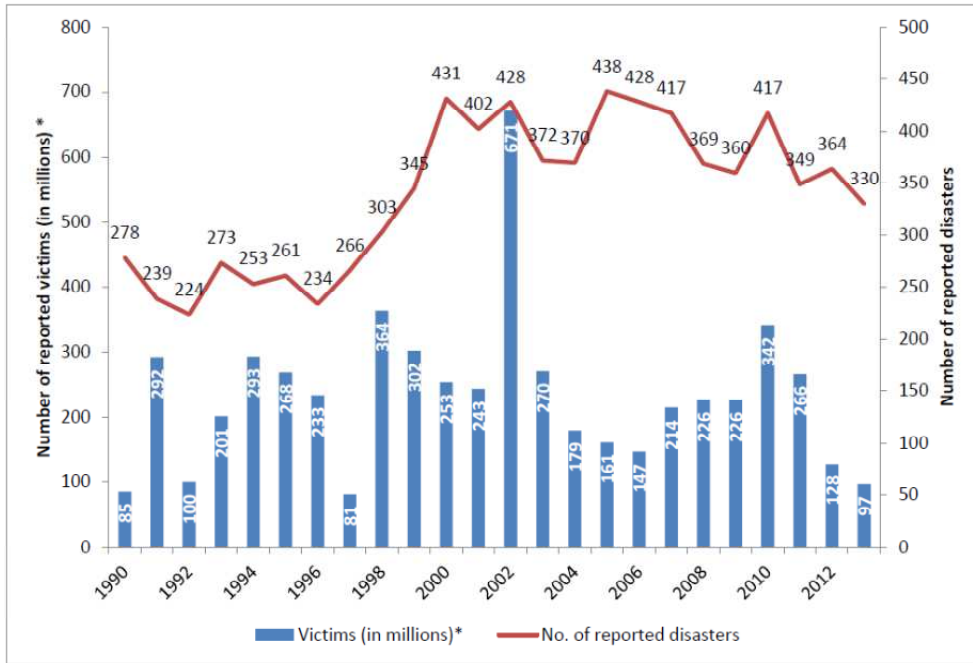


Figure 1. Trends in occurrence and victims (Death and total affected) [9]

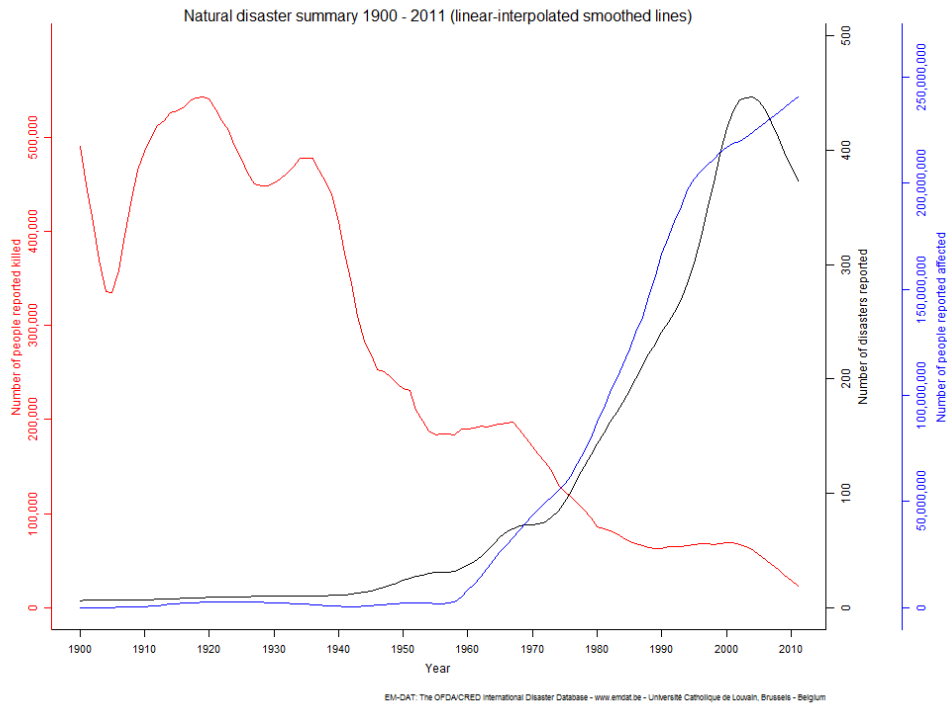


Figure 2. Natural disaster summary 1900-2011 (linear-interpolated smoothed lines)[11]

2.2. Drought as a hazard

Due to the increase of population and development of agricultural energy and industrial sectors, the request for water has increased many fold and even water scarcity has been occurring each year in many parts of the world. Other factors, such as contamination of water resources and climate change, have further contributed to the water scarcity (See Figure 3). [12]

Drought is an insidious hazard of nature. It originates from a deficiency of precipitation that results in a water shortage for some activity or some group. Drought differs from other natural hazards (e.g., floods, tropical cyclones, and earthquakes) in several ways. First since the effects of drought often accumulate slowly over a considerable period of time, and many linger for years after the termination of the event, a drought's onset and end are difficult to determine. Second the absence of a precise and universally accepted definition of drought adds to the confusion about whether or not a drought exist and, if it does, its severity. Realistically, definitions of drought must be region and application (or impact) specific. Third, drought impacts are less obvious and are spread over a larger geographical area than are damages that result from other natural hazards.[13]

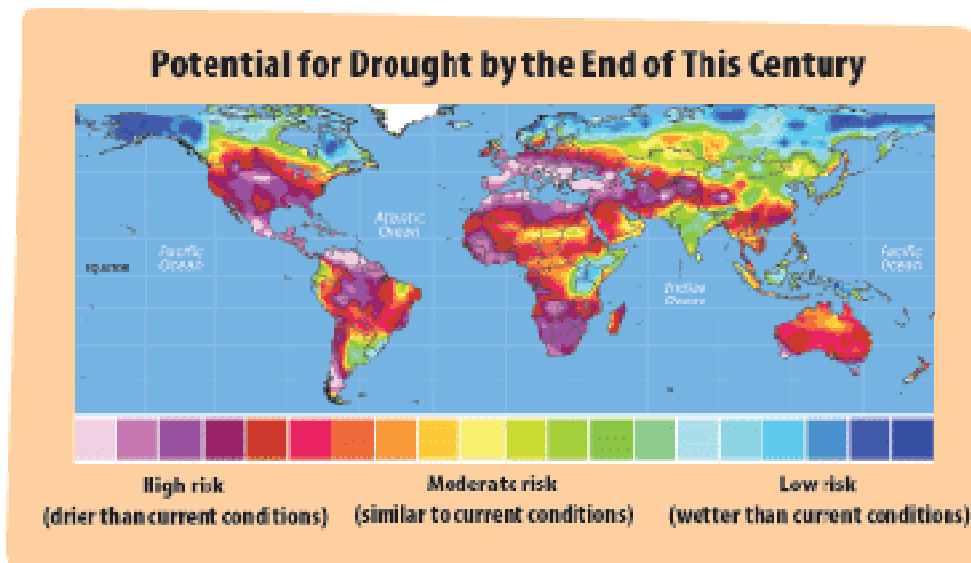


Figure 3. Map showing drought potential by the end of the current century.[14]

Drought can have devastating effects on communities and the surrounding environment. The degree of devastation is directly correlated with the strength of the drought and the length of time an area is considered to be in drought conditions.

One impact of drought on communities is its effect on water supply, impacting both surface and ground water resources. Drought can impact surface water quality in many ways. Reduced stream and river flows can increase the concentration of pollutants in water and cause stagnation. Higher water temperatures in

lakes and reservoirs lead to reduced oxygen levels, which can affect aquatic life and water quality. Runoff from drought-related wildfires can carry extra sediment, ash, charcoal, and woody debris to surface waters, killing fish and other aquatic life by decreasing oxygen levels in the water.

Reduced precipitation and increased evaporation of surface water can impact the recharge of groundwater supplies over time. Of all groundwater systems, shallow groundwater aquifers that exchange water with surface waters are likely to be the most affected by drought. [15]

Water may become especially polluted during times of drought due to the lack of rain water to dilute industrial and agricultural chemicals. This toxic water can be harmful to plants and animals that use it and make it difficult to clean for drink water. In the worst droughts, farmers are unable to maintain their fields because of the drought conditions and the restrictions placed on water.

Another impact of drought is the reduction of electrical generation. In the areas where the power generation depends on the use of water for hydropower, if water use is restricted, then power plants need to be shut down and more expensive kinds of energy generation may be need to be used.

For humans, the health implications of drought are numerous and far reaching. Some drought-related health effects are experienced in the short-term and can be directly observed and measured. However, the slow rise or chronic of drought can result in longer term, indirect health implications that are not always easy to anticipate or monitor. The quality and quantity of food supply can be affected by drought conditions, which can potentially lead to several types of adverse health effects.[15]

Country	Date	No Killed
Somalia, Drought	February 1, 2010	20000
Pakistan, Drought	January 1, 2014	180
China P Rep, Drought	May 1, 2006	134
Paraguay, Drought	September 1, 2008	4
Kenya, Drought	July 1, 2008	4

Table 1. Top 10 most important Drought disasters for the period 2006 to 2015 sorted by numbers of killed at the country level. [11]

Country	Date	No Total Affected
China P Rep, Drought	October 1, 2009	60000000
China P Rep, Drought	December 1, 2010	35000000
China P Rep, Drought	August 1, 2014	27500000
China P Rep, Drought	May 1, 2006	18000000
Thailand, Drought	April 1, 2008	10000000
Niger, Drought	September 1, 2009	7900000
Thailand, Drought	March 1, 2010	6482602
Ethiopia, Drought	May 1, 2008	6400000
Ethiopia, Drought	January 1, 2009	6200000
China P Rep, Drought	January 1, 2013	5000000

Table 2. Top 10 most important Drought disasters for the period 2006 to 2015 sorted by numbers of total affected people at the country level. [11]

2.3. Types of Drought

Many definitions of drought exist because the characteristics of drought differ between regions. Drought impacts also vary significantly between locations because of differences in economic, social and environmental characteristics at the micro and macro scales. All droughts originate from a deficiency of precipitation.[16]

Nevertheless, three principals types of drought can be identified (see Figure 4): meteorological, agricultural, and hydrological. Meteorological drought is mainly defined by the deficit of precipitation from expected amount over an defined period of time. Agricultural drought may be characterized by a deficiency in water availability for crop or plant growth. Although precipitation deficiencies are important, agricultural drought severity is frequently associated with deficiencies in soil moisture, the most significant factor in defining crop production potential. Agricultural drought usually occurs after the meteorological drought, depending on the reserve of water in the soil. Some soils are more resilient to drought because of high water holding capacity. Vulnerability is highest on soils with a low water holding capacity, although appropriate soil management practices can reduce the impacts of drought on crops. Hydrological drought is defined by deficiencies in surface and ground water resources, which lead to a lack of water availability to meet normal and specific water demands. Hydrological or water supply drought usually occurs after the agricultural drought because considerable time elapses between precipitation deficiencies and declines in ground water and reservoir levels. Similarly, these components of the hydrologic system are usually the last to recover from longer-term droughts. [16]

Moreover, there is another type of drought know as socioeconomic drought, which associates the supply and demand of some economic good with elements of meteorological, hydrological, and agricultural drought. It differs from the other types because its incidence depends on the time and space processes of supply and demand to identify or classify droughts. The supply of many economic goods, such as water, forage, food grains, fish, and hydroelectric power, depends on weather. Because of the natural variability of climate, water supply is abundant in some years but unable to meet human and environmental needs in other years. Socioeconomic drought occurs when the demand for an economic good exceeds supply as a result of a weather-related shortfall in water supply. [17]

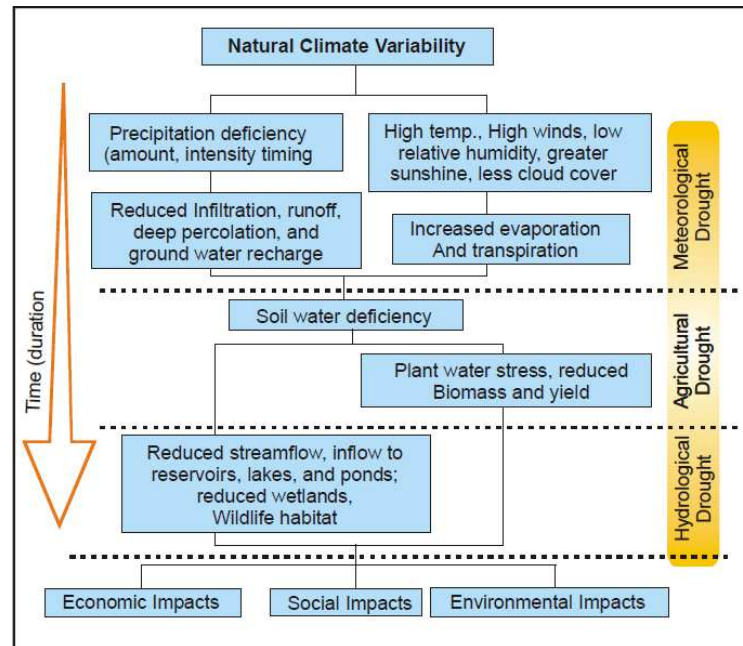


Figure 4. Sequence of Drought Impacts[18]

On the basis of a set of defined criteria, the intensity and duration of drought is expressed with a drought index developed as a means to measure drought. Usually, drought index integrates various parameters like rainfall, temperature, evapotranspiration, runoff and other water supply indicators into a single number and gives a comprehensive picture for decision-making. In fact, different types of drought require different indices that can be used to quantify the moisture condition of a region and thereby detect the onset and measure the severity of drought events. This can assist in quantifying the spatial extent of a drought event thereby allowing a comparison of moisture supply condition between[19].

2.4. The role of remote sensing for drought monitoring

In recent years, the rising population and overstress on natural resources, decrease in water resources, soil degradation, and future projected climate change scenarios have become important areas of concern. The implication on food security and a hold up in agricultural and fodder production leads to socio-economic unrest especially in developing countries[20]. Then, management of natural resources in developing as well as developed countries requires information on the state and changes in a range of biophysical variables.

In many zones of the world, droughts still to be a potential disaster and consequently, there is a need for appropriate quantification of drought impacts and monitoring and reporting of drought development in economically and environmentally susceptible areas. However, the detection, monitoring and mitigation of disasters require gathering of fast and continuous relevant information that are not to be reached through traditional means. Since disasters that cause vast social and economic disruptions normally affect big areas or territories and are linked to global change, it is not possible to efficiently collect continuous data using conventional methods. For example, meteorological data from the ground stations can be a good source of information that can be used for agricultural drought assessment. However, the poor density of weather stations makes it difficult to get sufficient temporal and spatial data to make consistent assessment and risk mapping. In addition, the data collected from existing meteorological stations are incomplete, limited in area coverage and not available timely.[21]

With the aim to management the crisis generate for the possible drought impacts, remote sensing data is an valid choice[18], [22] and is currently utilized worldwide[23]–[25]. The remote sensing tools offer excellent possibilities of collecting general information and data, useful to monitoring the drought events. This is because the technology has capability of collecting information at global and regional scales fast and frequently and the data is collected in digital form. According to Westen[26], for the management of natural disasters a large quantity of multi-temporal spatial data is necessary and satellite remote sensing is the ideal tool for disaster management, because it offers information over big areas, and at short time intervals. Furthermore, observation from space provides permanent data archive, additional visual information, and enables to have regular and repetitive view of nearly the earth's entire surface[20]. This technique make possible to quickly acquire information fast over big areas by means of sensors operating in several spectral bands mounted on satellites. A satellite, which orbits the earth, is able to explore the whole surface in a few days and repeat the survey of the same area at regular intervals, whilst an aircraft can give a more complete analysis of a smaller area, if a specific need occurs. The spectral bands used by these sensors cover the whole range between visible and microwaves.

The development and advancements in space technology, to address issues like drought detection, monitoring and assessment have been dealt with very successfully and helped in formulation of plans to deal with this slow onset disaster. With the help of environmental satellites, drought could be detected before and delineated more correctly, and its impact on agriculture would be diagnosed far in advance of harvest, which is the most vital for global food security and trade [20]. For a precise assessment of the occurrence, extent and severity of drought, it is essential to get a correct picture of the spatial and temporal distribution of a number of hydrological, meteorological, and surface variables. Space observation technologies having this potential has made a significant contribution in this field.

3. LITERATURE REVIEW

In this chapter a review of drought situation in Africa and some system and indicators that are fundamentals to develop this study are reported.

3.1. An Overview of drought situation in Africa

Sustainable development in Africa has been affected by drought and desertification in the last years. These problems have far reaching adverse impacts on human health, food security, economic activity, physical infrastructure, natural resources and the environment and national and global security.

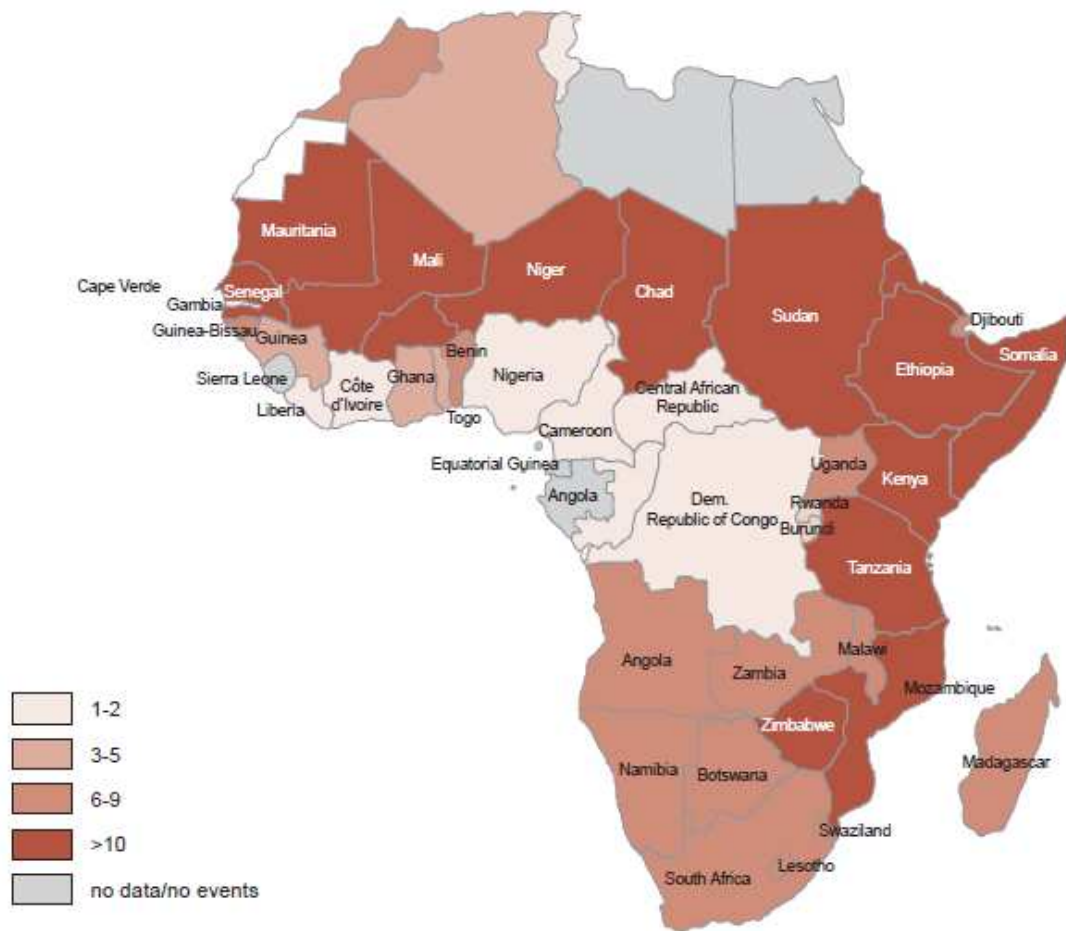
The most important variable of drought in Africa is the water deficit, that result in a water shortage for some activity, group, or environmental sector. A more in-depth definition of drought includes four sub definitions including meteorological, hydrological, agricultural and socio-economic drought

The underlying cause of most droughts can be related to changing weather patterns manifested through the excessive build up of heat on the earth's surface, meteorological changes which result in a reduction of rainfall, and reduced cloud cover, all of which results in greater evaporation rates. The resultant effects of drought are exacerbated by human activities such as deforestation, overgrazing and poor cropping methods, which reduce water retention of the soil, and improper soil conservation techniques, which lead to soil degradation.[27]

Desertification on the other hand is defined as a process of land degradation in arid, semi-arid and dry sub-humid areas, resulting from various factors, including climatic variations and human activities. There are different direct and indirect factors that causes desertification. Normally the phenomenon occurs because there are some ecosystems (e.g. drylands) that are extremely vulnerable to over-exploitation and inappropriate land use, generating underdevelopment of economies and in entranced poverty among the affected populations. [27]

Two thirds of Africa is classified as deserts or drylands. These are concentrated in Sahelian region, the Horn of Africa and the Kalahari in the south. Africa is especially susceptible to land degradation and bears the greatest impact of drought and desertification. It is estimated that two-thirds of African land is already degraded to some degree and land degradation affects at least 485 million people or sixty five percent of the entire African population. Desertification especially around the Sahara has been pointed out as one the potent symbols in Africa of the global environment crisis. Climate change is set to increase the area susceptible to drought, land degradation and desertification in the region. Under a range of climate scenarios, it is projected that there will be an increase of 5-8% of arid and semi Arid lands in Africa. [27]

With regard to drought, Africa presented a high frequency of occurrence and severity of drought. This is one of the most important natural disasters in the continent. A study from Bristol University projects that areas of western were at most risk from decreasing water supply and droughts as a result of rising temperatures. Actually, some climate scenarios predict that the driest regions of the world will become even drier, presenting a risk of persistence of drought in many areas of Africa which will consequently bear greater and sustained negative impacts. [27]



Source: Adapted from Noojin, Leah 2006. *Factors that influence famine in Sub-Saharan African Countries*

Figure 5. Drought Events per country from 1970 to 2004 within Sub-Saharan Africa [27]

3.2. Impacts of drought

Drought generate impacts that spans many sectors of the economy and reaches well beyond the area experiencing physical drought. This complexity exists because water is integral to society's ability to produce goods and provide services.

Impacts are commonly referred to as direct and indirect. Direct impacts include reduced water levels, increased livestock and wildlife mortality rates, and damage to wildlife and fish habitat. The consequences of these direct impacts illustrate indirect impacts. For example, a reduction in crop, and forest productivity may result in reduced income for farmers and agribusiness, increased prices for food and timber, unemployment, reduced tax revenues because of reduced expenditures, foreclosures on bank loans to farmers and businesses, migration, and disaster relief programs.[28]

3.2.1. Economic impacts

Many economic impacts occur in agriculture and related sectors, because of the reliance of these sectors on surface and groundwater supplies. In addition to losses in yields in crop and livestock production, drought is associated with insect infestations, plant disease, and wind erosion. The incidence of forest and range fires increases substantially during extended periods of droughts, which in turn places both human and wildlife populations and higher levels of risk.

Income loss is another indicator used in assessing the impacts of drought. Reduced income for farmers has a ripple effect. Retailers and other who provide goods and services to farmers face reduced business. This leads to unemployment, increased credit risk for financial institutions, capital shortfalls, and eventual loss of tax revenue for local, state, and federal governments. Prices for food, energy, and other products increase as supplies are reduced. In some cases, local shortages of certain goods result in importing these goods from outside the drought-stricken region. Reduced water supply impairs the navigability of rivers and results in increased transportation cost because products must be transported by alternative means. Hydropower production may also be significantly affected. [28]

3.2.2. Environmental impacts

Environmental losses are their result of damages to plant and animal species, wildlife habitat, and air and water quality, forest and range fires, degradation of landscape quality, loss of biodiversity, and soil erosion. Some of these effects are short-term conditions returning to normal following the end of the drought. Other environmental effects last for some time and may even become permanent. Wildlife habitat, for example, may be degraded through the loss of wetlands, lakes, and vegetation. However, many species eventually recover from this temporary aberration. The degradation of landscape quality, including increased soil erosion, may lead to a more permanent loss of biological productivity. [28]

3.2.3. Social impacts

Social impacts involve public safety, health, conflicts between water users, reduced quality of life, and inequities in the distribution of impacts and disaster relief. Many of the impacts identified as economic and environmental have social components as well. Population migration is a significant problem in many countries, often stimulated by a greater supply of food and water elsewhere. Migration is usually to urban areas within the stressed vicinity, or to regions outside the drought affected area or may even be to adjacent countries and usually when the drought has abated, the migrants seldom return home, depriving rural areas of valuable human resources. The drought migrants place increasing pressure on the social infrastructure of the urban areas, leading to increased poverty and social unrest. [28]

3.3. Drought impacts in Africa

It is common knowledge that land degradation and desertification constitutes major causes of forced human migration and environmental refugees, deadly conflicts over the use of dwindling natural resources, food insecurity and starvation, destruction of critical habitats and loss of biological diversity, socio-economic instability and poverty and climatic variability through reduced carbon sequestration potential. The impacts of drought and desertification are among the most costly events and processes in Africa. The widespread poverty, the fact that a large share of Africa's economies depend on climate-sensitive sectors mainly rain fed agriculture, poor infrastructure, heavy disease burdens, high dependence on and unsustainable exploitation of natural resources, and conflicts render the consistent especially vulnerable to impacts of drought and desertification. The consequences are mostly borne by the poorest people and the Small Island Developing States (SIDS). In the region, women and children in particular, bear the greatest burden when land resources are degraded and when drought sets in. As result of the frequent droughts and desertification, Africa has continued to witness food insecurity including devastating famines, water scarcity, poor health, economic hardship and social and political unrest.[27]

3.3.1. Impact on economic growth and poverty reduction

The majority fo the population in most African countries live on marginal lands in rural areas practicing rain-fed agriculture. The impact of drought and climatic variability in both economic and mortality terms is generally larger for relatively simple and predominantly agricultural economies. These types of economies dominate Africa. In 2004, the UNCCD estimated that some six million hectares of productive land was being lost every year since 1990, due to land degradation. This in turn had caused income losses worldwide of US\$ 42 billion per year. With two-thirds of arable land expected to be lost in Africa by 2025, land degradation currently leads to the loss of an average of more than 3 percent annually of agriculture GDP in the Sub-Saharan Africa region. In Ethiopia, GDP loss from reduced agricultural productivity is estimated at \$ 130 million per year. In Uganda land degradation in the dry lands threatens to cause havoc on the country's economy and escalate poverty. This is because these dry lands constitute the Uganda cattle corridor, which accounts for over 90 percent of the national cattle herd and livestock production contributes 7.5 percent to the GDP and 17 percent to the agricultural GDP.

Drought and floods account for 80 percent of loss of life and 70 percent of economic losses linked to natural hazards in Sub-Saharan Africa. The drought of 1990/1991 in Zimbabwe resulted in a 45 percent drop in agricultural production but also a 62 percent decline in the value of the stock market, a 9 percent drop in manufacturing output and a GDP drop of 11 percent. As a proportion of the national economy this is a very significant loss and can best be thought of as 2.5 billion dollars of foregone development, for example, hospitals and schools not built.

3.3.2. Impact on food security

The poor households that are affected by drought and desertification do not have adequate resources to deal with food shortages leading to food insecurity and hunger that affects millions of people. If land degradation continues at the current pace, it is projected that more than a half of cultivated agricultural area in Africa could be unusable by the year 2050 and the region may be able to feed just 25 percent of its population by 2025. Agriculture being one of the main economic activities in Africa, this would lead to a catastrophe with unprecedented repercussions.

The most severe consequence of drought is famine. Food aid to subcontinent accounts for approximately 50 percent of the yearly budget of the World Food Aid Programme. The consecutive droughts that have occurred in the southern Africa since 2001 have led to serious food shortages. The drought of 2002-03 resulted in a food deficit of 3.3 million tonnes, with an estimated 14.4 million people in need of assistance. At the height of the Horn of Africa's drought in 2000, 3.2 million Kenyans were dependent on food aid, and malnutrition reached 40 percent of the population, more than 3 times the normal level. In 2005, Concern, in partnership with the Diocese of Malindi, Kenya, provided seed and technical support to 2,129 farm households who were severely affected by drought. During the same year 2005 many other African countries faced food shortages because of the combined effects of severe droughts[29], [30] and desertification that could become semi-permanent under climate change. The worst affected countries included Ethiopia, Zimbabwe, Malawi, Eritrea and Zambia, a group of countries where at least 15 million people would go hungry without aid[31]. The situation in Niger, Djibouti and Sudan also deteriorated rapidly. Many of these countries had their worst harvest in more than 10 years and were experiencing their third or fourth consecutive severe drought.

3.3.3. Impact on water

Drought influence water availability, which is projected to be one of the greatest constraints to economic growth in the future. In Africa, climate change is expected to intensify the continent's increasingly critical water situation. Reduced annual average rainfall and its run-off would worsen desertification in southern Africa. This sub-region being one of many water-stressed regions could thus see a further decrease in streams flow and the ability of groundwater to 'recharge'. Furthermore, it is projected that by 2025 Southern Africa will also join most countries in North Africa that can already be classified as having absolute water scarcity today. This means that countries in these regions will not have sufficient water resources to maintain their current level of per capita food production from irrigated agriculture – even at high levels of irrigation efficiency – and also to meet reasonable water needs for domestic, industrial, and environmental purposes. To sustain their needs, water will have to be transferred out of agriculture into other sectors, making these countries or regions increasingly dependent on imported food. By the year 2025, it is thus estimated that nearly 230 million Africans will be facing water scarcity, and 460 million will live in water-stressed countries.

In the Nile region, most scenarios estimate a decrease in river flow up to more than 75 per cent by the year 2100. This would have significant impacts on agriculture, as a reduction in the annual flow of the Nile above 20 per cent will interrupt normal irrigation. Such a situation could cause conflict because the current allocation of water, negotiated during periods of higher flow, would become untenable.

The situation of women and children who are responsible for fetching water for the households is therefore worsened by drought and desertification. These can add hours of labor to an already fully charged workday.

3.3.4. Impact on biodiversity

Biodiversity existing in dry lands and other habitats underpin ecosystem services that vital for livelihoods of millions of people in Africa. It is the foundation for sustainable development in the region and globally. The dry areas of the world are the origin of a large number of globally important cereals and food legumes, such as barley, wheat, faba beans and lentils. Four hundred million people, two thirds of sub-Sahara African population, rely on forest goods and services for their livelihood. Drought, land degradation and desertification have had serious threats to the management, sustainable use and equitable sharing of benefits of biodiversity. The projected devastating impacts of climate change in the region including exacerbating these factors will escalate biodiversity degradation and loss associated with drought, land degradation and desertification. These factors affect biodiversity directly and indirectly. Onsite impacts include habitat and species degradation and loss, leading to overall loss of economic and biological productivity. For instance on rangelands, overgrazing not only reduces the overall protective soil cover and increases soil erosion, but also leads to a long-term change in the composition of the vegetation. Plant biodiversity will change over time, unpalatable species will dominate, and total biomass production will be reduced. These in turn trigger and contribute to indirect or offsite impacts. Soil erosion will contribute to denudation and pollution of wetlands and water bodies. As biological and economic productivity deteriorates, communities are forced migrate to other areas or engage in other coping activities that too contribute biodiversity degradation.

According to the Africa Environment Outlook II, approximately half of Africa's terrestrial eco-regions have lost more than 50 per cent of their area to cultivation, degradation or urbanization. It also states that some eco-regions such as the Mandara Plateau mosaic, Cross-Niger transition forests, Jos Plateau forest-grassland mosaic, and Nigerian lowland forests have gone more than more than a 95 percent transformation. Nine other eco-regions have lost more than 80 per cent of their habitat, including the species-rich lowland Fynbos and Renosterveld and the forest and grasslands of the Ethiopian Highlands; the Mediterranean woodlands and forests have lost more than 75 per cent of their original habitat, and the few remaining blocks of habitat are highly fragmented.

In the sand dune areas of countries such as Mauritania, Mali, Niger, Nigeria and Senegal major river basins siltation processes accumulate debris and materials that engulf natural vegetation, such as the *Acacia nilotica* riparian forests. Soil erosion contributes to moving the seed capital of the fround, uprooting grassy as well as woody species, and in accumulation areas it smothers valuable species.

In West Africa the movement of people south towards sub-humid to humid tropical areas has resulted into loss of primary forests and woodlands, repeated logging of the secondary vegetation, and depletion into loss of primary forests and woodlands, repeated logging of the secondary vegetation, and depletion of

a number of species. More diffuse degradation of land resources also occurs in the arid and sub-humid parts. These include the extraction of tree resources outside forests for charcoal making, and the use of high value woods.

3.3.5. Impact on Energy

The impacts of drought and desertification on the energy sector are felt primarily through losses in hydropower potential for electricity generation and the effects of increased runoff on hydropower generation. The gravity of impacts of electricity generation is further demonstrated by the case of Ghana where for the first half of 2007, the water level at the Akosombo dam had fallen below the minimum level of 240 feet. This led to reduction in hydro-electricity generation and hence load shedding of electricity in the whole country. Energy impacts are also experience through changes in the growth rates of trees on which a vast majority of the people in the region rely for fuel wood.

Due to the limited alternatives available to them and low priority accorded to meet their needs in times of scarcity, the rural areas and the urban poor bear the greatest cost of decrease in energy resources. This undermines efforts to pull these categories of people out of the poverty trap.

3.4. Indices for drought monitoring

On the basis of a set of defined criteria, the measure of the intensity and duration of drought is expressed through a drought index. That integrates into a single number, different parameters like rainfall, evapotranspiration, runoff, temperature and some water supply indicators, giving a complete summary for decision-making. Actually, each type of drought require different indices that can be used to measure the severity and the spatial extents of droughts events, allowing a comparison between different regions [19]. It is important to taking into account that for monitoring drought using a combination of monitoring tools integrated together is preferable instead to use a single indicator [32].

3.4.1. Meteorological drought indices

Meteorological indices measures how much precipitation for a given period of time has deviated from historically established norms. Some of the widely used drought indices include Palmer Drought Severity Index (PDSI), Crop Moisture Index (CMI), Standardized Precipitation Index (SPI), and Surface Water Supply Index (SWSI).

3.4.1.1. *Palmer Drought Severity Index (PDSI)*

Palmer, 1965 developed an index to measure the departure of moisture availability based on the supply and demand concept of the water balance equation, taking into account more than just the precipitation deficit as specific locations. The objective of the Palmer Drought Severity Index (PDSI) is to provide standardized measurements of moisture conditions so that comparison could be made between locations and between months. As a meteorological drought index it is responsive to abnormal weather conditions either on dry or abnormally wet side but was specifically designed to treat the drought problem in semiarid an sub humid climate with cautions that extrapolation beyond these conditions may lead to unrealistic results.

PDSI has been used in west Hungary as soil moisture indicator and also widely utilized in the United States for drought monitoring and as a tool to trigger actions associated with drought contingency plans. However, several researchers have shown its limitation. The Palmer Drought Severity Index has a time scale of about 9 months which does not allow identification of droughts at shorter time scales[33]. Moreover, this index has many other shortcomings related to calibration and spatial comparability [34]–[36]. Furthermore, it is designed for agriculture thus does not accurately represent the hydrological impact resulting from longer droughts[37]. As a solution to these problems, the Standardized Precipitation Index (SPI) was developed, an index which can be calculated at different time scales to monitor droughts in the different usable water resources[38].

3.4.1.2. Standardized Precipitation Index (SPI)

The standard precipitation index, developed by Mckee et al. (1993) [38], is the most widely utilized index for understanding the magnitude and duration of drought events. The purpose of employing the SPI is to assign a single numeric value to the precipitation that can be compared across regions with markedly different climates. Technically, it is the number of standard deviations that the observed value would deviate from the long-term mean, for a normally distributed random variable. The calculation for any location is based on the historical precipitation record that is fitted to a probability distribution, which is then transformed into a normal distribution so that mean SPI for the location and desired period is zero[39].

According to Thavorntam and Mongkolsawat (2006)[40], SPI helps in examining the severity and spatial patterns of drought in a given region. Besides, it offers a quick, handy and simple approach with minimal data requirements[41]. The index is designed to quantify the impacts of precipitation deficit on groundwater, reservoir storage, soil moisture, and stream flow for multiple time scales. Precipitation deficits can be effectively quantified for multiple time scales which reflect the impact of drought on the availability of the different water resources. Thus, Mckee et al. (1993) [38] originally calculated the SPI for 3, 6, 12, 14, and 48 months time scales.

Compared to the Palmers Drought Severity Index (PDSI), SPI is easy to determine and has greater spatial consistence therefore a more recommendable drought index. Moreover, it can be used in risk assessment analysis and making decisions with special ability for adjustments to time periods for which the users are interested, for example, short time periods in life cycle of crops or longer periods regarding water resources [33]. According to Mckee et al. (1993) [38], soil moisture conditions respond to precipitation anomalies on a relatively short time scale while groundwater, stream flow, and reservoir storage reflect the longer-term precipitation anomalies. Normally, drought occurs every time when SPI is negative or its intensity comes to -1.0 or lower, while drought stops when SPI is positive. Each drought event, therefore, has a duration defined by its beginning and end, and intensity for each month that the event continues. The positive sum of the SPI for all the months within a drought event can be termed the drought's "magnitude".

<i>SPI Values</i>	<i>Drought Category</i>
0 to -0.99	Mild drought
-1.00 to -1.49	Moderate drought
1.50 to -1.99	Severe drought
≤ -2.00	Extreme drought

Table 3. Drought intensity categories defined for values of SPI[38]

3.4.1.3. *Crop Moisture Index (CMI)*

The Crop Moisture Index (CMI) is based on weekly mean temperature and precipitation which was specifically designed as an agricultural drought index[42]. It depends on the drought severity at the beginning of the week and the evapotranspiration, soil deficit or soil moisture recharge during the week [43]. The index measures both evapotranspiration deficits (drought) and excessive wetness (more than enough precipitation to meet evapotranspiration demand and recharge the soil). Designed to monitor short-term moisture conditions affecting a developing crop, it is not a good long-term drought monitoring tool. The CMI's rapid response to changing short-term conditions may provide misleading information about long-term conditions. Nemani et al. (1992) [44] used CMI for estimating surface moisture status, because it depicts changes in soil moisture situation more rapidly than PDSI. It was found that CMI indicates more favorable moisture conditions over a particularly wet or dry month even in the middle of a serious long-term wet or dry period.

3.4.1.4. *Standardized Water Supply Index (SWSI)*

Shafer and Dezman (1982)[45] developed the Surface Water Supply Index (SWSI) to complement the Palmer Index for moisture conditions across the state of Colorado. This index, computed with only snowpack, precipitation, and reservoir storage in the winter, compliments the Palmer index for moisture condition and is dependent on the season. During the summer months, stream flow replaces snowpack as a component within the SWSI equation. SWSI has been used along with PDSI, to trigger the activation and deactivation of the Colorado drought plan. However, although is easy to calculate yet it has the limitation that values between basins or a region is difficult to compare[46].

3.4.2. Satellite based drought indices for drought characterization

The use of point measurement using station to calculate drought indices, that is normally implemented, could not reflect spatial details particularly where station density is poor. Reed et al. (2002)[47] showed how the lack of spatial detail could be the major disadvantage of station based drought indicators, affecting reliability of the drought index. In consequence at present, some drought indices have been calculated using remote sensing. Furthermore, vegetation based drought indices have been developed and widely utilized to address drought related investigations.

3.4.2.1. Normalized Difference Vegetation Index (NDVI)

Tucker first suggested NDVI in 1979 as an index of vegetation health and density[48] and it has been considered as the most important index for mapping of agricultural drought[49].

In satellite image, vegetation appears very different at different light spectrum particularly in the visible and near infrared wavelengths. Healthy or dense vegetation absorbs most of the visible light and reflects a large portion of the near infrared light whereas the unhealthy or sparse vegetation reflects more visible light and less near infrared light. Comparing these two, visible and near infrared light, scientists measure the relative amount of vegetation and its vigor using a vegetation index. NDVI is an index of vegetation health and density computed from the satellite image using spectral radiance in red and near infrared reflectance using the following formula: $NDVI = \frac{(NIR-R)}{(NIR+R)}$, where NIR and R refer to the near infrared and the red band reflectance respectively.

NDVI is a powerful indicator to monitor the vegetation cover of wide areas, and to detect the frequent occurrence and persistence of droughts[40]. The index provides a measure of the amount and vigor of vegetation at the land surface where the magnitude of NDVI is related to the level of photosynthetic activity in the observed vegetation. In general, higher values indicate greater vigor and amount of vegetation.

Since climate is one of the most important factors affecting vegetation conditions, AVHRR-NDVI data have been used to evaluate climatic and environmental changes at regional and global scales[50]–[52]. NDVI is a good indicator of green biomass, leaf area index and patterns of production [22]. Furthermore, it can be used not only for accurate description of continental land cover, vegetation classification and vegetation vigor but is also effective for monitoring rainfall and drought, estimating net primary production of vegetation, crop growth conditions and crop yields, detecting weather impacts and other events important for agriculture, ecology and economic [51]. NDVI has been used successfully to identify stressed

and damaged crops and pastures but only in homogeneous terrain. In more heterogeneous terrain regions their interpretation becomes more difficult [51], [53]. Many studies have been done in some areas in the world indicating meaningful direct relationships between NDVI derived from NOAA AVHRR satellites, rainfall and vegetation cover and biomass.

3.4.2.2. Vegetation Condition Index (VCI)

The vegetation condition index is an indicator of the status of the vegetation cover, first suggested by Kogan (1997)[54] as a function of the NDVI minimum and maxima encountered for a given ecosystem over many years. The index is defined as: $VCI_j = \frac{NDVI_j - NDVI_{min}}{NDVI_{max} - NDVI_{min}} \times 100$ where, $NDVI_{min}$ and $NDVI_{max}$ are calculated from long-term record for a particular month and j is the index of the current month. It shows how close the NDVI of the current month is to the minimum NDVI calculated from the long-term record. The condition of the ground vegetation presented by VCI is measured in percent and values between 50% and 100% indicate optimal or above normal conditions whereas VCI values close to zero percent reflect an extreme dry month.

VCI has been used by Kogan and Uganani, 1998[55] for estimation of corn yield in South Africa, drought detection in Argentina[56]; drought monitoring over India[57]; monitoring droughts in the southern Great Plains, USA[58]; drought detection and monitoring in the Mediterranean region[53] and drought assessment and monitoring in Southwest Asia[48]. These studies suggest that VCI captures rainfall dynamics better than NDVI particularly in geographically non-homogeneous areas. Also, VCI values indicate how much the vegetation has advanced or deteriorated in response to weather. It was concluded from the above studies that VCI has provided an assessment of spatial characteristics of drought, as well as its duration and severity and were in good agreement with precipitation patterns.

3.4.2.3. Temperature Condition Index (TCI)

TCI was also suggested by Kogan (1997) [54], [22]. It was developed to reflect vegetation response to temperature i.e. the higher the temperature is the more extreme drought. TCI is based on brightness temperature and represents the deviation of the current month's value from the recorded maximum. TCI is defined as: $TCI_j = \frac{BT_{max} - BT_j}{BT_{max} - BT_{min}} \times 100$ where, BT is the brightness temperature BT_{max} and BT_{min} are maximum and minimum BT values calculated from the long-term record of remote sensing images for a particular period j .

TCI has been used for drought monitoring in the USA, China, Zimbabwe and the Former Soviet Union. A study in Argentina for drought detection revealed that the index is useful to assess the spatial characteristics, duration and severity of droughts, and were in good agreement with precipitation patterns[56].

3.4.3. Water Requirement Satisfaction Index (WRSI)

WRSI is a geospatial model that was developed by the Food and Agricultural Organization (FAO) for use with satellite data to monitor water supply and demand for rainfed crop throughout the growing season[59]. It is also a crop performance index based on the availability of water in the soil.

For example in Ethiopia, crop yields are to a large extent predicted by the amount of available water compared to water requirement. Taking this into account a new software environment for drought indexing, namely Livelihood Early Assessment and Protection (LEAP) was designed specifically for the Ethiopian context commissioned by the World Food Program (WFP) in 2006[60]. One of the goals of LEAP is to serve as a platform for calculation of weather based indices starting out with the calculation of a crop water balance indicator, WRSI. In addition, it uses relevant soil information from DAO digital soil map and topographical parameters derived from the GTOPO30 digital elevation model (DEM)[61].

The performance of the crop during the growing season is one of the indicators of agricultural drought. Currently, crop moisture stress on grain crop can be monitored using satellite based crop performance index, WRSI[62]. This index indicates the extent to which the water requirement of the crop has been satisfied in the growing season[60]. WRSI can be related to crop production using a linear yield reduction function to a crop and the reduction of crop yield due to water deficit is simulated from it. WRSI is currently operational as monitoring and forecasting tool for region wide food security analyses in drought prone countries in Sub-Saharan Africa. Furthermore, Senay and Verdin[63] evaluated the performance of the model using district level crop yield data from Ethiopia. Historical yield data from 1996-1999 were used to evaluate the performance of a seasonal WRSI for sorghum. The reported district yield data were significantly correlated ($r=0.77$) to the WRSI values and the model particularly found successful in capturing the response of the crop during a relatively dry year.

3.5. Experiences on monitoring drought conditions in Africa

Important in the efforts to manage impacts of drought and to tackle desertification are effective systems for understanding, monitoring and forecasting drought and land degradation as well as mechanisms for identifying and prioritizing appropriate responses, and evaluating the impact of the interventions.

In terms of monitoring interventions to combat drought, a good practice in establishing Desertification Information System (DIS) for National Action Programme (NAP) implementation is demonstrated by case of Tunisia. Generally however, the progress in setting up of similar systems in other countries of the region has been slow and variable depending on country specificities. This slow progress and indeed lack of DIS is witnessed even among some countries that have adopted their NAPs. Countries attribute this to limitations of human and financial resources.

Tunisia has established a monitoring and evaluation system for steering the NAP. It aims to assess the impact of investments made in fighting desertification and to enable the compilation of management chart for national policy-makers at different levels. In addition, a desertification information pooling system (DIS) has been set up to provide crucial information for national planning, helping ensure sustainable development by helping decision-makers to make appropriate choices. The DIS consists of the desertification issue chart at national level, which shows the quantities and qualities of the various natural resources, the causes of desertification in each region and monitoring indicators pertaining to the resources.

Drought monitoring and early warning systems and programs are being developed and made operational.

Regional Climate Outlook Forums are convened annually by the World Meteorological Organization (WMO) in the Greater Horn of Africa, in South Africa and in West Africa, to elaborate and ensure appropriate dissemination of consensual regional outlooks, bulletins and products about the next rainy season. These outlooks are directed towards the needs of users from agriculture, health, water management and energy, based upon their input and feedback.

Climate for Development in Africa (ClimDev Africa) Programme is being developed under the auspices of Global Climate Observing System (GCOS) in collaboration with ECA. The purpose of the three-phase programme is to guide the effective integration of climate information and services into development planning for Africa and to ensure the mainstreaming of climate considerations in achievement of the Millennium Development Goals. Outcomes of the programme will be achieved under the following main results areas: policy (awareness, accountability and advocacy); climate Risk management; climate services

including National Meteorological and Hydrological Services (NMHSs) and other climate service; and observations, data management, and infrastructure.

To support drought monitoring, WMO and the United Nations Development Programme (UNDP) have provided support in the establishment of IGAD Climate Prediction and Applications Centre (ICPAC) in Nairobi as a specialized institution of the Intergovernmental Authority on Development (IGAD). The participating countries are Burundi, Djibouti, Eritrea, Ethiopia, Kenya, Rwanda, Somalia, Sudan, Uganda and United Republic of Tanzania. Another centre is established in Harare, Zimbabwe. These centres are charged with timely monitoring of drought intensity, geographical extent, duration and impact on agricultural production, and issuing early warnings. The African Centre of Meteorological Applications for Development (ACMAD) is also in place and provides similar services. ICPAC has linked its drought and conflict monitoring activities into the Conflict Early Warning and Response Mechanism (CEWARN) whose drought-monitoring centre reports on drought and forage conditions and makes food projections. This is enhancing ICPAC capacity to monitor pastoral conflicts and provide to member states timely information on specific events and their causes, thus helping countries to prevent escalation of such conflicts.

The World Hydrological Cycle Observing Systems (WHICOS) contributes towards an easily accessible source of hydrological information that provides the basic building blocks for sustainable development through water resources assessment and planning, ecosystem and water quality monitoring, flood forecasting and drought monitoring and prediction. In this regard, WMO is also providing advisory services to the countries in their efforts to reorganize and strengthen the national hydrological services for Volta, Niger and later Senegal Basins.

Few early warning systems have been established at country level. Zambia has an Early Warning System that has assisted the country to intervene and take necessary measures where drought has occurred. However, even though there has been regular collection of rainfall data and regular forecasting there has been little utilization of this information by most of decision makers because the information appears complex.[27]

4. DATA AND METHODOLOGY

In the ITHACA drought Early Warning System (EWS) vegetation monitoring procedures are based on phenological parameters that describe the dynamics of the different types of vegetation over time. The continuous monitoring of these parameters allows to identify the condition of vegetation and the duration of growing season. In order to correctly integrate SPI based precipitation monitoring procedures in the ITHACA system, a preliminary investigation of existing relationships between the vegetation and precipitation dynamics was necessary. For this aim, in this study, the statistical correlation between time-series of vegetation phenological parameters and fortnightly cumulated precipitation using different cumulating periods (namely, 1, 3, 6 and 9 months) has been analysed. The description of the methodologies and base data adopted in order to carry out this goal are the object of this chapter.

For the purposes of this study, after a preliminary analysis of vegetation dynamics, the behavior of the precipitation cumulated in different periods of time has been studied and rainy seasons that have a considerable impacts on the development of the vegetation have been identified. The selected periods of time were defined taking into consideration the outcomes of previous research studies [38]. In particular, for this study, the periods corresponding to 1, 3, 6 and 9 months were selected. Furthermore, for each of these periods, a SPI dataset has been calculated using the whole available precipitation time-series (1998-2013) in order to identify historical meteorological drought events and to define effective near real-time precipitation monitoring procedures to be used in the current ITHACA drought EWS.

4.1. Vegetation Monitoring and ITHACA drought Early Warning System (EWS)

ITHACA developed a system for the early detection and monitoring of vegetation stress and agricultural drought events on a global scale. The system mainly relies on satellite derived data.

The system is based on the near real-time monitoring of a selection metric derived from vegetation index time-series that allows the early detection of vegetation stress conditions and the assessment of vegetation productivity and its projection at the end of the observed growing season [64].

The final aim of the system is the timely detection of critical conditions in vegetation health and productivity, during a vegetative growing season and at its end. By consequence the system can pinpoint agricultural areas with increased crop or pasture failure thus enabling end-users to better plan the interventions. Moreover, a simplified vulnerability model, applied to the hazard data, yields the food security conditions for the affected areas. The model includes agricultural indicators and socio-economic factors linked to people's strategy to supply the food they need.

Currently, the development of a webGIS service suitable for the visualization and distribution of final monitoring products (near real-time and historical maps) is ongoing.

4.1.1. Data input and Methodology

The maps about vegetation conditions, produced fortnightly by the system, derive from the near real-time analysis of parameters related to vegetation phenology. Vegetation phenology concerns the study of periodic vegetative events, such as the annual cycles of green-up, or growth, and senescence. In particular, developed Vegetation monitoring procedures are based on extracting and elaborating, for each considered vegetation growing season (see Figure 6), a set of phenological parameters from the yearly Normalized Difference Vegetation Index (NDVI) function (the regular curve depicted in Figure 6) that best fits the original yearly NDVI time-series (the irregular curve depicted in Figure 6) using, as a base data MODIS datasets. This data is provided every 16 days projected on a 0.05 degree (5600-meter) geographic Climate Modelling Grid (CMG). Considering the availability of the input vegetation data the Drought EWS is updated every fortnight during the solar year.

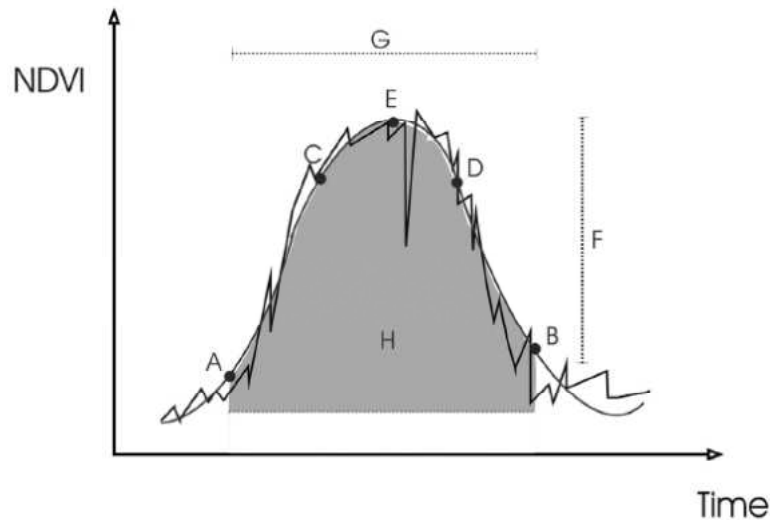


Figure 6. Diagram of NDVI/time and derived phenological parameters (A-H) for a vegetation growing season.

Starting from the yearly NDVI function (see Figure 6), the following phenological parameters can be extracted and used in order to describe the current vegetation growing season:

1. the time for the start of the season (SoS) [A]: time for which the left edge of the NDVI fitted function has increased to a user defined level measured from the left minimum level;
2. the time for the end of the season (EoS) [B]: time for which the right edge has decreased to a user defined level measured from the right minimum level;
3. the length of the season (Len)[G]: time from the start to the end of the season;
4. the base level (Base): given as the average of the left and right minimum values;
5. the time for the mid of the season (MID): computed as the mean value of the time for which, respectively, the left edge has increased to the 80 % level [C] and the right edge has decreased to the 80 % level [D].
6. the largest data value (Larg)[E] for the fitted NDVI function during the season;
7. the seasonal amplitude (Amp)[F]: difference between the maximal value and the base level;
8. the rate of increase at the beginning of the season (Incr): calculated as the ratio between the values evaluated at the season start and at the left 80% level [C] divided by the corresponding time difference;
9. the rate of decrease at the end of the season (Decr): calculated as the ratio between the values evaluated at the season end and at the right 80% level [D] divided by the corresponding time difference;
10. the small seasonal integral (Smi)[H]: integral of the difference between the function describing the season and the base level from season start to season end. This is the integral over the growing season giving the area between the fitted function and the average of the left and right minimum values.

Monitoring procedures proposed in the ITHACA drought EWS are currently based on the Start of The Season (SoS) and the Small Seasonal Integral (Smi). For the purposes of this study, instead all the presented parameters have been taken into consideration and calculated for the whole Africa for all the seasons contained in the years 2000-2013. The same calculation can be performed globally.

The basic idea behind the system developed by ITHACA is that phenological parameters for a given growing season, are related to the seasonal vegetation productivity. The parameters take into account both agricultural production and available biomass in pastoral areas. Therefore, comparing phenological values with the average values and the minimum and maximum ones computed using the whole time-series (2000 to present) of NDVI data, helps to better explain and understand the performances of the considered vegetative season (in case of historical analyses). In case of near real-time monitoring, the analysis provides an estimation of a season expected productivity.

The simple Deviation (D) and Percent Deviation (PD) from the average value are the proposed metrics to quantify the deviation of the examined vegetation season conditions from the historical normal behavior:

$$D = x - \mu_x \quad [1]$$

$$PD = (x - \mu_x) / \mu_x \cdot 100 \quad [2]$$

where μ_x is the historical average value of the considered phenological parameter, estimated using the whole available time-series.

Mapping the distribution of the deviation indexes [1] and [2] allows to identify areas of reduced vegetation productivity. This base information, evaluated continuously on a fortnightly basis and completed by ancillary data, such as the distribution of cultivated areas and the type of prevailing cultivation, helps to early detect critical conditions in agricultural productivity for a specific vegetative season in order to predict future crop failures and food crises.

Two outputs are produced in the framework of the ITHACA vegetation monitoring system, (i) monitoring products generated on a fortnightly basis in near real-time showing the distribution of deviation indexes for the Start of the Season and the Seasonal Small Integral parameters for the current growing season, (ii) historical maps showing the distribution of the same deviation indexes for all the identified vegetation growing seasons from 2000 to present (2 seasons/year, that is 2 maps/year).

The *Seasonal Small Integral PD imagery* describes vegetation condition for the main and secondary growing seasons for the years 2000 to present (two images per year) using the Sml parameter extracted from MODIS NDVI time-series. Figure 7 shows, for instance, the distribution of the PDs (see equation [2]) for the selected phenological parameter, estimated on a pixel basis (0.05 degrees). In addition, in order to provide a more effective display of the most affected areas, raw results are also aggregated at the second level administrative boundary (Figure 8), according to a higher frequency distribution rule. As an example, in the maps reported in in Figure 7 and in Figure 8, areas where the Seasonal Small Integral parameter for the examined vegetation season has a negative deviation from the average value are shown using light orange to red colors.

It should be noted that the considered growing seasons, for the different areas of the world, refer to different months in the year, according to the specific agro-climatic zoning. For areas with two different seasons in their vegetation/crop calendar, mapped Small Integral PDs for main and secondary seasons refer respectively to the first and second season encountered from the start of the considered year; for the areas where a unique growing season is detected, only the first season is mapped (i.e. in the second season image these areas are indicated as areas where no growing season has been detected during the analyses). Besides, in the output imagery, barren areas, urban and built-up areas, evergreen/deciduous needle leaf/broadleaf forest areas, swamp vegetation, water bodies, and, in general, areas where no growing season has been detected during the analyses, are excluded from the analyses and given a specific fill value.

Moreover, raw imagery (0.05 degrees) showing the distribution of the original Seasonal Small Integer parameter (*Raw Seasonal Small Integral imagery*) for examined areas for the main and secondary growing seasons (for 2000 to present; 2 images per year) are also produced in order to allow direct vegetation productivity comparisons between two or more growing seasons specifically selected by end-users.

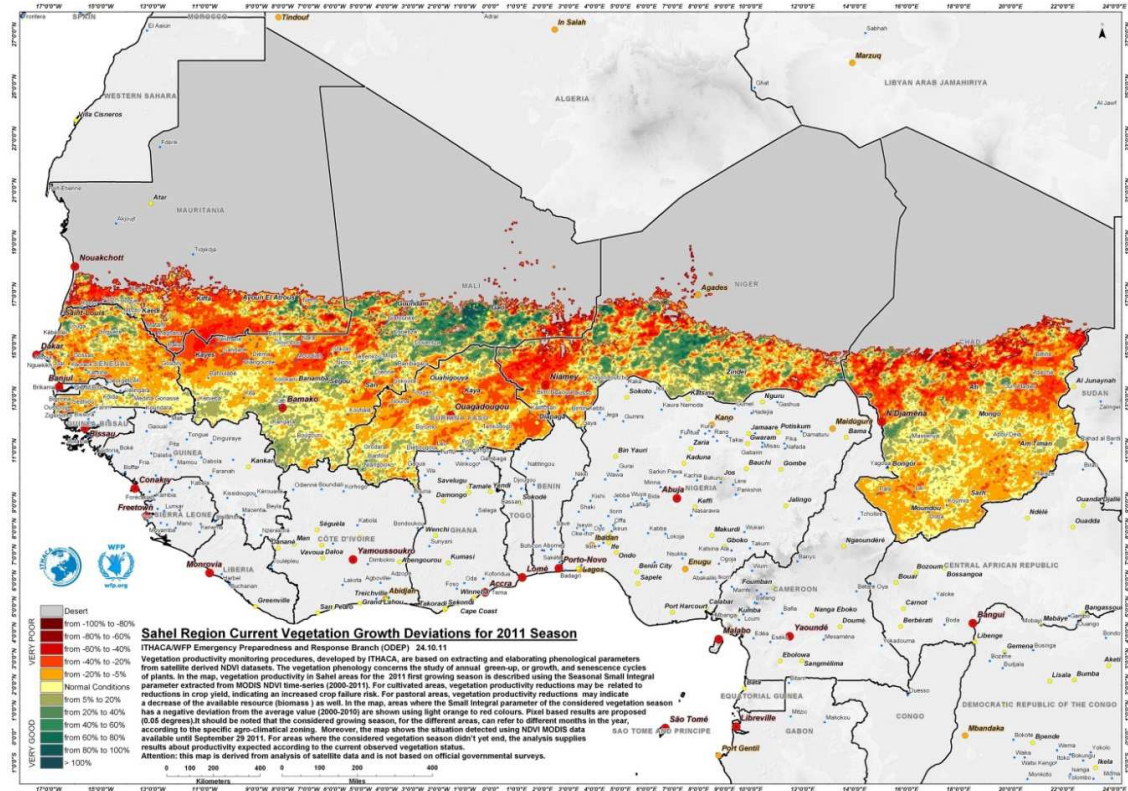


Figure 7. Pixel based output of the Percent Deviations (PDs) of the phenological parameter Season Small Integral for the 2011 growing season for the Sahel area.

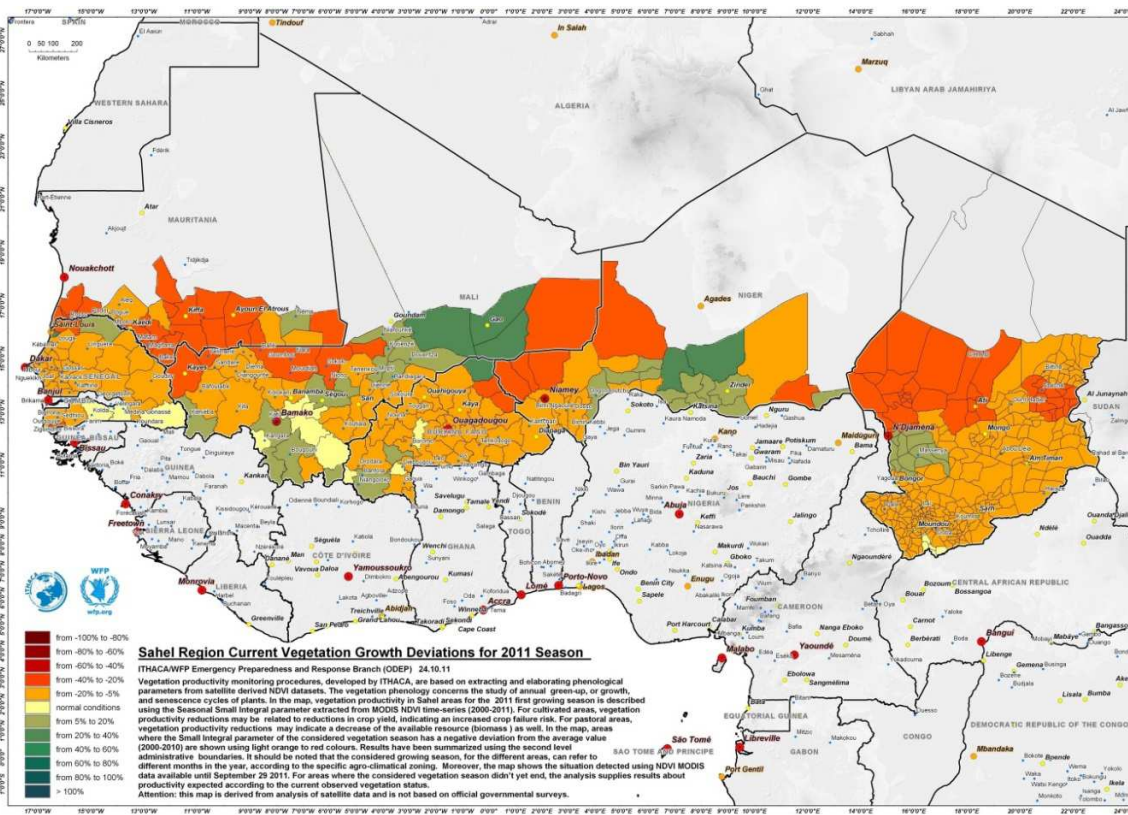


Figure 8. Aggregated on the second level administrative boundary output of the Percent Deviations (PDs) of the phenological parameter Seasonal Small Integral for the 2011 growing season for the Sahel area.

4.1.2. Derived Products

Value-added products/information that can be derived from the above mentioned base datasets are the following:

- direct vegetation productivity comparisons, based on raw *Seasonal Small Integral imagery*, between two or more growing seasons specifically selected. Besides, the Condition Index (CI), which provides a measure of the proximity of the considered value, or an examined year, of the selected parameter to the minimum (CI=0) and maximum (CI=1) ones, can be estimated using raw *Seasonal Small integral imagery*. The CI is expressed as:

$$CI = \frac{x - \min_x}{\max_x - \min_x} * 100 \quad [3]$$

where

x is the value of the phenological parameter for the examined growing season; \min_x and \max_x are the minimum and maximum values of the parameter considered, extracted from the whole available historical time-series (2000 to present).

- drought historical products, that is the investigation of the historical occurrence of vegetation stress events in a region through the aggregation of the Seasonal Small Integral Percent Deviation values for selected years. This analysis allows the identification of the areas showing the greatest number of negative vegetation productivity deviations in subsequent growing seasons. For instance, areas most affected by poor vegetation growth in the selected time interval could be considered more vulnerable in case of future drought events (Figure 10). This dataset allows drought hazard identification, which is a required step in drought risk assessment and identification. Refinement though is possible by coupling historical vegetation productivity information with ancillary data, such as the distribution of cultivated areas and the type of prevailing cultivation, or the livelihood zones distribution.

4.1.3. Drought vulnerability

Vulnerability is considered as the entirety of factors that exacerbate or mitigate the possible effects of hazard hitting a populated area. Measuring the effects of a disaster implies firstly the identification and definition of what those effects are. As Peduzzi et al. [65] stated in 2009, casualties normally. Previous studies ([66], [65]) had pointed out that the estimation of affected people is highly complex and inaccurate to some extent compared to that of other natural disasters. In fact, drought-related mortality is caused by impacts on livelihoods, which contributes to reduce food intake, exacerbate migration, and creation of water and sanitation problems, leading to deterioration of health conditions, augmenting diseases, and eventually death [67]. However official national statistics of drought affected population are often unavailable or based on different assumptions, which causes data to be barely comparable.

The food security condition of any households or individuals, here considered as the ultimate drought effect, is the outcome of the interaction of a broad range of agro-environmental, socio-economic and biological factors [68]. The concept of food security, as it is widely accepted, rests on three pillars: availability, access, and utilization of food. In the frame of this study only the availability of and the access to food were taken into consideration, the first analyzed with indicators for crop production anomalies and the second modeled considering physical accessibility to markets.

Two different raster layers (i.e. an agricultural vulnerability layer and a risk surface one) serve as basis of the vulnerability model which is applied to the drought hazard layer resulting from the vegetation monitoring. Details of agricultural vulnerability, risk surface and final alerts are provided in the following paragraphs.

4.1.3.1. Agricultural vulnerability

The Agricultural Vulnerability layer is built by considering three indicators: (i) the soil suitability for crop production (FAO Global Agro-Ecological Zones database), (ii) the percentage of irrigated area (FAO Global Map of Irrigation Areas dataset) and (iii) the Crops Diversity Index (modified after Julich, 2006; based on FAO CountrySTAT administrative level 1 production database). The above mentioned indicators are combined in order to take into account, respectively: (i) the agricultural potential of soils themselves; (ii) the presence of irrigation facilities which is subjected to augment the agricultural potential; (iii) the diversification of cultivated crops, which is supposed to play an important role in the degree of vulnerability of a cropland area.

4.1.3.2. Risk surfaces

Specific risk units, shaped on the basis of people's strategy to sell and buy staple foods, were defined. In this way the hazard that hits a particular area is subdivided into homogeneous units in which the potential impacts could occur. The risk surfaces here presented (see Figure 11left) were created by considering an accessibility term and a gravity model integrated with market flows. The first accounts for both physical distance and travel times to identified food source locations (i.e. markets). The second models the people attraction exerted by the different market categories and their interconnections.

- **Accessibility:** it refers to the distance to a location of interest and the ease with which this location can be reached [70]. In this work it assumes a value inferring the probability, for people living in a determined area, to be able to displace for selling and buying commodities at a specific location. A considered country is subdivided into market catchment areas calculated on the basis of the easiness to access important markets, identified through a market survey. The accessibility is intended as a "friction surface" that takes into account distance and travel times to markets, considered equally important at this stage. Travel times are calculated as suggested by Pozzi & Robinson, 2008 [71].
- **Gravity model:** market areas own an economic sense that does not correspond to other more commonly used territorial or administrative divisions. The theories of delineation of trade areas, though not conceived for the purpose of market analysis in developing countries, are considered promising in the context of this work.

According to literature, the attractiveness of market center is essentially measured using two variables: center population (i.e. the mass term), which exerts a positive attraction over consumers, and distance (i.e. the friction term), which discourage consumers from moving [72], [73]. Huff (1962) improved the spatial-interaction model by introducing a probabilistic approach for the definition of trade areas; i.e. each trade center has a certain probability of being patronized. To determine the probability of a consumer in i visiting a particular store in j (P_{ij}), Huff postulates that this probability equals the ratio of the utility of the considered store (U_{ij}) to the sum of utilities of all the stores in the analyzed area (U_{ik}):

$$P_{ij} = \left(\frac{U_{ij}}{\sum_{i=1}^k U_{ik}} \right) = \left(\frac{S_j \cdot D_{ij}}{\sum_{i=1}^k S_k \cdot D_{ik}} \right) \quad (1)$$

where P_{ij} = probability of consumer at i visiting store j ; k = is the set of competing stores in the region; U_{ij} = utility of store j for individual at i ; S_j = size of outlet j ; D_{ij} = Euclidean distance between consumer at i and store j .

In order to adapt Huff's law to the present study several adjustments were made:

- the size of the store (S) was substituted with an importance factor related to the type of market (wholesale, assembly and retail);
- the Euclidean distance (D) was replaced by the distance calculated with the accessibility model in order to take into account physical hindrances and therefore rather realistic travel times.

The modified Huff gravity model has been implemented in a GIS environment to obtain a raster containing: (i) the maximum probability value for each pixel and (ii) an identifier of the specific market to which this maximum value belongs.

The gravity model output was then integrated with data related to known flows of staple food from a market to another. In fact it has been proven that, especially in developing countries, traditional production surplus areas supply those areas that cannot satisfy their population food needs with local production, this occurring even during average production years. The market flow analysis (available only for few countries) is used in the present study in order to distribute the alerts that relapse on traditionally food surplus areas over the areas that are normally supplied by the latter. In the same way, when food deficit areas are alerted, the surplus areas where the food comes from are screened and if none or minimal alert is found, then the deficit area alerts are diminished.

4.1.3.3. Final alerts

The output of the drought EWS, hereafter called final alert, (see Figure 11right), furnishes a value linked to the food security conditions of a determined area.

For the near real-time production of the final alerts, the hazard layer produced during the fortnightly monitoring activities is firstly superimposed and weighted with the Agricultural Vulnerability layer. The hazard raster is clipped with the crop areas in order to consider only the alerts that are meaningful because impacting a valuable land; then each retained hazard pixel is multiplied by the Agricultural Vulnerability value. The resulting map is expressed in the same units as the hazard. The ratio of the number of alerted pixels to the total number of crop pixels is then calculated per each risk surface unit; where this ratio

surpasses a threshold value of 20% the corresponding risk surface unit is alerted. The alert value that is associated with each risk surface unit is the mean value of the alerted pixel multiplied by the previously calculated ratio, giving an account for the relevance of the considered anomalies on the basis of the portion of the impacted cropland.

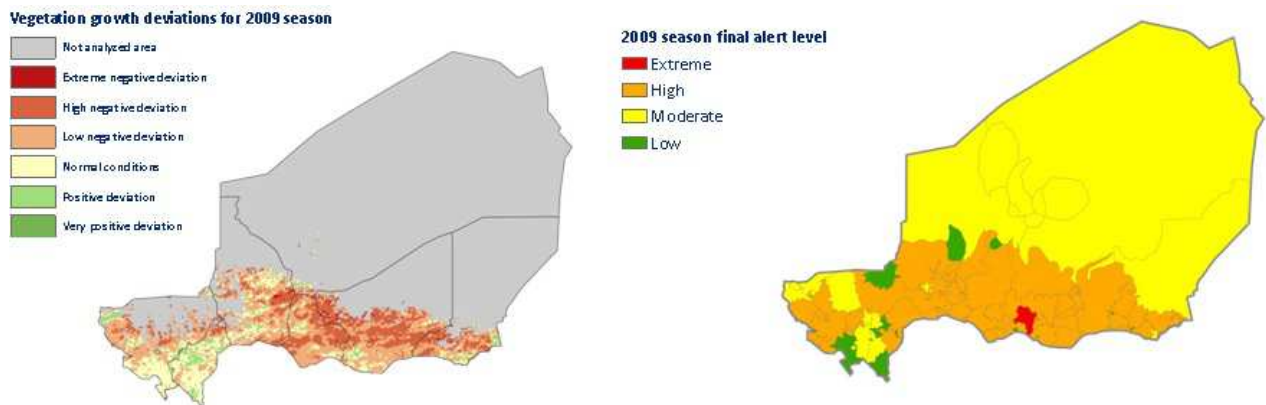


Figure 11. On the left: agricultural vulnerability and risk surfaces calculated for Niger, on the right: final alert calculated for 2009 season in Niger and distributed over the risk surfaces.

4.2. Precipitation monitoring for drought Early Warning purposes

In the hydrologic cycle, precipitation is fundamental linking the atmosphere with land surface processes. In addition, this variable has the most important role in the terrestrial climate system. Precise measurements of precipitation on a variety of space and time scales are important not only to weather forecasters and climate scientists, but also to a wide range of decision makers, including hydrologists, agriculturalists, and industrialists[75]. Extreme values of precipitation can cause impact to life and environment generating floods and droughts.[76].

Therefore, in order to improve the effectiveness of the ITHACA Drought EWS, the inclusion of proper precipitation monitoring procedures has been planned. Taking into account the nature of this system, which provide a global coverage drought monitoring, the Tropical Rainfall Measuring Mission (TRMM) rainfall estimation dataset was selected. TRMM data is generated from remotely sensed sources in almost real-time and it is free-of-charge.

4.2.1. Data

The Tropical Rainfall Measuring Mission (TRMM) is a joint USA-Japan satellite mission to monitor tropical and subtropical precipitation[77]. The mission includes 5 instruments, but just 2 are normally used for precipitation measurement purpose: TRMM Microwave Imager (TMI) and Precipitation Radar (PR)[78]. The TRMM Multi-satellite Precipitation Analysis (TMPA) provides a calibration-based sequential scheme for combining precipitation estimates from multiple satellites, as well as gauge analyses, where feasible, at fine scales ($0.25^\circ \times 0.25^\circ$ and 3 hourly). TMPA is available in two formats; based on calibration by *the TRMM combined instrument* that is available with two months of delay and *TRMM microwave imager precipitation products* that is available in almost real time. Both datasets cover the latitude band 50° N-S for the period from 1998 to present[79]. TMPA 3B43 monthly precipitation averages and TMPA 3B42 daily and sub-daily(3h) averages are probably the most relevant TRMM-related products for climate research[78].

Considering the different types of drought impacts, as already discussed in chapter 2 (See Figure 4), it is necessary to study the rainfall and its scarcity considering different observation time intervals, in order to identify a possible drought event and completely describe its behavior. Particularly, in the case of an agricultural drought event is appropriate to choice monthly, three-monthly, six-monthly and nine-monthly cumulative. In the Figure 12, there is an example of different cumulative rainfall maps obtained for a selected date and considering different accumulation time intervals preceding this date.

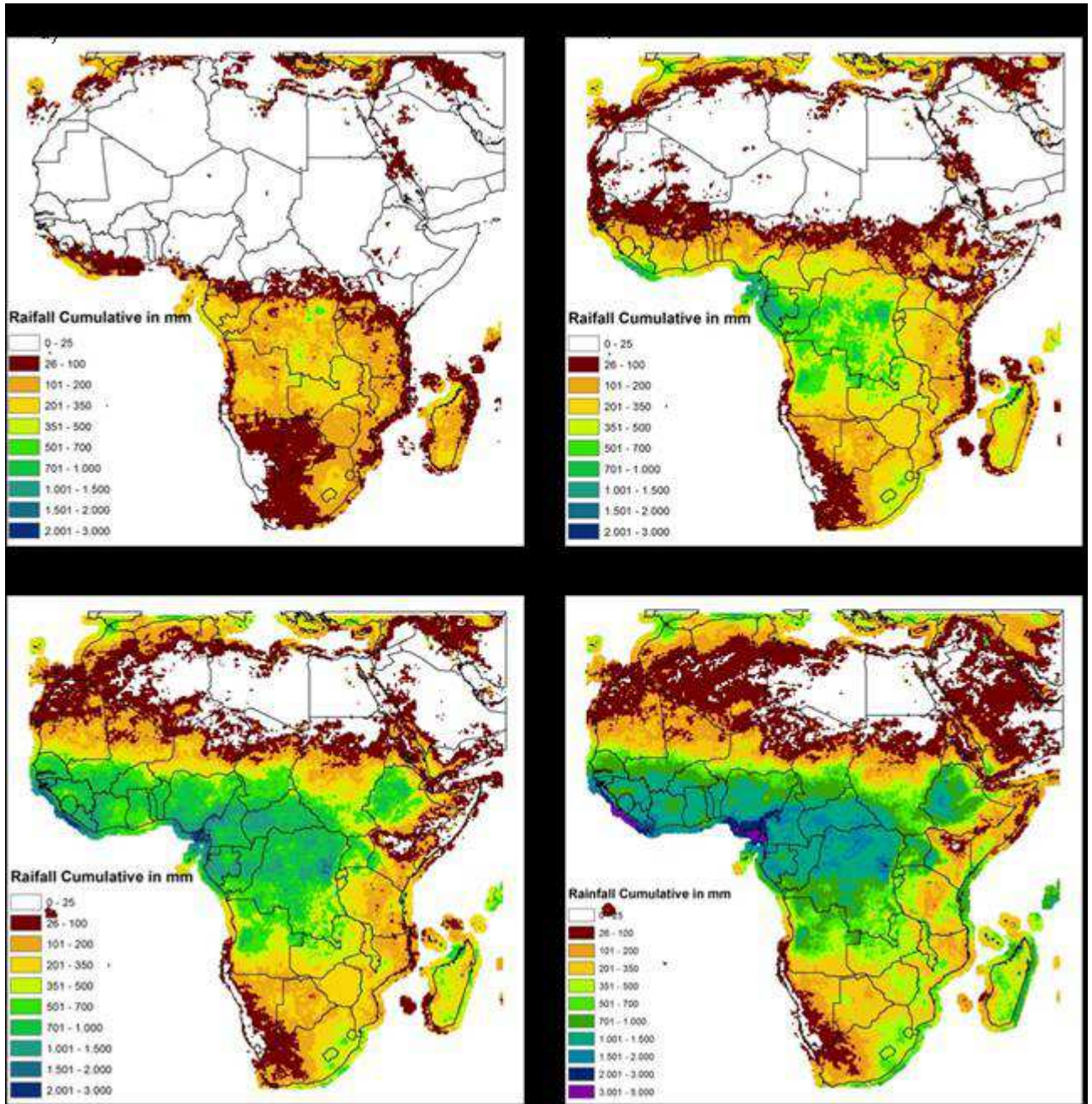


Figure 12. TRMM Cumulative Rainfall 16 January 2011. a) 1Month, b) 3Months, c)6Months, d)9Months

4.2.2. Standardized Precipitation Index

For the purposes of the ITHACA drought EWS, the monitoring of rainfall conditions using the Standardized Precipitation Index (SPI) has been proposed, and required a procedures for its calculation starting from TRMM data have been implemented..

The SPI provides a measure of the rarity of observed rainfall for a given location and accumulation period from usual conditions.

Usually, a drought event is defined as a period in which the SPI is continuously negative and where the SPI reaches a value of -1.0 or less. SPI values are usually classified in ranges with values between -1.0 and 1.0 defined as near-normal conditions. Values between -1.0 and -1.50 are moderately dry, values from -1.50 to -2.0 are severely dry, and any value less than -2 is extremely dry. At the other end, values between 1.0 and 1.50 are moderately wet, 1.50 to 2.0 values are very wet, and values greater than 2 are extremely wet conditions.

In this study the SPI for different cumulative periods of rainfall was calculated, as discussed in 4.2.1. A python script has been developed in order to calculate on a pixel basis the SPI fitting a gamma probability density function to a given frequency distribution of precipitation totals.

In the drought monitoring frame, the SPI is commonly used in order to identify drought events with large impacts on human lives and the environment. As an example, using the implemented procedures for SPI calculation, the severe drought event located between southern Somalia, southern ETHIOPIA, eastern Kenya and north-eastern Tanzania has been identified. This area was located considering the failure of the 2 subsequent rainy seasons (October-December 2010 and March-May 2011) (see Figure 13, Figure 14, and Figure 15), which was revealed in severe anomalies in SPI values, implying a significant drought impact on vegetation, including crops[80].

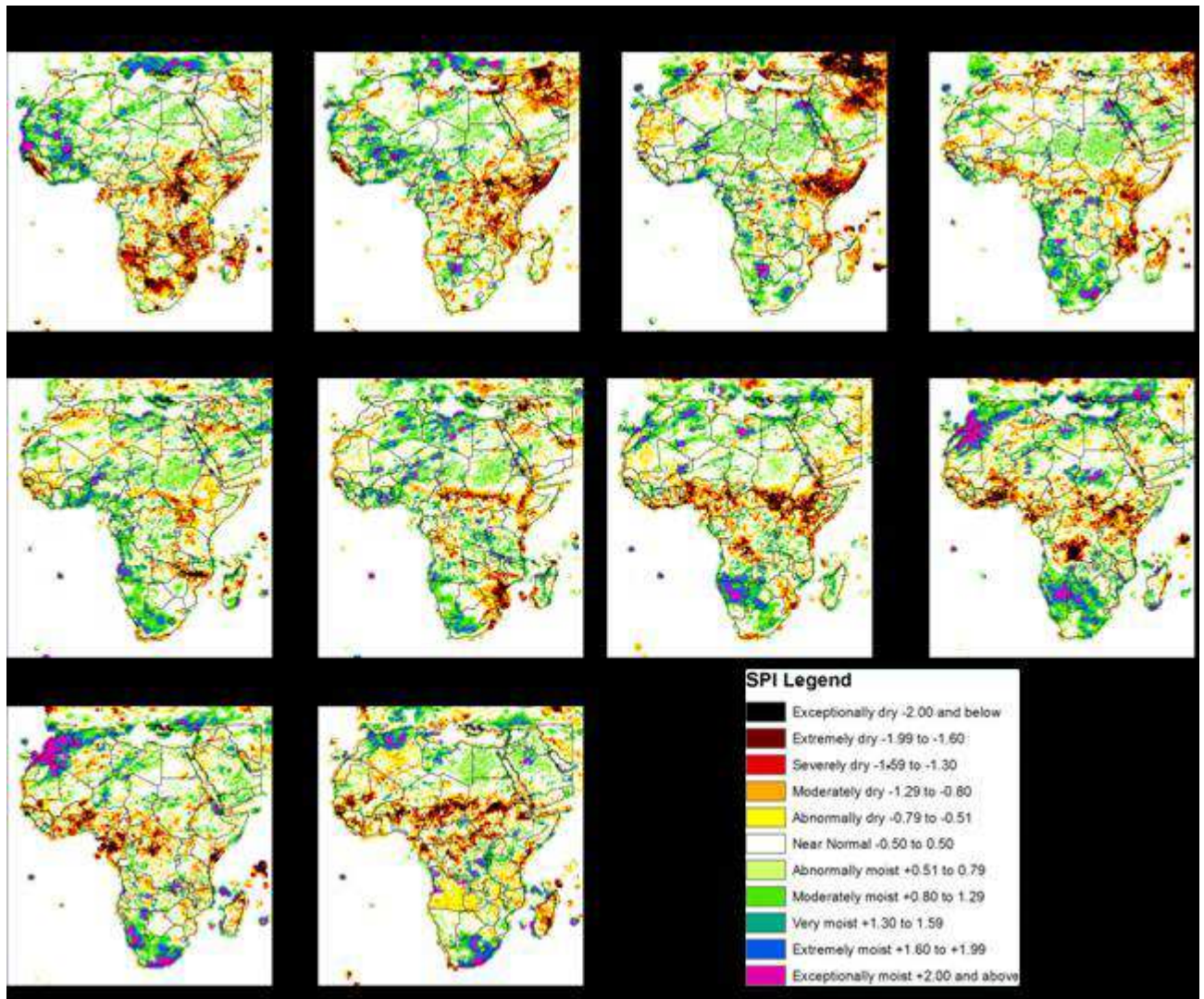


Figure 13. Evolution of the SPI for 1-month TRMM rainfall accumulations (SPI01)

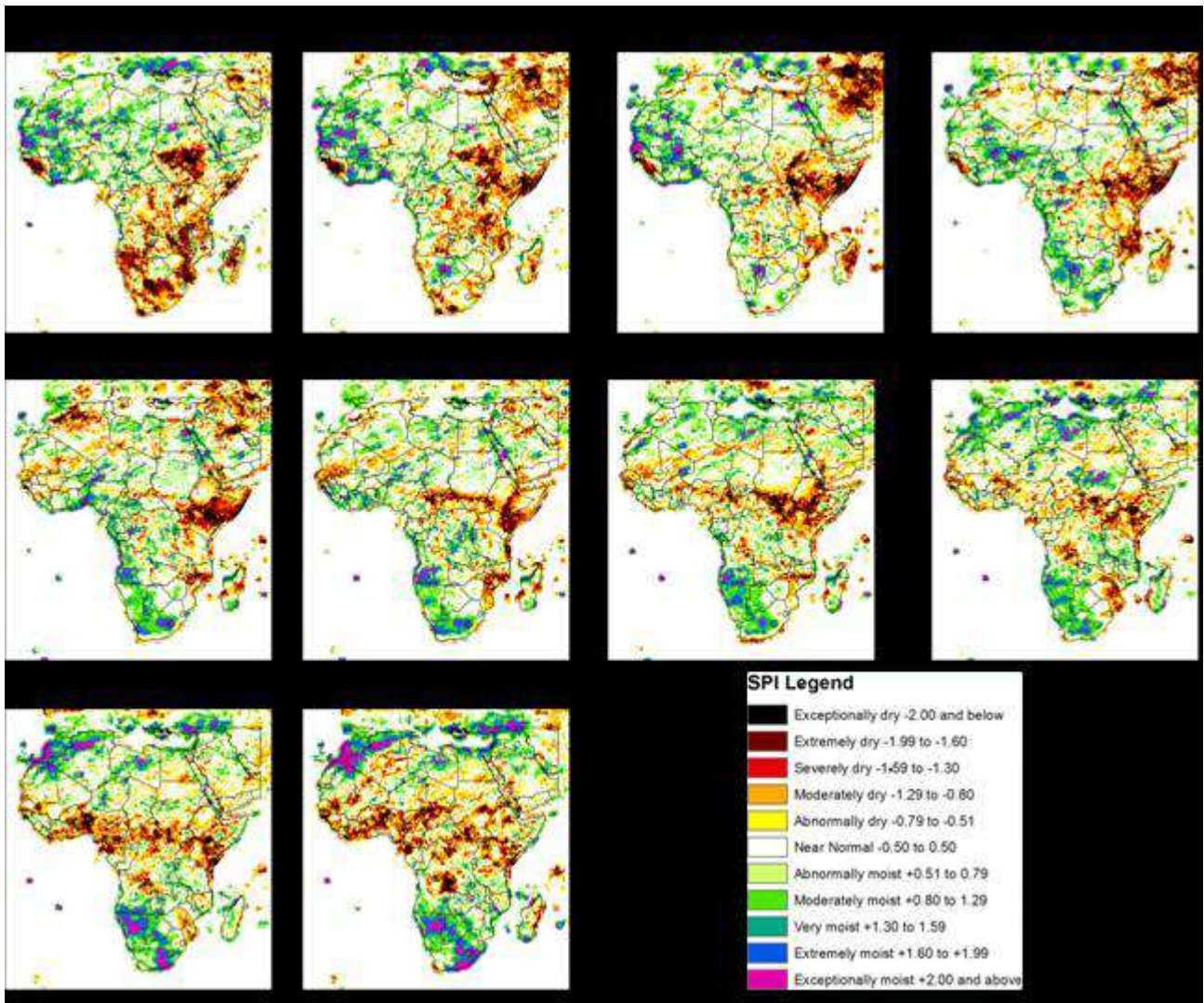


Figure 14. Evolution of the SPI for 3-months TRMM rainfall accumulations (SPI03).

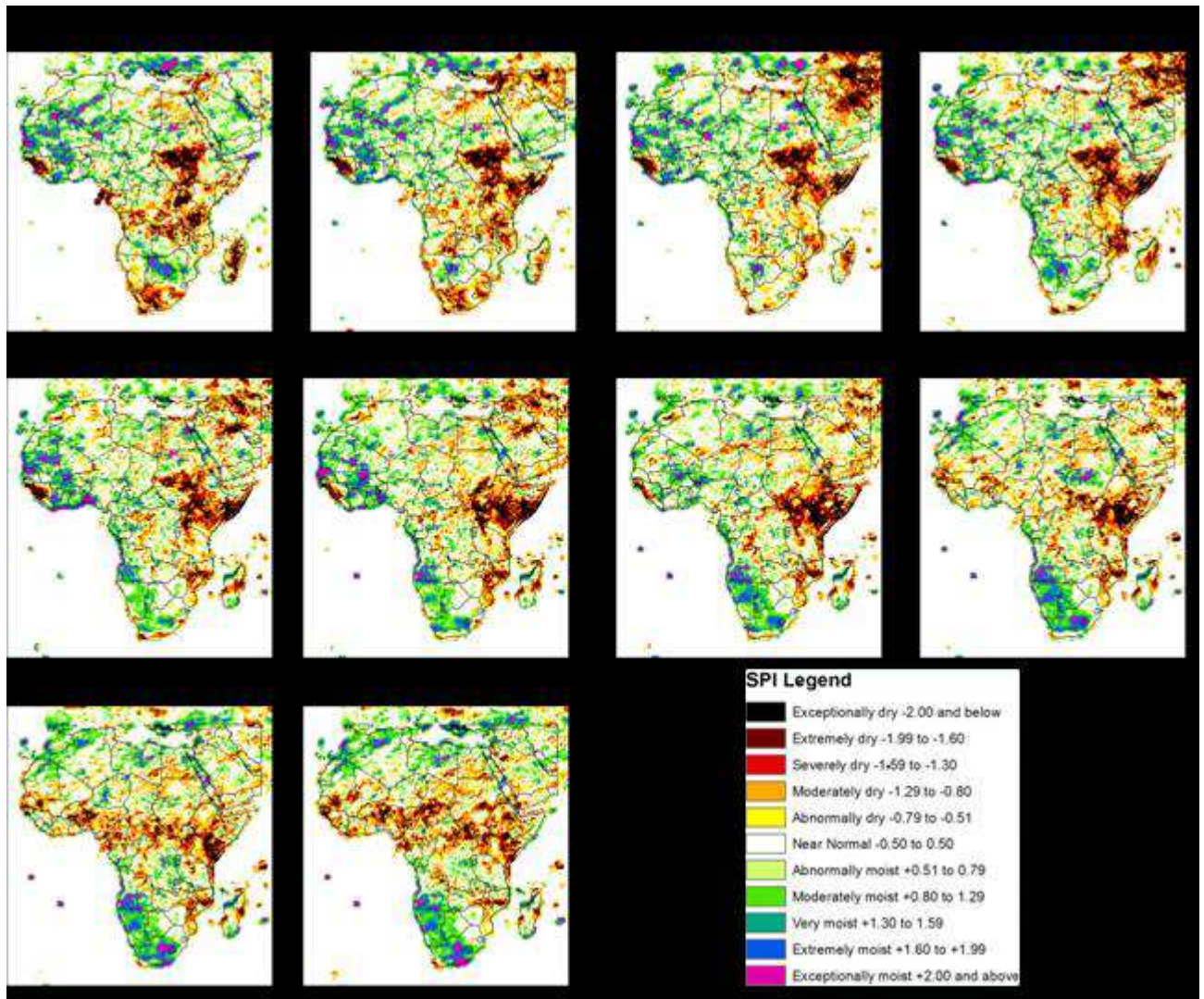


Figure 15. Evolution of the SPI for 6-months TRMM rainfall accumulations (SPI06)

4.3. Climate and rainfall analysis

In this chapter the methodology adopted in order to carry out the study of climatology and land cover distribution for the African continent is described. The aim of this study was to preliminarily identify possible areas where the correlation between rainfall and vegetation is affected by the climate.

4.3.1. Additional data used

To describe the Africa climate and land cover, two database with the same resolution and spatial coverage were used.

4.3.1.1. Climate Classification

Climate is a complex, abstract concept involving data on all aspects of Earth's environment. The climate of an area is the combination of the environmental conditions that have prevailed there over a long period of time. This synthesis involves both averages of the climatic elements and measurements of variability.

Climate classification is the formalization of systems that recognize, clarify and simplify climatic similarities and differences between geographic areas in order to enhance the scientific understanding of climates. Such classification schemes rely on efforts that sort and group vast amounts of environmental data to uncover patterns between interacting climatic processes.

With the aim to analyze the climate conditions impacts in the correlation between the vegetation and rainfall in the area of study, it was decided to study the Köppen-Geiger Climate Classification map. This is the most frequently used climate classification system, it was presented in the first time by Wladimir Köppen in 1900 and was updated by Rudolf Geiger in 1961. Recently, a new version world map of Köppen-Geiger classification was published by Kottek et al. (2006) [81]. Furthermore, an updated of this product that shows the shift of climate zones in the past, present and future were presented[82].

To generate the latest version of the classification maps and the shift of climate zones in the past, two global datasets of climate observations were selected. Both are available on a regular 0.5 degree latitude/longitude grid with monthly temporal resolution. The first dataset is provided by the Climatic Research Unit (CRU) of the University of East Anglia[83] and delivers grids of monthly climate observations from meteorological stations comprising nine climate variables from which only temperature is used in this study. This dataset, referred to as CRU TS 2.1, covers the global land areas excluding Antarctica. The second dataset, provided by the Global Precipitation Climatology Centre (GPCC) located at the German Weather

Service, is the so called GPCP's Full Data Reanalysis Version 4 for 1901-2007[84]. This recently updated gridded precipitation dataset covers the global land areas excluding Greenland and Antarctica.

The classification mainly consist of 3 letters that are related with precipitation or temperature. The first letter represented the main climate. The second one refers to a subsequent precipitation conditions (see Table 4). There is a particular case, the polar climate (E) without precipitation differentiations. The key to calculate this letters implies that the polar climates (E) have to be determined first, followed by the arid climates (B) and subsequent differentiations into the equatorial climates (A) and the warm temperature and snow climates (C) and (D), respectively. [81]

The annual mean near-surface (2m) temperature is denoted by T_{ann} and the monthly mean temperatures of the warmest and coldest months by T_{max} and T_{min} respectively. P_{ann} is the accumulated annual precipitation and P_{min} is the precipitation of the driest month. Additionally P_{smin} , P_{smax} , P_{wmin} and P_{wmax} are defined as the lowest and highest monthly precipitation values for the summer and winter half-years on the hemisphere considered. [81]

In addition to these temperature and precipitation values a dryness threshold P_{th} in mm is introduced for the arid climates (B), which depends on the absolute measure of the annual mean temperature in °C [T_{ann}], and on the annual cycle of precipitation[81]:

$$P_{th} = \begin{cases} 2\{T_{ann}\} & \text{if at least } \frac{2}{3} \text{ of the annual precipitation occurs in winter,} \\ 2\{T_{ann}\} + 28 & \text{if at least } \frac{2}{3} \text{ of the annual precipitation occurs in summer,} \\ 2\{T_{ann}\} + 14 & \text{otherwise.} \end{cases}$$

Type	Description	Criteria
A	Equatorial climates	$T_{\min} \geq +18^{\circ}\text{C}$
Af	Equatorial rainforest, fully humid	$P_{\min} \geq 60 \text{ mm}$
Am	Equatorial monsoon	$P_{\text{ann}} \geq 25(100 - P_{\min})$
As	Equatorial savannah with dry summer	$P_{\min} < 60 \text{ mm in summer}$
Aw	Equatorial savannah with dry winter	$P_{\min} < 60 \text{ mm in winter}$
B	Arid climates	$P_{\text{ann}} < 10 P_{\text{th}}$
BS	Steppe climate	$P_{\text{ann}} > 5 P_{\text{th}}$
BW	Desert climate	$P_{\text{ann}} \leq 5 P_{\text{th}}$
C	Warm temperature climates	$-3^{\circ}\text{C} < T_{\min} < +18^{\circ}\text{C}$
Cs	Warm Temperature climate with dry summer	$P_{\text{smin}} < P_{\text{wmin}}, P_{\text{wmax}} > 3P_{\text{smin}}$ and $P_{\text{smin}} < 40 \text{ mm}$
Cw	Warm Temperature climate with dry winter	$P_{\text{wmin}} < P_{\text{smin}}$ and $P_{\text{smax}} > 10 P_{\text{wmin}}$
Cf	Warm Temperature climate, fully humid	neither Cs nor Cw
D	Snow climates	$T_{\min} \leq -3^{\circ}\text{C}$
Ds	Snow climate with dry summer	$P_{\text{smin}} < P_{\text{wmin}}, P_{\text{wmax}} > 3P_{\text{smin}}$ and $P_{\text{smin}} < 40 \text{ mm}$
Dw	Snow climate with dry winter	$P_{\text{wmin}} < P_{\text{smin}}$ and $P_{\text{smax}} > 10 P_{\text{wmin}}$
Df	Snow climate, fully humid	neither Ds nor Dw
E	Polar climates	$T_{\text{max}} < +10^{\circ}\text{C}$
ET	Tundra climate	$0^{\circ}\text{C} \leq T_{\text{max}} < +10^{\circ}\text{C}$
EF	Frost climate	$T_{\text{max}} < 0^{\circ}\text{C}$

Table 4. Key to calculate the climate formula of Köppen and Geiger for the main climates and subsequent precipitation conditions, the first two letters of the classification[81]

The scheme how to determine the additional temperature conditions (third letter) for the arid climates (B) as well as for the warm temperature (C) and snow climates (D), is given in the Table 5[81].

Type	Description	Criterion
h	Hot steppe/desert	$T_{\text{ann}} \geq +18^{\circ}\text{C}$
k	Cold steppe/desert	$T_{\text{ann}} < +18^{\circ}\text{C}$
a	Hot summer	$T_{\text{max}} \geq +22^{\circ}\text{C}$
b	Warm summer	not (a) and at least 4 $T_{\min} \geq +10^{\circ}\text{C}$
c	Cool summer and cold winter	not (b) $T_{\min} > -38^{\circ}\text{C}$

d extremely continental like (c) but $T_{\min} \leq -38^{\circ}\text{C}$

Table 5. Key to calculate the climate formula of Köppen and Geiger, the third letter temperature classification[81]

In the Figure 16 is illustrated the Köppen-Geiger Map Classification with all the respective categories for the whole Africa continent.

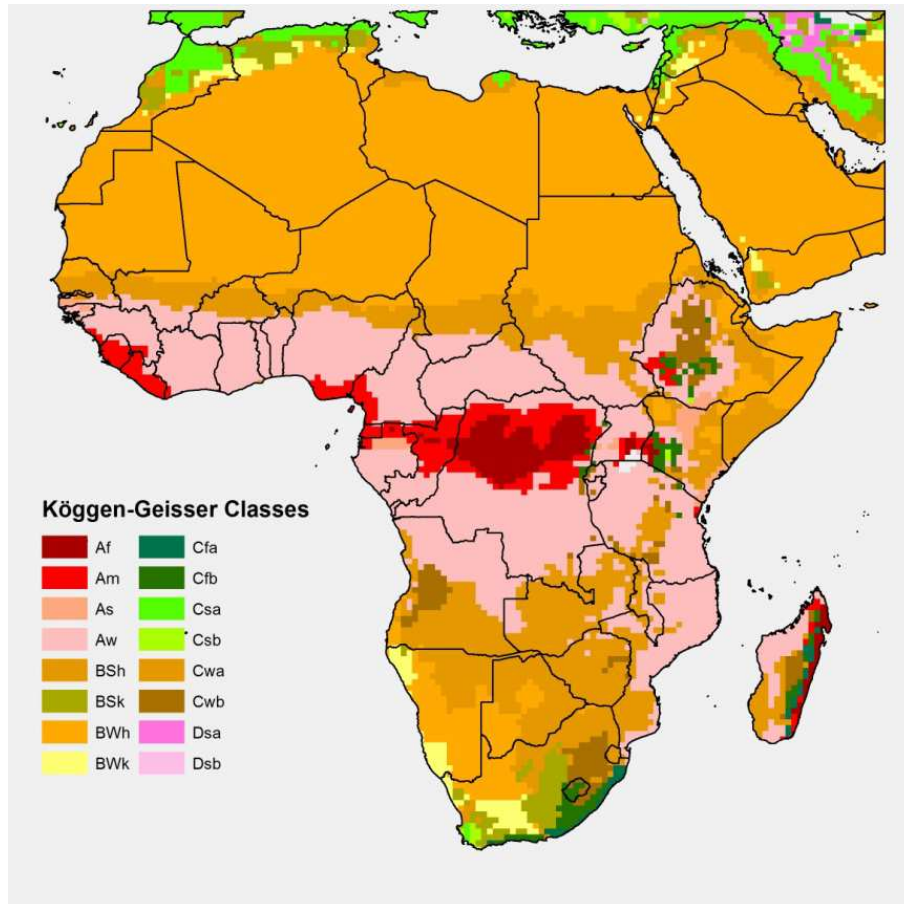


Figure 16. Africa Köppen-Geiger Map Classification

4.3.1.2. Land Cover Classification

Global land cover datasets provide thematic characterizations of the Earth's surface that capture biotic and abiotic properties and that are closely tied to the ecological condition of land areas. Information related to land cover is fundamental in the context of global change science. In the past decade available data sources and methodologies for creating global land cover maps from remote sensing have evolved rapidly[85]. In particular, for the purpose of the proposed study The MODIS land cover product has been selected.

There are two MODIS global land cover classification grids with different spatial resolution. The first grid is the MODIS Land Cover Type product (MCD12Q1), that includes five main layers for each calendar year in which land cover is mapped using different classification systems. This Product is generated at 500-m spatial resolution.

Moreover, the second grid, the Land Cover Type Climate Modeling Grid (CMG) product (MCD12C1), provides the dominant land cover types and also the sub-grid frequency distribution of land cover classes at a lower spatial resolution (0.05°) compared to MCD12Q1. MCD12C1 is derived using the same algorithm that produces MCD12Q1. It contains three classification schemes, which describe the land cover properties derived from observations spanning a year's input of Terra and Aqua MODIS data.

With the aim to have spatial coherence between the rainfall, climate, vegetation monitoring and the land cover product was decided to use the MCD12C1 product, selecting the International Geosphere Biosphere Programme (IGBP) land cover scheme that identifies 17 land cover classes, which includes 11 natural vegetation classes, 3 developed and mosaicked land classes, and 3 non-vegetated land (See Table 6 and Figure 17).

Class	Land Cover Type (IGBP)
0	Water
1	Evergreen Needleleaf forest
2	Evergreen Broadleaf forest
3	Deciduous Needleleaf forest
4	Deciduous Broadleaf forest
5	Mixed forest
6	Closed shrublands
7	Open shrublands
8	Woody savannas
9	Savannas
10	Grasslands
11	Permanent wetlands
12	Croplands
13	Urban and built-up
14	Cropland/Natural vegetation mosaic
15	Snow and ice
16	Barren or sparsely vegetated
255	Fill Value/Unclassified

Table 6. MODIS (MCD12C1) IGBP Land Cover Types

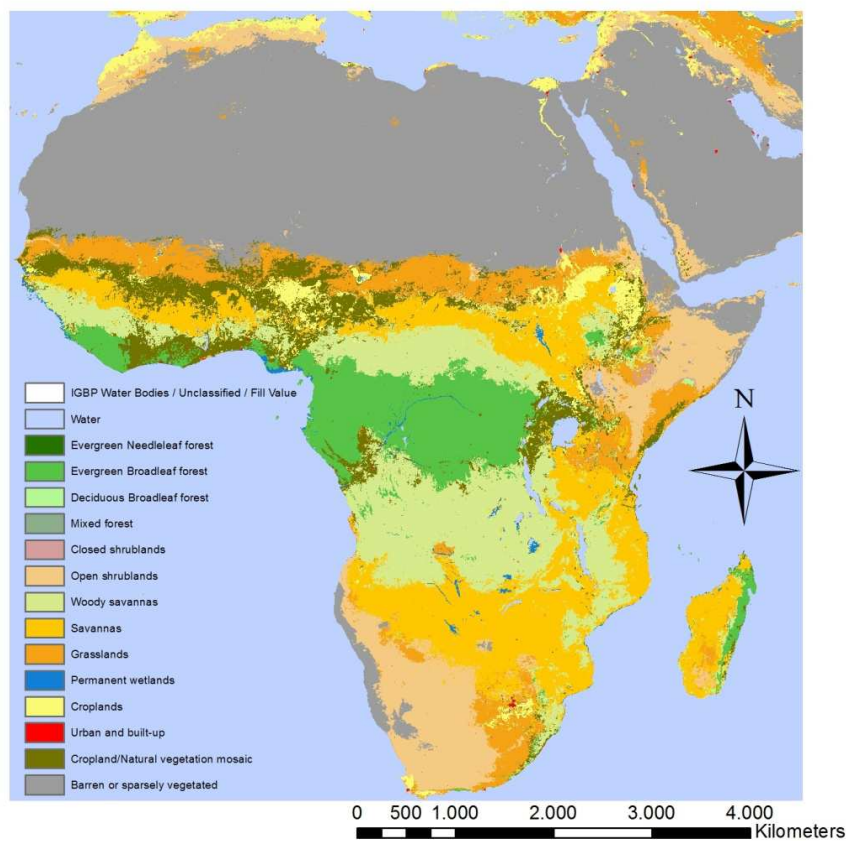


Figure 17. Africa MCD12C1 IGBP Land Cover

4.3.1.3. Geographical Vegetation Mask

Considering the different climate and geographical conditions that characterize the African continent and their variability, it was fundamental to make a preliminary analysis with the aim to identify the areas where the results of the vegetation monitoring activities proposed in the ITHACA Drought EWS are produced with insufficient reliability. These areas have been excluded and masked during the statistical analysis carried out in this study.

Considering the climate classification it can be noticed that the area with reduced reliability are classified as Equatorial rainforest, fully humid (Af) and Equatorial Monsoon (Am). These areas have the particularity that are humid zones with high values of rainfall and with a vegetation without a defined seasonal behavior. In addition, most of the areas covered by the evergreen needleleaf forest type and characterized by Af or Am climate types, were not included in the correlation analysis implemented in this study. Finally, in the procedures, the areas classified as barren or sparsely vegetated are obviously discarded.

Figure 18 shows the final masked area (white area) that was kept out of the statistical analyses.

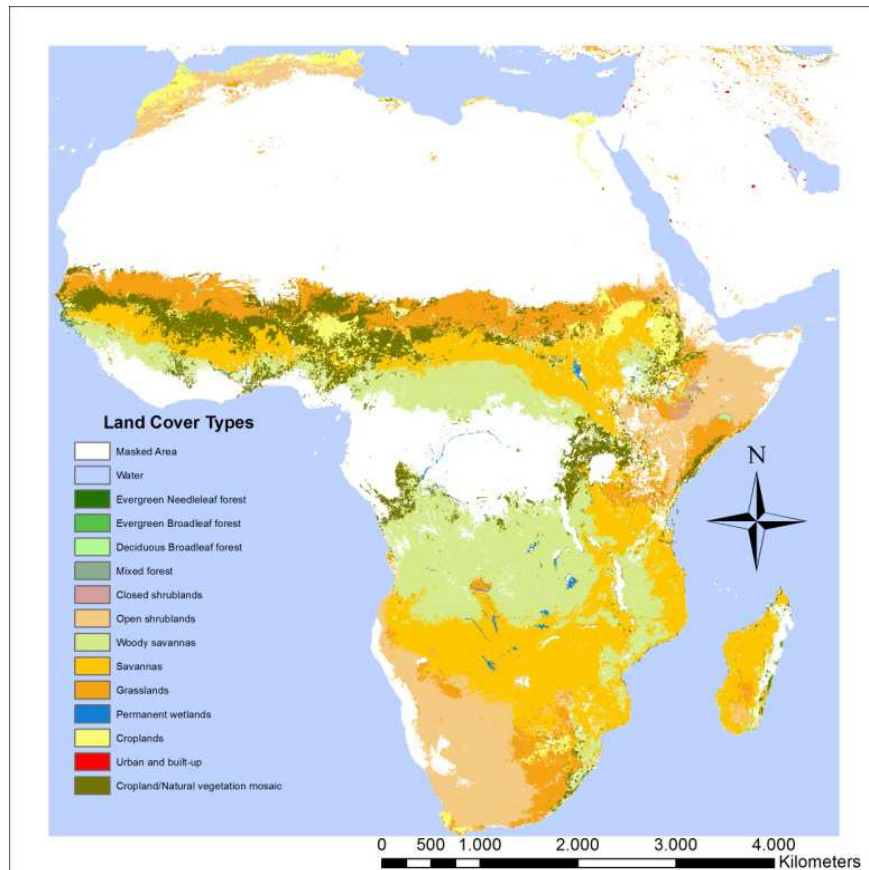


Figure 18. Geographical Masked Area

4.3.2. Climate and rainfall analysis

Considering the importance of the climate conditions in the origin and development of drought events, a preliminary phase of this study was to make an analysis of the climate in the whole Africa with special attention to the rainfall data.

Initially, a set of cumulative rainfall periods that could have directly impacts in the normal development of the vegetation was defined. In this case, using the TRMM daily data, a dataset was generated accumulating rainfall in periods of one, three, six and nine months, selected considering the growing season of vegetation and the rainfall season presented in a solar year. This cumulative rainfall was calculated in a dynamic temporal window corresponding to MODIS-NDVI fortnightly data presented in the vegetation monitoring dataset, creating a file for each cumulative period and for each fortnight in a solar year. With the aim to have vegetation and rainfall datasets at same geographical projection and taking into account the different resolution between the rainfall data and the vegetation monitoring data, the cumulative rainfall files were projected and downscaled to the spatial resolution of the original vegetation data.

Furthermore, considering the availability of the different data sets, for the analysis a period of 14 years corresponding to the time between 2000 and 2013, was selected..

With the aim to identify the rainfall behavior in the different areas of the continent, for each cumulative period and for each fortnight the value of average cumulative precipitation in the 14 years of data was calculated. Then, the fortnight interval that presented the maximum value for the different calculated average values at the same time was identified.

Then, using the monthly averages was possible identify the parameters that identify the rainfall season for each region in the continent; it was possible to define the rainfall start of the season, the duration of the rainfall season, the areas with two rainfall seasons in the year and the areas with extreme meteorological conditions (The areas with values lower than 25 mm per month).

This information is essential to understand the relationship between rainfall and vegetation growth, especially in the areas where both have similar temporal behavior. In the Figure 19 and Figure 20, is showed the evolution of the monthly and three-monthly average rainfall accumulation.

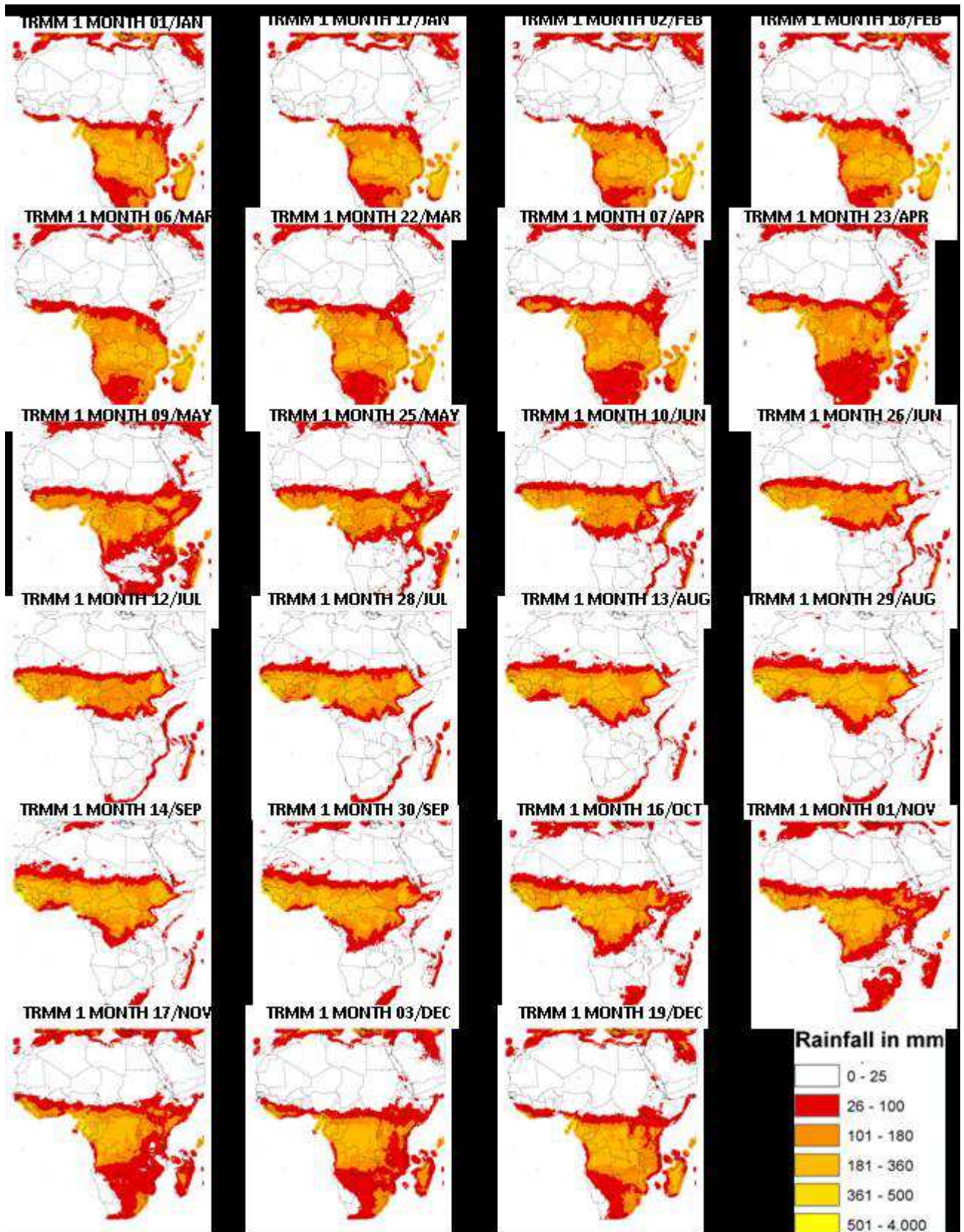


Figure 19. Behavior of the cumulative monthly precipitation during the solar year distributed in fortnights

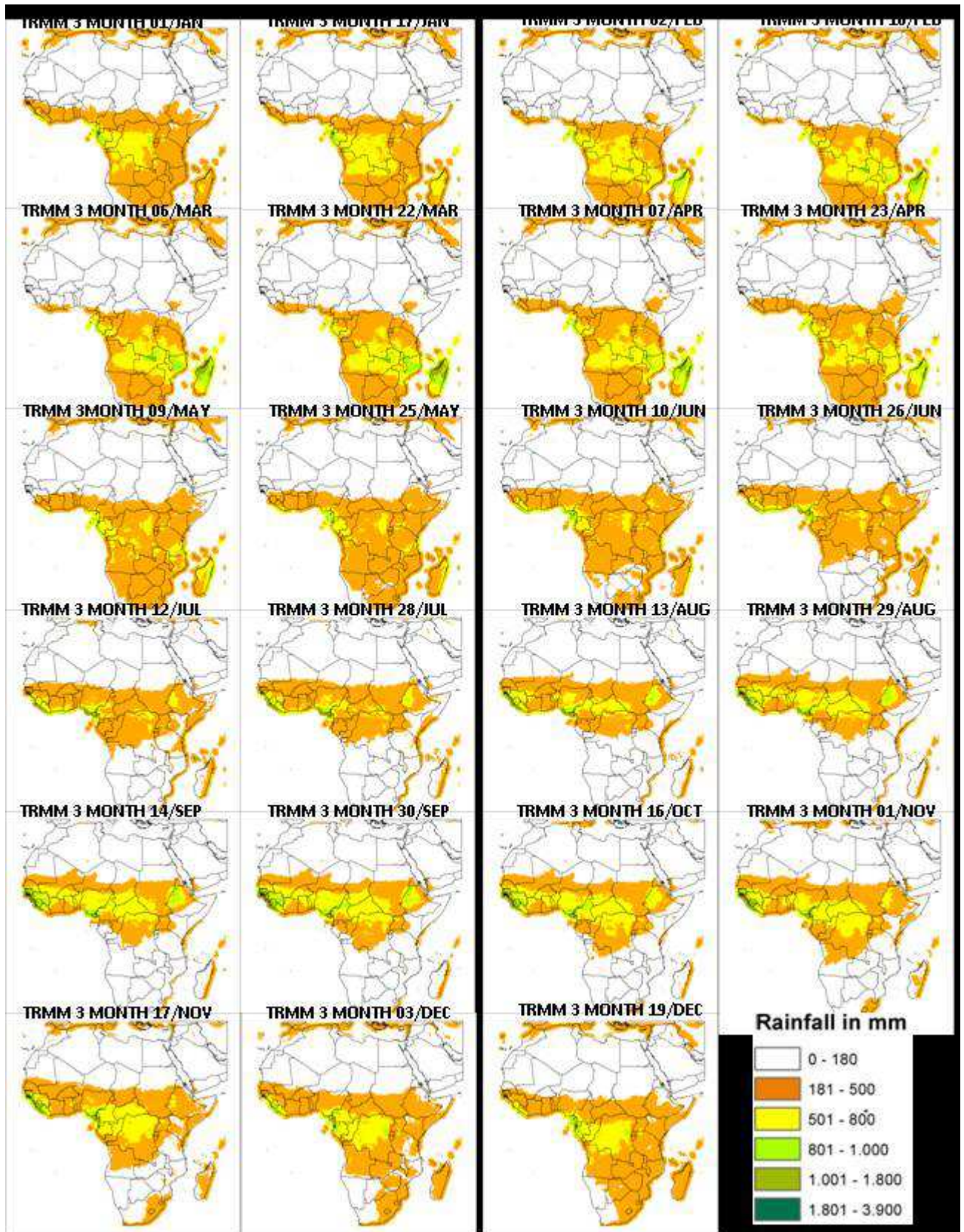


Figure 20. Behavior of the cumulative three-monthly precipitation during the solar year distributed in fortnights

4.4. Relationship between Vegetation and Rainfall data

In this chapter the methodology used to investigate the relationship between the vegetation and rainfall data is explained. To better understand this relationship, an analysis conducted on phenological parameters extracted through to the vegetation monitoring in ITHACA Drought EWS during the period between 2000 and 2013. The phenological parameters were correlated through the Pearson correlation coefficient with different cumulated rainfall values, obtained as defined in 4.3.2. Then, with the purpose of study the significance of the observed correlation a Student's t-test with significance level of 5 % was applied.

4.4.1. Correlation Analysis

A correlation analysis describes the linear relationship between two or more variables without attributing to one variable the effect generated in other one. This technique is useful because indicates if two variables have something in common. A correlation coefficient is an numerical indicator that defines the relationship between two variables; it is expressed numerically in a range between -1.00 and +1.00 and rises with the increase of the amount of the variance of a single variable that is shared by other variables[86]. The correlation can be direct or positive, which means that variables change in the same direction or it can be indirect or negative with variables changing in the opposite direction. The most important parameter in the correlation is not the sign, it is the absolute value.

In this study the correlation analysis was carried out using the Pearson correlation coefficient:

$$r_{xy} = \frac{\sum(X - \bar{X})(Y - \bar{Y})}{\sqrt{[\sum(X - \bar{X})^2][\sum(Y - \bar{Y})^2]}}$$

where,

r_{xy} = Pearson correlation coefficient

X = Individual observations of variable X.

Y = Individual observations of variable Y.

\bar{X} = Mean of variable X.

\bar{Y} = Mean of variable Y.

A proper IDL algorithm was implemented to calculate the value of the correlation coefficient between the different cumulated rainfall values and the phenological vegetation parameters.

For each considered phenological parameter a correlation analysis has been performed considering each 2000-2013 time-series of MODIS NDVI fortnightly values (23 fortnightly values in a solar year) and each fortnightly time-series of cumulated rainfall values (obtained using, as cumulating period, 1, 3, 6, or 9 months preceding the last day of the examined fortnightly interval, as already described). Concurrently, the analysis was implemented considering the presence of vegetations characterized by two growing seasons per year, therefore in some areas there were two correlation coefficients for the same parameter.

For instance, in the Figure 21 and Figure 22 are represented the Pearson correlations coefficients in the whole Africa correspondent to the relationship between the Amplitude of the vegetation and the cumulative rainfall for 1 month and 3 months respectively.

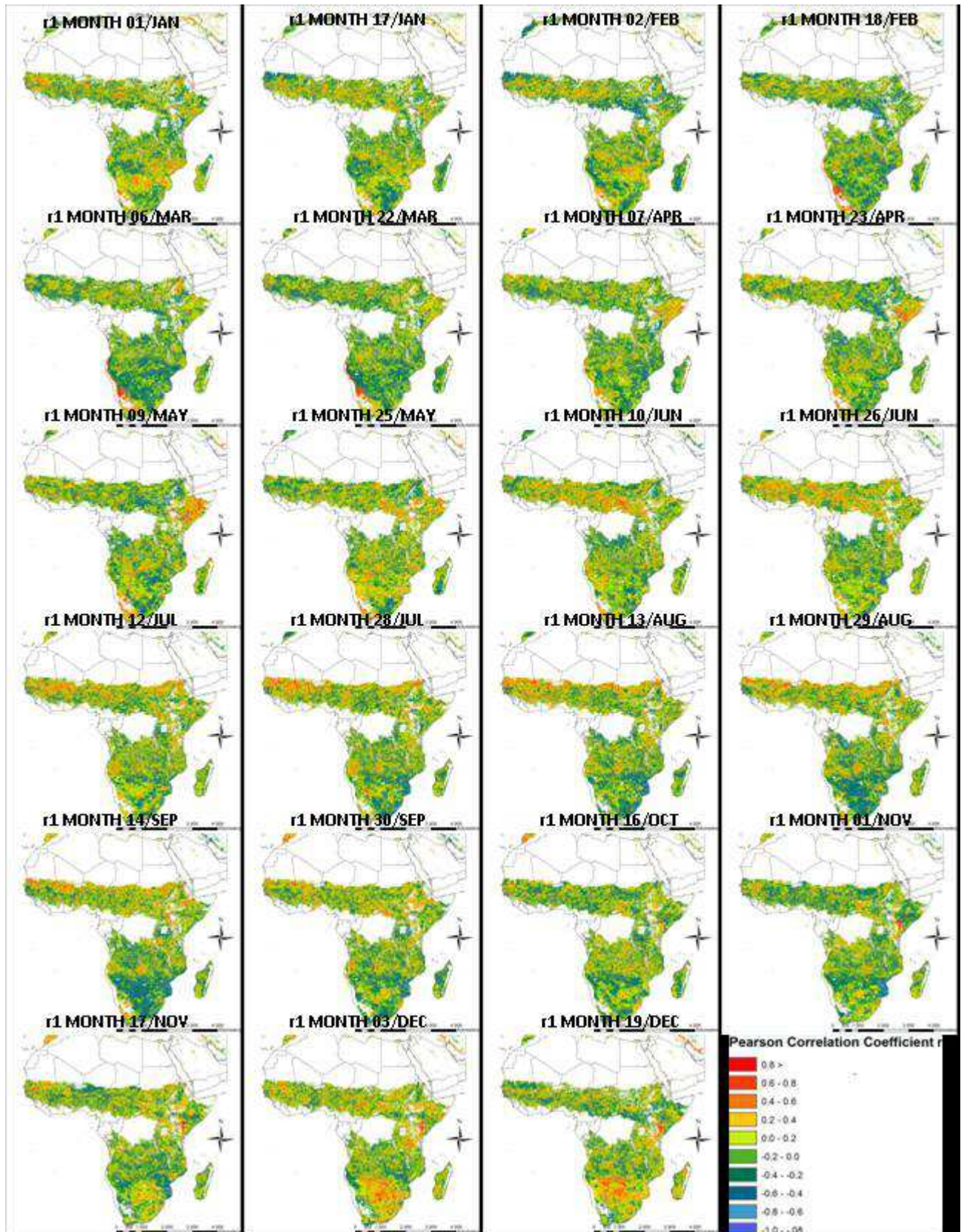


Figure 21. Evolution of the Pearson correlation coefficient (r) between cumulative rainfall for 1 month and the Amplitude in the period between 2000-2013 for the first (In some areas the only one) season of the solar year

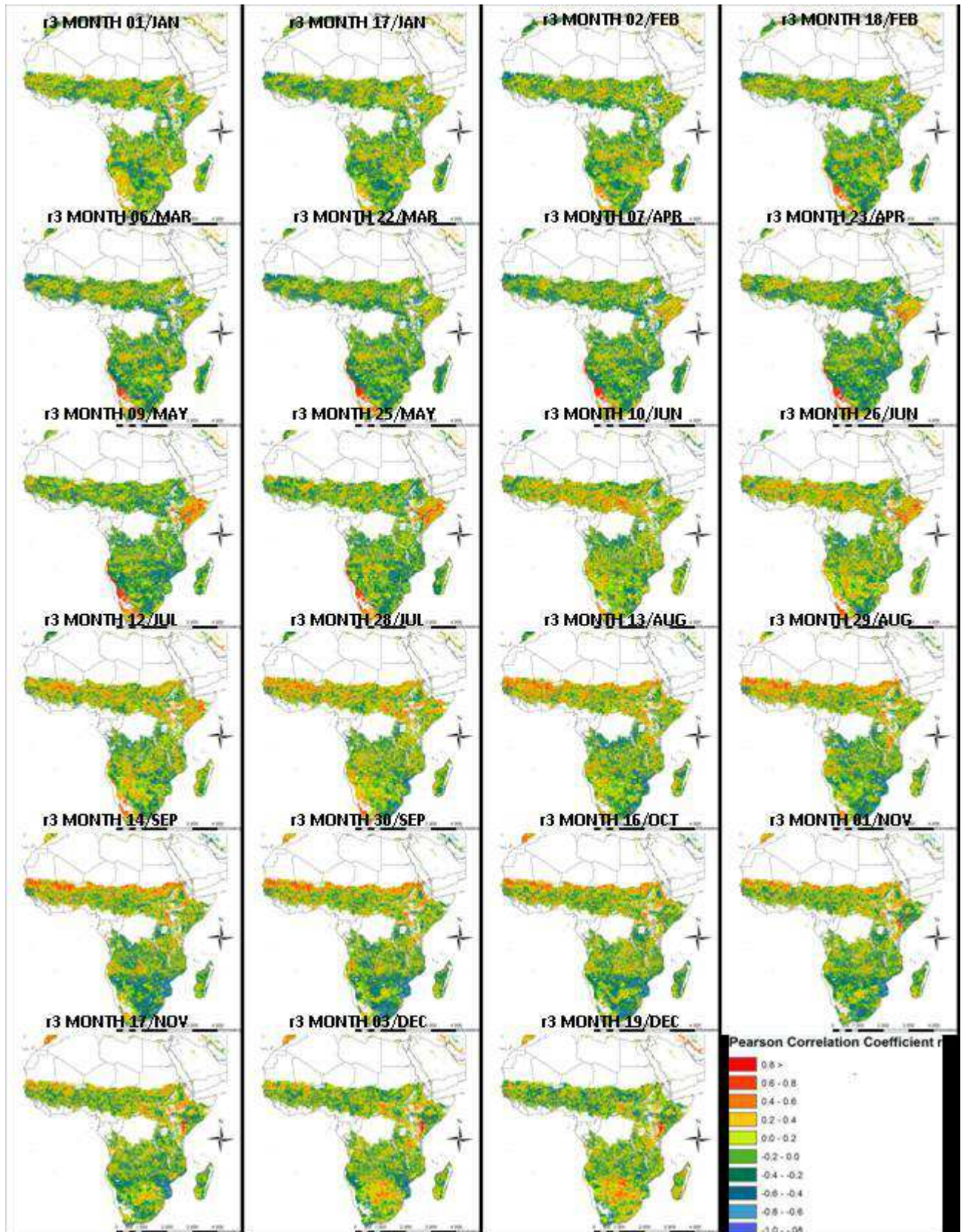


Figure 22. Evolution of the Pearson correlation coefficient (r) between cumulative rainfall for 3 months and the Amplitude in the period between 2000-2013 for the first (In some areas the only one) season of the solar year

4.4.2. Test of Statistical Significance

The statistical significance is defined like the likelihood that a result or relationship is caused by something other than mere random chance. With the aim to determine the significance of the correlation coefficient an analysis through a Student's t-test with significance level of 5 %, was implemented.

A correlation coefficient is significant if it is possible to assert with certain probability that it is different to zero. Normally a test of statistical significance presented two hypothesis ; a null hypothesis and an alternative hypothesis. In this case the main objective of the test was to determine the existence of a linear relationship using the null hypothesis that the true correlation coefficient is equal to 0, thus the alternative hypothesis was that the true correlation coefficient is different to 0. It was demonstrated that the correlations sampling distribution from a population characterized by a correlation coefficient equal to zero follow a student distribution with N-2 degrees of freedom, where N is the number of observations and deviation type:

$$s_r = \sqrt{\frac{1 - r_{xy}^2}{N - 2}}$$

where,

r_{xy} = Correlation Coefficient between variables x and y.

Consequently, for a determinate correlation coefficient (r_{xy}) it is checked if it is possible that r_{xy} is in the sampling distribution under the null hypothesis. Considering the student distribution, it is calculated the value of the test statistic using the following formula:

$$t = \frac{r_{xy} - 0}{\sqrt{\frac{1 - r_{xy}^2}{N - 2}}}$$

With the value of the test statistics (t) and the degrees of freedom (N-2) is obtained a P-value that is calculated using a statistical software package or statistical tables. This value is compared with the level of significance to decide if the null hypothesis is accepted or rejected. In the case in which the null hypothesis is rejected, the correlation is defined as significant and is considered that the test of significance is passed.

Considering the type of data used in this research, a proper IDL algorithm was implemented, to identifying the areas where the test of significance was passed.

In Figure 23 is illustrated the correlation coefficients between cumulative rainfall for 3 months and the small integral in the whole area (a) and the same information with the mask generated by the correlation coefficients that have not passed the test (b).

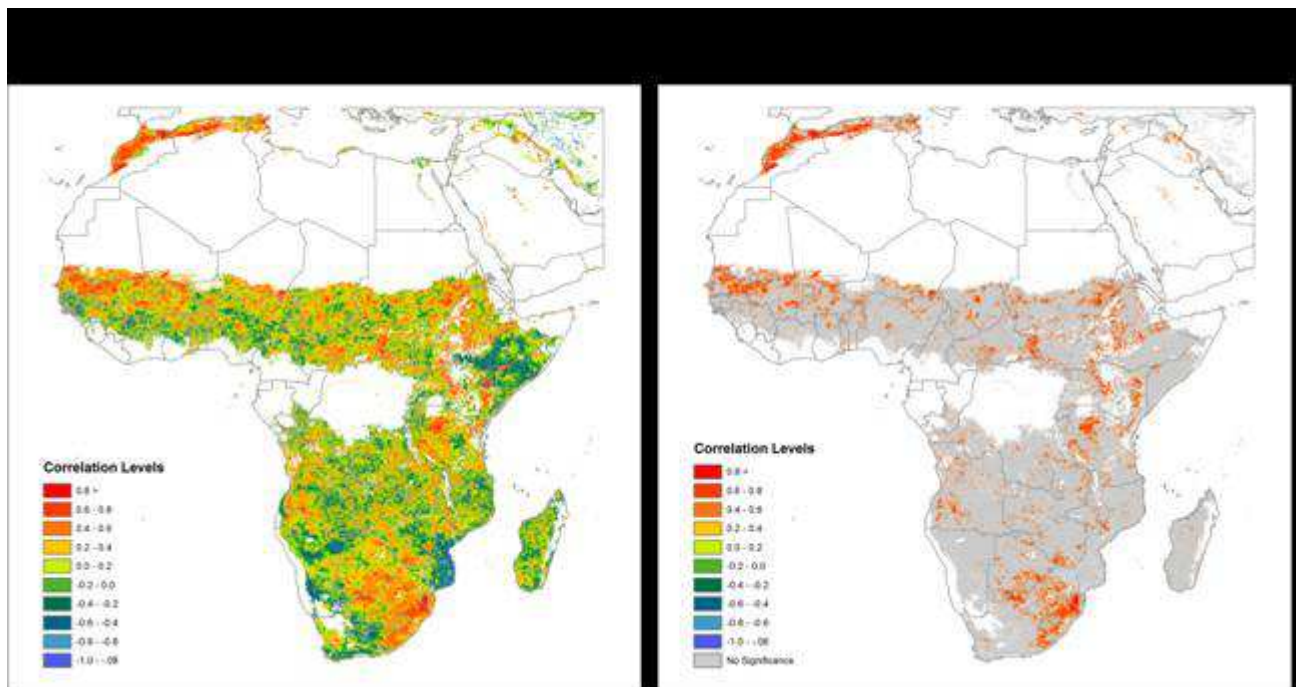


Figure 23. a) Pearson correlation coefficient (r) between cumulative rainfall for 3 months and the Small Integral for the period corresponded to 11 November to b) Pearson correlation coefficient (r) between cumulative rainfall for 3 months and the Small Integral for the period corresponded to 11 November with the no significance correlation areas.

5. OUTCOMES AND DISCUSSION

5.1. Land Cover Analysis

Considering the Land Cover classification described in 4.3.1.2, a preliminary analysis was conducted to determine the distribution of areas covered by the different land cover classes in Africa, excluding the areas that not correspond to a vegetation type (See Figure 24). These classes cover in total an area of **17.295,00Km²**.

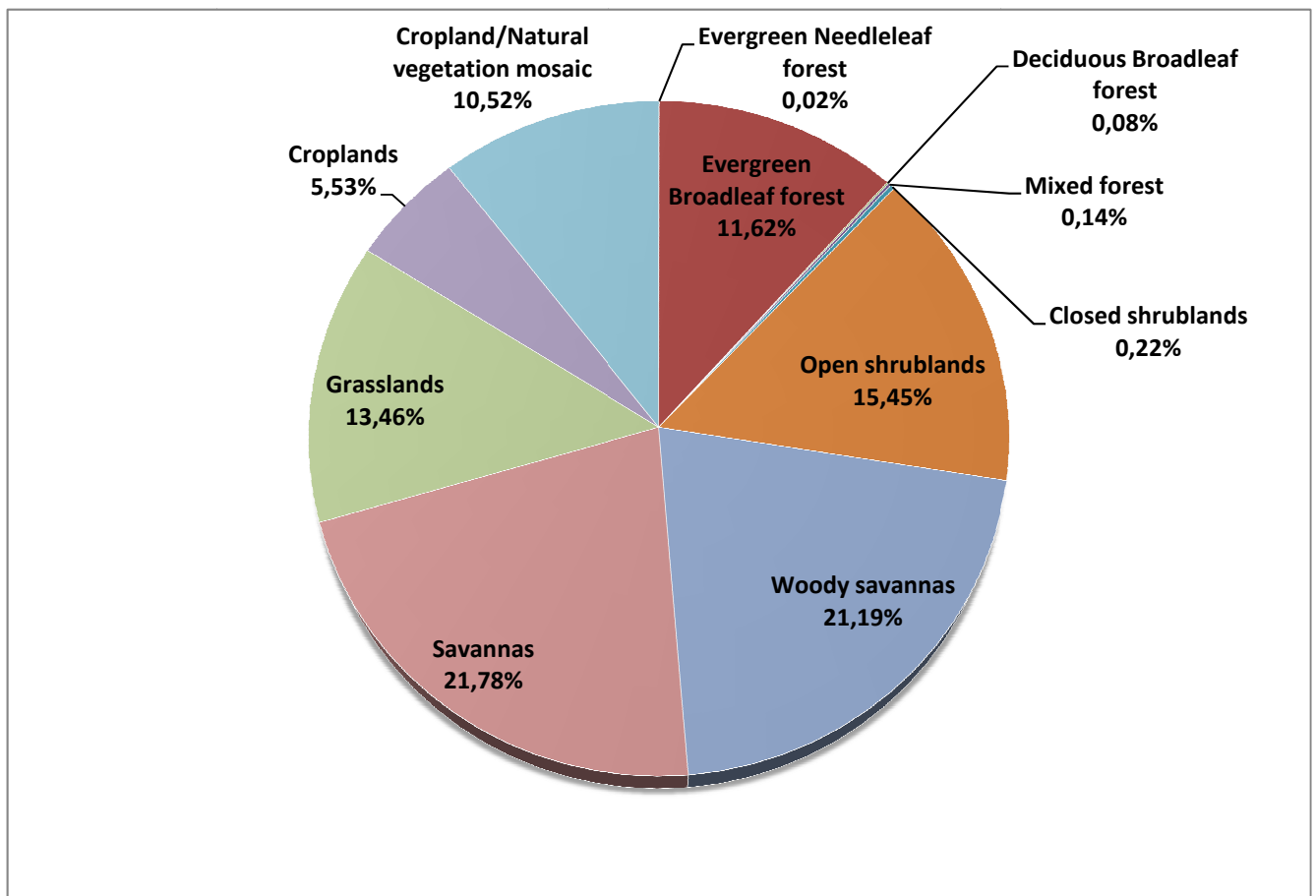


Figure 24. Vegetation Land Cover Distribution in Africa (MCD12C1)

In addition, a small area is characterized by a bi-seasonal behavior, presenting two growing seasons per solar year. This area corresponding to the 11% of the vegetation classes in the whole of African continent (1.882,63Km²). The distribution of the classes with bi-seasonal behavior is illustrated in the Figure 25.

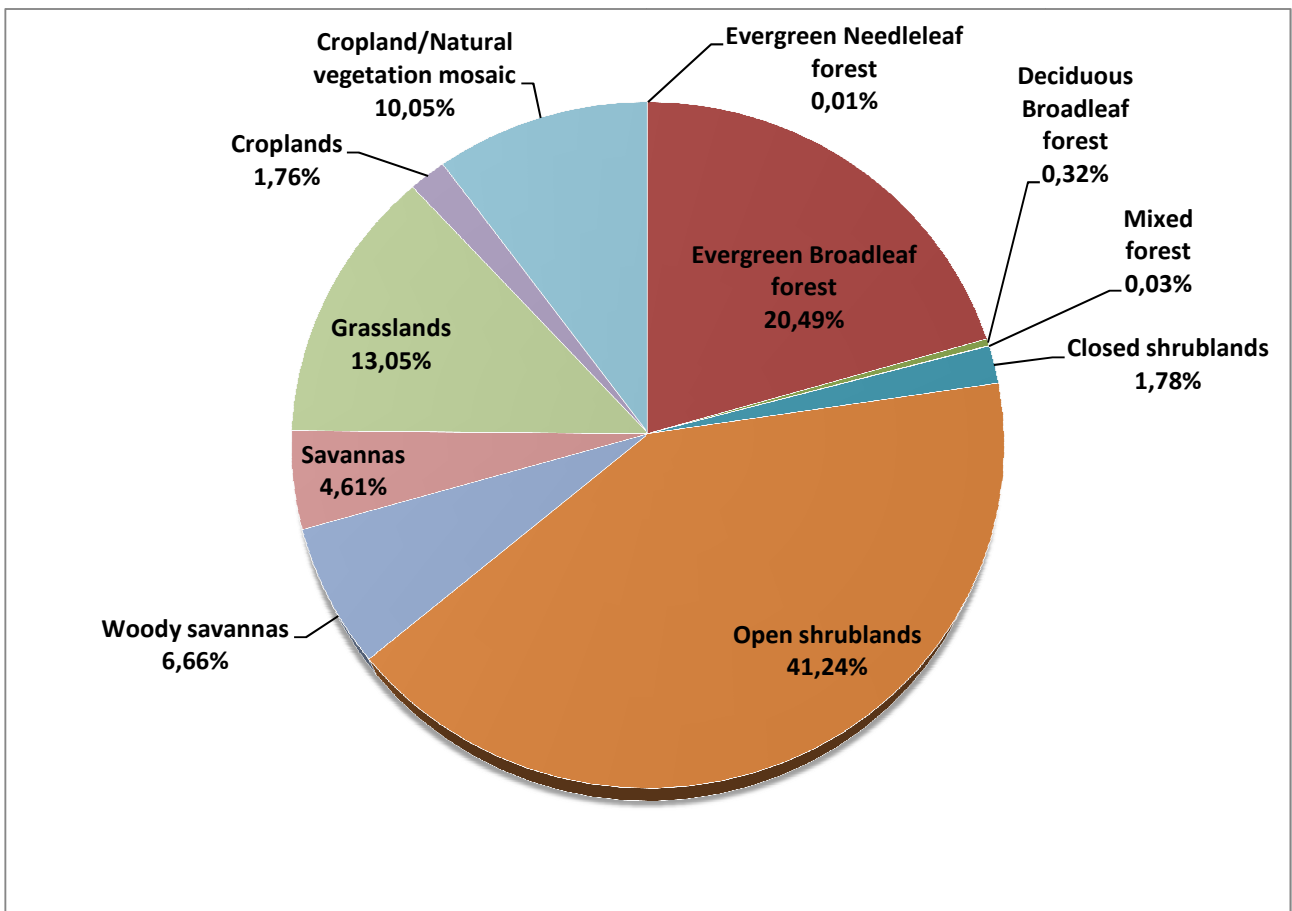


Figure 25. Vegetation Land Cover with two growing season at year, Land Cover Distribution in Africa (MCD12C1)

As shown in Figure 24 and Figure 25, the Deciduous Broadleaf forest, Mixed forest, Closed shrublands, and Evergreen Needleleaf forest classes cover a really small area of the whole African continent. Therefore, considering also their casual distribution and the spatial resolution of the datasets used in this study (0.05 deg) , these land cover types were considered as not representative, and consequently excluded in the subsequent analyses.

Furthermore, as already described in 4.3.1.3, the areas where the ITHACA drought EWS is implemented with insufficient reliability, which mainly correspond to the Evergreen Broadleaf forest land cover class, were also excluded. In conclusion, with the aim to conduct a reliable analysis, the Open shrublands, Woody savannas, Savannas, Grasslands, Croplands and Cropland/Natural vegetation mosaic classes, as shown in See Figure 26,were considered for the subsequent statistical analyses.

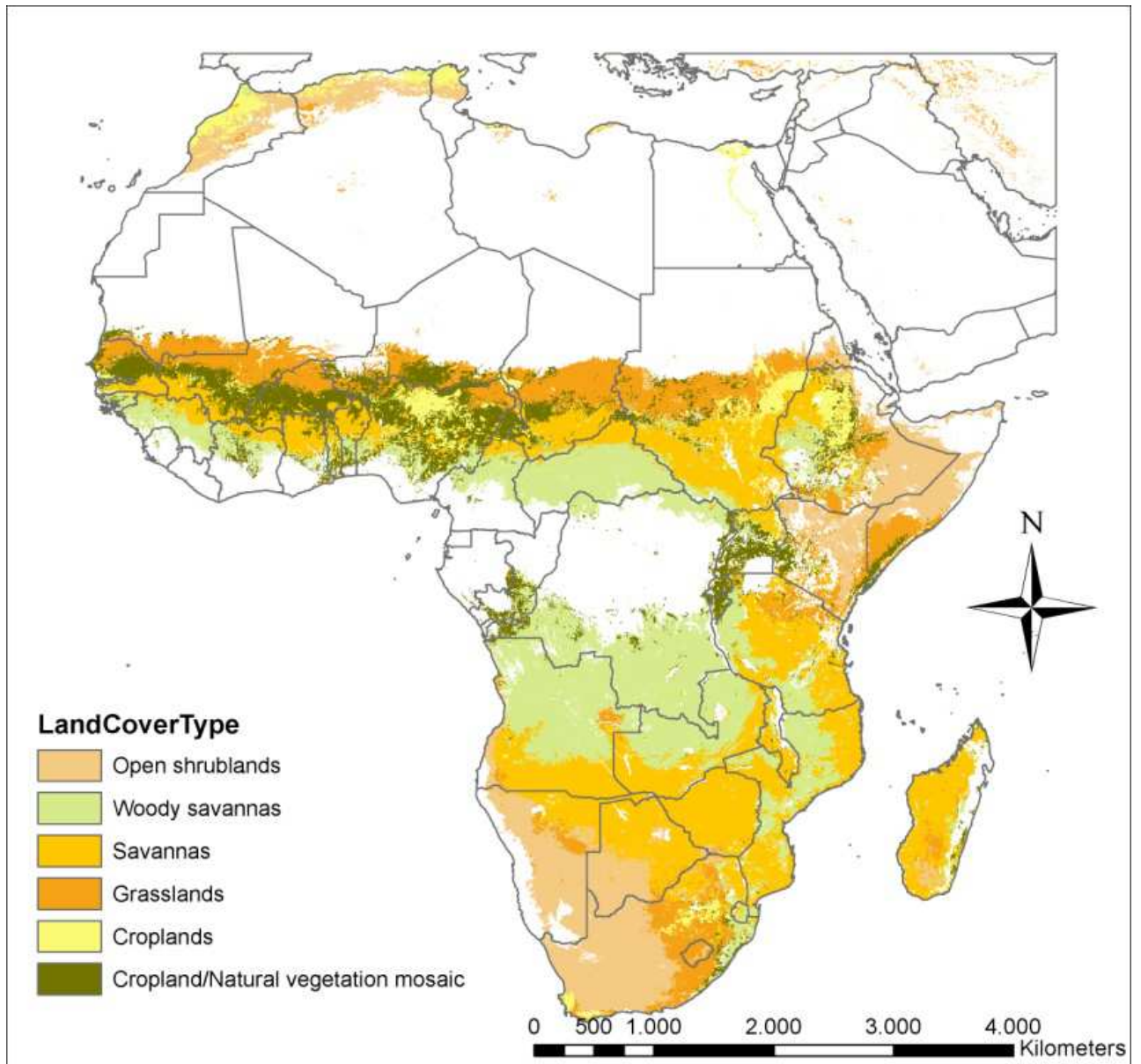


Figure 26. Vegetation Land Cover classes used in the analysis. Excluded areas are in white.

5.2. Test of Significance Analysis

According to the defined significance test described in 4.4.2, an analysis of the results obtained was conducted and final outcomes are proposed in this paragraph. The analysis was implemented for all the land cover types defined in the precedent paragraph. For each analyzed land cover type the areas that passed the significance Student t-test were identified and expressed as a percentage of the total area corresponding to the considered land cover class. The main purpose was to identify, for each vegetation type, the phenological parameters that would be potentially affected by the rainfall behavior.

5.2.1. Open shrublands

5.2.1.1. First vegetation growing season

The Open Shrublands land cover type corresponds to a 15.45 % of the vegetated area in the whole African continent, and the correlation coefficients calculated between the cumulated rainfall (1, 3, 6 months) and the different considered phenological parameters shows positive and significant values over a large portion of this area.

The largest areas with positive correlation coefficient values between all the phenological parameters and the cumulated rainfall are obtained considering 1 month as cumulating interval. Moreover, the smallest areas with positive correlation correspond to the 6 months cumulating period (See Table 7).

Phenological Parameter	SEASON 1		
	TEST PASSED		
	TRMM 1 Month	TRMM 3 Months	TRMM 6 Months
Amp	67,53%	61,23%	56,27%
Base	68,45%	65,33%	58,44%
Decr	66,50%	53,99%	44,13%
Incr	71,89%	57,73%	48,02%
Larg	64,77%	61,13%	56,00%
Len	74,71%	68,32%	55,97%
Sml	77,99%	73,26%	67,14%

Table 7. Percentage of the Open Shrublands areas that passed the Student t-test for the correlation between cumulate rainfall and phenological parameters in the first vegetation growing season.

On the other hand, taking into consideration the different examined phenological parameters, the Seasonal Small Integral (SMI) presented, in all the cumulated periods, the largest percentage of area with positive correlation values with respect to the remaining parameters. The Amplitude (Amp) and the Large (Larg) parameters presented a similar behavior, characterized by an evident reduction of the areas showing positive correlation when considering the 6 month cumulated rainfall. This is in agreement with what was expected, given that these parameters are directly related. Finally, it can be noticed that also the Decrease (Decr) and the Increase (Incr) parameters presented considerable reduction if the 3 and 6 months cumulating periods are taken into consideration, with respect to the 1 month period.

Moreover, with the aim to better understand the data given in Table 7, an analysis of the spatial distribution of the outcomes of the significance test was carried out (See Figure 27). Thus, considering the different areas of Africa covered by open shrublands, it was observed that the area where all the phenological parameters presented larger zones with no significant values of the correlation coefficient, is located in the south of the continent (specifically, this area extends between the Angola, Botswana, Namibia and South Africa countries). This area does not present a particular climate classification, then the causes of lower values of the correlation coefficient, which require further investigations, are to be sought in geographical or topographical factors.

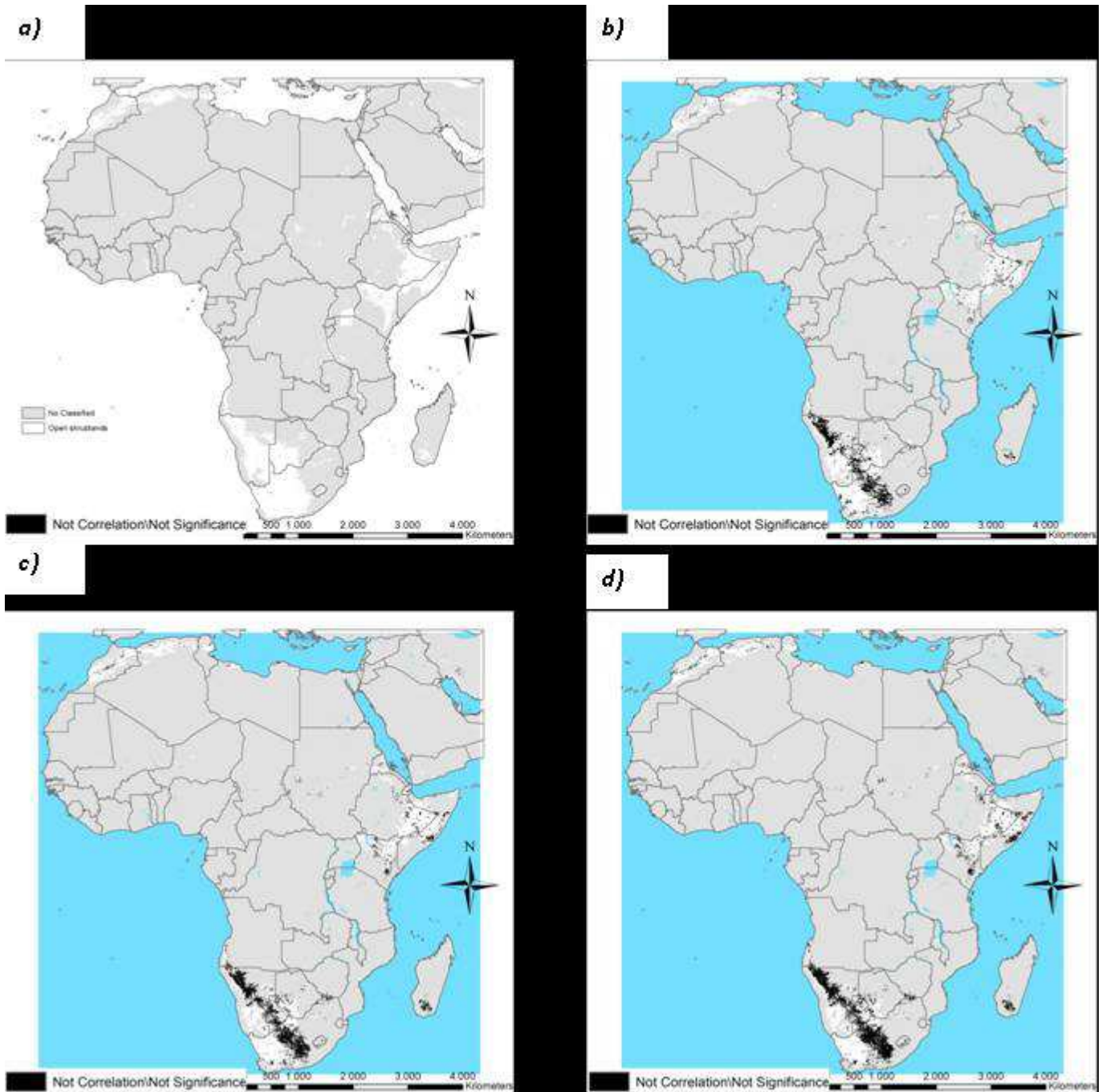


Figure 27. Outcomes of the Student t-test for the correlation between the Seasonal Small Integral (Sml) and cumulated rainfall (b) 1 month , c) 3 months d) 6 months) for the Open Shrublands vegetation type (a) in the first vegetation season.

5.1.1.1. Second vegetation growing season

The 41.24 % of the area covered by Open Shrublands shows a yearly bi-modal NDVI function that correspond to the presence of two different vegetation growing seasons. The correlation analysis carried out between the cumulated rainfall (1, 3, 6 months) and the different phenological parameters related to the second growing season showed positive and significant values over a large portion of these areas (See Table 8).

As for the first season analysis, the largest areas with positive correlation coefficient values between all the phenological parameters and the cumulated rainfall are obtained considering 1 month as cumulating interval. Moreover, the smallest areas showing positive correlation coefficients correspond to the 6 months cumulating period (See Table 8).

Open Shrub	SEASON 2		
	TEST PASSED		
	TRMM 1 Month	TRMM 3 Months	TRMM 6 Months
Amp	87,14%	78,57%	70,66%
Base	62,90%	60,59%	53,38%
Decr	78,63%	68,71%	56,49%
Incr	82,21%	67,12%	56,73%
Larg	83,85%	76,57%	68,15%
Len	77,50%	59,02%	45,40%
Sml	91,55%	82,32%	73,19%

Table 8. Percentage of the Open Shrublands areas that passed the Student t-test for the correlation between cumulate rainfall and phenological parameters in the second vegetation growing season.

On the other hand, taking into consideration the different examined phenological parameters, the Seasonal Small Integral (SMI) presented, in all the cumulated periods, the largest percentage of area with positive correlation values with respect to the remaining parameters. The Amplitude (Amp) and the Large (Larg) parameters presented a similar behavior, characterized by an evident reduction of the areas showing positive correlation when considering the 6 month cumulated rainfall. This is in agreement with what was expected, given that these parameters are directly related. Finally, it can be noticed that also the Decrease (Decr) and the Increase (Incr) parameters presented considerable reduction if the 3 and 6 months cumulating periods are taken into consideration, with respect to the 1 month period.

Furthermore, it can be noticed that, for all the phenological parameters, the percentage values given in Table 8 are generally greater than those obtained for the first vegetation growing season. This is in agreement with what was expected, given that the area analysed for the significance test in this case is significantly reduced compared to the previous case and, more importantly, is practically concentrated in a single region of Africa (Horn of Africa, see Figure 28).

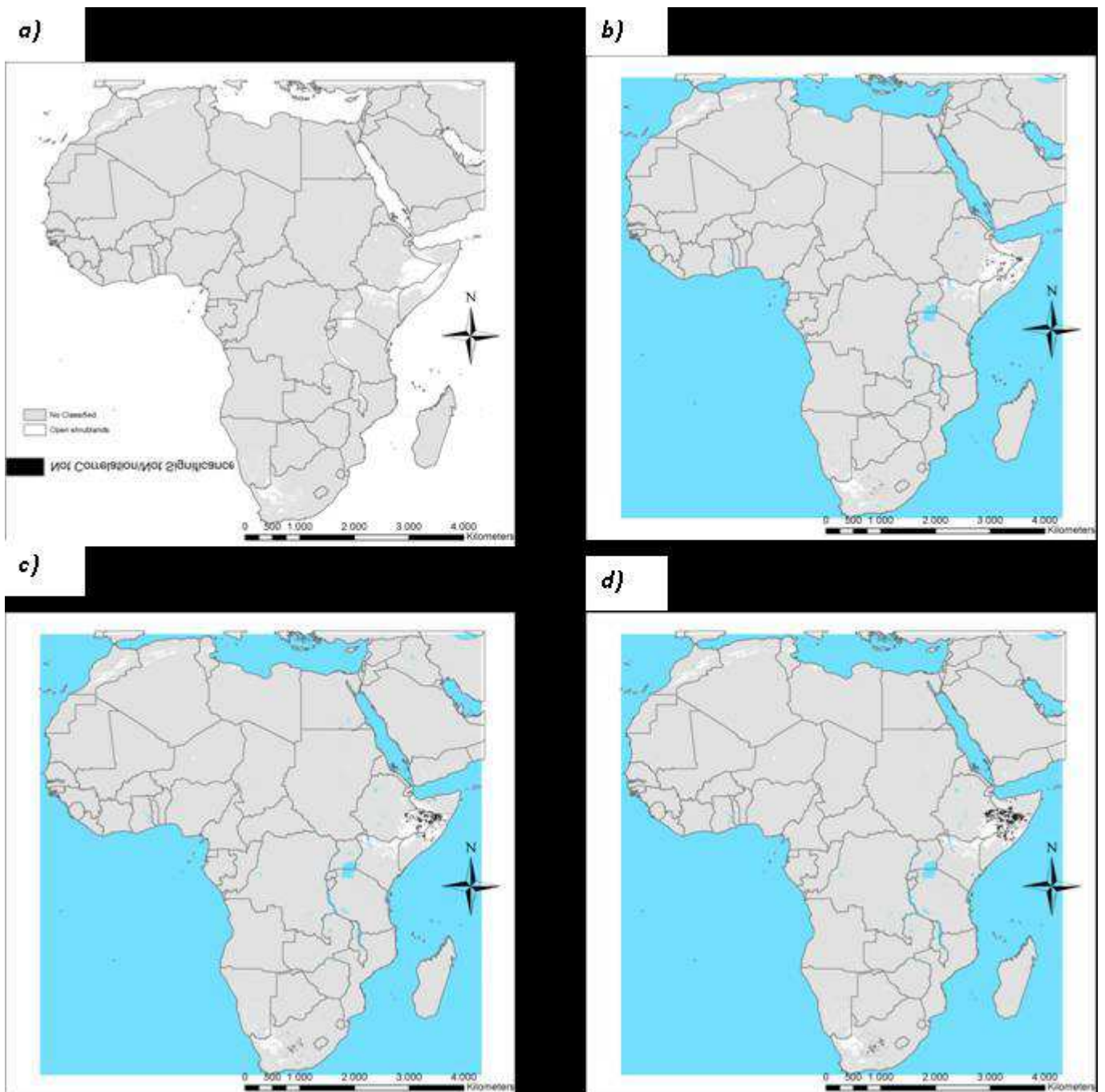


Figure 28. Outcomes of the Student t-test for the correlation between the Seasonal Small Integral (Smi) and cumulated rainfall (b) 1 month , c) 3 months d) 6 months) for the Open Shrublands vegetation type (a) in the second vegetation season.

5.2.2. Woody savannas

5.2.2.1. First vegetation growing season

The Woody savannas land cover type corresponds to a 21.19 % of the vegetated area in the whole African continent, and the correlation coefficients calculated between the cumulated rainfall (1, 3, 6 months) and the different considered phenological parameters shows some particular conditions over a large portion of this area.

The largest areas with positive correlation coefficient values between all the phenological parameters and the cumulated rainfall are obtained considering 1 month as cumulating interval. Moreover, the smallest areas with positive correlation correspond to the 6 months cumulating period (See Table 9).

Woody Sav	SEASON 1		
Phenological Parameter	TEST PASSED		
	TRMM 1 Month	TRMM 3 Months	TRMM 6 Months
Amp	52,42%	35,44%	23,64%
Base	74,78%	65,12%	50,87%
Decr	58,05%	39,82%	26,56%
Incr	72,53%	55,32%	43,30%
Larg	61,15%	47,26%	34,84%
Len	69,01%	56,01%	42,70%
Sml	60,32%	44,60%	33,15%

Table 9. Percentage of the Woody Savannas areas that passed the Student t-test for the correlation between cumulate rainfall and phenological parameters in the first vegetation growing season.

On the other hand, taking into consideration the different examined phenological parameters, the Base presented, in all the cumulated periods, the largest percentage of area with positive correlation values with respect to the remaining parameters.. The Amplitude (Amp) presented, in all the cumulated periods, the smallest percentage of area with positive correlation values with respect to the remaining parameters. Finally, it can be noticed that the Decrease (Decr) and the Increase (Incr) parameters presented considerable reduction if the 3 and 6 months cumulating periods are taken into consideration, with respect to the 1 month period.

Moreover, with the aim to better understand the data given in Table 9, an analysis of the spatial distribution of the outcomes of the significance test was carried out (See Figure 29). Thus, considering the different areas of Africa covered by woody savannas, it was observed that the area where all the

phenological parameters presented larger zones with no significant values of the correlation coefficient is distributed uniformly in the whole area identified in this class . Considering the distribution and the larger areas with no significant values, it was concluded that this type of vegetation does not presented a dependence of the rainfall behavior.

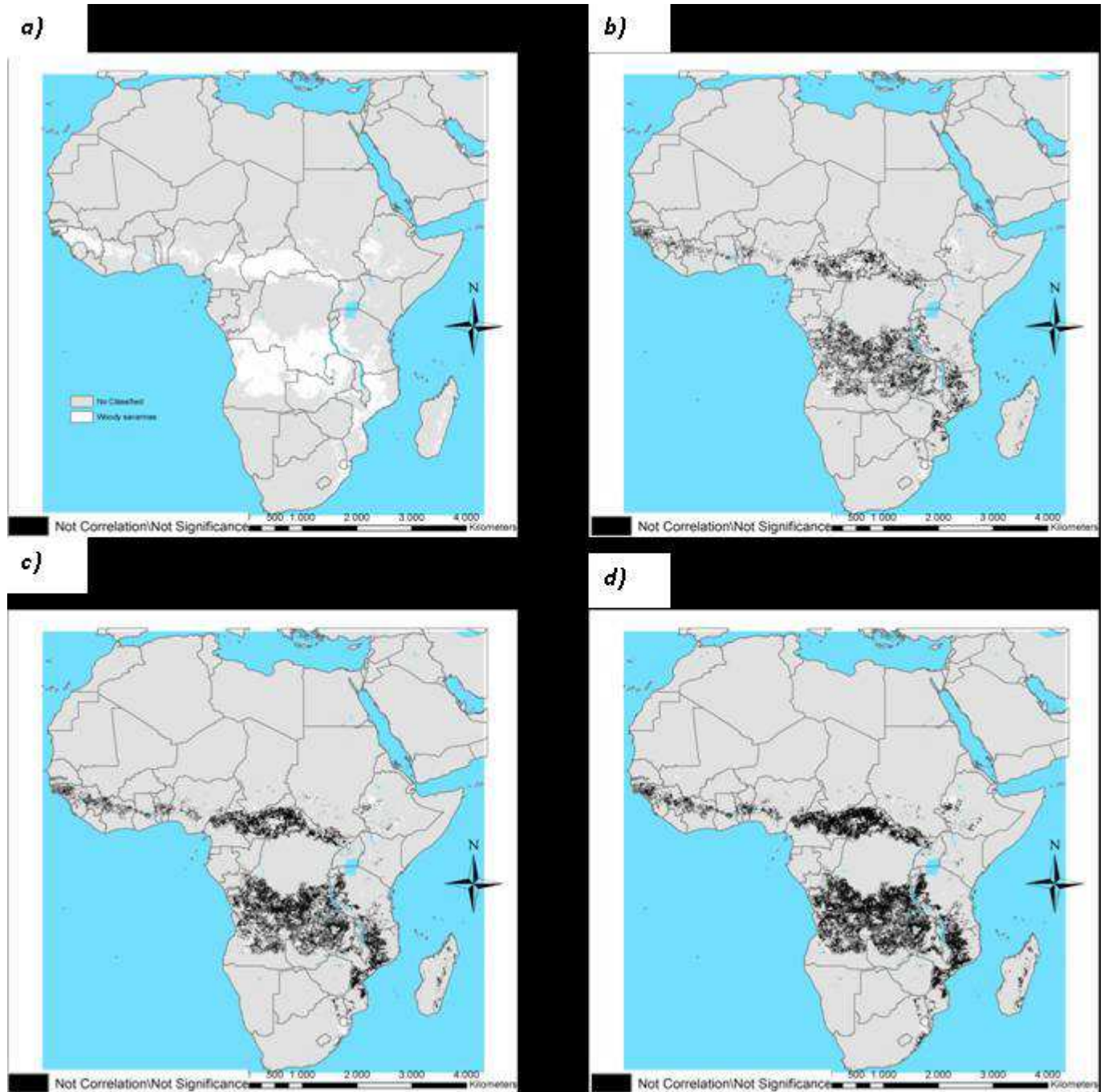


Figure 29. Outcomes of the Student t-test for the correlation between the Seasonal Small Integral (Smi) and cumulated rainfall (b) 1 month , c) 3 months d) 6 months) for the Woody savannas vegetation type (a) in the second vegetation season

5.2.3. Savannas

5.2.3.1. First vegetation growing season

The Savannas land cover type corresponds to a 21.78 % of the vegetated area in the whole African continent, and the correlation coefficients calculated between the cumulated rainfall (1, 3, 6 months) and the different considered phenological parameters shows some particular conditions over a large portion of this area.

The largest areas with positive correlation coefficient values between all the phenological parameters and the cumulated rainfall are obtained considering 1 month as cumulating interval. Moreover, the smallest areas with positive correlation correspond to the 6 months cumulating period (See Table 10).

Phenological Parameter	SEASON 1		
	TEST PASSED		
	TRMM 1 Month	TRMM 3 Months	TRMM 6 Months
Amp	56,16%	38,43%	27,68%
Base	82,26%	74,89%	65,69%
Decr	59,79%	41,87%	28,98%
Incr	71,47%	50,19%	37,61%
Larg	66,12%	51,61%	40,13%
Len	75,70%	66,08%	57,32%
Sml	69,15%	54,99%	45,34%

Table 10. Percentage of the Savannas areas that passed the Student t-test for the correlation between cumulate rainfall and phenological parameters in the first vegetation growing season.

On the other hand, taking into consideration the different examined phenological parameters, the Base presented, in all the cumulated periods, the largest percentage of area with positive correlation values with respect to the remaining parameters.. The Amplitude (Amp) presented, in all the cumulated periods, the smallest percentage of area with positive correlation values with respect to the remaining parameters. Finally, it can be noticed that the Decrease (Decr) and the Increase (Incr) parameters presented considerable reduction if the 3 and 6 months cumulating periods are taken into consideration, with respect to the 1 month period.

Moreover, with the aim to better understand the data given in Table 10, an analysis of the spatial distribution of the outcomes of the significance test was carried out (See Figure 30). Thus, considering the different areas of Africa covered by savannas, it was observed that the area where all the phenological

parameters presented larger zones with no significant values of the correlation coefficient is distributed uniformly in the whole area identified in this class . Considering the distribution and the larger areas with no significant values, it was concluded that this type of vegetation does not presented a dependence of the rainfall behavior.

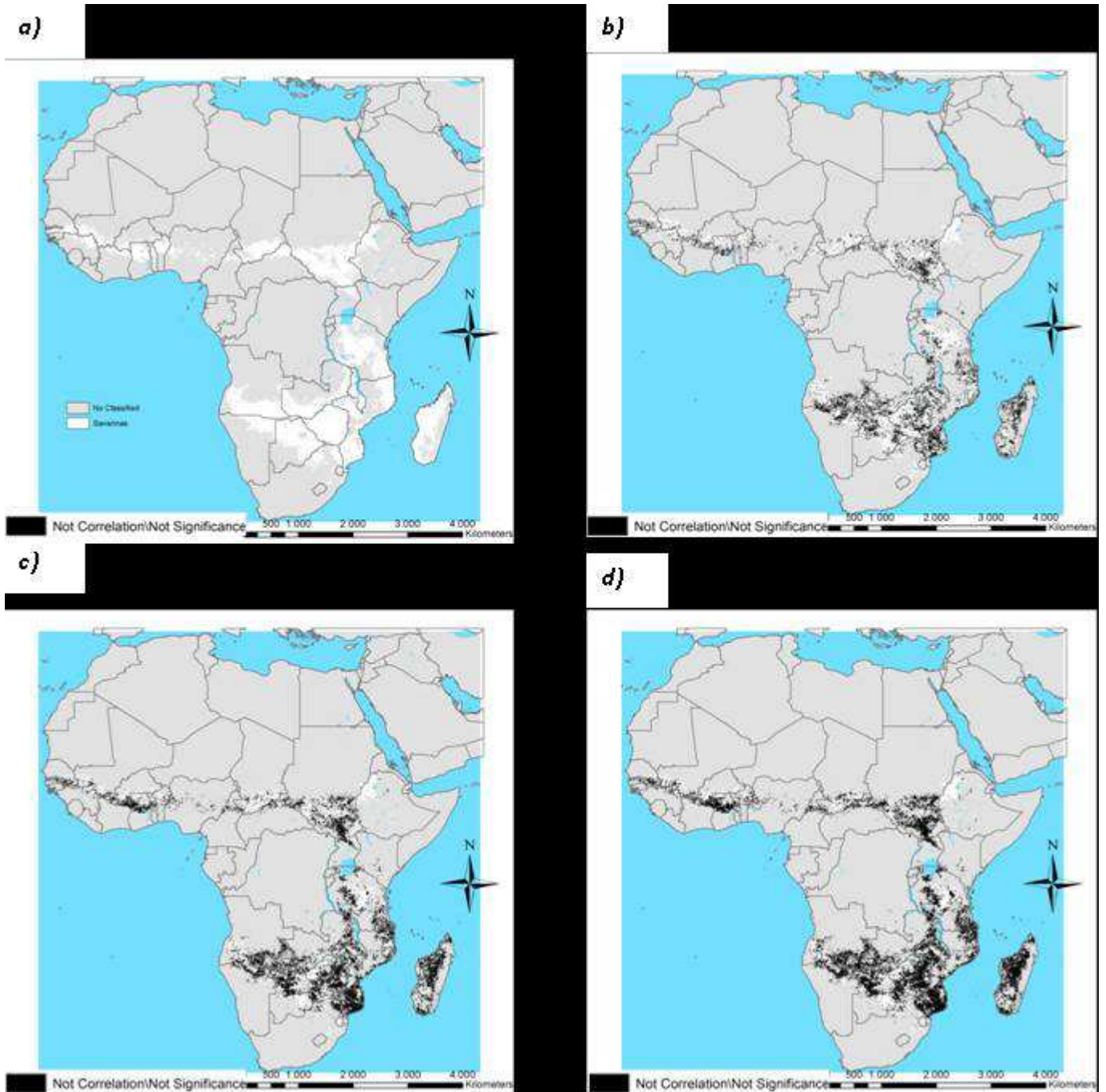


Figure 30. Outcomes of the Student t-test for the correlation between the Seasonal Small Integral (Sml) and cumulated rainfall (b) 1 month , c) 3 months d) 6 months) for the Savannas vegetation type (a) in the second vegetation season

5.2.4. Grasslands

5.2.4.1. First vegetation growing season

The Grasslands land cover type corresponds to a 13.46 % of the vegetated area in the whole African continent, and the correlation coefficients calculated between the cumulated rainfall (1, 3, 6 months) and the different considered phenological parameters shows positive and significant values over a large portion of this area.

The largest areas with positive correlation coefficient values between all the phenological parameters and the cumulated rainfall are obtained considering 1 month as cumulating interval. Moreover, the smallest areas with positive correlation correspond to the 6 months cumulating period (See Table 10).

Phenological Parameter	SEASON 1		
	TEST PASSED		
	TRMM 1 Month	TRMM 3 Months	TRMM 6 Months
Amp	65,87%	57,37%	51,30%
Base	73,06%	65,94%	62,44%
Decr	59,92%	46,63%	37,30%
Incr	67,58%	49,20%	38,68%
Larg	66,71%	58,93%	54,15%
Len	82,26%	76,43%	66,47%
Sml	84,07%	78,86%	71,70%

Table 11. Percentage of the Grasslands areas that passed the Student t-test for the correlation between cumulate rainfall and phenological parameters in the first vegetation growing season.

On the other hand, taking into consideration the different examined phenological parameters, the Seasonal Small Integral (SMI) presented, in all the cumulated periods, the largest percentage of area with positive correlation values with respect to the remaining parameters. The Amplitude (Amp) and the Large (Larg) parameters presented a similar behavior, characterized by an evident reduction of the areas showing positive correlation when considering the 6 month cumulated rainfall. This is in agreement with what was expected, given that these parameters are directly related. Finally, it can be noticed that also the Decrease (Decr) and the Increase (Incr) parameters presented considerable reduction if the 3 and 6 months cumulating periods are taken into consideration, with respect to the 1 month period.

Moreover, with the aim to better understand the data given in Table 11, an analysis of the spatial distribution of the outcomes of the significance test was carried out (See Figure 31). Thus, considering the different areas of Africa covered by grasslands, it was observed that the area where all the phenological

parameters presented larger zones with no significant values of the correlation coefficient, is located in the south of the continent (specifically located in South Africa). This area present a particular climate classification regarding to the whole area classified such grassland, this could be considered such a possible cause of lower values of the correlation coefficient, which require further investigations.

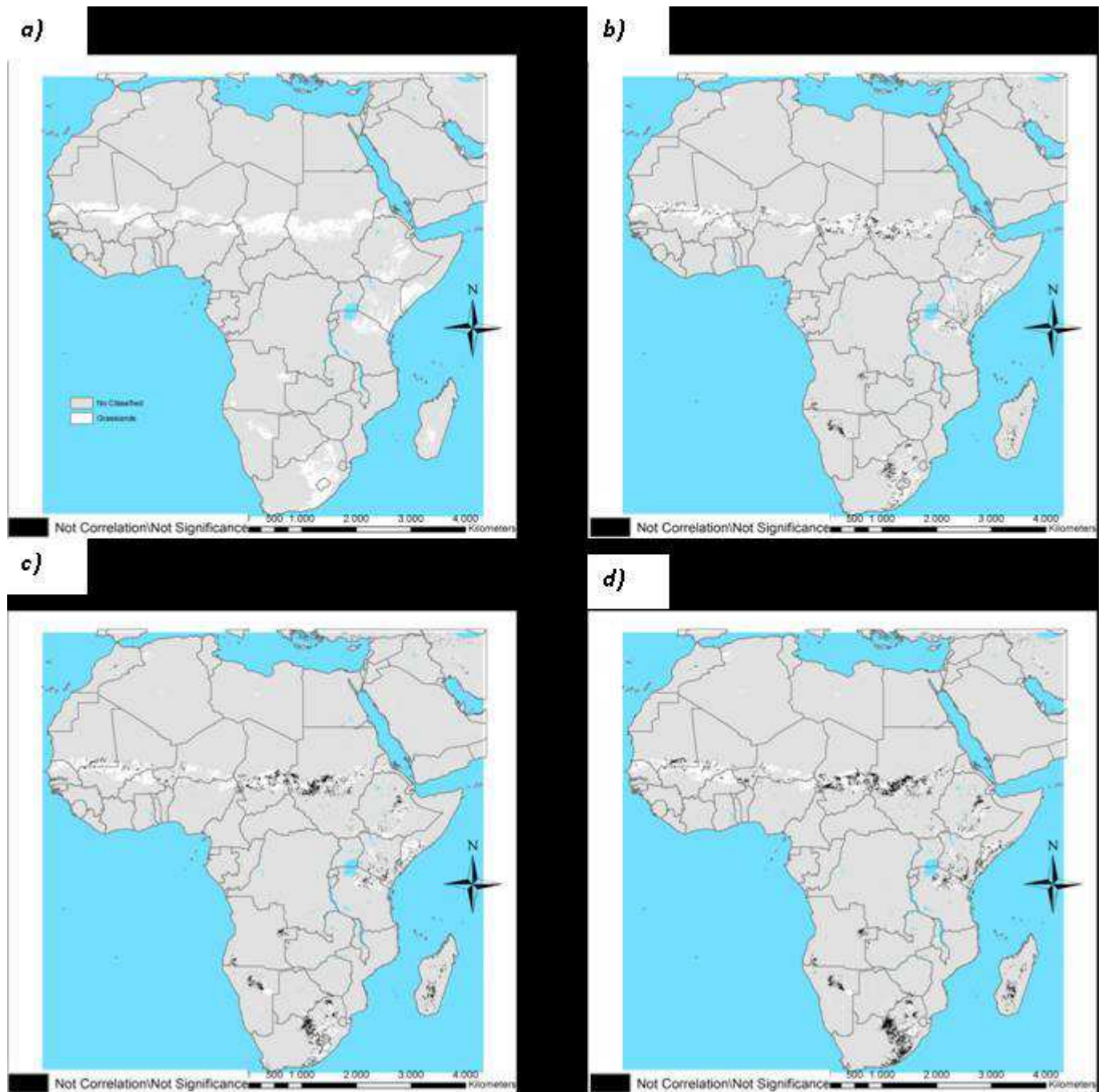


Figure 31. Outcomes of the Student t-test for the correlation between the Seasonal Small Integral (Sml) and cumulated rainfall (b) 1 month , c) 3 months d) 6 months) for the Grasslands vegetation type (a) in the second vegetation season

5.1.1.1. Second vegetation growing season

The 13.05 % of the area covered by Grasslands shows a yearly bi-modal NDVI function that correspond to the presence of two different vegetation growing seasons. The correlation analysis carried out between the cumulated rainfall (1, 3, 6 months) and the different phenological parameters related to the second growing season showed positive and significant values over a large portion of these areas (See Table 12).

As for the first season analysis, the largest areas with positive correlation coefficient values between all the phenological parameters and the cumulated rainfall are obtained considering 1 month as cumulating interval. Moreover, the smallest areas showing positive correlation coefficients correspond to the 6 months cumulating period (See Table 12).

Grassland	SEASON 2		
Phenological Parameter	TEST PASSED		
	TRMM 1 Month	TRMM 3 Months	TRMM 6 Months
Amp	86,57%	80,08%	70,01%
Base	73,90%	70,66%	60,12%
Decr	71,28%	54,41%	40,70%
Incr	70,31%	49,88%	34,30%
Larg	84,50%	80,51%	70,75%
Len	91,20%	85,69%	77,18%
Sml	96,41%	93,23%	85,68%

Table 12. Percentage of the Grasslands areas that passed the Student t-test for the correlation between cumulate rainfall and phenological parameters in the second vegetation growing season.

On the other hand, taking into consideration the different examined phenological parameters, the Seasonal Small Integral (SMI) presented, in all the cumulated periods, the largest percentage of area with positive correlation values with respect to the remaining parameters. The Amplitude (Amp) and the Large (Larg) parameters presented a similar behavior, characterized by an evident reduction of the areas showing positive correlation when considering the 6 month cumulated rainfall. This is in agreement with what was expected, given that these parameters are directly related. Finally, it can be noticed that also the Decrease (Decr) and the Increase (Incr) parameters presented considerable reduction if the 3 and 6 months cumulating periods are taken into consideration, with respect to the 1 month period.

Furthermore, it can be noticed that, for all the phenological parameters, the percentage values given in Table 12 are generally greater than those obtained for the first vegetation growing season. This is in agreement with what was expected, given that the area analysed for the significance test in this case is significantly reduced compared to the previous case and, more importantly, is practically concentrated in a single region of Africa (Horn of Africa, see Figure 32).

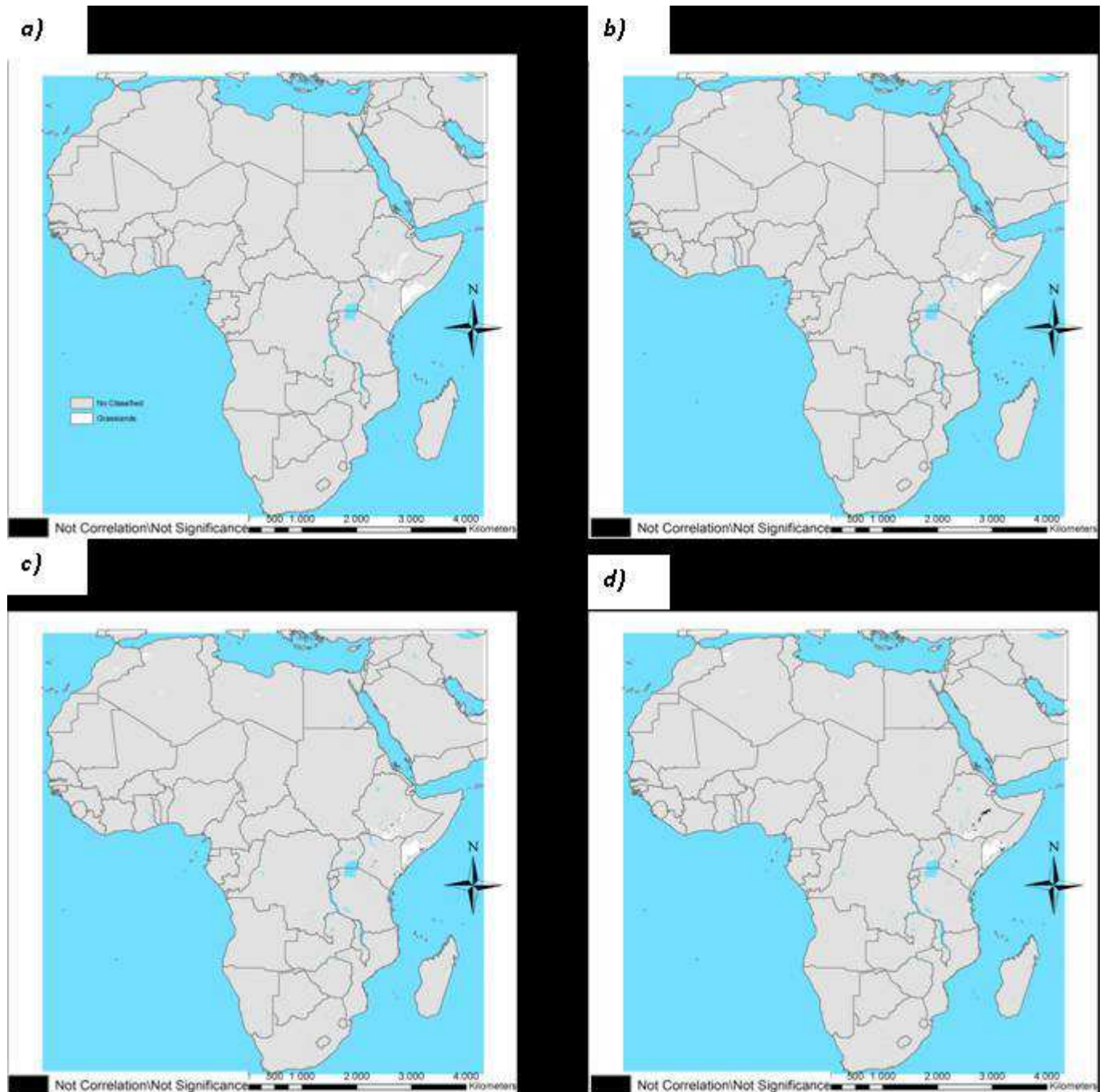


Figure 32. Outcomes of the Student t-test for the correlation between the Seasonal Small Integral (Smi) and cumulated rainfall (b) 1 month , c) 3 months d) 6 months) for the Grasslands vegetation type (a) in the second vegetation season

5.2.5. Croplands

5.2.5.1. First vegetation growing season

The Croplands land cover type corresponds to a 5.53 % of the vegetated area in the whole African continent, and the correlation coefficients calculated between the cumulated rainfall (1, 3, 6 months) and the different considered phenological parameters shows positive and significant values over a large portion of this area.

The largest areas with positive correlation coefficient values between all the phenological parameters and the cumulated rainfall are obtained considering 1 month as cumulating interval. Moreover, the smallest areas with positive correlation correspond to the 6 months cumulating period (See Table 13).

Cropland	SEASON 1		
Phenological Parameter	TEST PASSED		
	TRMM 1 Month	TRMM 3 Months	TRMM 6 Months
Amp	61,14%	51,60%	40,58%
Base	78,22%	73,49%	64,86%
Decr	58,79%	45,58%	29,01%
Incr	67,30%	50,96%	36,47%
Larg	64,42%	57,34%	46,93%
Len	80,96%	73,82%	63,36%
Sml	81,17%	73,88%	64,27%

Table 13. Percentage of the Cropland areas that passed the Student t-test for the correlation between cumulate rainfall and phenological parameters in the first vegetation growing season.

On the other hand, taking into consideration the different examined phenological parameters, the Seasonal Small Integral (SMI) presented, in all the cumulated periods, the largest percentage of area with positive correlation values with respect to the remaining parameters. The base of the season, the Length of the season(Len) and the Seasonal Small Integral parameters presented a similar behavior, characterized by an evident reduction of the areas showing positive correlation when considering the 6 month cumulated rainfall. The Amplitude (Amp) presented a small percentage of area with positive correlation values with respect to other vegetation class. Finally, it can be noticed that also the Decrease (Decr) and the Increase (Incr) parameters presented considerable reduction if the 3 and 6 months cumulating periods are taken into consideration, with respect to the 1 month period.

Moreover, with the aim to better understand the data given in Table 13, an analysis of the spatial distribution of the outcomes of the significance test was carried out (See Figure 33). Thus, in this case considering the different areas of Africa covered by croplands, it was observed that there is not a particular area where all the phenological parameters presented larger zones with no significant values of the correlation coefficient. These areas are presented specially in the 6 months cumulative interval.

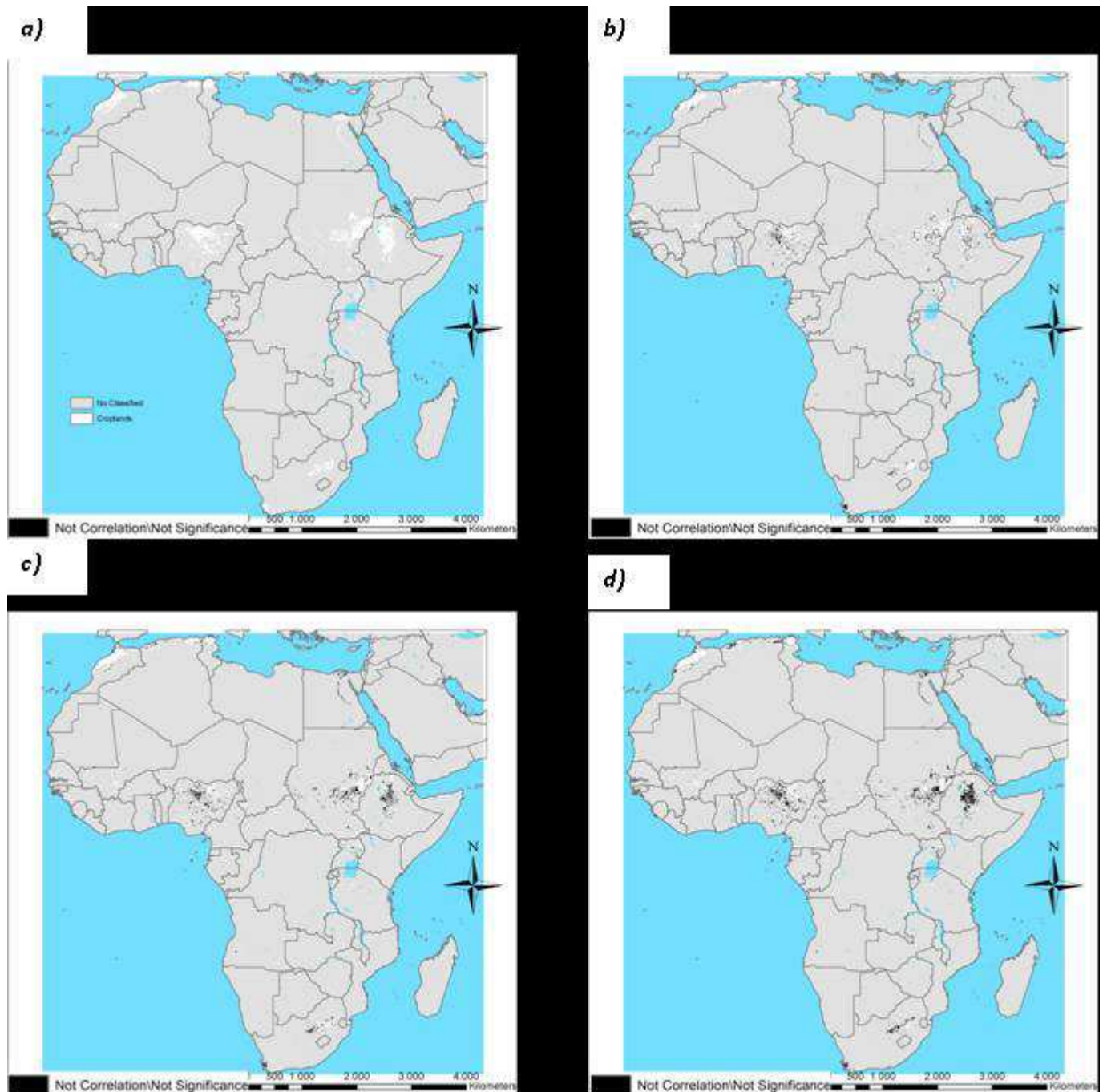


Figure 33. Outcomes of the Student t-test for the correlation between the Seasonal Small Integral (Smi) and cumulated rainfall (a) in the first vegetation season (b) 1 month , c) 3 months d) 6 months)

5.2.6. Cropland/Natural vegetation mosaic

5.2.6.1. First vegetation growing season

The Cropland/Natural vegetation mosaic land cover type corresponds to a 10.52 % of the vegetated area in the whole African continent, and the correlation coefficients calculated between the cumulated rainfall (1, 3, 6 months) and the different considered phenological parameters shows positive and significant values over a large portion of this area.

The largest areas with positive correlation coefficient values between all the phenological parameters and the cumulated rainfall are obtained considering 1 month as cumulating interval. Moreover, the smallest areas with positive correlation correspond to the 6 months cumulating period (See Table 14).

Crop/NatMos	SEASON 1		
Phenological Parameter	TEST PASSED		
	TRMM 1 Month	TRMM 3 Months	TRMM 6 Months
Amp	66,72%	53,69%	42,79%
Base	71,69%	64,23%	53,07%
Decr	62,07%	48,48%	35,39%
Incr	70,24%	52,03%	37,86%
Larg	69,24%	59,03%	48,89%
Len	78,09%	68,89%	58,50%
Sml	78,47%	69,34%	61,22%

Table 14. Percentage of the Cropland/Natural vegetation mosaic areas that passed the Student t-test for the correlation between cumulate rainfall and phenological parameters in the first vegetation growing season.

On the other hand, taking into consideration the different examined phenological parameters, the Seasonal Small Integral (SMI) presented, in all the cumulated periods, the largest percentage of area with positive correlation values with respect to the remaining parameters. The Seasonal Small Integral (SMI) and the Length of the season (Len) parameters presented a similar behavior, characterized by an evident reduction of the areas showing positive correlation when considering the 6 month cumulated rainfall. This is in agreement with what was expected, given that these parameters are directly related. Finally, it can be noticed that also the Decrease (Decr) and the Increase (Incr) parameters presented considerable reduction if the 3 and 6 months cumulating periods are taken into consideration, with respect to the 1 month period.

Moreover, with the aim to better understand the data given in Table 14, an analysis of the spatial distribution of the outcomes of the significance test was carried out (See Figure 31). Thus, considering the

different areas of Africa covered by Cropland/Natural vegetation mosaic, it was observed that the area where all the phenological parameters presented larger zones with no significant values of the correlation coefficient, is located in the east of the continent (specifically located in Uganda). This area present a particular climate classification regarding to the whole area classified such Cropland/Natural vegetation mosaic, this could be considered such a possible cause of lower values of the correlation coefficient, which require further investigations.

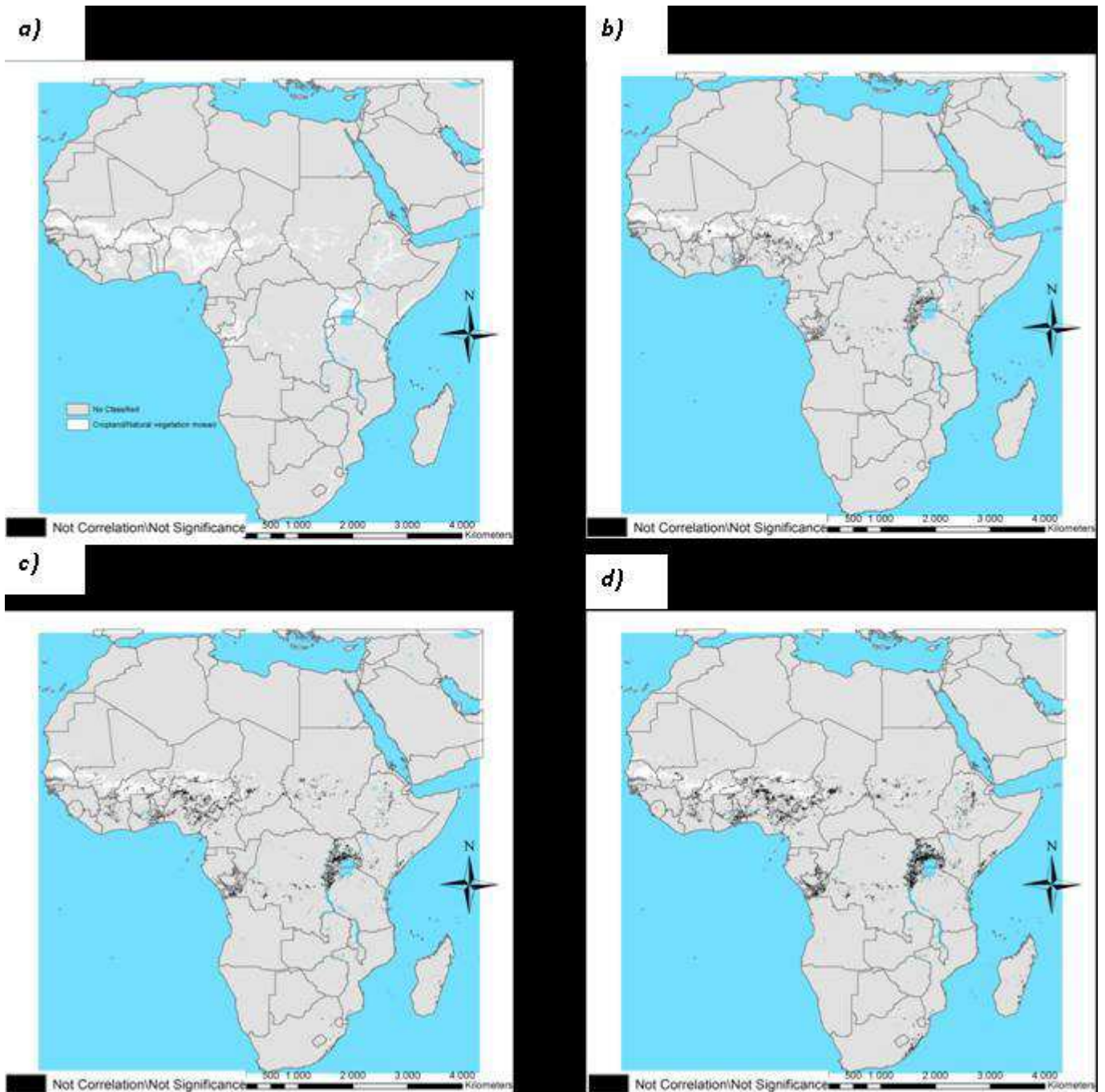


Figure 34. Outcomes of the Student t-test for the correlation between the Seasonal Small Integral (Sml) and cumulated rainfall (b) 1 month , c) 3 months d) 6 months) for the Cropland/Natural vegetation mosaic type (a) in the first vegetation season

5.1.1.1. Second vegetation growing season

The 10.05 % of the area covered by Cropland/Natural vegetation mosaic shows a yearly bi-modal NDVI function that correspond to the presence of two different vegetation growing seasons. The correlation analysis carried out between the cumulated rainfall (1, 3, 6 months) and the different phenological parameters related to the second growing season did not show positive and significant values over a large portion of these areas (See Table 15).

As for the first season analysis, the largest areas with positive correlation coefficient values between all the phenological parameters and the cumulated rainfall are obtained considering 1 month as cumulating interval. Moreover, the smallest areas showing positive correlation coefficients correspond to the 6 months cumulating period (See Table 15).

Crop/NatMos	SEASON 2		
	TEST PASSED		
Phenological Parameter	TRMM 1 Month	TRMM 3 Months	TRMM 6 Months
Amp	60,38%	40,72%	25,60%
Base	62,96%	53,95%	43,03%
Decr	63,92%	39,81%	32,37%
Incr	62,46%	37,13%	23,08%
Larg	59,85%	48,73%	37,89%
Len	67,10%	49,69%	36,31%
Sml	67,95%	50,06%	37,25%

Table 15. Percentage of the Cropland/Natural vegetation mosaic areas that passed the Student t-test for the correlation between cumulate rainfall and phenological parameters in the second vegetation growing season

On the other hand, taking into consideration the different examined phenological parameters, the Seasonal Small Integral (SMI) presented, in all the cumulated periods, the largest percentage of area with positive correlation values with respect to the remaining parameters. The Seasonal Small Integral (SMI) and the Length of the season (Len) parameters presented a similar behavior, characterized by an evident reduction of the areas showing positive correlation when considering the 6 month cumulated rainfall. This is in agreement with what was expected, given that these parameters are directly related. Finally, it can be noticed that also the Decrease (Decr) and the Increase (Incr) parameters presented considerable reduction if the 3 and 6 months cumulating periods are taken into consideration, with respect to the 1 month period.

Moreover, with the aim to better understand the data given in Table 15, an analysis of the spatial distribution of the outcomes of the significance test was carried out (See Figure 35). Thus, considering the different areas of Africa covered by Cropland/Natural vegetation mosaic in the second growing season, it

was observed that the area where all the phenological parameters presented larger zones with no significant values of the correlation coefficient is distributed uniformly in the whole area identified in this class. Considering the distribution and the larger areas with no significant values, it was concluded that this type of vegetation does not presented a dependence of the rainfall behavior in the second season.

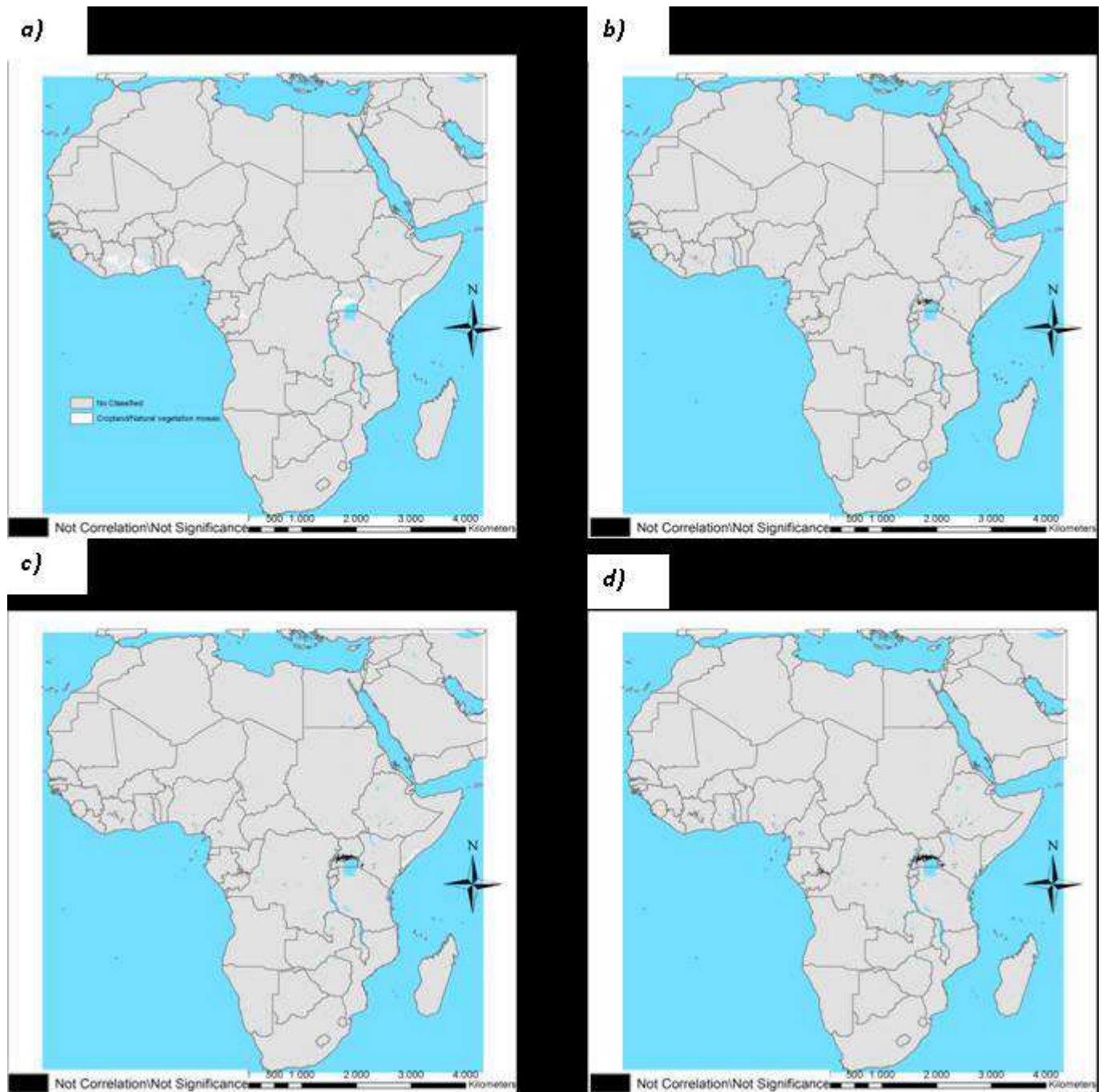


Figure 35. Outcomes of the Student t-test for the correlation between the Seasonal Small Integral (Smi) and cumulated rainfall (b) 1 month , c) 3 months d) 6 months) for the Cropland/Natural vegetation mosaic type (a) in the second vegetation season

5.3. Correlation Analysis

Based on the significance test outcomes described in the precedent paragraph, an analysis of the obtained correlation coefficients was conducted, with the main aim to identify the areas where a relationship between vegetation and cumulated rainfall exists. For this purpose, three intervals of correlation were defined in order to better describe the existing relationship in the analyzed areas: Medium Correlation (0.4-0.6), High Correlation (0.6-0.8) and Very High Correlation (0.8-1.0).

This kind of analysis was conducted for the Open shrublands, Grasslands and Cropland/Natural vegetation mosaic land cover types because of they are the classes that covered larger areas in the African continent and are characterized by a positive and significant values of correlation in all the phenological parameters considered in this study. For each analyzed land cover type, the different areas classified in the adopted intervals of correlation were identified and expressed as a percentage of the total area corresponding to the considered land cover class.

5.3.1. Open shrublands

The correlation coefficients calculated between the cumulated rainfall (1, 3, 6 months) and the different considered phenological parameters show positive and significant values over a large portion of the Open Shrublands area in the whole African continent.

Considering the Medium Correlation level, largest areas are in correspondence to 1 month cumulated rainfall for all the considered phenological parameters. Moreover, the smallest areas with the same correlation level correspond to the 6 months cumulating period (see Table 16).

Open Shrub	SEASON 1		
	Medium Correlation		
	TRMM 1 Month	TRMM 3 Months	TRMM 6 Months
Amp	31,92%	23,33%	20,52%
Base	35,60%	31,97%	29,73%
Decr	33,61%	26,12%	21,38%
Incr	32,32%	25,64%	22,35%
Larg	34,40%	26,48%	22,81%
Len	40,46%	33,56%	29,19%
Sml	32,75%	23,72%	22,21%

Table 16. Percentages of Open Shrublands areas showing Medium Correlation level between the phenological parameters and cumulated rainfall for the first growing season

On the other hand, the Length of the season (Len) parameter presents, for all the cumulating periods, the largest percentage of area with Medium Correlation level with respect to the remaining parameters; on the contrary, the Amplitude (Amp) parameter presents, in all the cumulated periods, the smallest percentage of area.

Comparing the percentages obtained for the High Correlation level with those related to the Medium Correlation one, the Increase (Incr) and the Seasonal Small Integral (Smi) parameters present an increase considering all the rainfall cumulating intervals. On the other hand, the percentage values obtained for the Base, Decrease (Decr) and Length of the season (Len) parameters present a notable reduction. The Amplitude (Amp) and the Large (Larg) parameters present a similar behavior, characterized by a reduction if the 1 month cumulating interval is considered, and an increase in the remaining cases. (see Table 17).

Open Shrub	SEASON 1		
Phenological Parameter	High Correlation		
	TRMM 1 Month	TRMM 3 Months	TRMM 6 Months
Amp	30,89%	27,36%	24,93%
Base	30,48%	29,05%	25,32%
Decr	28,86%	23,47%	19,21%
Incr	34,27%	26,97%	21,79%
Larg	27,65%	27,85%	25,67%
Len	32,11%	31,83%	24,71%
SMI	40,30%	38,23%	32,64%

Table 17. Percentages of Open Shrublands areas showing High Correlation level between the phenological parameters and cumulated rainfall for the first growing season

Finally, considering the areas showing Very High Correlation levels, it can be noticed that the Seasonal Small Integral (Smi) and the Amplitude (Amp) parameters present similar behavior, characterized by large percentages of area in correspondence of the 3 and 6 months rainfall cumulating intervals (See Table 18). The areas showing Very High Correlation levels may be considered, with particular prudence, areas where the examined land cover type presents some vulnerability to rainfall anomalies.

Open Shrub	SEASON 1		
Phenological Parameter	Very High Correlation		
	TRMM 1 Month	TRMM 3 Months	TRMM 6 Months
Amp	4,72%	10,54%	10,82%
Base	2,37%	4,31%	3,40%
Decr	4,04%	4,40%	3,54%
Incr	5,31%	5,12%	3,88%
Larg	2,72%	6,79%	7,53%
Len	2,14%	2,93%	2,07%
SMI	4,95%	11,32%	12,29%

Table 18. Percentages of Open Shrublands areas showing Very High Correlation level between the phenological parameters and cumulated rainfall for the first growing season

In accordance with this hypothesis, it can be stated that the Seasonal Small Integral (Smi) parameter presents a condition of vulnerability higher respect to the remaining parameters, as described Figure 36.

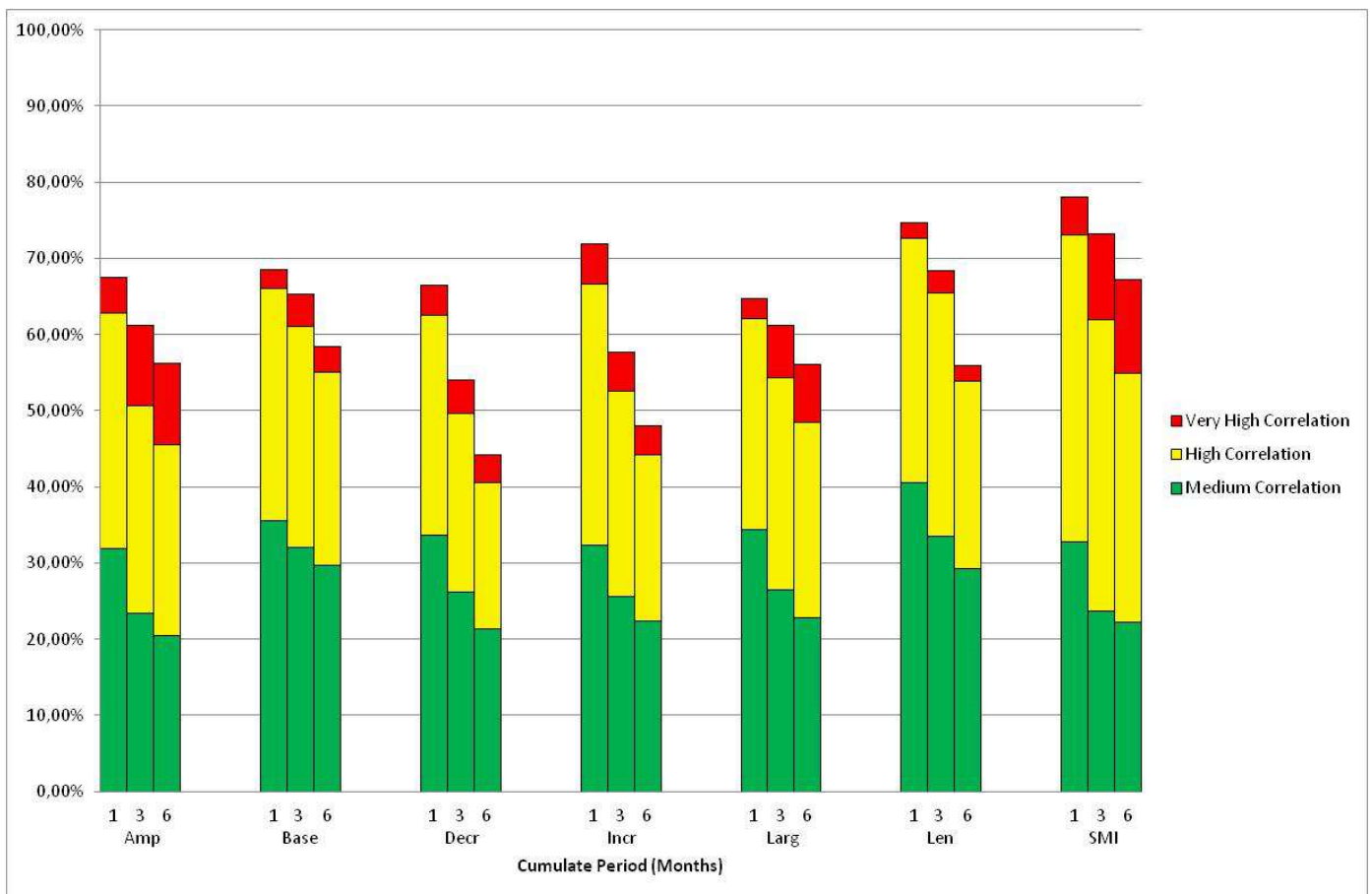


Figure 36. Correlation Analysis for the Open Shrubland land cover type, first growing season

5.3.2. Grasslands

The correlation coefficients calculated between the cumulated rainfall (1, 3, 6 months) and the different considered phenological parameters show positive and significant values over a large portion of the Grasslands area in the whole African continent

Considering the Medium Correlation level, largest areas are in correspondence to 1 month cumulated rainfall for all the considered phenological parameters. Moreover, the smallest areas with the same correlation level correspond to the 6 months cumulating period (See Table 19).

Grassland	SEASON 1		
	Medium Correlation		
	TRMM 1 Month	TRMM 3 Months	TRMM 6 Months
Amp	37,53%	29,15%	26,00%
Base	39,76%	33,00%	30,72%
Decr	33,03%	25,85%	22,21%
Incr	35,36%	29,08%	24,25%
Larg	38,65%	30,09%	27,41%
Len	38,91%	32,22%	29,89%
SMI	37,54%	30,39%	28,56%

Table 19. Percentages of Grasslands areas showing Medium Correlation level between the phenological parameters and cumulated rainfall for the first growing season

On the other hand, the Base parameter presents, for all the cumulating periods, the largest percentage of area with Medium Correlation level with respect to the remaining parameters; on the contrary, the Decrease (Decr) parameter presents, in all the cumulated periods, the smallest percentage of area.

Comparing the percentages obtained for the High Correlation level with those related to the Medium Correlation one, the Length of the season (Len) and the Seasonal Small Integral (Smi) parameters present an increase considering all the rainfall cumulating intervals. On the other hand, the percentage values obtained for the Amplitude(Amp), Base, Decrease (Decr), Increase (Incr) and Large (Large) parameters present a notable reduction. (See Table 20).

Grassland	SEASON 1		
Phenological Parameter	High Correlation		
	TRMM 1 Month	TRMM 3 Months	TRMM 6 Months
Amp	26,92%	25,35%	22,55%
Base	31,21%	29,85%	28,46%
Decr	24,16%	18,64%	14,11%
Incr	29,56%	18,69%	13,53%
Larg	26,73%	26,21%	23,99%
Len	40,17%	39,45%	32,88%
SMI	42,81%	41,84%	36,77%

Table 20. High Percentages of Grasslands areas showing High Correlation level between the phenological parameters and cumulated rainfall for the first growing season

Finally, considering the areas showing Very High Correlation levels, it can be noticed that the Seasonal Small Integral (Smi) and the Length of the season (Len) parameters present similar behavior, characterized by large percentages of area in correspondence of the 3 and 6 months rainfall cumulating intervals (See Table 21). The areas showing Very High Correlation levels may be considered, with particular prudence, areas where the examined land cover type presents some vulnerability to rainfall anomalies.

Grassland	SEASON 1		
Phenological Parameter	Very High Correlation		
	TRMM 1 Month	TRMM 3 Months	TRMM 6 Months
Amp	1,42%	2,86%	2,75%
Base	2,10%	3,10%	3,26%
Decr	2,74%	2,14%	0,97%
Incr	2,66%	1,43%	0,90%
Larg	1,33%	2,62%	2,76%
Len	3,17%	4,76%	3,70%
SMI	3,72%	6,63%	6,36%

Table 21. Percentages of Grasslands areas showing Very High Correlation level between the phenological parameters and cumulated rainfall for the first growing season

In accordance with this hypothesis, it can be stated that the Seasonal Small Integral (Smi) parameter presents a condition of vulnerability higher respect to the remaining parameters, as described Figure 37.

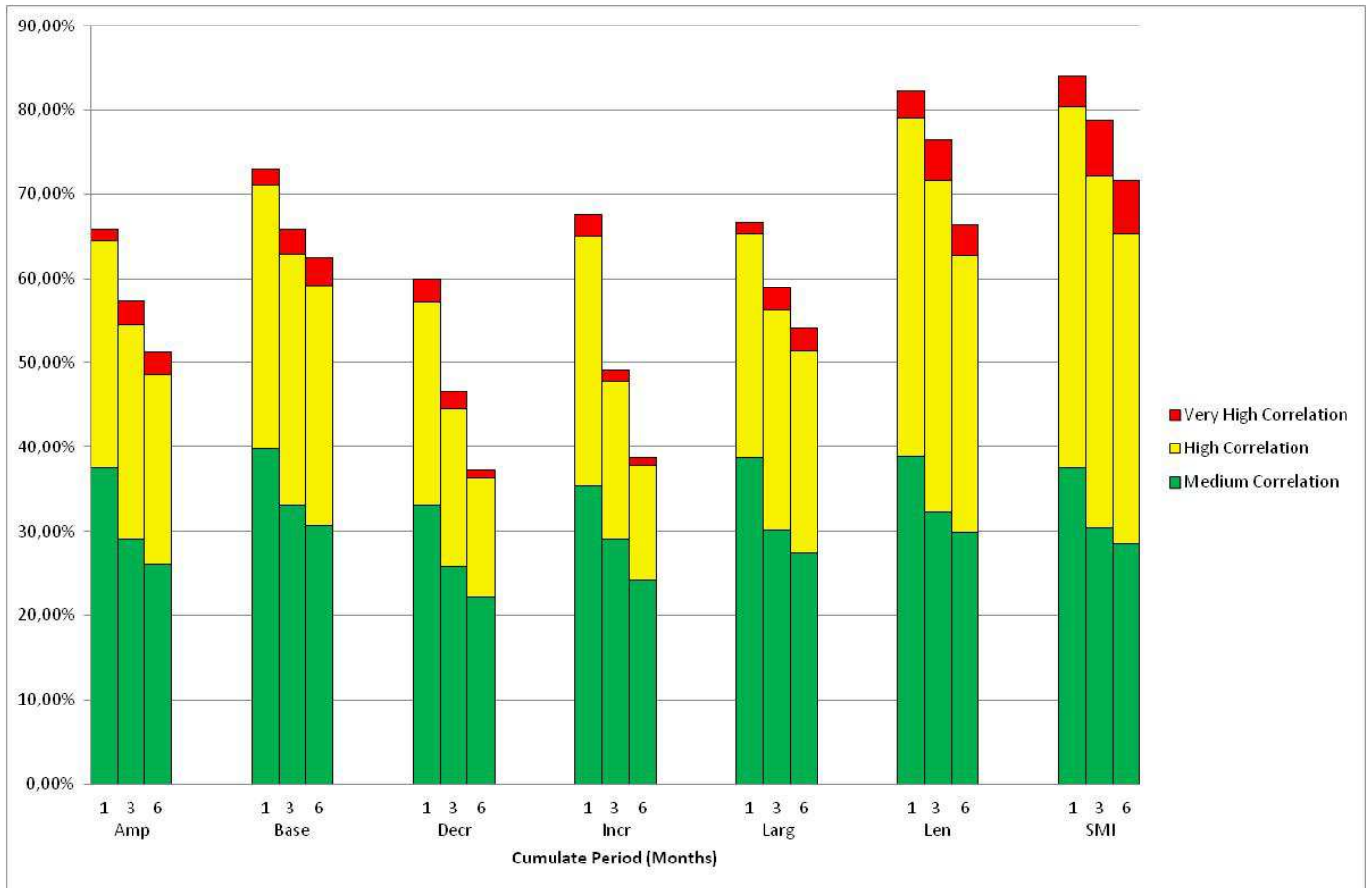


Figure 37. Correlation Analysis for the Grasslands land cover type, first growing season

5.3.3. Cropland/Natural vegetation mosaic

The correlation coefficients calculated between the cumulated rainfall (1, 3, 6 months) and the different considered phenological parameters show positive and significant values over a large portion of the Cropland/Natural vegetation mosaic area in the whole African continent.

Considering the Medium Correlation level, largest areas are in correspondence to 1 month cumulated rainfall for all the considered phenological parameters. Moreover, the smallest areas with the same correlation level correspond to the 6 months cumulating period (See Table 22).

Crop/NatMos	SEASON 1		
	Medium Correlation		
	TRMM 1 Month	TRMM 3 Months	TRMM 6 Months
Amp	40,73%	31,50%	25,25%
Base	41,22%	35,41%	29,42%
Decr	36,06%	29,10%	22,38%
Incr	36,56%	30,03%	23,37%
Larg	41,18%	33,02%	27,44%
Len	39,97%	33,02%	28,70%
SMI	38,05%	29,23%	25,38%

Table 22. Percentages of Cropland/Natural vegetation mosaic areas showing Medium Correlation level between the phenological parameters and cumulated rainfall for the first growing season

On the other hand, the Base parameter presents, for all the cumulating periods, the largest percentage of area with Medium Correlation level with respect to the remaining parameters; on the contrary, the Decrease (Decr) parameter presents, in all the cumulated periods, the smallest percentage of area.

Comparing the percentages obtained for the High Correlation level with those related to the Medium Correlation one, the Seasonal Small Integral (Smi) parameter presents an increase considering all the rainfall cumulating intervals. On the other hand, the percentage values obtained for the Length of the season (Len) parameter present a larger percentage of area with high correlation respect to the remaining parameters (See Table 23).

Crop/NatMos	SEASON 1		
Phenological Parameter	High Correlation		
	TRMM 1 Month	TRMM 3 Months	TRMM 6 Months
Amp	24,88%	20,84%	16,39%
Base	29,03%	27,14%	22,05%
Decr	23,95%	17,86%	12,24%
Incr	30,36%	20,37%	13,56%
Larg	26,73%	24,33%	19,81%
Len	35,88%	32,82%	27,20%
SMI	37,59%	35,31%	30,88%

Table 23. High Percentages of Cropland/Natural vegetation mosaic areas showing High Correlation level between the phenological parameters and cumulated rainfall for the first growing season

Finally, considering the areas showing Very High Correlation levels, it can be noticed that the Seasonal Small Integral (Smi) and the Length of the season (Len) parameters present similar behavior, characterized by large percentages of area in correspondence of the 3 and 6 months rainfall cumulating intervals (See Table 24). The areas showing Very High Correlation levels may be considered, with particular prudence, areas where the examined land cover type presents some vulnerability to rainfall anomalies.

Crop/NatMos	SEASON 1		
Phenological Parameter	Very High Correlation		
	TRMM 1 Month	TRMM 3 Months	TRMM 6 Months
Amp	1,11%	1,35%	1,15%
Base	1,45%	1,69%	1,60%
Decr	2,07%	1,52%	0,77%
Incr	3,33%	1,62%	0,93%
Larg	1,33%	1,69%	1,64%
Len	2,23%	3,05%	2,60%
SMI	2,83%	4,80%	4,96%

Table 24. Percentages of Cropland/Natural vegetation mosaic areas showing Very High Correlation level between the phenological parameters and cumulated rainfall for the first growing season

In accordance with this hypothesis, it can be stated that the Seasonal Small Integral (Smi) parameter presents a condition of vulnerability higher respect to the remaining parameters, as described Figure 38.

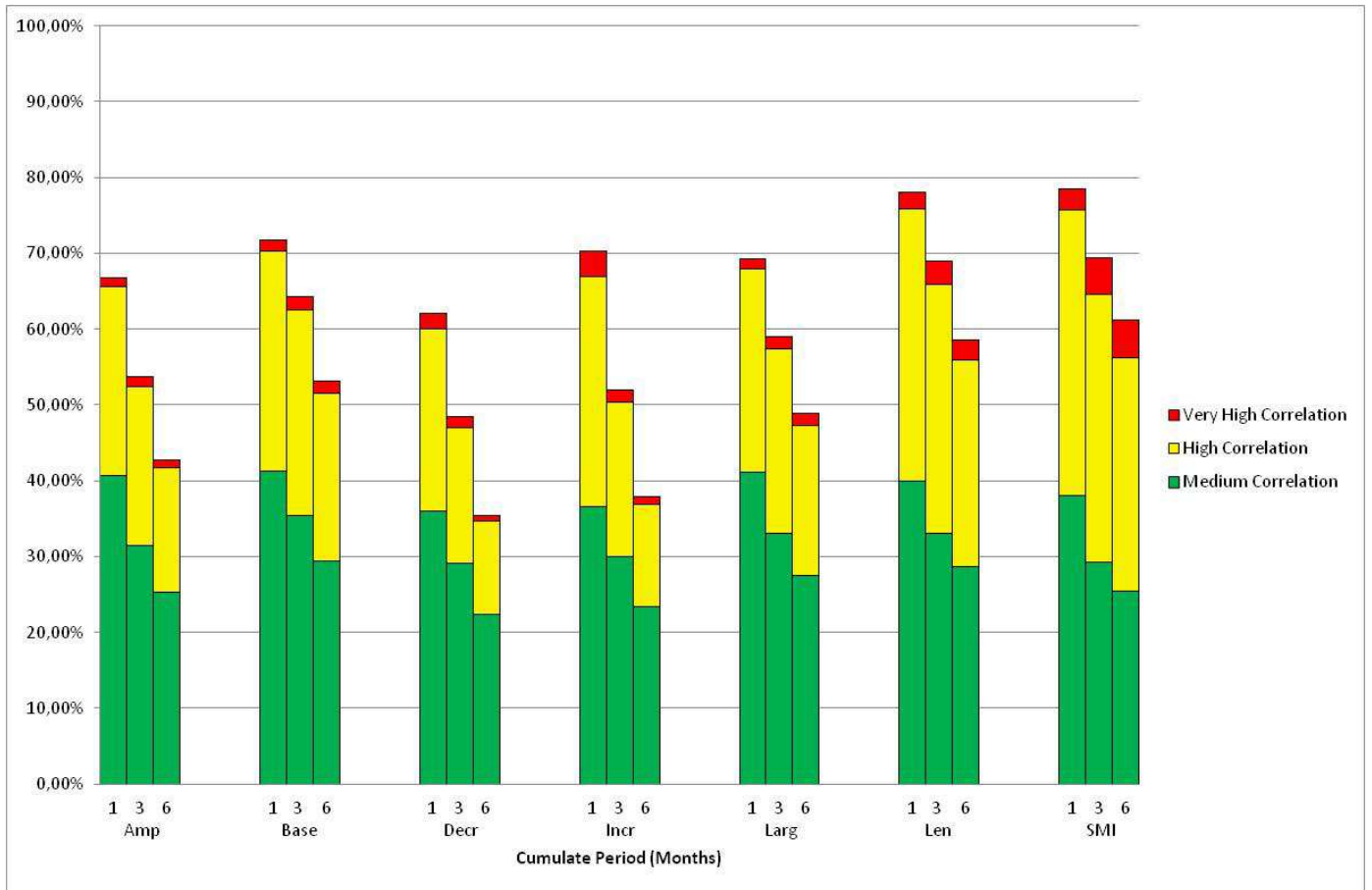


Figure 38. Correlation Analysis for the Cropland/Natural vegetation mosaic land cover type, first growing season

5.4. Integration Analysis

With the aim to better investigate and summarize the results of the correlation analysis, described in the precedent paragraph, a spatial correlation analysis was conducted using the correlation intervals already defined and the cumulative rainfall intervals corresponding to the maximum values of correlation.

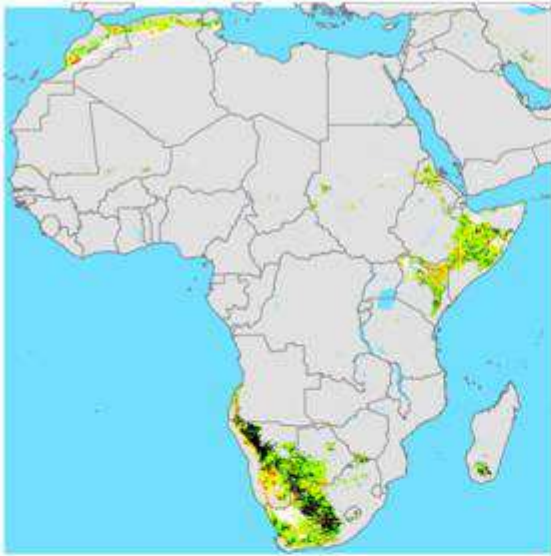
In addition, using the percentages of the areas classified in the different correlation levels for each vegetation land cover type, an integrated index was calculated with the purpose to assign a level of possible vulnerability to each land cover type. Finally, the cumulating rainfall interval corresponding to the maximum vulnerability value, was identified and a dataset integrating the two parameters, was generated.

5.4.1. Spatial Correlation Analysis

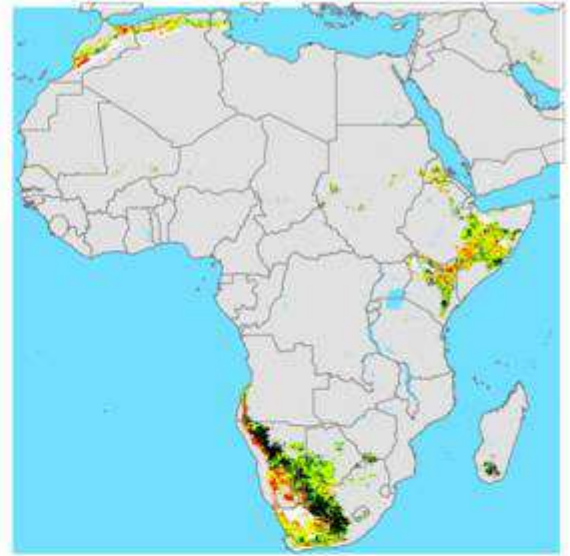
Considering the maximum values of the correlation coefficients calculated for each vegetation land cover type between the phenological parameters and the different cumulated rainfalls and with the aim to use this information for the purposes of the ITHACA Drought EWS, a spatial analysis was implemented on a pixel basis in the whole African continent. For this analysis, each pixel is classified according to the correlation interval levels defined in the precedent paragraph.

In particular, the analysis was implemented considering all the examined rainfall cumulating intervals (see Figure 39) with the main purpose to identify the areas characterized by different levels of correlation and, consequently, different levels of possible vulnerability. The final dataset produced in this phase was a map containing the weights to be applied to the rainfall alerts generated in near real-time in the ITHACA Drought EWS, before their integration with the vegetation based alerts.

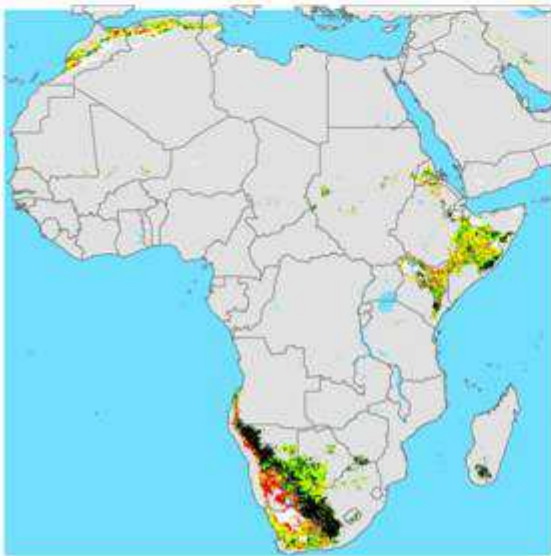
a)



b)



c)



Correlation Level

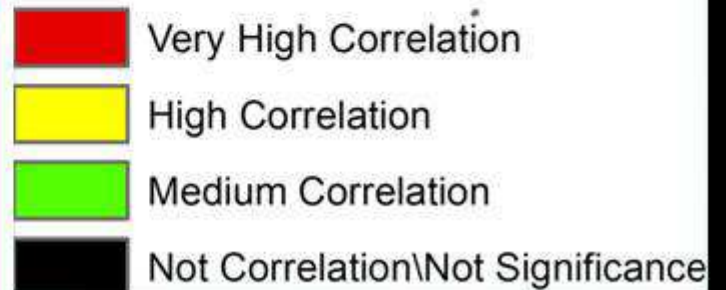


Figure 39. Maps showing the Maximum Correlation levels for the Seasonal Small Integral (Smi) on a pixel basis for each cumulating intervals (a) 1 month, b) 3 months, c) 6months) for the Open shrublands vegetation land cover type (first growing season)

In addition, a comparative analysis was conducted, for each vegetation land cover type, in order to identify, on a pixel basis, the examined rainfall cumulating interval that corresponds to the obtained absolute maximum value of correlation. The output of this analysis showed the maximum correlation to be reached for each area in the whole African continent, classified considering the already discussed correlation levels. Finally, the rainfall cumulating interval corresponding to each maximum absolute correlation value, evaluated on a pixel basis, allowed to identify the proper rainfall cumulating interval to be used for near real-time SPI calculation in the ITHACA drought EWS (see Figure 40)

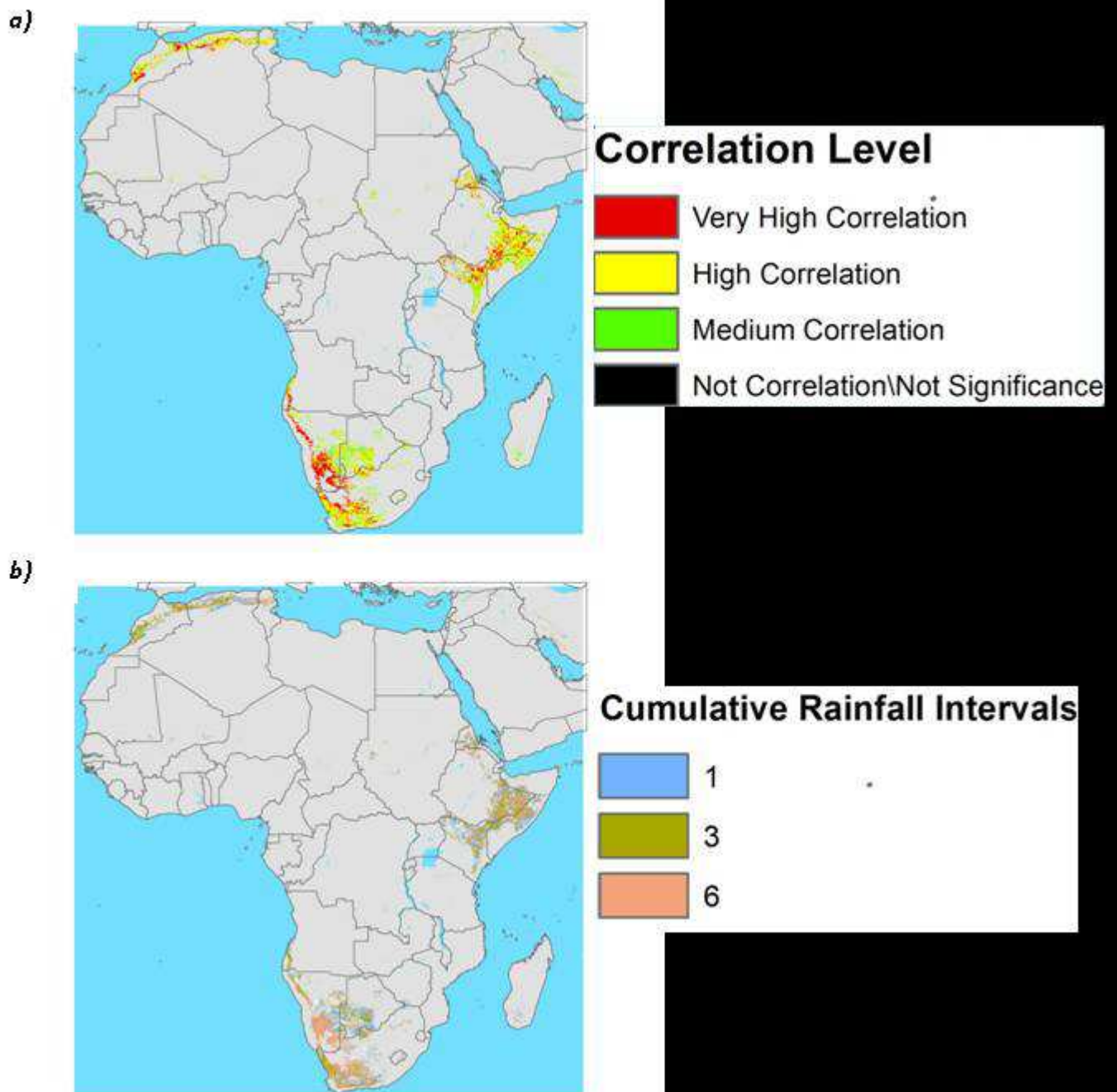


Figure 40.a) Maximum Absolute Correlation levels for the Seasonal Small Integral (Sml) on a pixel basis for the Open shrublands vegetation cover type for the first growing season, b) rainfall cumulating intervals corresponding to the absolute maximum correlation level for the Seasonal Small Integral (Sml) on a pixel basis for the Open shrublands vegetation cover type for the first growing season

5.4.2. Vulnerability Analysis.

As already discussed, for some land cover classes high correlation values may indicate, with prudence, a greater vulnerability to the vegetation to rainfall anomalies. Therefore, with the aim to carry out a preliminary investigation about the vulnerability of the vegetation to the cumulated rainfall, a vulnerability index was defined based on the correlation levels described in the precedent paragraph. Outcomes obtained in this phase were used to propose recommendations to be applied in the existing ITHACA Drought EWS.

Considering that obtained correlation values were classified into three intervals, in order to propose a vulnerability index a scale between 0 and 3 was selected. In this scale, the value 0 was adopted as the minimum value, that corresponds to the areas where not significant correlation values are found, the value 1 was adopted as the value of vulnerability index corresponding to a Medium Correlation level, while the values 2 and 3 were used for the High and Very High Correlation levels, respectively.

The proposed index was calculated for all examined vegetation land cover types, generating an index for all selected phenological parameters and rainfall cumulating intervals. A value of vulnerability between 0 and 3 was calculated starting from Tables discussed in 5.3 using the following formula:

$$V_{ij} = 1W_{Mij} + 2W_{Hij} + 3W_{VHij}$$

where,

V_{ij} = Vulnerability index for each phenological parameter i and for each cumulative rainfall interval j .

W_{Mij} = Weight assigned to the areas classified in the medium correlation interval for each phenological parameter i and for each cumulative rainfall interval j .

W_{Hij} = Weight assigned to the areas classified in the high correlation interval for each phenological parameter i and for each cumulative rainfall interval j .

W_{VHij} = Weight assigned to the areas classified in the very high correlation interval for each phenological parameter i and for each cumulative rainfall interval j .

The calculation of the proposed vulnerability index allowed to integrate the outcomes of all the previous phases, related to the significance test and the correlation analysis, and is used in order to make a complex evaluation of the existing relationship between vegetation and rainfall dynamics. In particular, in this study, for each vegetation land cover type the vulnerability index corresponding to all examined phenological parameters were calculated and assigned to all the pixels in the whole African continent belonging in the same vegetation class.

Considering the Open Shrubland land cover type, the study of the vulnerability index revealed that the parameter that is the most vulnerable to rainfall anomalies among the examined phenological parameters, is the Seasonal Small Integral (Sml), and that, in this case, the highest vulnerability coefficient value is obtained considering a 3 months rainfall cumulating interval. In addition, it can be noticed that all the phenological parameters present a vulnerability index close to the value corresponding to the Medium Correlation level (See Table 25).

Open_Shrubland_Season1	Vulnerability Index		
Phenological Parameters	TRMM 1 Month	TRMM 3 Months	TRMM 6 Months
Amp	1,079	1,097	1,028
Base	1,037	1,030	0,906
Decr	1,034	0,863	0,704
Incr	1,168	0,949	0,776
Larg	0,979	1,026	0,967
Len	1,111	1,060	0,848
SMI	1,282	1,341	1,244

Table 25. Vulnerability Index for the phenological parameters using different rainfall cumulating intervals for the Open Shrubland land cover type and for the first growing season.

Considering the Grasslands land cover type, the study of the vulnerability index revealed that the parameter that is the most vulnerable to rainfall anomalies among the examined phenological parameters, is the Seasonal Small Integral (Sml), and that, in this case, the highest vulnerability coefficient value is obtained considering a 1 month rainfall cumulating interval. In addition, it can be noticed that all the phenological parameters present a vulnerability index close to the value corresponding to the Medium Correlation level (See Table 26).

Grasslands_Season1	Vulnerability Index		
Phenological Parameters	TRMM 1 Month	TRMM 3 Months	TRMM 6 Months
Amp	0,956	0,884	0,793
Base	1,085	1,020	0,974
Decr	0,896	0,696	0,533
Incr	1,025	0,708	0,540
Larg	0,961	0,904	0,837
Len	1,288	1,254	1,068
SMI	1,343	1,340	1,212

Table 26. Vulnerability Index for the phenological parameters using different rainfall cumulating intervals for the Grasslands Vegetation cover type and for the first growing season.

Considering the Open Shrubland land cover type, the study of the vulnerability index revealed that the parameter that is the most vulnerable to rainfall anomalies among the examined phenological parameters, is the Seasonal Small Integral (Smi), and that, in this case, the highest vulnerability coefficient value is obtained considering a 1 month rainfall cumulating interval. In addition, it can be noticed that all the phenological parameters present a vulnerability index close to the value corresponding to the Medium Correlation level. On the other hand, the Amplitude (Amp), the Decrease (Decr) and the Increase (Incr) presented lower values of vulnerability in the cumulative intervals corresponding to 1 and 3 months (See Table 27).

Crop/Nat_Veg_Mos_Season1	Vulnerability Index		
Phenological Parameters	TRMM 1 Month	TRMM 3 Months	TRMM 6 Months
Amp	0,938	0,772	0,615
Base	1,036	0,947	0,783
Decr	0,902	0,694	0,492
Incr	1,073	0,756	0,533
Larg	0,986	0,867	0,720
Len	1,184	1,078	0,909
SMI	1,217	1,143	1,020

Table 27. Vulnerability Index for the phenological parameters using different rainfall cumulating intervals for the Cropland/Natural vegetation mosaic cover type and for the first growing season.

With the aim to convert the results obtained in this study into effective suggestions for the integration of rainfall data into the ITHACA drought EWS, a dataset showing, for each analyzed land cover class, the maximum vulnerability index for each phenological parameter and the corresponding rainfall cumulating interval, was generated for the whole African continent (see Figure 41). This information may help, indeed, to correctly identify, for each type of land cover, the rainfall cumulating interval to be used for the purposes of inclusion in the ITHACA Drought EWS of effective procedures for near real-time SPI calculation. Moreover, the vulnerability values, obtained for each land cover class, may be used in order to allow a preliminary weight operation of the alerts generated using the rainfall anomalies index.

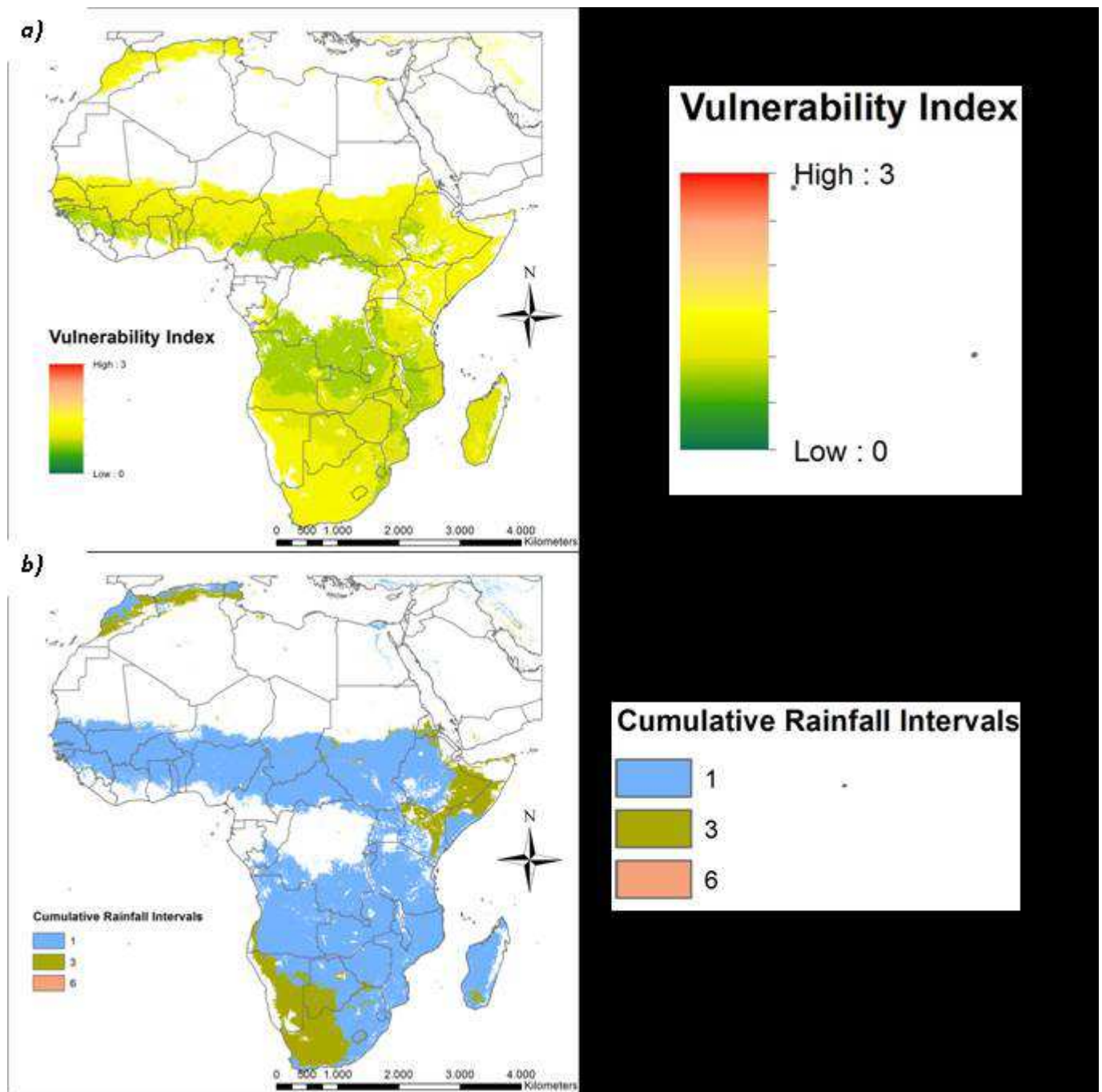


Figure 41. a) Maximum vulnerability Index identified for the whole African continent, for the Seasonal Small Integral (Smi) in the first growing season, and b) corresponding rainfall cumulating interval..

6. CONCLUSIONS AND RECOMMENDATION

The first purpose of this study was to complete the existing ITHACA drought EWS, based on the monitoring of vegetation conditions based on phenological parameters, introducing proper procedures able to monitor rainfall conditions in near real-time. Consequently, considering the available precipitation datasets the Standardized Precipitation Index (SPI) was selected as the parameter to identify the possible meteorological drought events directly related with the rainfall. Proper procedures for the calculation of the SPI on a global scale for different cumulative rainfall intervals have been implemented.

Furthermore, a research has been conducted to identify the possible relationships between vegetation and rainfall in the whole Africa through a correlation analysis of several phenological vegetation parameters and the cumulated rainfall corresponding to the cumulative intervals of 1, 3 and 6 months. The main purpose of this step of the study was to identify the areas and the parameters that correctly support the planning and definition of effective procedures for the integration, where it is meaningful, of the vegetation monitoring procedures and the rainfall anomalies calculated through the SPI in the final ITHACA drought EWS. Obviously, due to the simplifications related to the resolution of spatial data used for the conducted analysis (0.05 deg), final recommendations and operative proposals may need further validation on a regional scale using also local datasets, where available.

In order to implement the research and considering the impacts that the drought events generate in the population, the whole African continent was selected as study area. First of all, a preliminary analysis aimed at identifying the areas where the results of the vegetation monitoring activities proposed in the ITHACA drought EWS are produced with insufficient reliability, was conducted. Then, an analysis of the land cover dataset was performed. In particular, considering the spatial distribution of the land cover types and the spatial resolution of the datasets used in this study (0.05 deg), the *Croplands*, *Grasslands*, *Savannas*, *Woody Savannas*, *Open Shrublands* and *Cropland/Natural Vegetation Mosaic* classes were selected for the subsequent correlation analyses proposed in this study.

A preliminary test of statistical significance of the correlation values obtained has been carried out. The main outcome of this test was the identification of the rainfall cumulating interval, specifically the 1 month interval, that produced larger areas with positive and significant correlation values for all the examined phenological parameters and land cover classes. Consequently, the monitoring of rainfall anomalies calculated using the 1 month SPI, which presents a higher likelihood to be the correct and effective information to be used in order to complete the vegetation conditions monitoring, has been initially proposed for its use in the ITHACA drought EWS. In addition, for the *Woody Savannas* and *Savannas* land cover types considerable areas with significant and positive correlation values could not be identified,

therefore it can be expected that, in these areas, the alerts generated through the vegetation monitoring would be independent to the rainfall anomalies.

Based on the outcomes of the test of statistical significance, a correlation analysis was conducted. The vegetation Seasonal Small Integral (Sml) and the Length of the growing Season (Len) phenological parameters were found to be the more correlated for all the examined vegetation land cover types. In addition, it was observed that the level of correlation of the Base, Amplitude (Amp) and Increase (Incr) phenological parameters depends of the considered vegetation land cover type. In particular, in the Increase parameter case, the correlation level decreases considerably considering a 6 months rainfall cumulating interval. On the other hand, the decrease (Decr) parameter presents the lower correlation values for all the vegetation land cover type. Therefore, through results obtained in this phase, it was possible to confirm the effectiveness of the use of the vegetation Seasonal Small Integral (Sml) parameter for drought early warning purposes. However, it was also proposed to investigate, in the future, the possible use of the Length of the growing Season (Len) as an alternative vegetation parameter or as a possible linked parameter between the rainfall and the vegetation.

Moreover, it was observed that the *Grasslands* and the *Open Shrublands* land cover classes presented, as a whole, the higher correlation values considering all the phenological parameters, except in the southern regions of the Africa, where large areas without significant correlations have been identified. However, the *Grasslands* land cover class presented large areas with high correlation values in the Horn of Africa area. In this area, this vegetation type shown to be directly correlated with the rainfall behavior in both the existing vegetation growing seasons.

Considering that, for some land cover classes, the obtained high correlation values may indicate, with prudence, a greater vulnerability to the vegetation to rainfall anomalies, a proper Vulnerability Index has been defined based on the different correlation levels found for each examined land cover class and investigated. The highest values of this index were found to be in correspondence to the 1month and 3 months rainfall cumulating intervals. Specifically, the areas that showed the highest values in correspondence to the 3 months rainfall cumulating interval are located in the south of the African continent (specifically, in the area that extends between the Botswana, Namibia and South Africa countries) and in the Horn of Africa, while the remaining areas presented highest values of vulnerability in correspondence to the 1 month rainfall cumulating interval.

Therefore, considering these results, it was proposed the possibility to use, in the ITHACA drought EWS, the developed Vulnerability Index in order to weight rainfall anomalies detected using the SPI, before the production of the final drought hazard dataset, which will be based on vegetation and precipitation anomalies detected in near real-time. In addition, based on the analysis of the Vulnerability Index, were also definitely identified and proposed, for each land cover type, the rainfall cumulating intervals (1, 3 or 6 months) to be correctly and effectively used for SPI calculation purposes, in order to complete the vegetation conditions monitoring.

7. REFERENCES

- [1] D. Wilhite, "Drought monitoring and early warning: Concepts, progress and future challenges," *World Meteorol. Organ. WMO*, 2006.
- [2] C. Shisanya, C. Recha, and A. Anyamba, "Rainfall variability and its impact on normalized difference vegetation index in arid and semi-arid lands of Kenya," *Int. J. ...*, 2011.
- [3] S. Rousvel, N. Armand, L. Andre, and S. Tengelen, "Comparison between vegetation and rainfall of bioclimatic ecoregions in central Africa," *Atmosphere (Basel)*., 2013.
- [4] T. Hilker and A. Lyapustin, "Vegetation dynamics and rainfall sensitivity of the Amazon," *Proc. ...*, 2014.
- [5] S. M. Herrmann, A. Anyamba, and C. J. Tucker, "Recent trends in vegetation dynamics in the African Sahel and their relationship to climate," *Glob. Environ. Chang.*, vol. 15, no. 4, pp. 394–404, Dec. 2005.
- [6] I. Angeluccetti, A. Demarchi, and F. Perez, "Vulnerability analysis for a drought Early Warning System," *EGU Gen. Assem. 2014*, vol. 16, no. i, p. 7525, 2014.
- [7] L. Eklundha and P. Jönssonb, "TIMESAT 3.1 software manual," *Lund Univ. Sweden*, 2012.
- [8] F. Perez, "The ITHACA Early Warning System for drought monitoring: first prototype test for the 2010 Sahel crisis," *Ital. J. Remote Sens.*, vol. 44, no. 1, pp. 181–195, 2012.
- [9] B. R. Guha-Sapir D, Hoyois Ph., "Annual Disaster Statistical Review 2013: The Numbers and Trends," 2014.
- [10] "National Disaster Management Guidelines- National Disaster Mangement Information and Communication System (NDMICS) 2011," 2012.
- [11] P. H.- D. Guha-Sapir, R. Below, "EM-DAT: International Disaster Database – www.emdat.be – Université Catholique de Louvain – Brussels – Belgium." .
- [12] A. K. Mishra and V. P. Singh, "A review of drought concepts," *J. Hydrol.*, vol. 391, no. 1–2, pp. 202–216, 2010.
- [13] D. A. (University of N. Wilhite, *Preparing for Drought: A Guidebook for Developing Countries*. Nairobi: United Nations Environment Programme., 1992.
- [14] A. Dai, "Drought under global warming: a review," *Wiley Interdiscip. Rev. Clim. Chang.*, 2011.
- [15] and A. W. W. A. C. for D. C. and P. U. E. P. A. National Oceanic and Atmospheric Agency, *When every drop counts: protecting public health during drought conditions - a guide for public health professionals*. Atlanta: Centers for Disease Control and Prevention, US. Environmental Protection Agency, National Oceanic and Atmospheric Agency, American Water Works Association, 2010, p. 56.
- [16] A. H. D. G. on drought ISDR, "Living With Risk: An Integrated Approach to Reducing Societal Vulnerability to Drought," 2004.

- [17] D. Wilhite and M. Glantz, "Understanding: the drought phenomenon: the role of definitions," *Water Int.*, 1985.
- [18] A. Jeyaseelan, "Droughts & floods assessment and monitoring using remote sensing and GIS," ... *Remote Sens. GIS Appl. Agric. ...*, pp. 291–313, 2003.
- [19] S. M. Quiring and T. N. Papakryiakou, "An evaluation of agricultural drought indices for the Canadian prairies," *Agric. For. Meteorol.*, vol. 118, pp. 49–62, 2003.
- [20] F. Kogan, "Global drought detection and impact assessment from space," *Drought a Glob. Assess.*, 2000.
- [21] G. M. Ambaw, "Satellite Based Remote Sensing of Soil Moisture for Drought Detection and Monitoring in the Horn of Africa," 2013.
- [22] V. U. Thenkabil, P.S., Gamage, M. S. D. N., Smakthin, "The_Use_of_Remote_Sensing_Data_for_Droug.pdf," Colombo, Sri Lanka, 2004.
- [23] a. Anyamba and C. J. Tucker, "Analysis of Sahelian vegetation dynamics using NOAA-AVHRR NDVI data from 1981-2003," *J. Arid Environ.*, vol. 63, pp. 596–614, 2005.
- [24] M. Mokhtari, "Agricultural drought Impact assessment using Remote Sensing: A case study Borkhar district Iran," *ITC, Enschede, Netherlands*, 2006.
- [25] T. M. Krishna, G. Ravikumar, and M. Krishnaveni, "Remote sensing based agricultural drought assessment in Palar basin of Tamil Nadu state, India," *J. Indian Soc. Remote Sens.*, vol. 37, no. March, pp. 9–20, 2009.
- [26] C. J. van Westen, "Remote sensing and geographic information systems for natural disaster management," *Inf. Syst.*, no. January, p. 27, 2000.
- [27] U. N. E. C. F. Africa, "Africa Review Report on: Drought and Desertification," Addis Ababa, Ethiopia, 2008.
- [28] J. Ferrer, M. A. Pérez, F. Pérez, and J. B. Artés, "Specific combined actions in Turia River during 2005-2007 drought," vol. d, no. 80, pp. 227–234, 2007.
- [29] F. Nhambura, "Africa must address food security; The Herald,(Zimbabwe) 14 February 2006," 2006.
- [30] J. Vidal and T. Radford, "One in six countries facing food shortage," *Guard.*, 2005.
- [31] "FAO," 2005. [Online]. Available: www.fao.org.
- [32] M. R. C. N. Sumanta Das, "Geospatial Assessment of Agricultural Drought," *Ijasr*, vol. 3, no. 1, pp. 1–28, 2013.
- [33] N. B. Guttman, "COMPARING THE PALMER DROUGHT INDEX AND THE STANDARDIZED PRECIPITATION INDEX' ties of the PDSI and its variations have been the referenced studies show that the intended," *J. Am. Water Resour. Assoc.*, vol. 34, no. 1, 1998.
- [34] N. Guttman, J. Wallis, and J. Hosking, "SPATIAL COMPARABILITY OF THE PALMER DROUGHT SEVERITY INDEX1," 1992.

- [35] T. R. Karl, "Some Spatial Characteristics of Drought Duration in the United States," *Journal of Climate and Applied Meteorology*, vol. 22. pp. 1356–1366, 1983.
- [36] W. M. Alley, "The Palmer Drought Severity Index: Limitations and Assumptions," *Journal of Climate and Applied Meteorology*, vol. 23. pp. 1100–1109, 1984.
- [37] F. N. KOGAN, "Remote sensing of weather impacts on vegetation in non-homogeneous areas," *Int. J. Remote Sens.*, vol. 11, no. 8, pp. 1405–1419, Aug. 1990.
- [38] T. B. Mckee, N. J. Doesken, and J. Kleist, "The relationship of drought frequency and duration to time scales," no. January, pp. 17–22, 1993.
- [39] D. Edwards and T. MCKEE, "Characteristics of twentieth century drought in the United States at multiple time scales," 1997.
- [40] N. Wattanakij, W. Thavorntam, and C. Mongkolsawat, "Analyzing Spatial Pattern of Drought in the Northeast of Thailand using multi-temporal Standardized Precipitation index (SPI)," *Asian Assoc. Remote Sens. - 27th Asian Conf. Remote Sensing, ACRS 2006*, pp. 1221–1226, 2006.
- [41] A. U. Komuscu, "Using the SPI to Analyze Spatial and Temporal Patterns of Drought in Turkey Using the SPI to Analyze Spatial and Temporal Patterns of Drought in Turkey," no. 1999, 2001.
- [42] W. Palmer, "Keeping track of crop moisture conditions, nationwide: The new crop moisture index," 1968.
- [43] R. Heim, "Drought indices: a review.," *Drought a Glob. Assess.*, 2000.
- [44] R. Nemani and L. Pierce, "Developing satellite-derived estimates of surface moisture status," *J. Appl. ...*, 1993.
- [45] B. Shafer and L. Dezman, "Development of a Surface Water Supply Index (SWSI) to assess the severity of drought conditions in snowpack runoff areas," *Proc. West. Snow Conf.*, 1982.
- [46] N. Doesken, T. McKee, and J. Kleist, "Development of a surface water supply index for the western United States: Final report," 1991.
- [47] J. F. Brown, B. C. Reed, M. J. Hayes, D. a. Wilhite, and K. Hubbard, "A prototype drought monitoring system integrating climate and satellite data," *PECORA 15/I. Satell. Inf. IV/ISPRS Comm. I/FIEOS 2002 Conf. Proc.*, 2002.
- [48] P. S. Thenkabail, E. a. Enclona, M. S. Ashton, and B. Van Der Meer, "Accuracy assessments of hyperspectral waveband performance for vegetation analysis applications," *Remote Sens. Environ.*, vol. 91, pp. 354–376, 2004.
- [49] M. H. Mokhtari, "Agricultural Drought Impact Assessment Using Remote Sensing Agricultural Drought Impact Assessment Using Remote Sensing," no. March, p. 137, 2005.
- [50] L. Ji and A. J. Peters, "Assessing vegetation response to drought in the northern Great Plains using vegetation and drought indices," *Remote Sens. Environ.*, vol. 87, no. 1, pp. 85–98, Sep. 2003.
- [51] F. . Ramesh, P.; Singh, P.; Roy, F.; Kogan, "Vegetation and temperature condition indices from NOAA AVHRR data for drought monitoring over India," *Int. J. Remote ...*, 2003.

- [52] J. Li, J. Lewis, J. Rowland, G. Tappan, and L. L. Tieszen, "Evaluation of land performance in Senegal using multi-temporal NDVI and rainfall series," *J. Arid Environ.*, vol. 59, pp. 463–480, 2004.
- [53] J. V Vogt, A. a Viau, I. Beaudin, S. Niemeier, and F. Somma, "DROUGHT MONITORING FROM SPACE USING EMPIRICAL INDICES AND PHYSICAL INDICATORS Jürgen V. VOGT, Alain A. VIAU, Isabelle BEAUDIN, Stefan NIEMEIER, Francesca SOMMA," no. November 1998, 2000.
- [54] F. N. Kogan, "Global Drought Watch from Space," *Bull. Am. Meteorol. Soc.*, vol. 78, pp. 621–636, 1997.
- [55] L. Unganai and F. Kogan, "Drought monitoring and corn yield estimation in Southern Africa from AVHRR data," *Remote Sens. Environ.*, 1998.
- [56] R. Seiler, F. Kogan, and J. Sullivan, "AVHRR-based vegetation and temperature condition indices for drought detection in Argentina," *Adv. Sp. Res.*, 1998.
- [57] C. Bhuiyan, R. P. Singh, and F. N. Kogan, "Monitoring drought dynamics in the Aravalli region (India) using different indices based on ground and remote sensing data," *Int. J. Appl. Earth Obs. Geoinf.*, vol. 8, pp. 289–302, 2006.
- [58] Z. Wan, P. Wang, and X. Li, "Using MODIS land surface temperature and normalized difference vegetation index products for monitoring drought in the southern Great Plains, USA," *Int. J. Remote Sens.*, 2004.
- [59] M. Frère and G. Popov, "Early Agrometeorological crop yield forecasting," *FAO, Plant Prod. Prot. Pap.*, 1986.
- [60] P. Hoefsloot, "Livelihood early assessment (LEAP) version 2.1," URL <http://vam.wfp.org/LEAP>, 2008.
- [61] D. B. Gesch, K. L. Verdin, and S. K. Greenlee, "New Land Surface Digital Elevation Model Covers the Earth," *Eos, Trans. Am. Geophys. Union*, vol. 80, no. 6, pp. 69–70, 1999.
- [62] U. S. Victor, N. N. Srivatsava, and B. V. Ramana Rao, "Quantification of crop yields under rainfed conditions using a simple soil water balance model," *Theor. Appl. Climatol.*, vol. 39, pp. 73–80, 1988.
- [63] G. Senay and J. Verdin, "Characterization of yield reduction in Ethiopia using a GIS-based crop water balance model," *Can. J. Remote Sens.*, 2003.
- [64] T. Bellone, P. Boccardo, and F. Perez, "Investigation of Vegetation Dynamics using Long-Term Normalized Difference Vegetation Index Time-Series," *Am. J. Environ. Sci.*, vol. 5, no. 4, pp. 461–467, 2009.
- [65] P. Peduzzi and H. Dao, "Assessing global exposure and vulnerability towards natural hazards: the Disaster Risk Index," ... *Hazards Earth ...*, 2009.
- [66] J. Birkmann, D. Krause, and N. Setiadi, "WorldRiskReport 2011," ... *Work. Berlin*, 2011.
- [67] A. de Waal, *Famine that kills: Darfur, Sudan, 1984–5*. Oxford, UK: Oxford University Press, Inc., 1989.
- [68] WFP, *Emergency Food Security Assessment Handbook*, Second edi. Rome, Italy, 2009.

- [69] S. Julich, "Drought risk indicators for assessing rural households," in *Summer Academy on Social Vulnerability*, 2006.
- [70] B. Goodall, *A Dictionary of Modern Human Geography.*, Penguin Bo. England, 1987.
- [71] F. Pozzi and T. Robinson, "Accessibility Mapping in the Horn of Africa : Applications for Livestock Policy," 11-08, 2008.
- [72] W. J. Reilly, *The Law of Retail Gravitation*. New York: Reilly, W.J., 1931.
- [73] C. Chasco Yrigoyen and J. Vicéns Otero, "Spatial interaction models applied to the design of retail trade areas," 1998.
- [74] D. L. Huff, "A Probabilistic Analysis of Consumer Spatial Behaviour," in *Emerging Concepts in Marketing*, 1962.
- [75] E. E. Ebert, J. E. Janowiak, and C. Kidd, "Comparison of near-real-time precipitation estimates from satellite observations and numerical models," *Bull. Am. Meteorol. Soc.*, vol. 88, no. January, pp. 47–64, 2007.
- [76] R. Teegavarapu, *Floods in a Changing Climate: Extreme Precipitation*. Cambridge University Press, 2012.
- [77] "TRMM," 2011. [Online]. Available: <http://trmm.gsfc.nasa.gov/>.
- [78] A. ;National C. for A. R. S. (Eds) Huffman, George J., Pendergrass, "'The Climate Data Guide: TRMM: Tropical Rainfall Measuring Mission.," 2014. [Online]. Available: <https://climatedataguide.ucar.edu/climate-data/trmm-tropical-rainfall-measuring-mission>.
- [79] G. J. Huffman, D. T. Bolvin, E. J. Nelkin, D. B. Wolff, R. F. Adler, G. Gu, Y. Hong, K. P. Bowman, and E. F. Stocker, "The TRMM Multisatellite Precipitation Analysis (TMPA): Quasi-Global, Multiyear, Combined-Sensor Precipitation Estimates at Fine Scales," *J. Hydrometeorol.*, vol. 8, pp. 38–55, 2007.
- [80] S. A. Barbosa P., Horion S., Micalé F., "Drought Bulletin for the Greater Horn of Africa : Situation in June 2011," 2011.
- [81] M. Kottek, J. Grieser, C. Beck, B. Rudolf, and F. Rubel, "World map of the Köppen-Geiger climate classification updated," *Meteorol. Zeitschrift*, vol. 15, no. 3, pp. 259–263, 2006.
- [82] F. Rubel and M. Kottek, "Observed and projected climate shifts 1901-2100 depicted by world maps of the Köppen-Geiger climate classification," *Meteorol. Zeitschrift*, vol. 19, no. 2, pp. 135–141, 2010.
- [83] T. D. Mitchell and P. D. Jones, "An improved method of constructing a database of monthly climate observations and associated high-resolution grids," *Int. J. Climatol.*, vol. 25, pp. 693–712, 2005.
- [84] M. Ziese, U. Schneider, A. Meyer-Christoffer, P. Finger, K. Schamm, A. Becker, and B. Rudolf, "Gridded Analysis Products provided by the Global Precipitation Climatology Centre (GPCP), and new Products getting operational 2013," *EGU Gen. Assem. Conf. Abstr.*, vol. 15, p. 4123, 2013.

- [85] M. a. Friedl, D. Sulla-Menashe, B. Tan, A. Schneider, N. Ramankutty, A. Sibley, and X. Huang, "MODIS Collection 5 global land cover: Algorithm refinements and characterization of new datasets," *Remote Sens. Environ.*, vol. 114, no. 1, pp. 168–182, 2010.
- [86] N. J. Salkind, *Métodos de investigación*. Pearson Educación, 1999, p. 380.

8. APPENDICES

8.1. Test of Significance Analysis

8.1.1. Open shrublands

8.1.1.1. First growing season

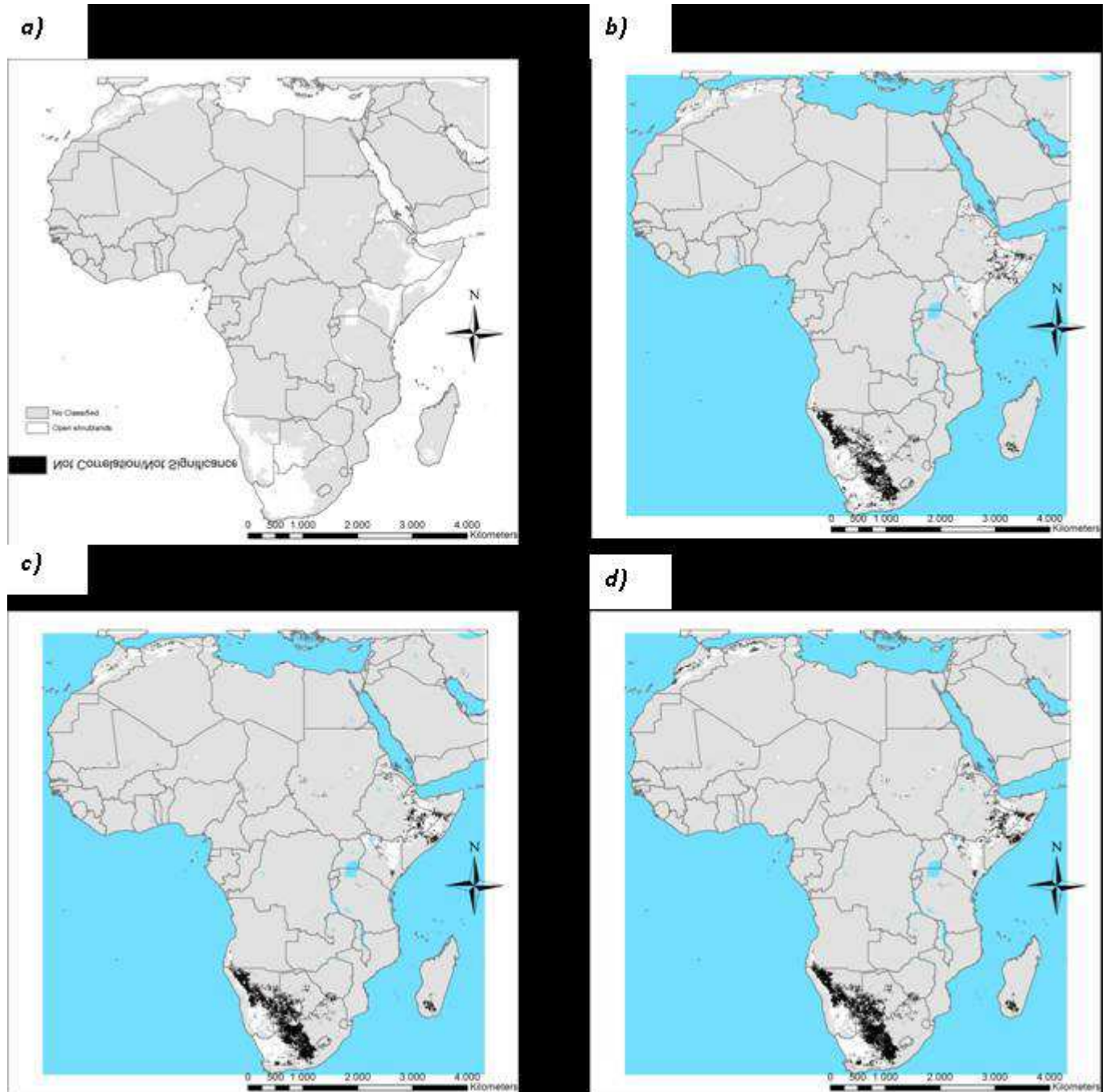


Figure 42. Outcomes of the Student t-test for the correlation between the Amplitude (Amp) and cumulated rainfall (b) 1 month , c) 3 months d) 6 months) for the Open Shrublands vegetation type (a) in the first vegetation season.

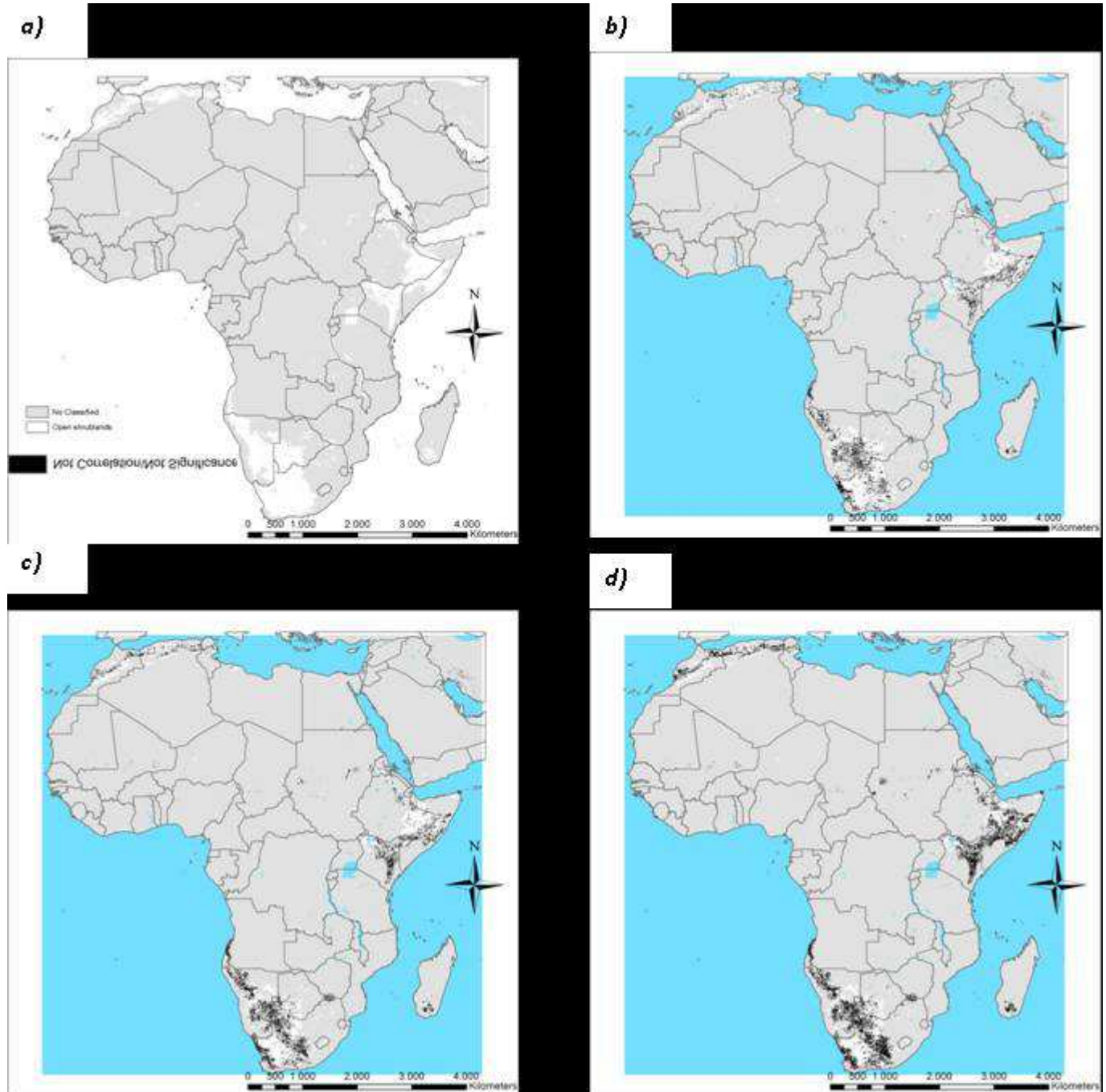


Figure 43. Outcomes of the Student t-test for the correlation between the Length (Len) and cumulated rainfall (b) 1 month , c) 3 months d) 6 months) for the Open Shrublands vegetation type (a) in the first vegetation season.

8.1.1.2. Second growing season

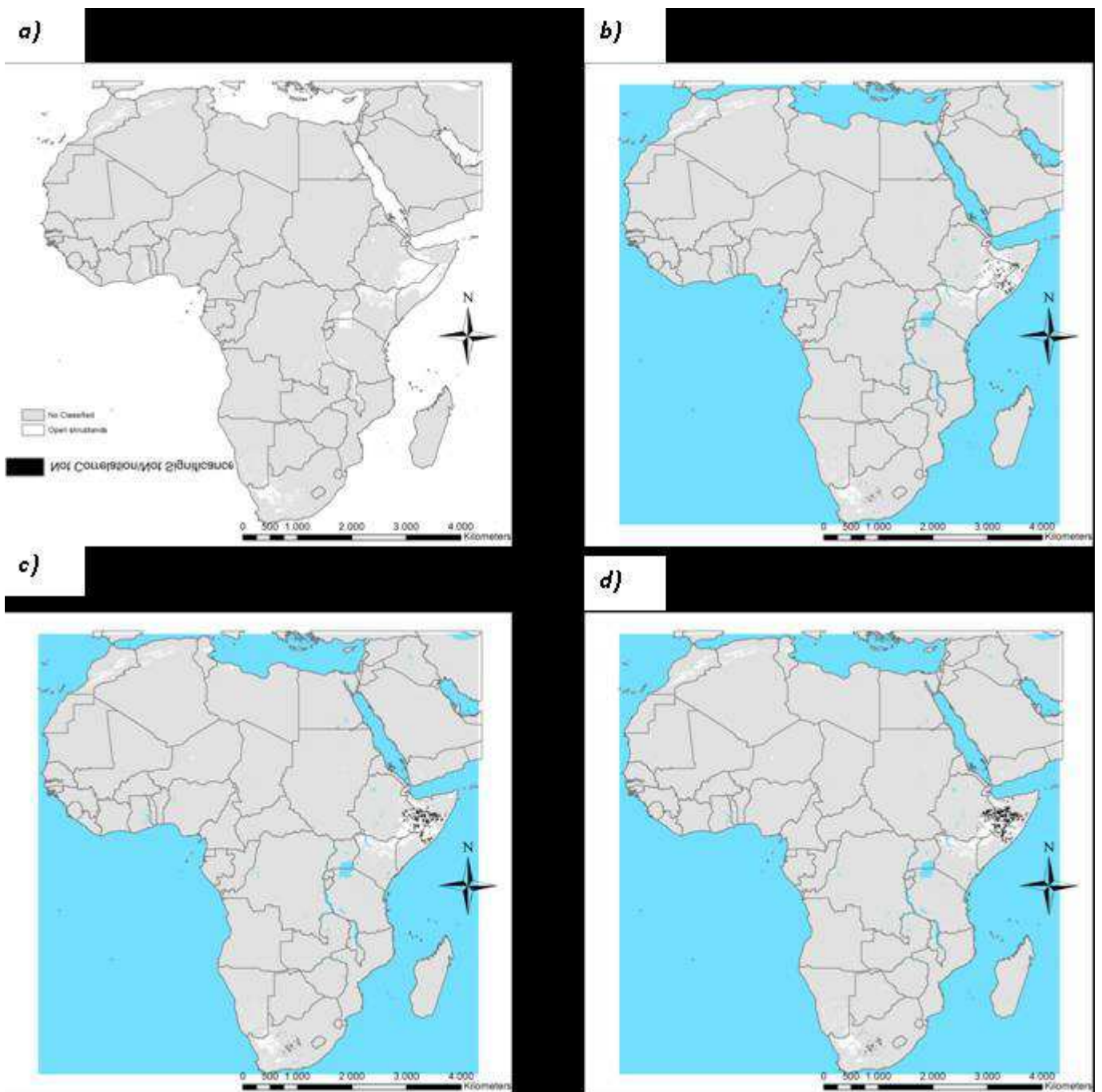


Figure 44. Outcomes of the Student t-test for the correlation between the Amplitude (Amp) and cumulated rainfall (b) 1 month , c) 3 months d) 6 months) for the Open Shrublands vegetation type (a) in the second vegetation season.

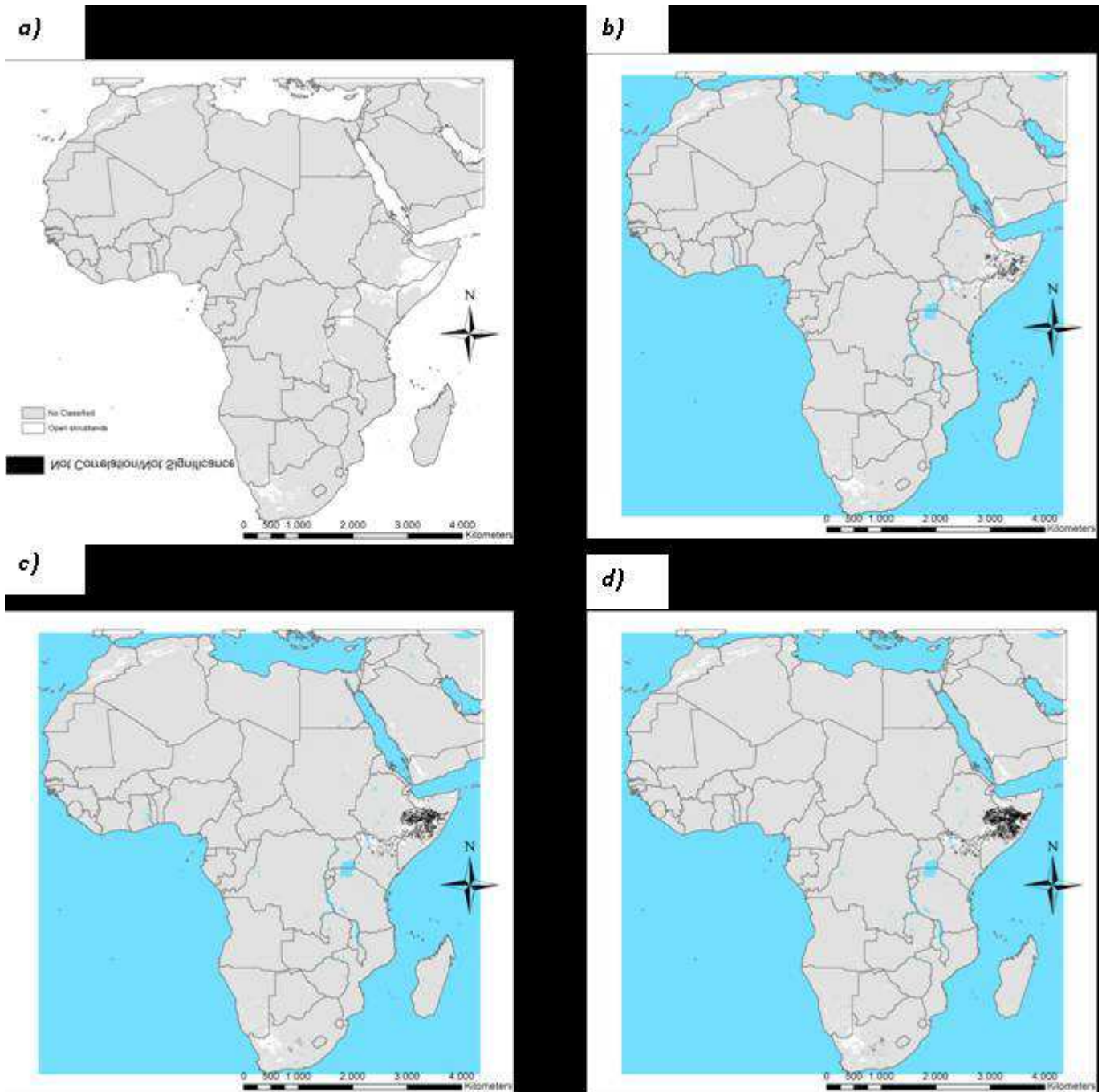


Figure 45. Outcomes of the Student t-test for the correlation between the Length (Len) and cumulated rainfall (b) 1 month , c) 3 months d) 6 months) for the Open Shrublands vegetation type (a) in the second vegetation season

8.1.2. Woody savannas

8.1.2.1. First growing season

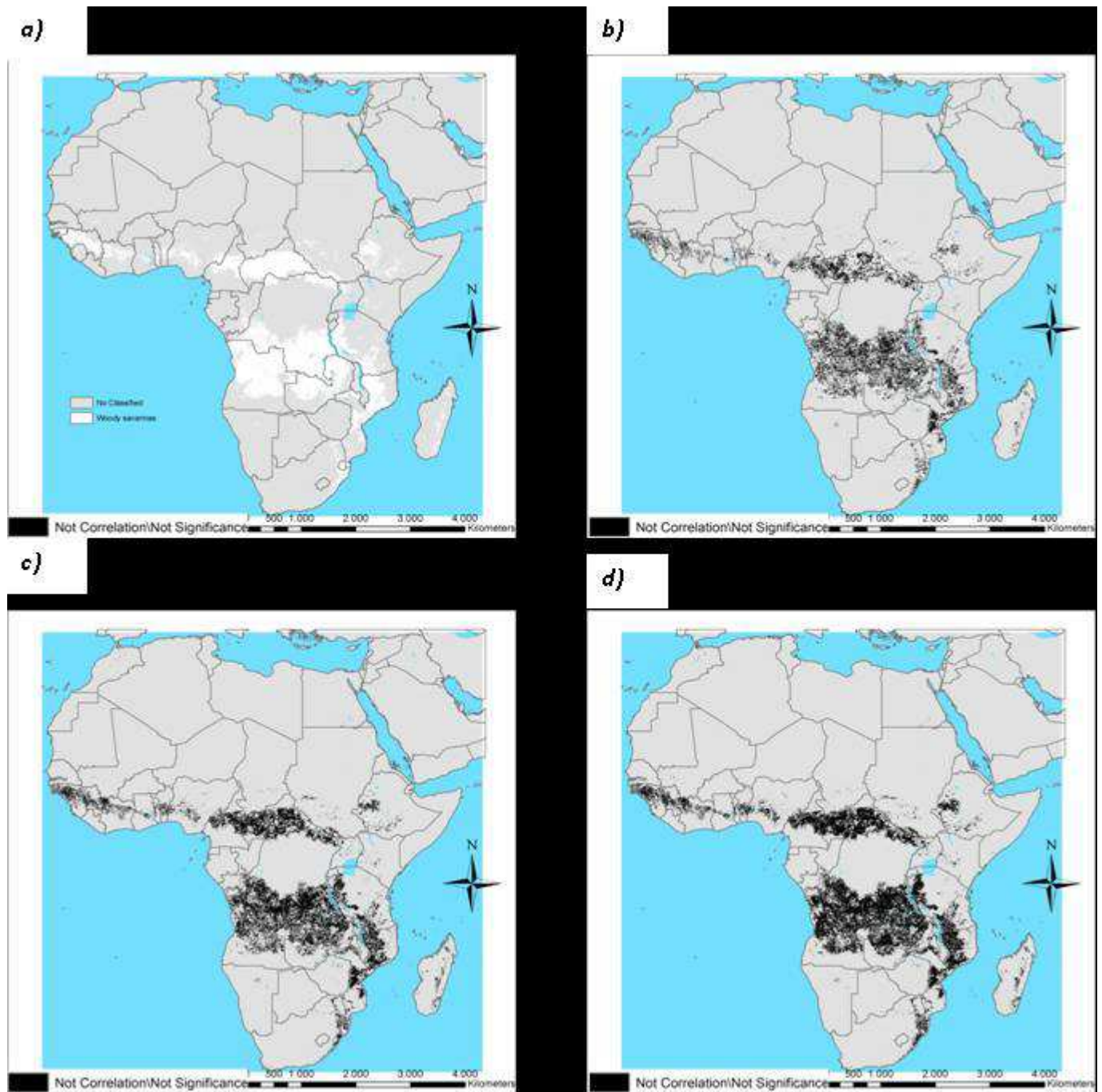


Figure 46. Outcomes of the Student t-test for the correlation between the Amplitude (Amp) and cumulated rainfall (b) 1 month, c) 3 months d) 6 months) for the Woody Savannas vegetation type (a) in the first vegetation season.

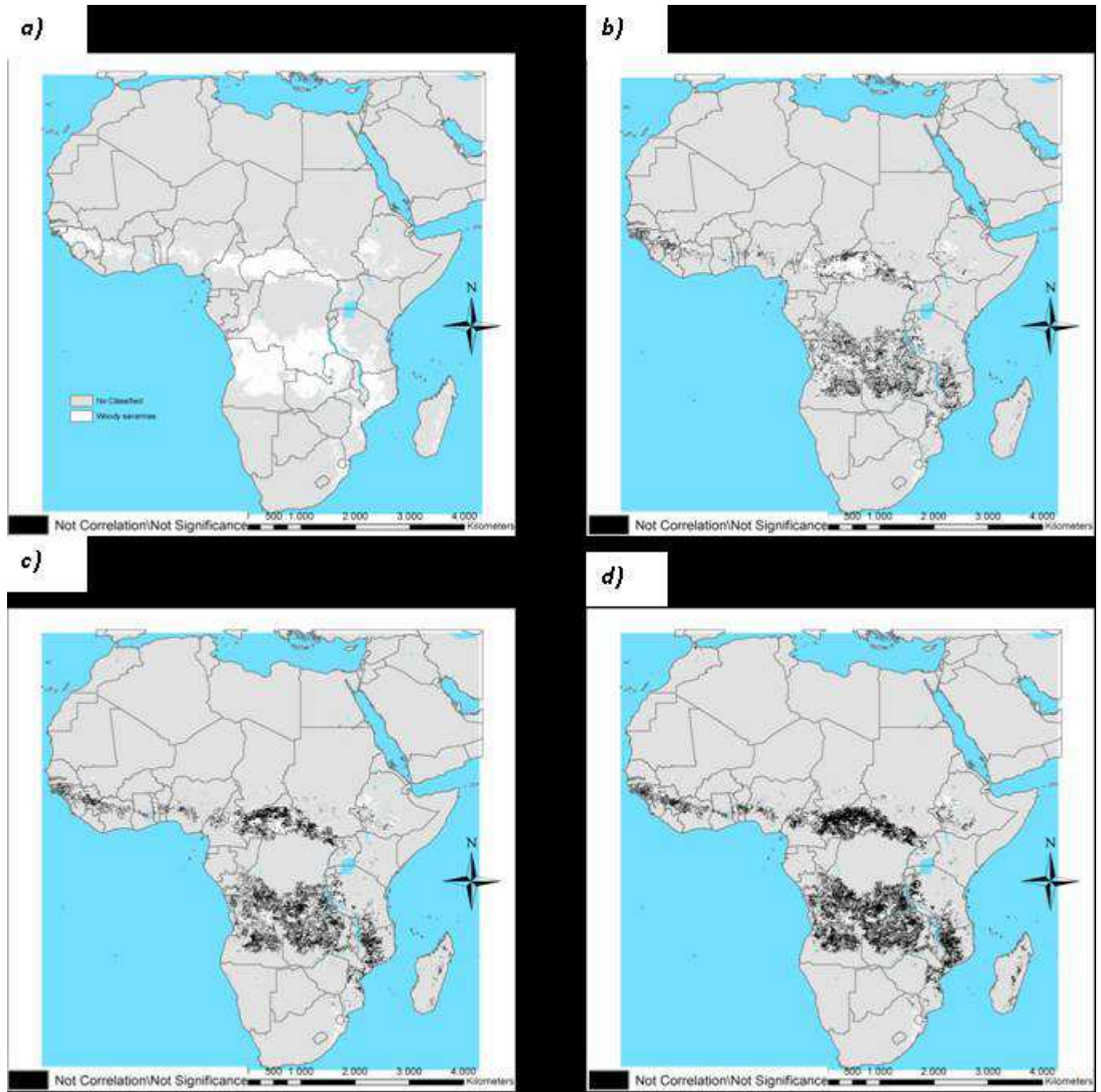


Figure 47. Outcomes of the Student t-test for the correlation between the Length (Len) and cumulated rainfall (b) 1 month , c) 3 months d) 6 months) for the Woody Savannas vegetation type (a) in the first vegetation season.

8.1.3. savannas

8.1.3.1. First growing season

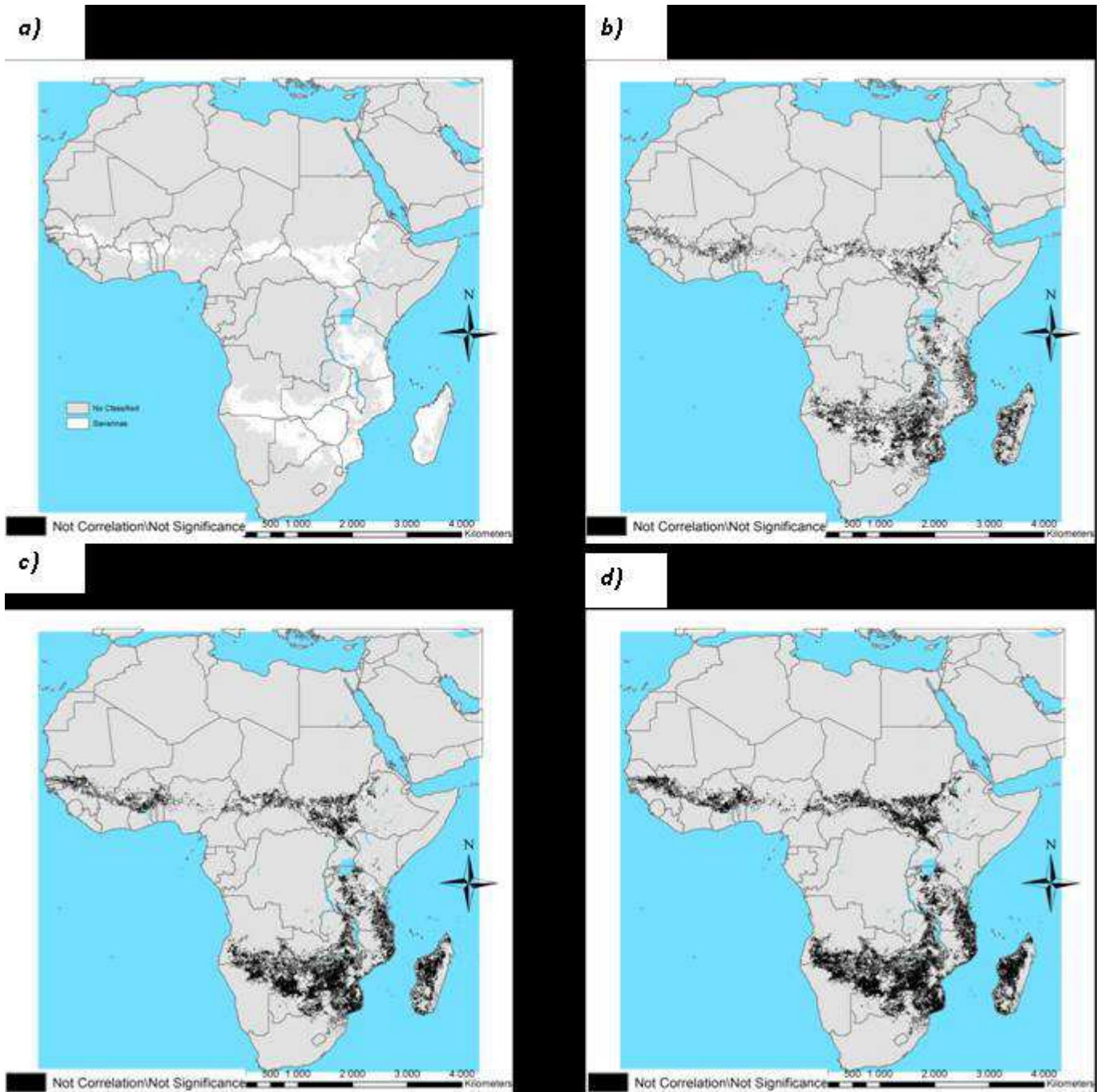


Figure 48. Outcomes of the Student t-test for the correlation between the Amplitude (Amp) and cumulated rainfall (b) 1 month, c) 3 months d) 6 months) for the Savannas vegetation type (a) in the first vegetation season.

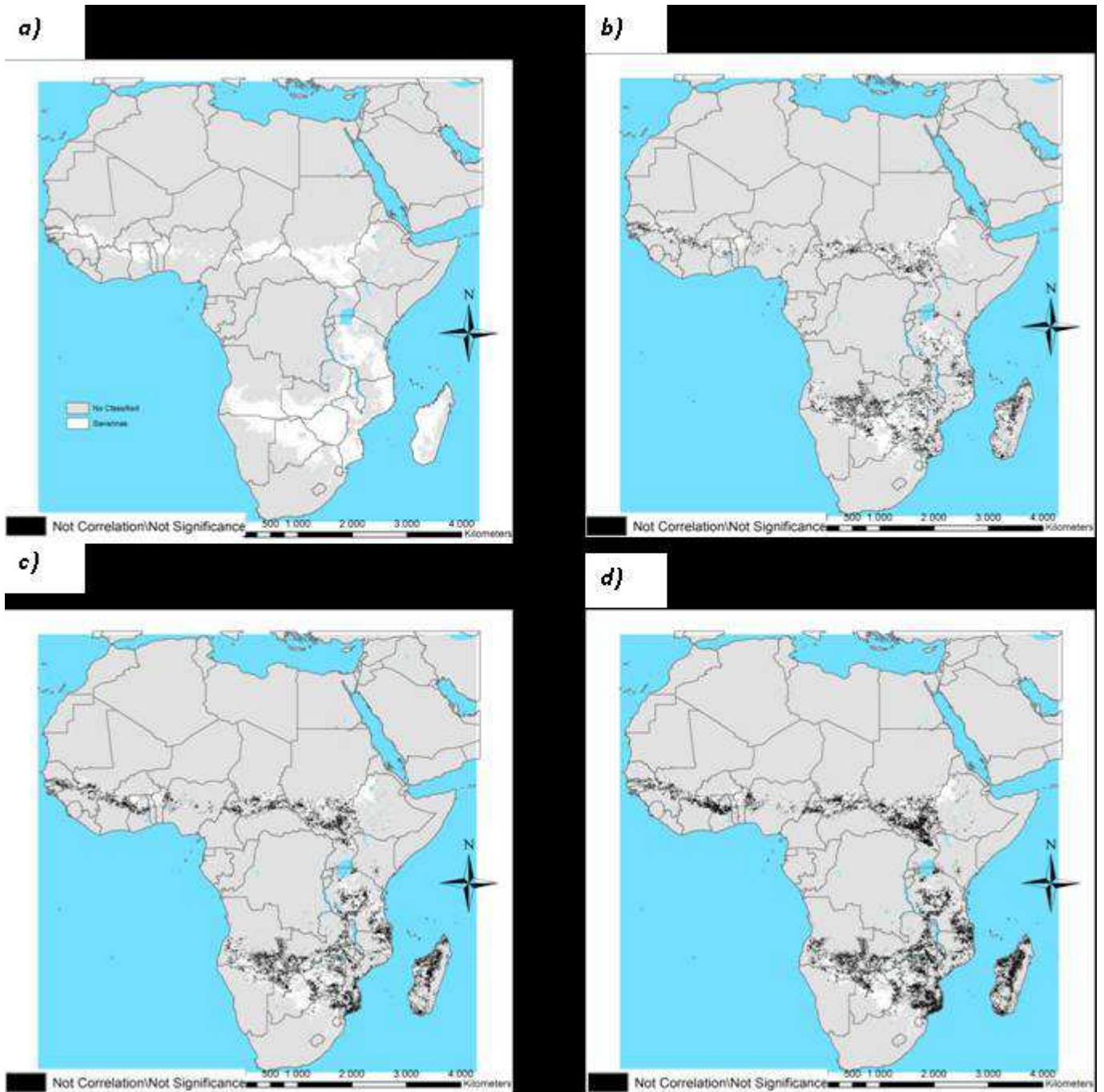


Figure 49. Outcomes of the Student t-test for the correlation between the Length (Len) and cumulated rainfall (b) 1 month , c) 3 months d) 6 months) for the Savannas vegetation type (a) in the first vegetation season

8.1.4. Grasslands

8.1.4.1. First growing season

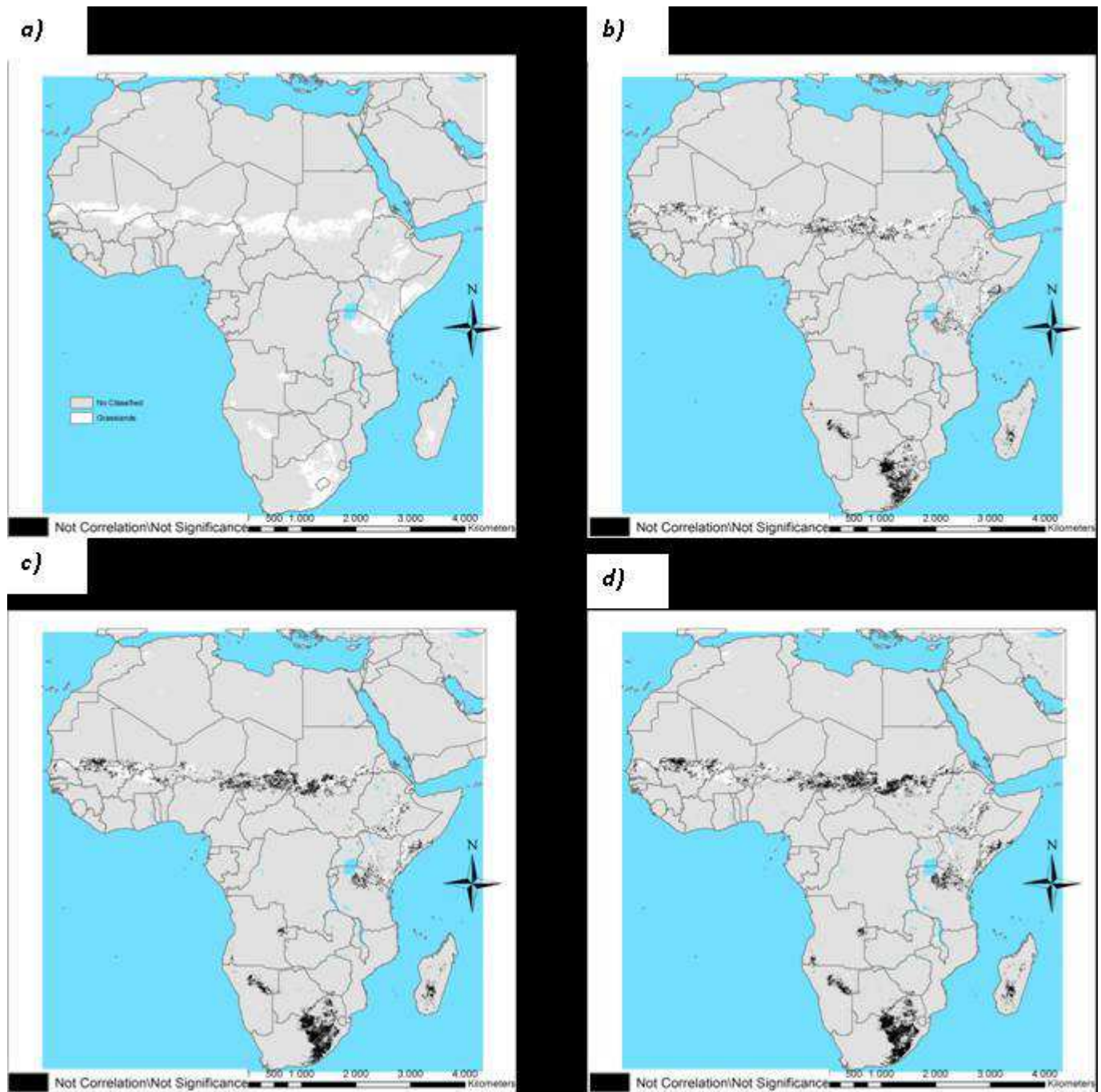


Figure 50. Outcomes of the Student t-test for the correlation between the Amplitude (Amp) and cumulated rainfall (b) 1 month , c) 3 months d) 6 months) for the Grasslands vegetation type (a) in the first vegetation season.

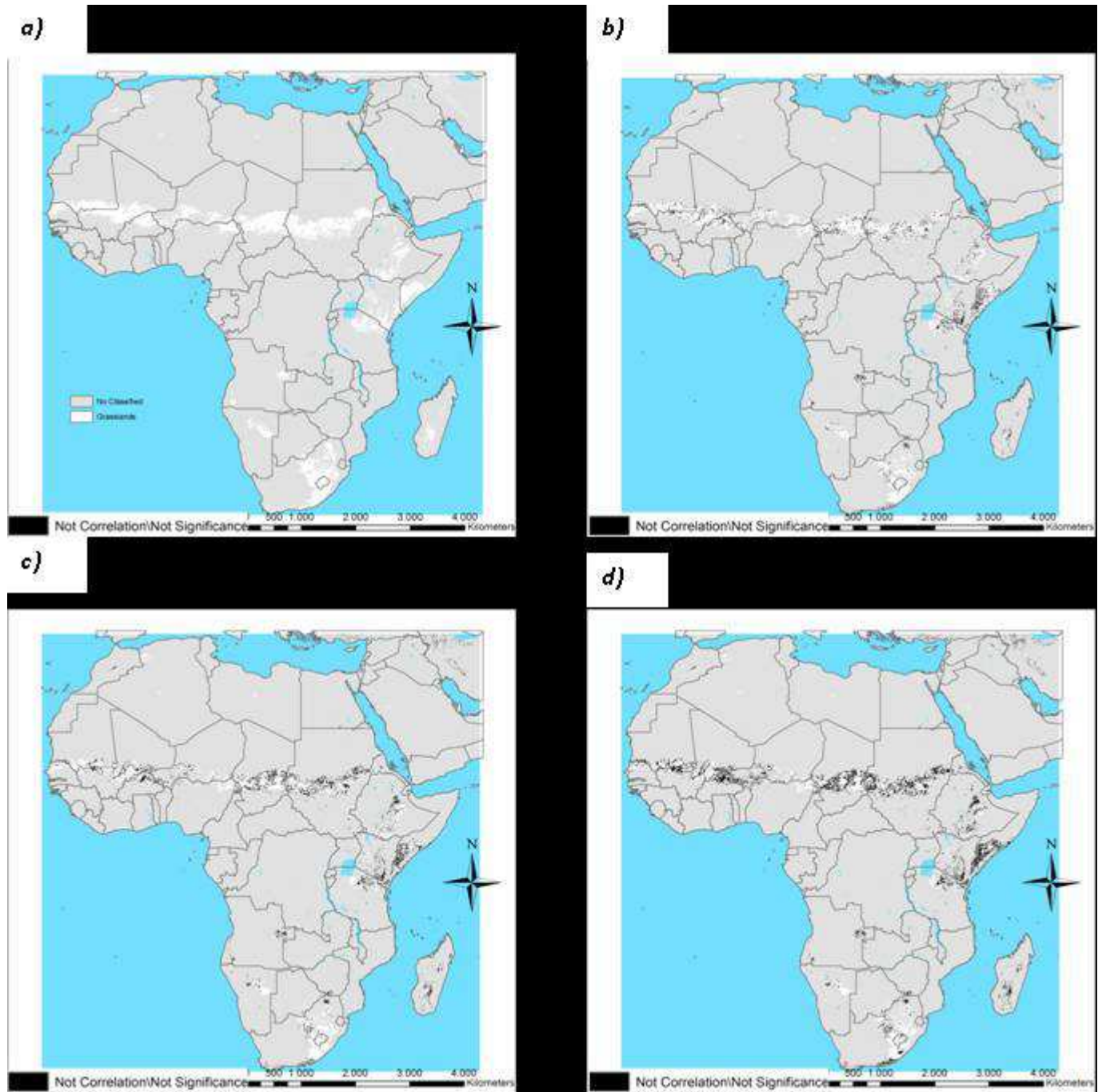


Figure 51. Outcomes of the Student t-test for the correlation between the Length (Len) and cumulated rainfall (b) 1 month , c) 3 months d) 6 months) for the Grasslands vegetation type (a) in the first vegetation season.

8.1.4.2. Second growing season

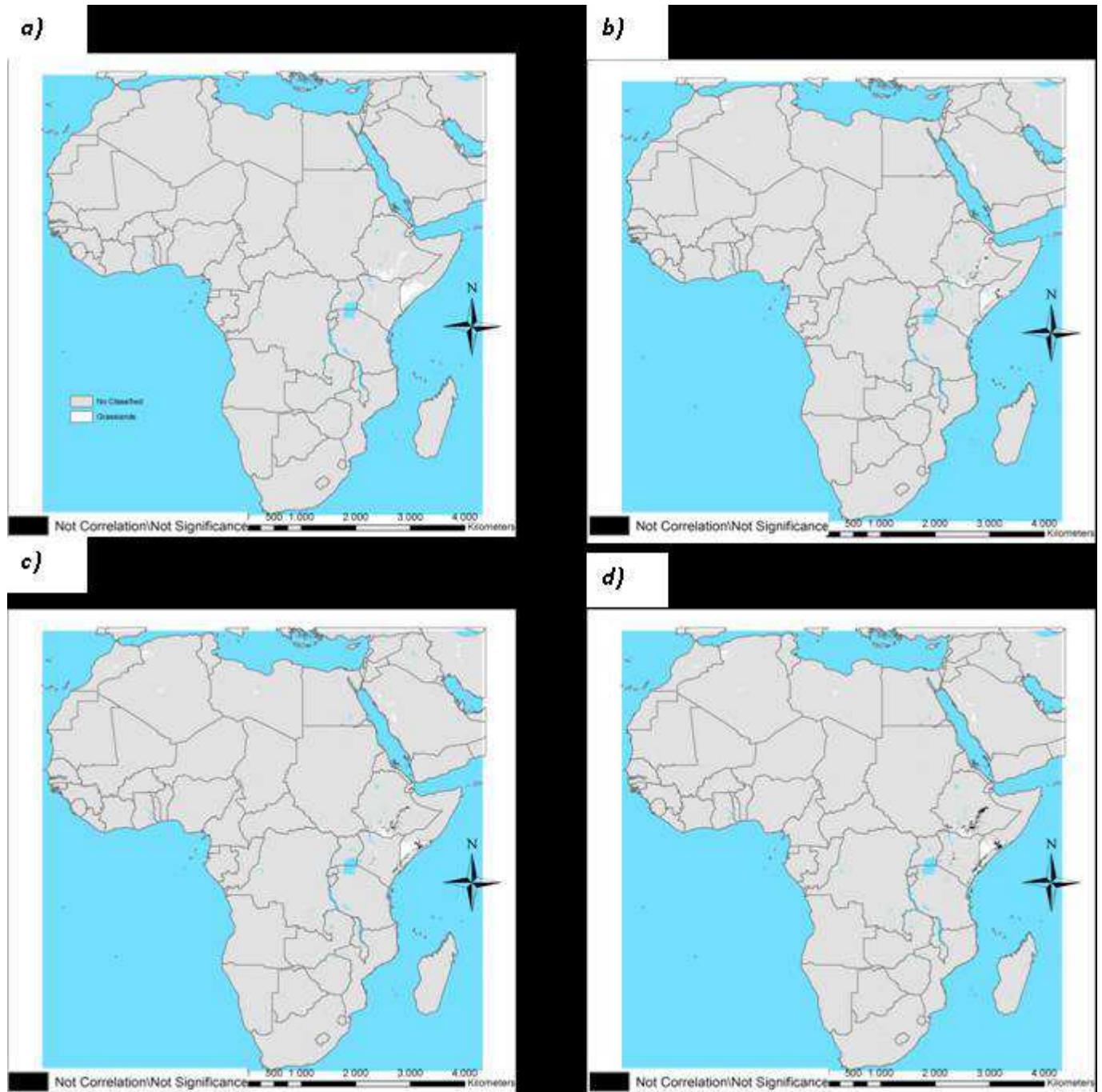


Figure 52. Outcomes of the Student t-test for the correlation between the Amplitude (Amp) and cumulated rainfall (b) 1 month , c) 3 months d) 6 months) for the Grasslands vegetation type (a) in the second vegetation season.

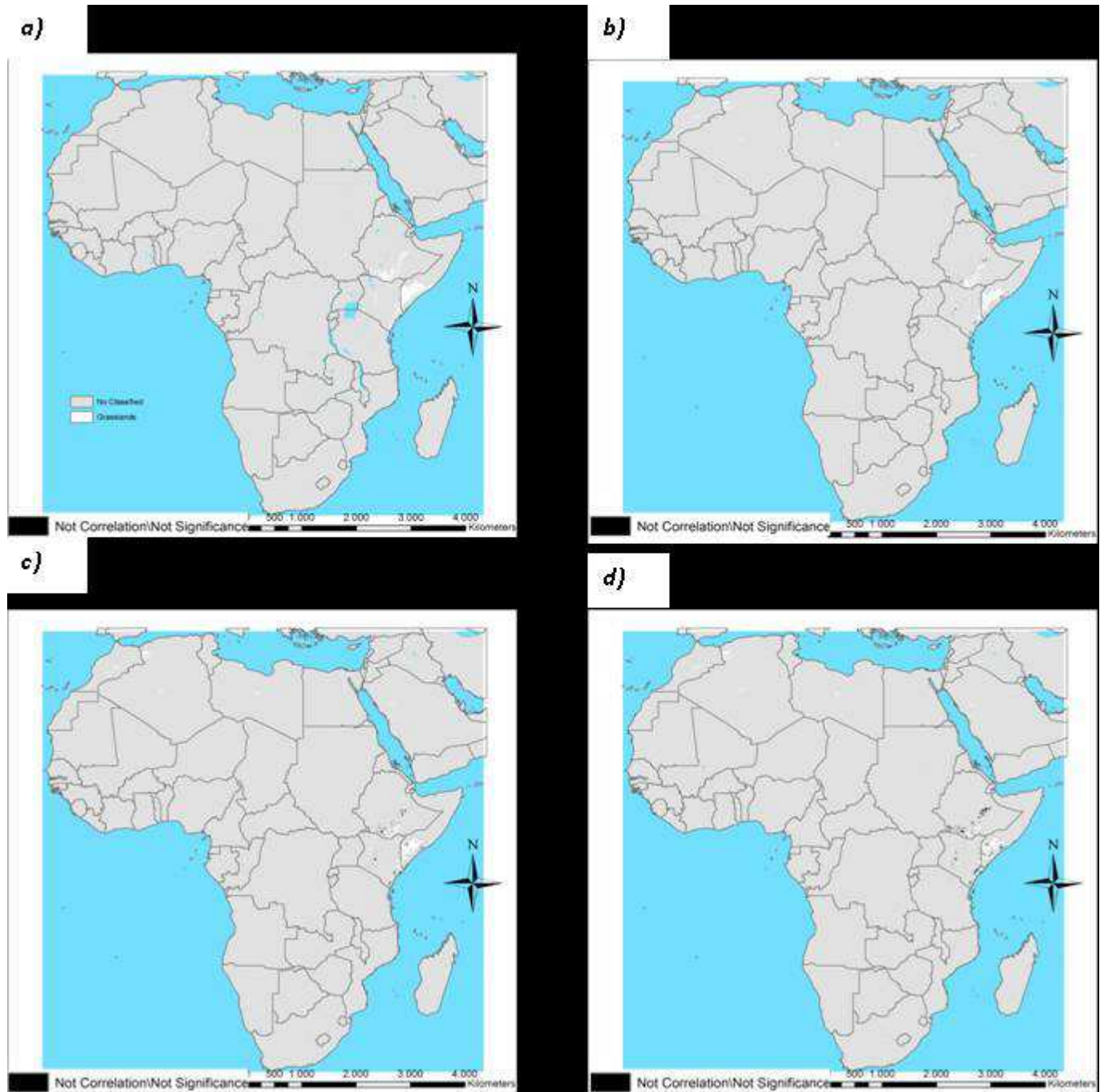


Figure 53. Outcomes of the Student t-test for the correlation between the Length (Len) and cumulated rainfall (b) 1 month , c) 3 months d) 6 months) for the Grasslands vegetation type (a) in the second vegetation season

8.1.5. Croplands

8.1.5.1. First growing season

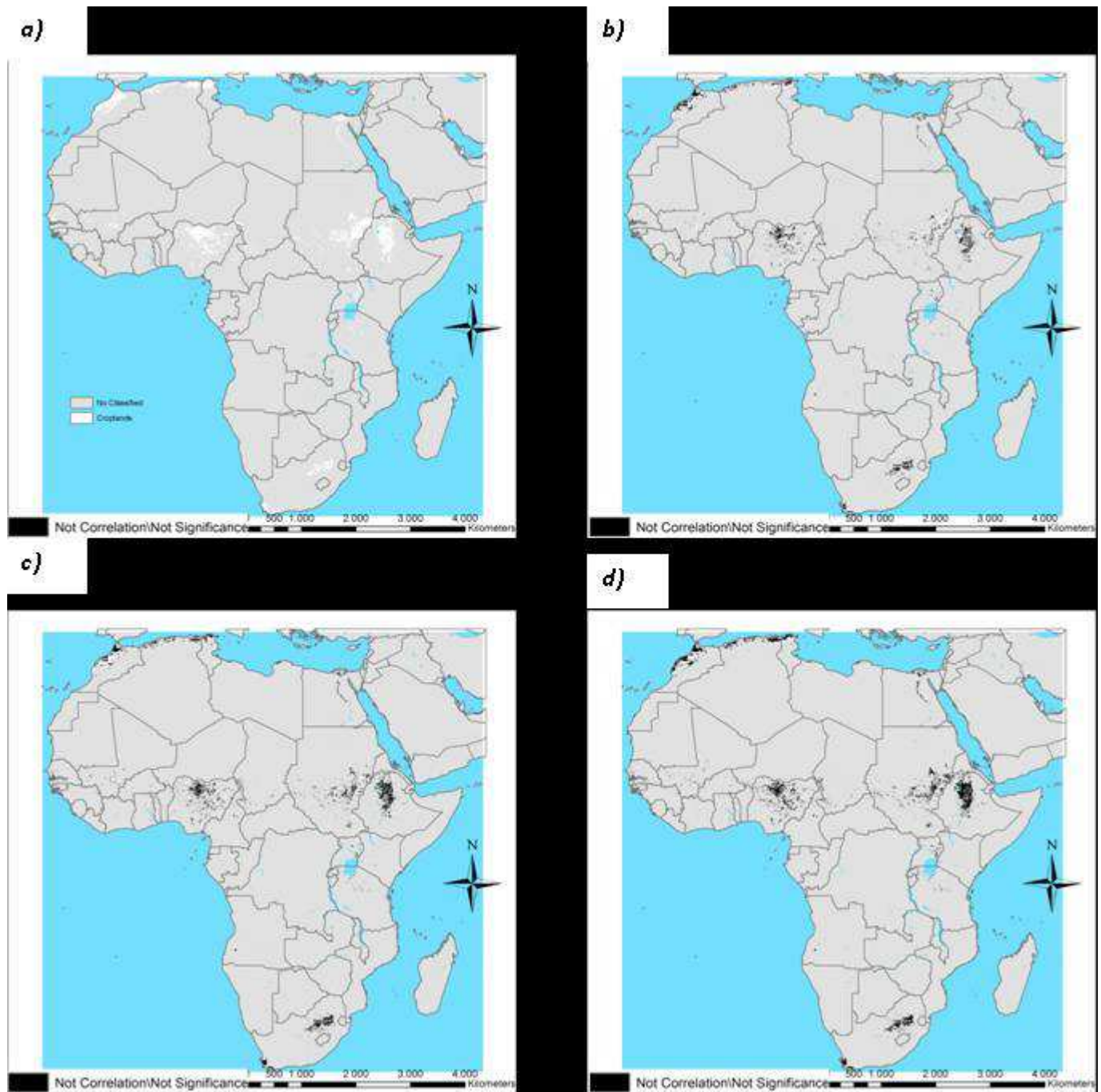


Figure 54. Outcomes of the Student t-test for the correlation between the Amplitude (Amp) and cumulated rainfall (b) 1 month, c) 3 months d) 6 months) for the Croplands vegetation type (a) in the first vegetation season

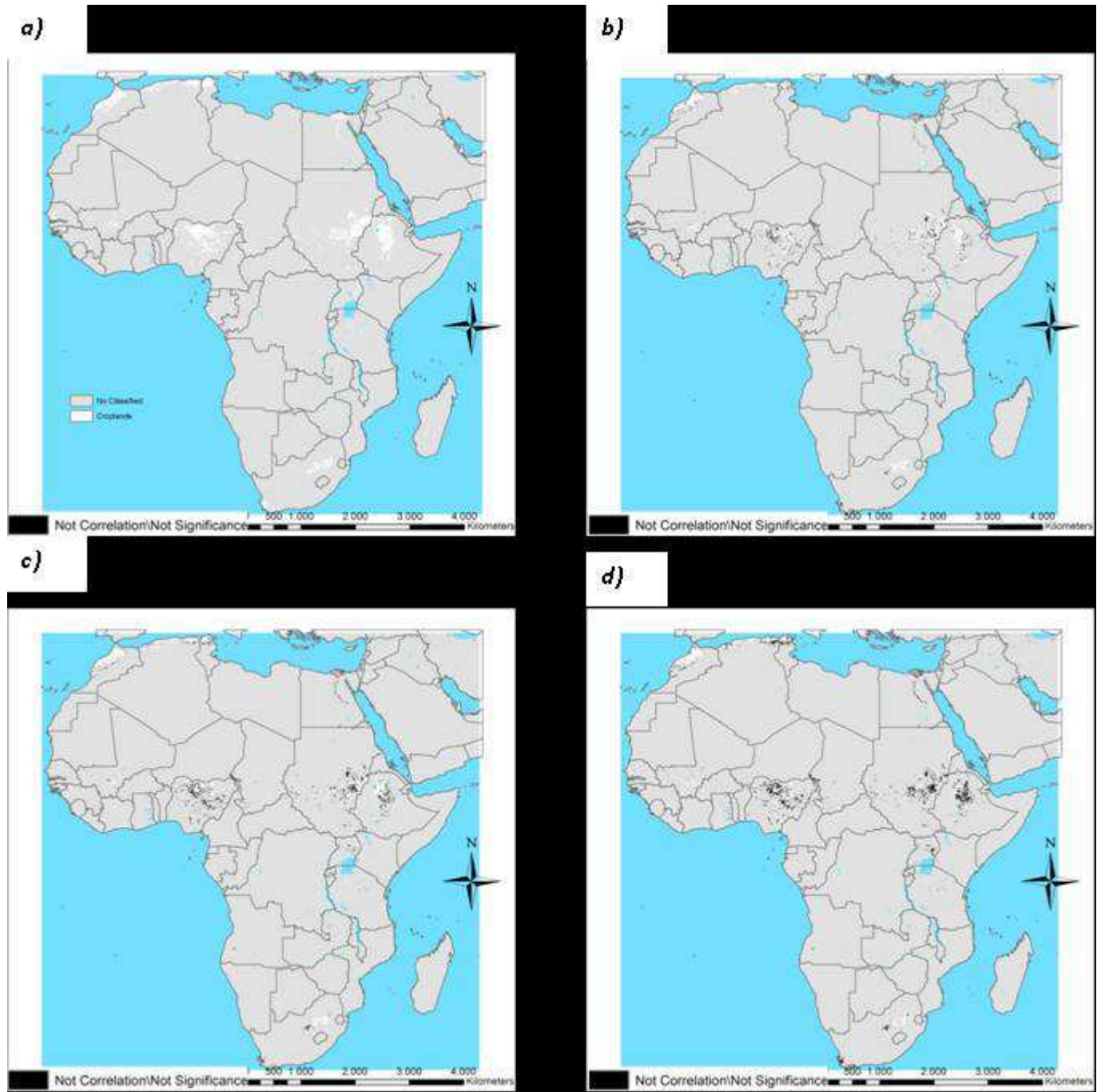


Figure 55. Outcomes of the Student t-test for the correlation between the Length (Len) and cumulated rainfall (b) 1 month , c) 3 months d) 6 months) for the Croplands vegetation type (a) in the first vegetation season

8.1.6. Cropland Natural Vegetation Mosaic

8.1.6.1. First growing season

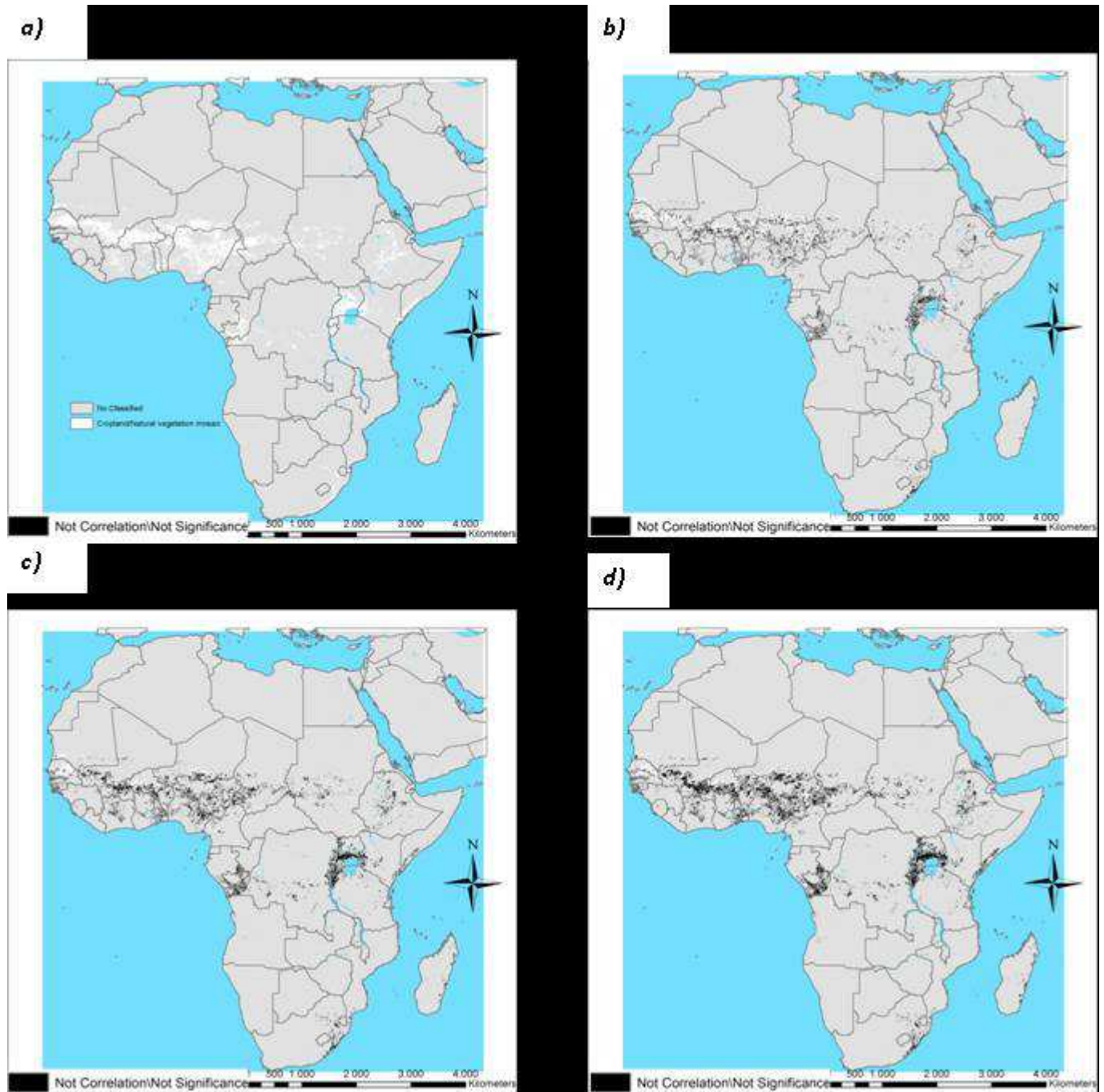


Figure 56. Outcomes of the Student t-test for the correlation between the Amplitude (Amp) and cumulated rainfall (b) 1 month, c) 3 months d) 6 months) for the Croplands/Natural vegetation mosaic type (a) in the first vegetation season

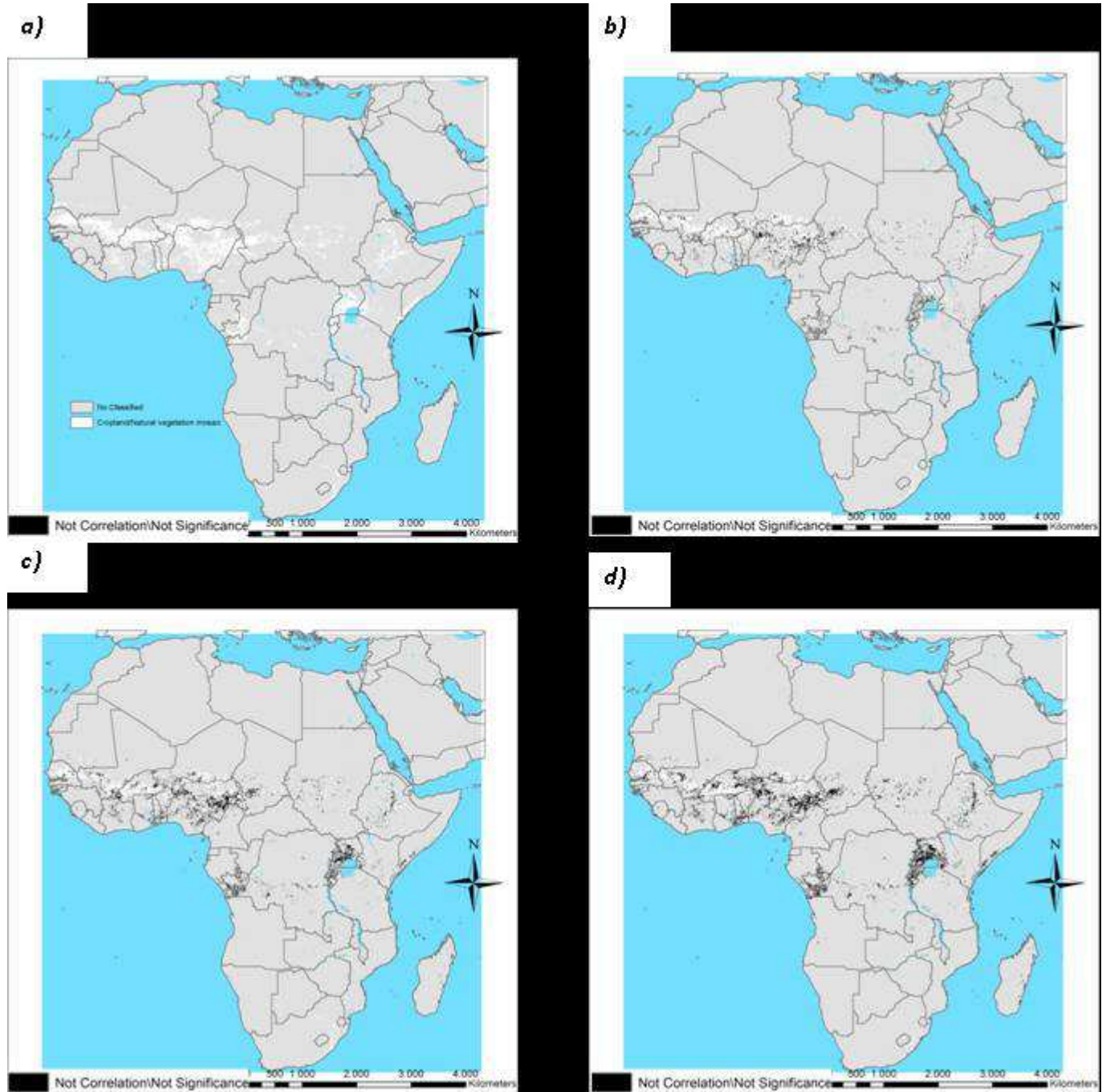


Figure 57. Outcomes of the Student t-test for the correlation between the Length (Len) and cumulated rainfall (b) 1 month , c) 3 months d) 6 months) for the Croplands/Natural vegetation mosaic type (a) in the first vegetation season

8.1.6.2. Second growing season

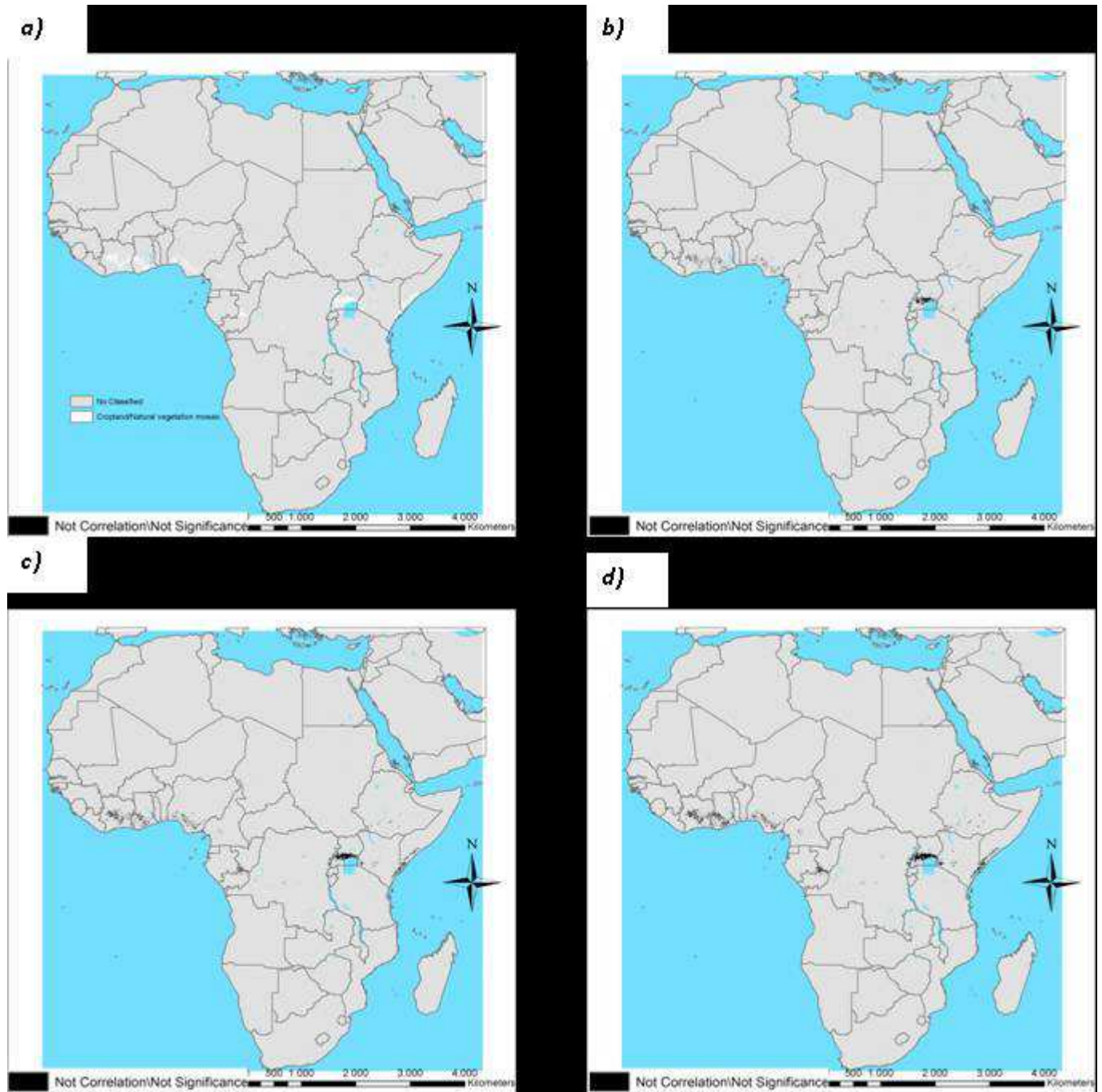


Figure 58. Outcomes of the Student t-test for the correlation between the Amplitude (Amp) and cumulated rainfall (b) 1 month , c) 3 months d) 6 months) for the Croplands/Natural vegetation mosaic type (a) in the second vegetation season

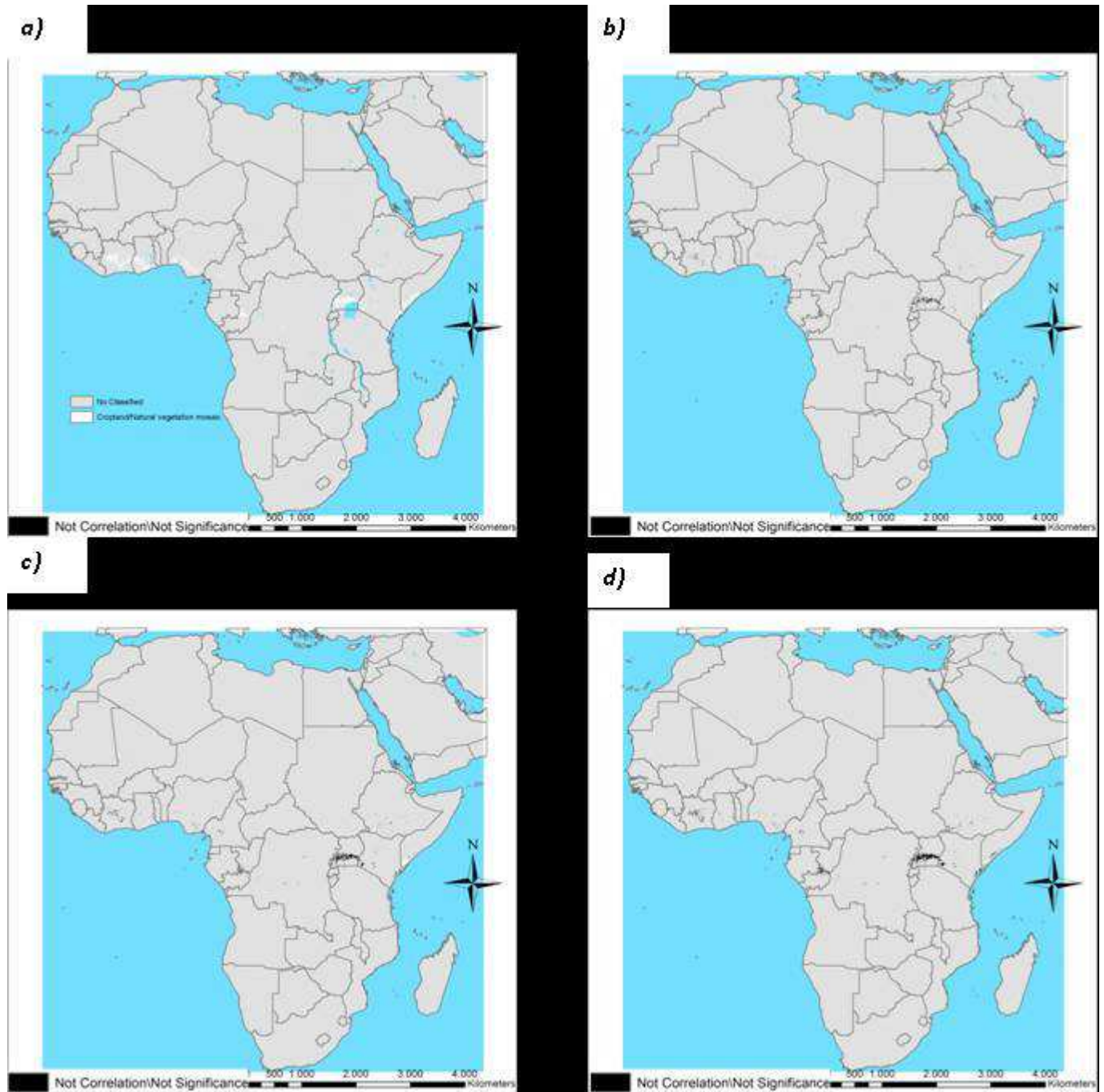


Figure 59. Outcomes of the Student t-test for the correlation between the Length (Len) and cumulated rainfall (b) 1 month , c) 3 months d) 6 months) for the Croplands/Natural vegetation mosaic type (a) in the second vegetation season

8.2. Correlation Analysis

8.2.1. Open Shrublands

8.2.1.1. Second growing season

Open Shrub	SEASON 2		
Phenological Parameter	Medium Correlation		
	TRMM 1 Month	TRMM 3 Months	TRMM 6 Months
Amp	32,06%	27,42%	26,41%
Base	35,57%	33,50%	28,67%
Decr	35,57%	31,95%	27,04%
Incr	35,34%	30,07%	26,39%
Larg	36,51%	29,30%	26,41%
Len	38,74%	31,80%	24,05%
SMI	26,56%	24,16%	22,89%

Table 28. Percentages of Open Shrublands areas showing Medium Correlation level between the phenological parameters and cumulated rainfall for the second growing season

Open Shrub	SEASON 2		
Phenological Parameter	High Correlation		
	TRMM 1 Month	TRMM 3 Months	TRMM 6 Months
Amp	42,68%	35,68%	30,51%
Base	24,56%	24,59%	22,31%
Decr	36,51%	30,15%	24,23%
Incr	40,30%	31,59%	25,99%
Larg	37,39%	34,77%	30,18%
Len	35,46%	24,76%	19,46%
SMI	46,60%	35,54%	29,86%

Table 29. Percentages of Open Shrublands areas showing High Correlation level between the phenological parameters and cumulated rainfall for the second growing season

Open Shrub	SEASON 2		
Phenological Parameter	Very High Correlation		
	TRMM 1 Month	TRMM 3 Months	TRMM 6 Months
Amp	12,40%	15,47%	13,75%
Base	2,78%	2,49%	2,40%
Decr	6,55%	6,61%	5,21%
Incr	6,57%	5,46%	4,35%
Larg	9,96%	12,50%	11,57%
Len	3,30%	2,47%	1,89%
SMI	18,40%	22,62%	20,43%

Table 30. Percentages of Open Shrublands areas showing Very High Correlation level between the phenological parameters and cumulated rainfall for the second growing season

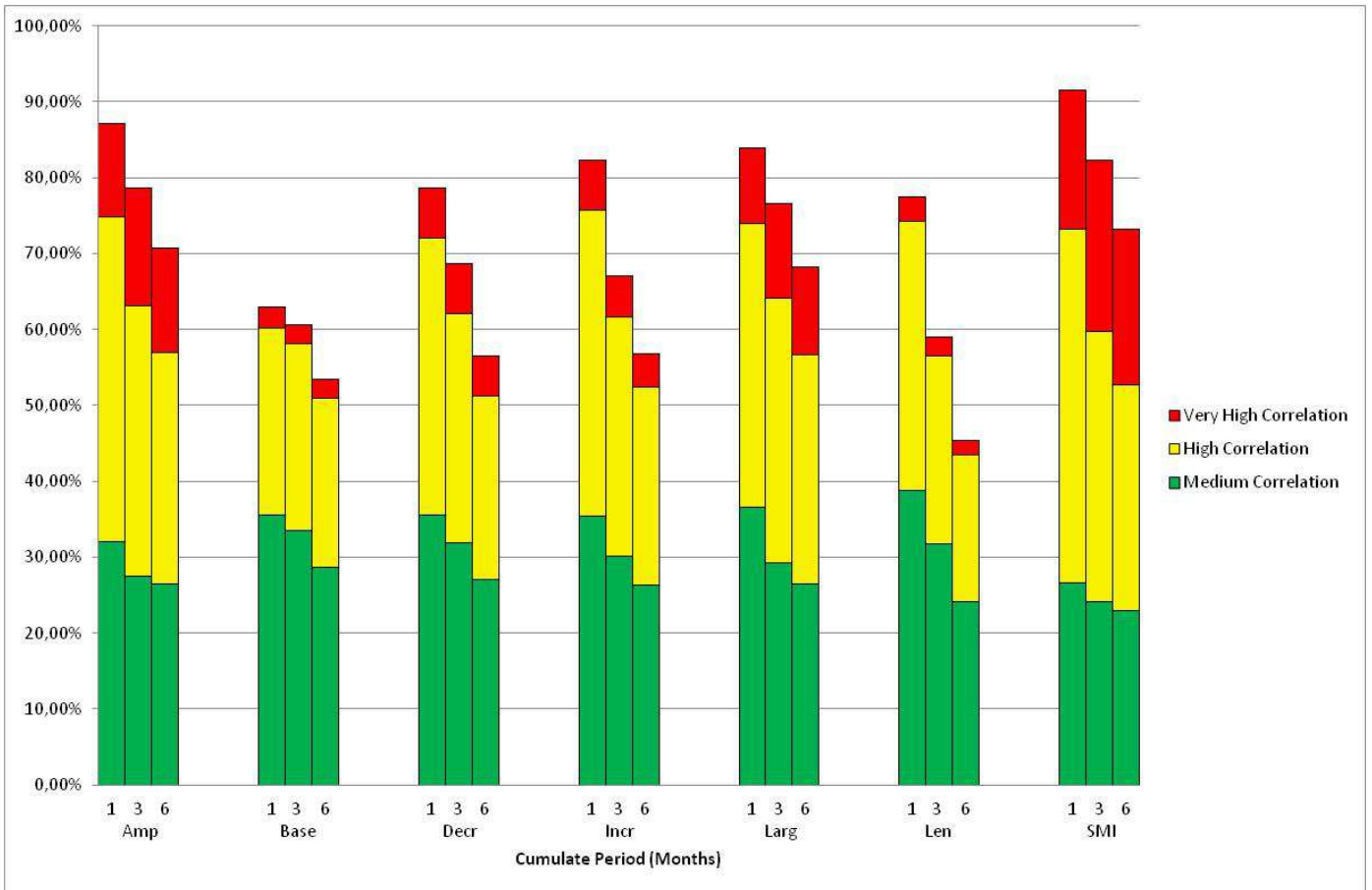


Figure 60. Correlation Analysis for the Open Shrubland land cover type, second growing season

8.2.2. Grasslands

8.2.2.1. Second growing season

Grassland	SEASON 2		
Phenological Parameter	Medium Correlation		
	TRMM 1 Month	TRMM 3 Months	TRMM 6 Months
Amp	31,69%	27,59%	25,09%
Base	36,53%	38,56%	31,97%
Decr	39,51%	31,39%	24,72%
Incr	40,19%	30,42%	21,47%
Larg	33,83%	29,70%	25,50%
Len	32,91%	28,57%	28,62%
SMI	16,70%	14,18%	15,99%

Table 31. Percentages of Grasslands areas showing Medium Correlation level between the phenological parameters and cumulated rainfall for the second growing season

Grassland	SEASON 2		
Phenological Parameter	High Correlation		
	TRMM 1 Month	TRMM 3 Months	TRMM 6 Months
Amp	47,11%	40,26%	34,34%
Base	33,92%	29,66%	25,40%
Decr	28,46%	20,64%	14,51%
Incr	28,44%	18,20%	11,88%
Larg	44,20%	39,44%	34,81%
Len	52,97%	49,17%	41,12%
SMI	57,92%	44,49%	38,01%

Table 32. Percentages of Grasslands areas showing High Correlation level between the phenological parameters and cumulated rainfall for the second growing season

Grassland	SEASON 2		
Phenological Parameter	Very High Correlation		
	TRMM 1 Month	TRMM 3 Months	TRMM 6 Months
Amp	7,76%	12,23%	10,57%
Base	3,46%	2,45%	2,75%
Decr	3,31%	2,39%	1,46%
Incr	1,68%	1,26%	0,95%
Larg	6,47%	11,36%	10,44%
Len	5,32%	7,95%	7,44%
SMI	21,79%	34,56%	31,68%

Figure 61. Percentages of Grasslands areas showing Very High Correlation level between the phenological parameters and cumulated rainfall for the second growing season

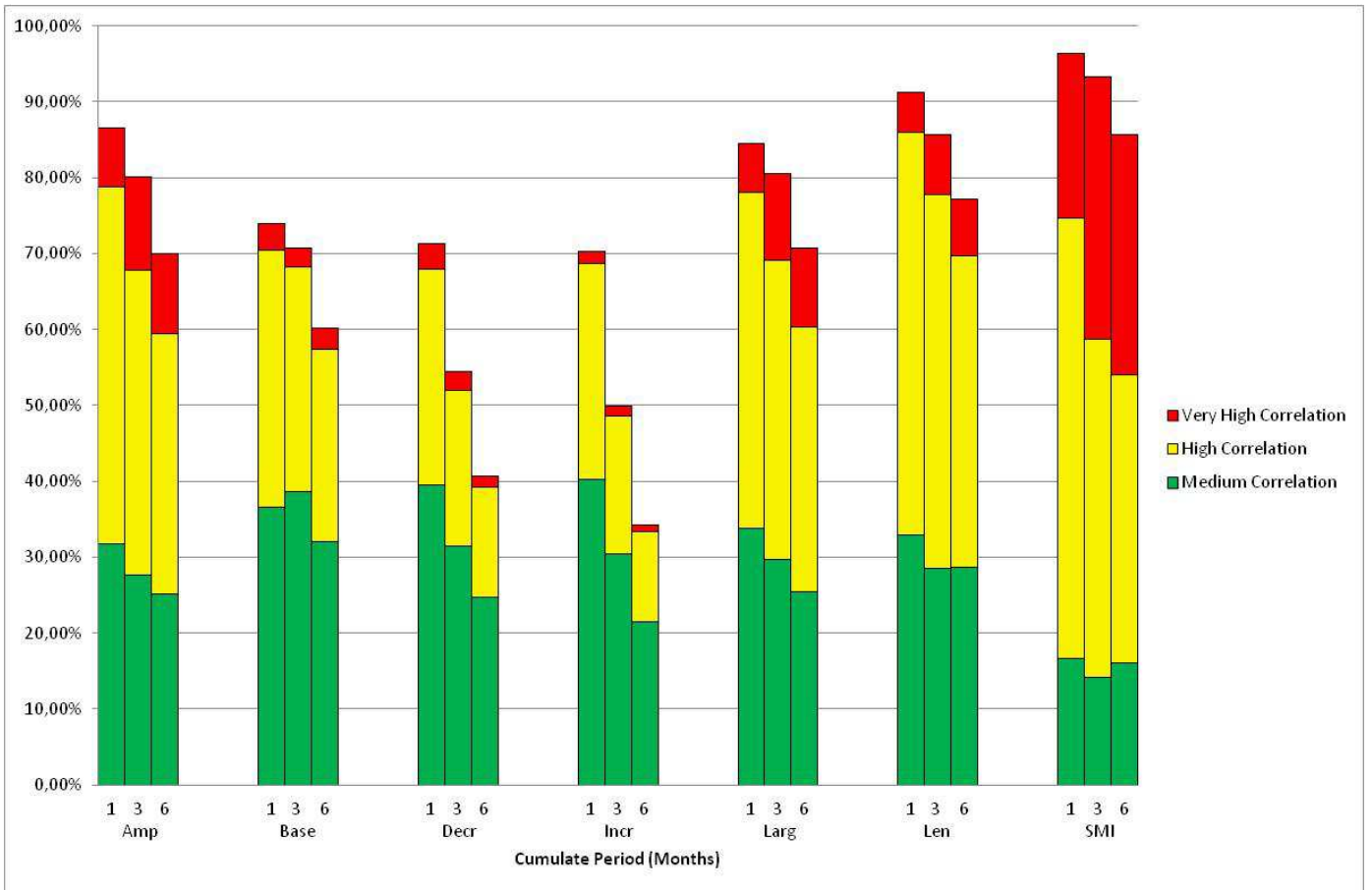


Figure 62. Correlation Analysis for the Grasslands land cover type, second growing season

8.2.3. Cropland Natural Vegetation Mosaic

8.2.3.1. Second growing season

Crop/NatMos	SEASON 2		
Phenological Parameter	Medium Correlation		
	TRMM 1 Month	TRMM 3 Months	TRMM 6 Months
Amp	38,78%	25,26%	17,07%
Base	35,92%	28,92%	23,29%
Decr	37,43%	25,76%	16,77%
Incr	36,83%	24,62%	15,99%
Larg	37,06%	28,92%	23,13%
Len	40,52%	26,06%	18,87%
SMI	34,18%	22,08%	16,33%

Table 33. Percentages of Cropland/Natural vegetation mosaic areas showing Medium Correlation level between the phenological parameters and cumulated rainfall for the second growing season

Crop/NatMos	SEASON 2		
Phenological Parameter	High Correlation		
	TRMM 1 Month	TRMM 3 Months	TRMM 6 Months
Amp	20,68%	14,39%	8,05%
Base	24,91%	22,72%	17,71%
Decr	24,43%	13,27%	8,08%
Incr	24,20%	11,76%	6,79%
Larg	21,96%	18,83%	13,80%
Len	25,28%	21,80%	16,01%
SMI	31,55%	23,24%	17,91%

Table 34. Percentages of Cropland/Natural vegetation mosaic areas showing High Correlation level between the phenological parameters and cumulated rainfall for the second growing season

Crop/NatMos	SEASON 2		
Phenological Parameter	Very High Correlation		
	TRMM 1 Month	TRMM 3 Months	TRMM 6 Months
Amp	0,92%	1,08%	0,48%
Base	2,13%	2,31%	2,04%
Decr	2,06%	0,78%	0,30%
Incr	1,42%	0,75%	0,30%
Larg	0,82%	0,98%	0,96%
Len	1,30%	1,83%	1,42%
SMI	2,22%	4,74%	3,00%

Table 35. Percentages of Cropland/Natural vegetation mosaic areas showing Very High Correlation level between the phenological parameters and cumulated rainfall for the second growing season

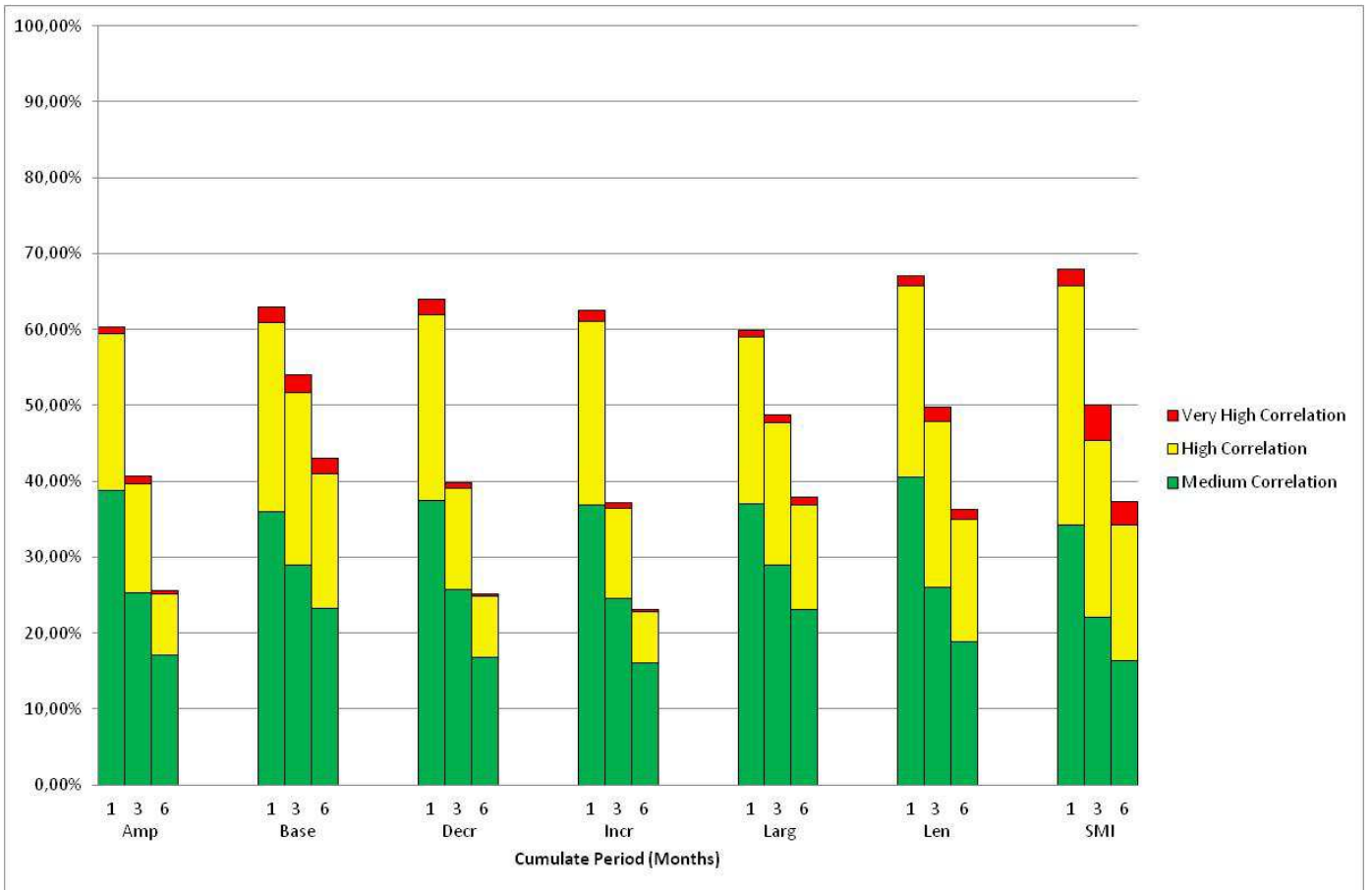


Figure 63. Correlation Analysis for the Cropland/Natural vegetation mosaic land cover type, second growing season

8.2.4. Woody savannas

8.2.4.1. First growing season

Woody Sav	SEASON 1		
Phenological Parameter	Medium Correlation		
	TRMM 1 Month	TRMM 3 Months	TRMM 6 Months
Amp	35,66%	24,21%	16,46%
Base	40,60%	34,68%	27,89%
Decr	34,81%	24,97%	17,64%
Incr	36,75%	30,11%	24,97%
Larg	38,76%	29,62%	22,16%
Len	41,62%	33,57%	26,35%
SMI	38,95%	28,15%	21,27%

Table 36. Percentages of Woody Savannas areas showing Medium Correlation level between the phenological parameters and cumulated rainfall for the first growing season

Woody Sav	SEASON 1		
Phenological Parameter	High Correlation		
	TRMM 1 Month	TRMM 3 Months	TRMM 6 Months
Amp	16,20%	10,82%	6,91%
Base	32,39%	28,42%	21,28%
Decr	21,19%	13,59%	8,36%
Incr	32,23%	23,06%	16,99%
Larg	21,53%	16,73%	11,94%
Len	26,26%	21,21%	15,38%
SMI	20,49%	15,50%	11,19%

Table 37. Percentages of Woody Savannas areas showing High Correlation level between the phenological parameters and cumulated rainfall for the first growing season

Woody Sav	SEASON 1		
Phenological Parameter	Very High Correlation		
	TRMM 1 Month	TRMM 3 Months	TRMM 6 Months
Amp	0,55%	0,41%	0,27%
Base	1,79%	2,02%	1,70%
Decr	2,05%	1,26%	0,56%
Incr	3,56%	2,15%	1,34%
Larg	0,86%	0,91%	0,74%
Len	1,13%	1,23%	0,97%
SMI	0,89%	0,94%	0,69%

Table 38. Percentages of Woody Savannas areas showing Very High Correlation level between the phenological parameters and cumulated rainfall for the first growing season

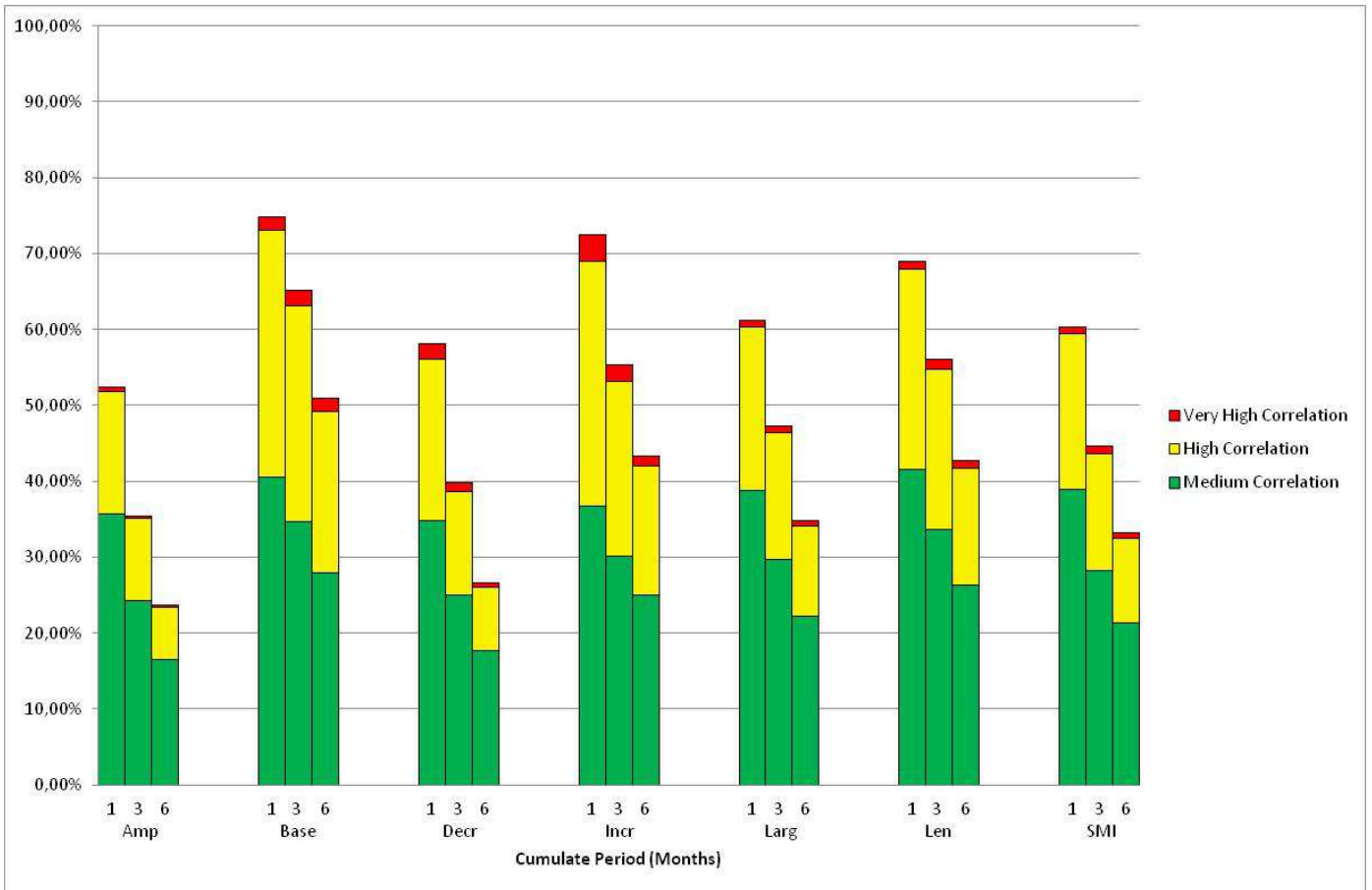


Figure 64. Correlation Analysis for the Woody Savannas land cover type, first growing season

8.2.5. Savannas

8.2.5.1. First growing season

Savannas	SEASON 1		
Phenological Parameter	Medium Correlation		
	TRMM 1 Month	TRMM 3 Months	TRMM 6 Months
Amp	36,87%	25,75%	19,13%
Base	38,53%	33,97%	30,81%
Decr	35,40%	26,02%	19,29%
Incr	35,79%	28,94%	23,38%
Larg	40,76%	32,13%	26,05%
Len	41,78%	35,34%	31,26%
SMI	40,50%	32,06%	26,49%

Table 39. Percentages of Savannas areas showing Medium Correlation level between the phenological parameters and cumulated rainfall for the first growing season

Savannas	SEASON 1		
Phenological Parameter	High Correlation		
	TRMM 1 Month	TRMM 3 Months	TRMM 6 Months
Amp	18,61%	12,14%	8,16%
Base	39,94%	36,68%	31,31%
Decr	22,36%	14,72%	9,17%
Incr	32,15%	19,75%	13,43%
Larg	24,38%	18,57%	13,43%
Len	32,45%	28,68%	24,14%
SMI	27,40%	21,63%	17,69%

Table 40. Percentages of Savannas areas showing High Correlation level between the phenological parameters and cumulated rainfall for the first growing season

Savannas	SEASON 1		
Phenological Parameter	Very High Correlation		
	TRMM 1 Month	TRMM 3 Months	TRMM 6 Months
Amp	0,69%	0,53%	0,40%
Base	3,79%	4,24%	3,57%
Decr	2,03%	1,13%	0,51%
Incr	3,53%	1,51%	0,80%
Larg	0,98%	0,91%	0,66%
Len	1,47%	2,05%	1,92%
SMI	1,25%	1,30%	1,16%

Table 41. Very Percentages of Savannas areas showing Very High Correlation level between the phenological parameters and cumulated rainfall for the first growing season

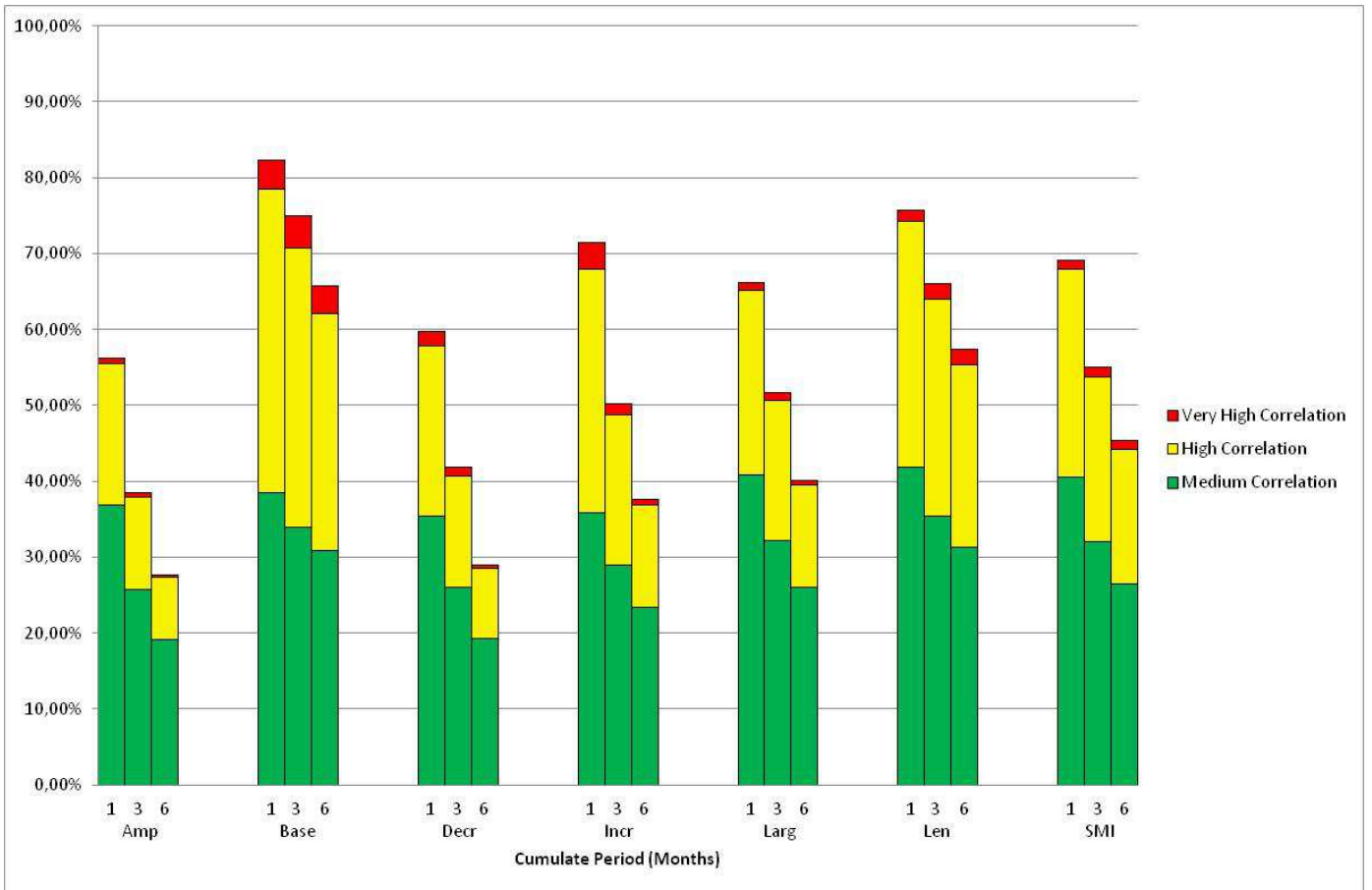


Figure 65. Correlation Analysis for the Savannas land cover type, first growing season

8.2.6. Croplands

8.2.6.1. First growing season

Cropland	SEASON 1		
Phenological Parameter	Medium Correlation		
	TRMM 1 Month	TRMM 3 Months	TRMM 6 Months
Amp	39,34%	30,95%	23,65%
Base	41,00%	33,62%	28,16%
Decr	34,42%	27,12%	18,63%
Incr	35,69%	28,34%	21,73%
Larg	41,03%	33,69%	26,53%
Len	41,13%	33,07%	29,86%
SMI	40,70%	31,23%	27,90%

Table 42. Percentages of Croplands areas showing Medium Correlation level between the phenological parameters and cumulated rainfall for the first growing season

Cropland	SEASON 1		
Phenological Parameter	High Correlation		
	TRMM 1 Month	TRMM 3 Months	TRMM 6 Months
Amp	20,81%	19,30%	15,61%
Base	34,97%	36,52%	32,99%
Decr	22,63%	16,88%	9,74%
Incr	28,54%	20,51%	13,66%
Larg	22,36%	22,25%	18,85%
Len	37,69%	36,79%	30,31%
SMI	38,51%	37,33%	31,18%

Table 43. Percentages of Croplands areas showing High Correlation level between the phenological parameters and cumulated rainfall for the first growing season

Cropland	SEASON 1		
Phenological Parameter	Very High Correlation		
	TRMM 1 Month	TRMM 3 Months	TRMM 6 Months
Amp	0,99%	1,35%	1,31%
Base	2,25%	3,34%	3,71%
Decr	1,74%	1,58%	0,64%
Incr	3,06%	2,11%	1,07%
Larg	1,02%	1,40%	1,56%
Len	2,14%	3,96%	3,19%
SMI	1,96%	5,32%	5,20%

Table 44. Percentages of Croplands areas showing Very High Correlation level between the phenological parameters and cumulated rainfall for the first growing season

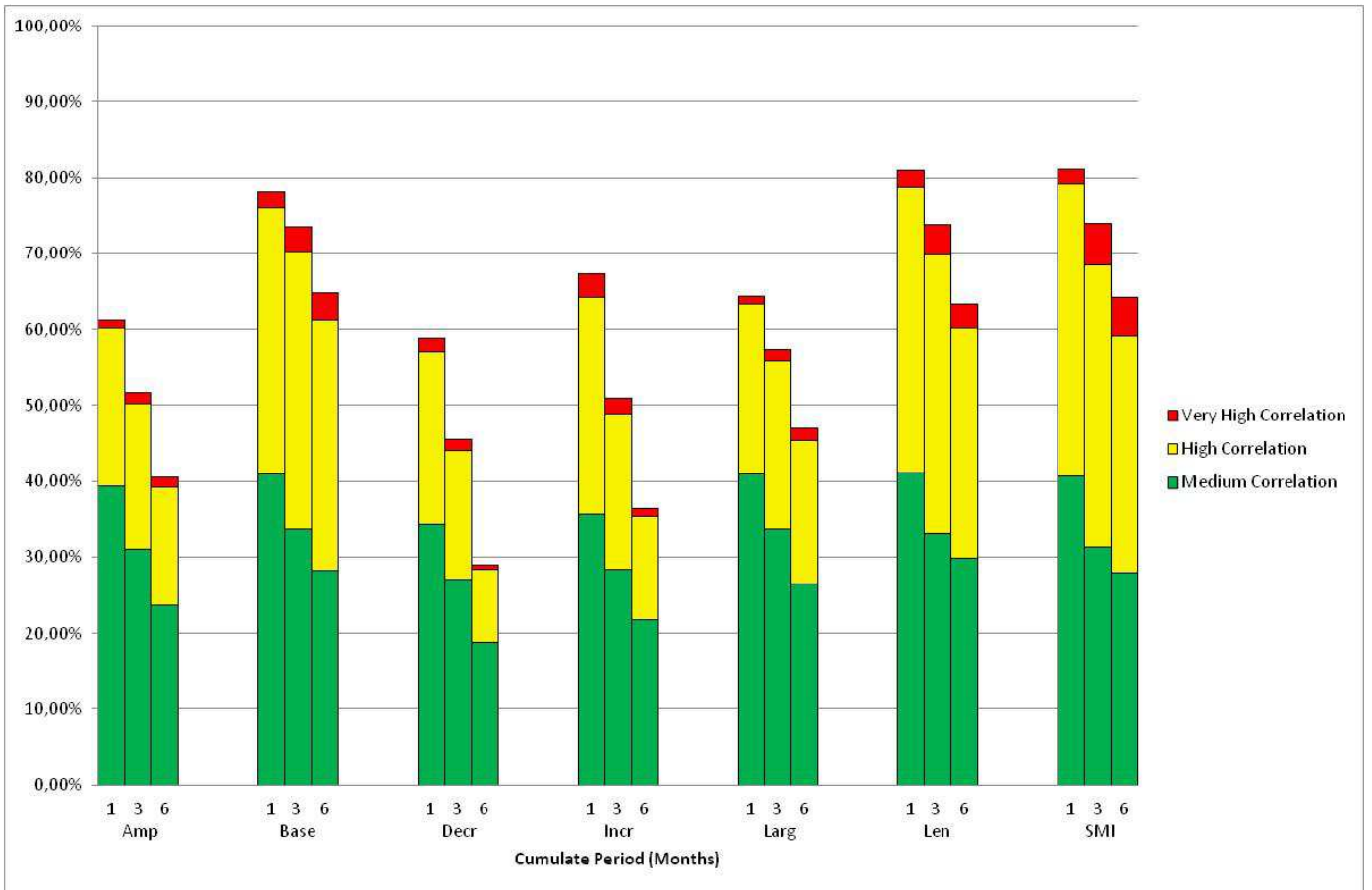


Figure 66. Correlation Analysis for the Croplands land cover type, first growing season

8.3. Integration Analysis

8.3.1. Spatial Correlation Analysis

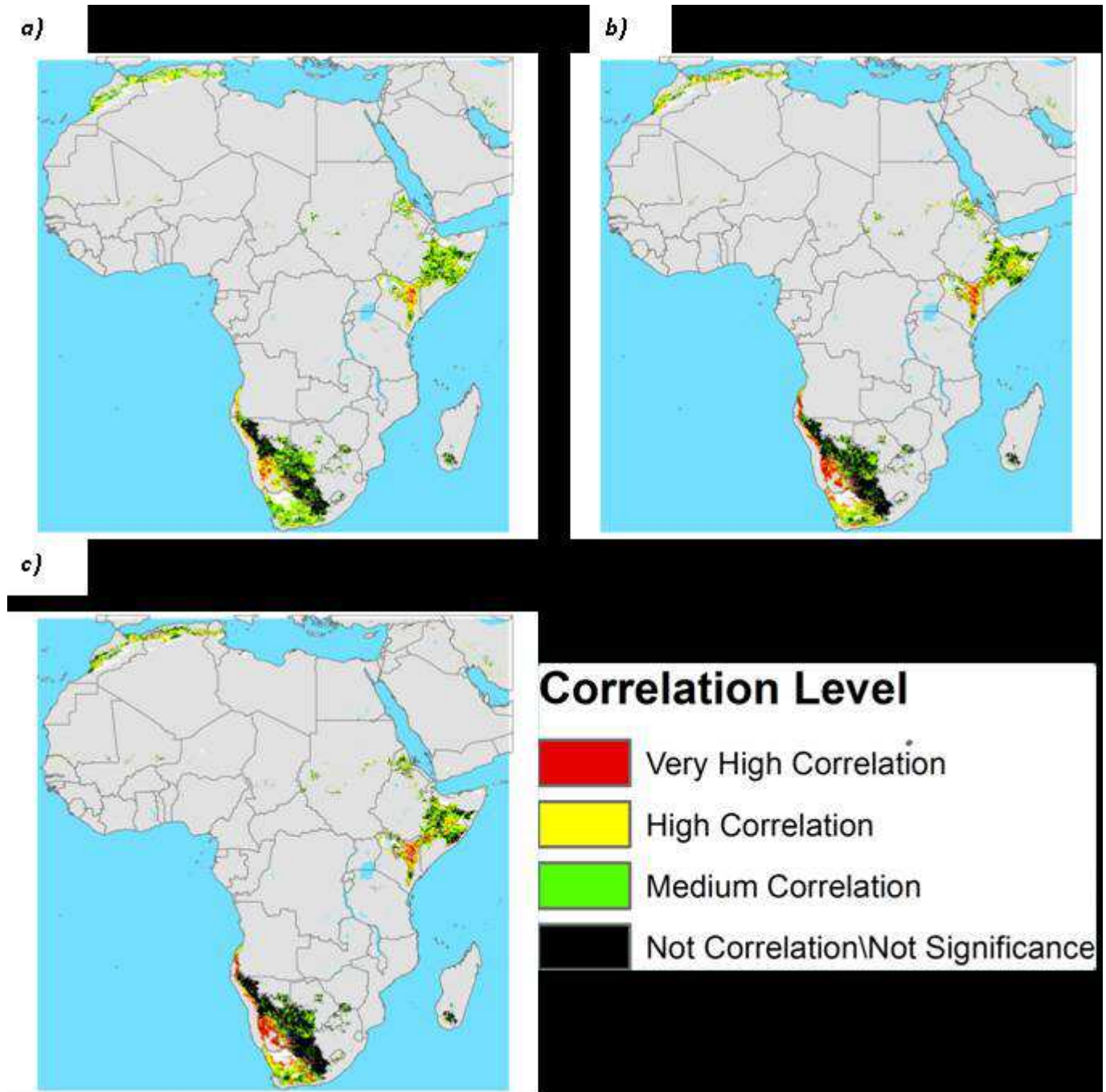


Figure 67. Maps showing the Maximum Correlation levels for the Amplitude (Amp) on a pixel basis for each cumulating intervals (a) 1 month, b) 3 months, c) 6 months) for the Open shrublands vegetation land cover type (first growing season)

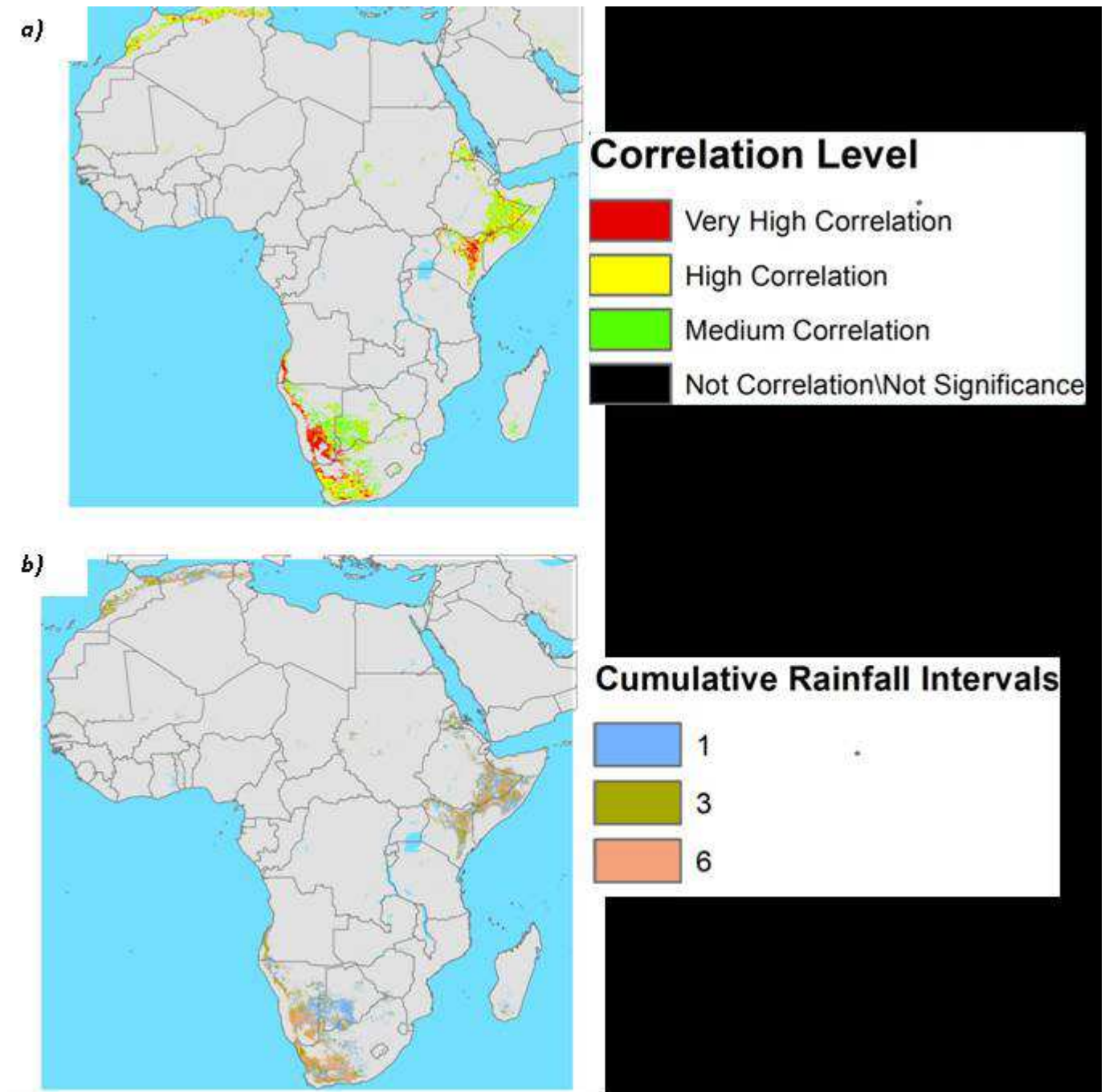


Figure 68.a) Maximum Absolute Correlation levels for the Amplitude (Amp) on a pixel basis for the Open shrublands vegetation cover type for the first growing season, b) rainfall cumulating intervals corresponding to the absolute maximum correlation level for the Amplitude (Amp) on a pixel basis for the Open shrublands vegetation cover type for the first growing season

a)



b)



c)



Correlation Level

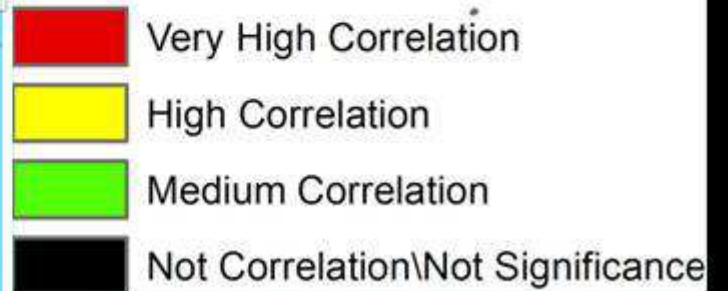


Figure 69. Maps showing the Maximum Correlation levels for the Length (Len) on a pixel basis for each cumulating intervals (a) 1 month, b) 3 months, c) 6 months) for the Open shrublands vegetation land cover type (first growing season)

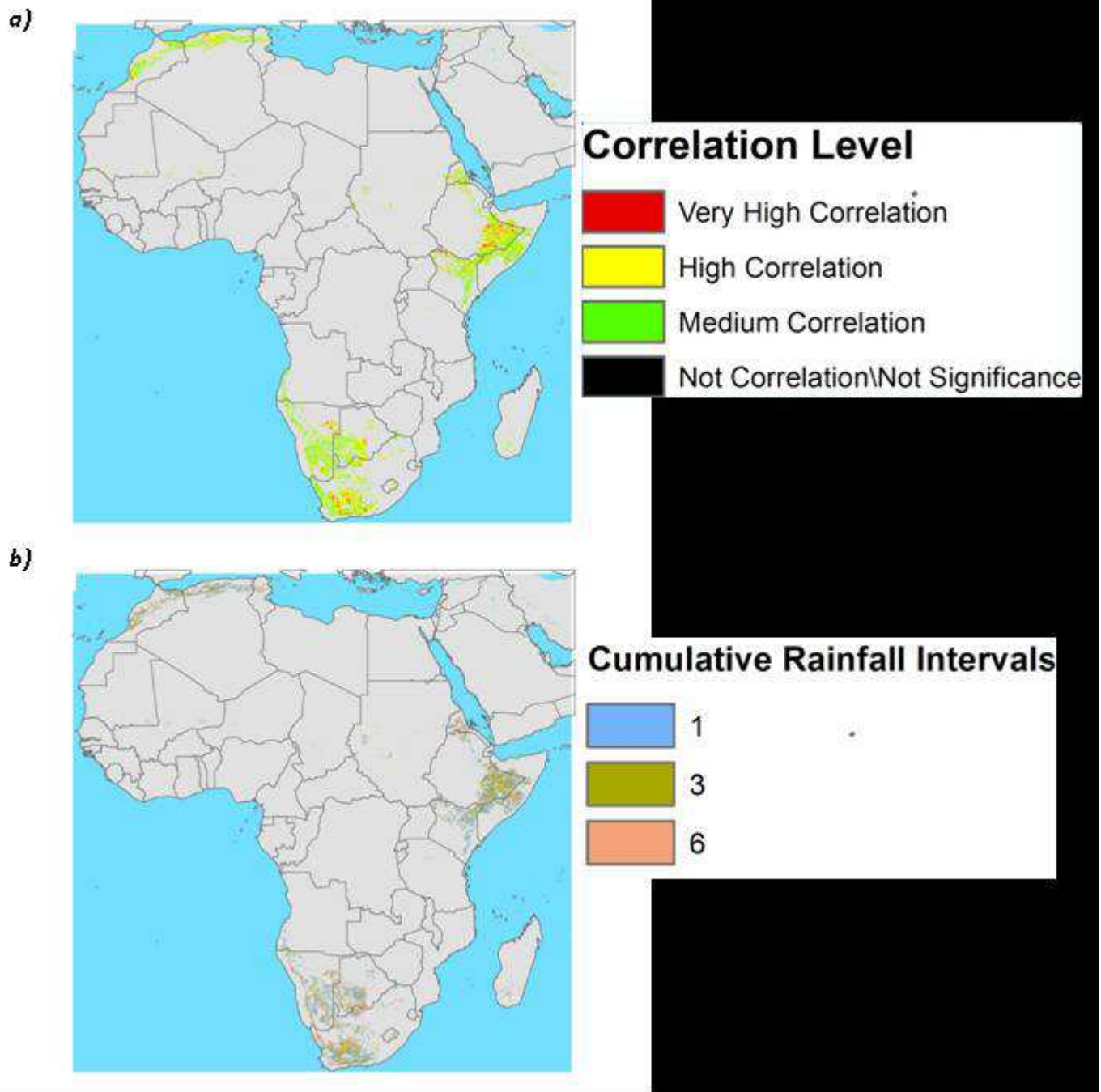
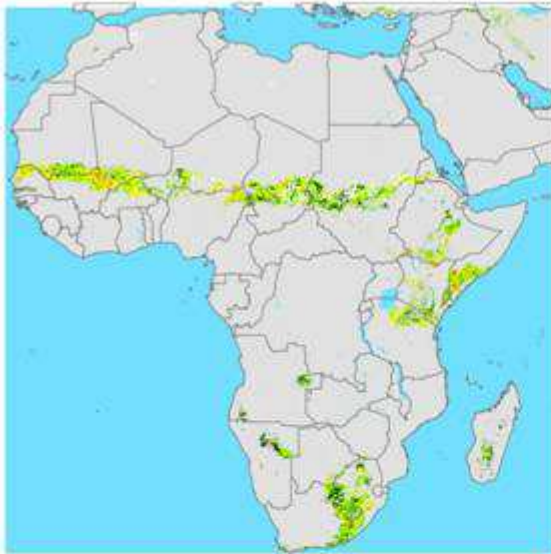
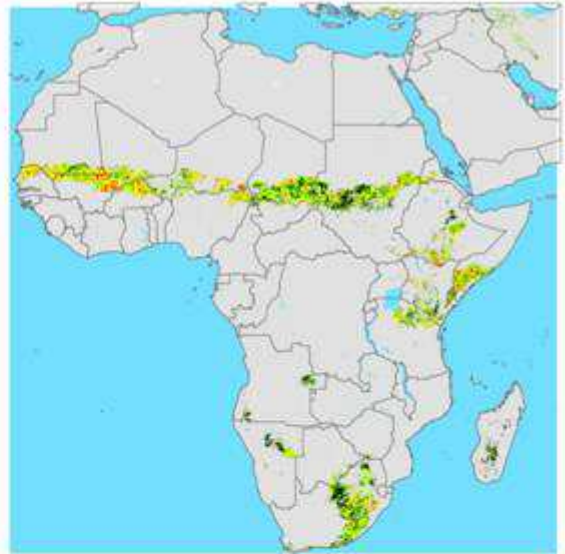


Figure 70. a) Maximum Absolute Correlation levels for the Length (Len) on a pixel basis for the Open shrublands vegetation cover type for the first growing season, b) rainfall cumulating intervals corresponding to the absolute maximum correlation level for Length (Len) on a pixel basis for the Open shrublands vegetation cover type for the first growing season

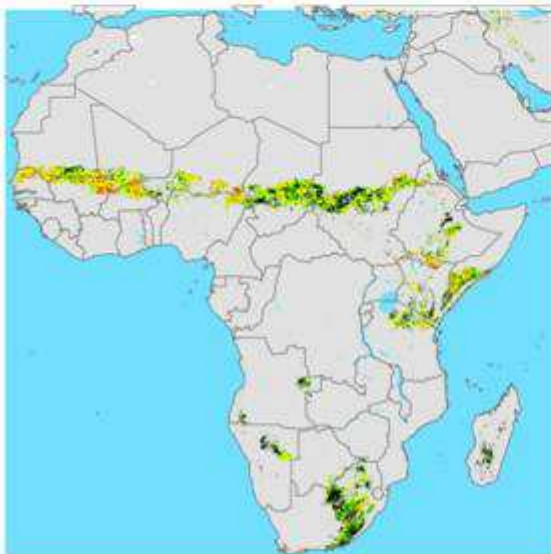
a)



b)



c)



Correlation Level

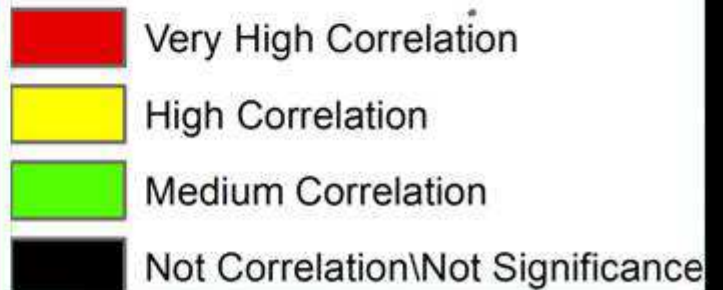


Table 45. Maps showing the Maximum Correlation levels for the Seasonal Small Integral (Smi) on a pixel basis for each cumulating intervals (a) 1 month, b) 3 months, c) 6months) for the Grasslands vegetation land cover type (first growing season)

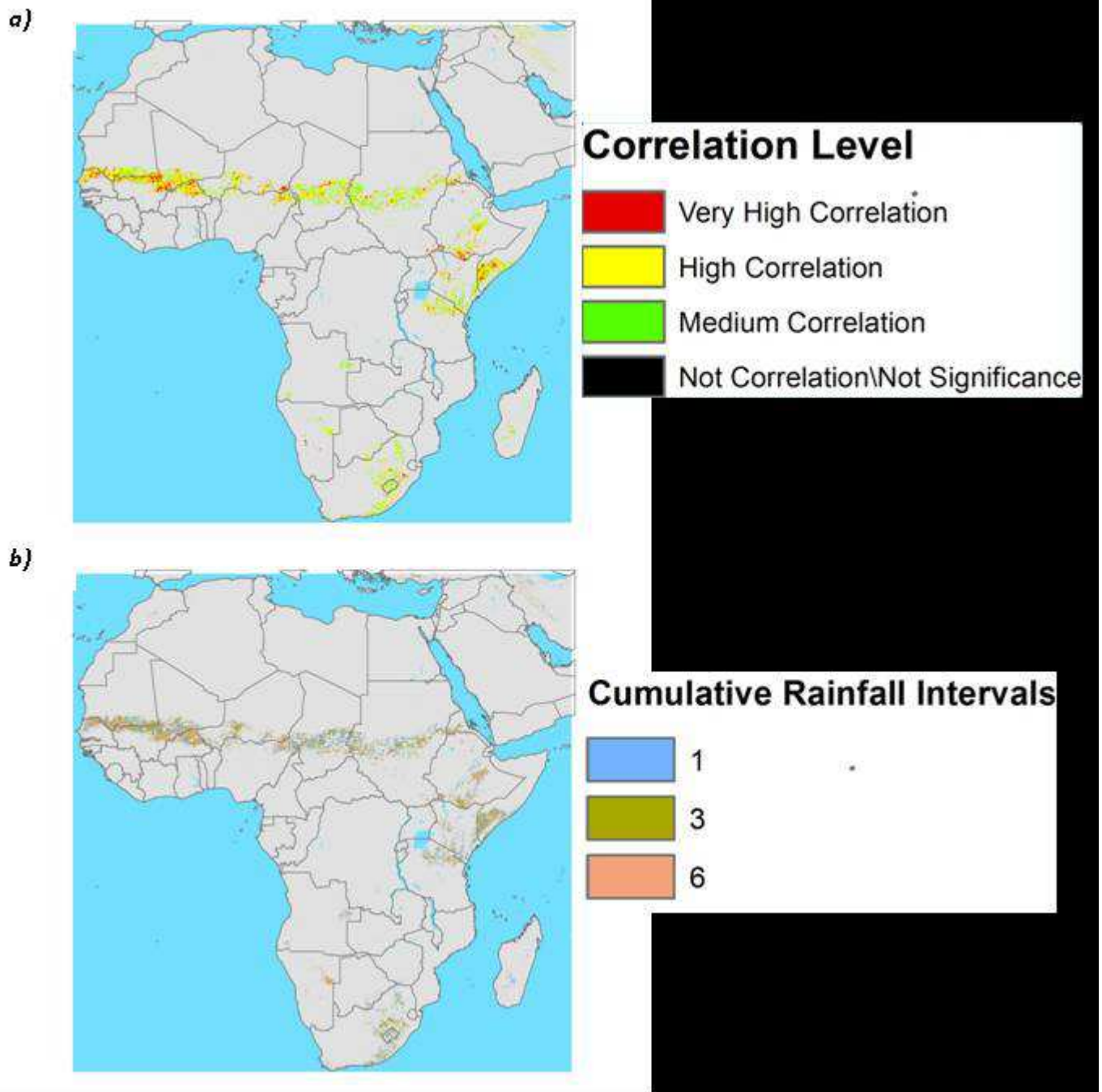


Table 46. a) Maximum Absolute Correlation levels for the Seasonal Small Integral (Sml) on a pixel basis for the Grasslands vegetation cover type for the first growing season, b) rainfall cumulating intervals corresponding to the absolute maximum correlation level for Seasonal Small Integral (Sml) on a pixel basis for the Grasslands vegetation cover type for the first growing season

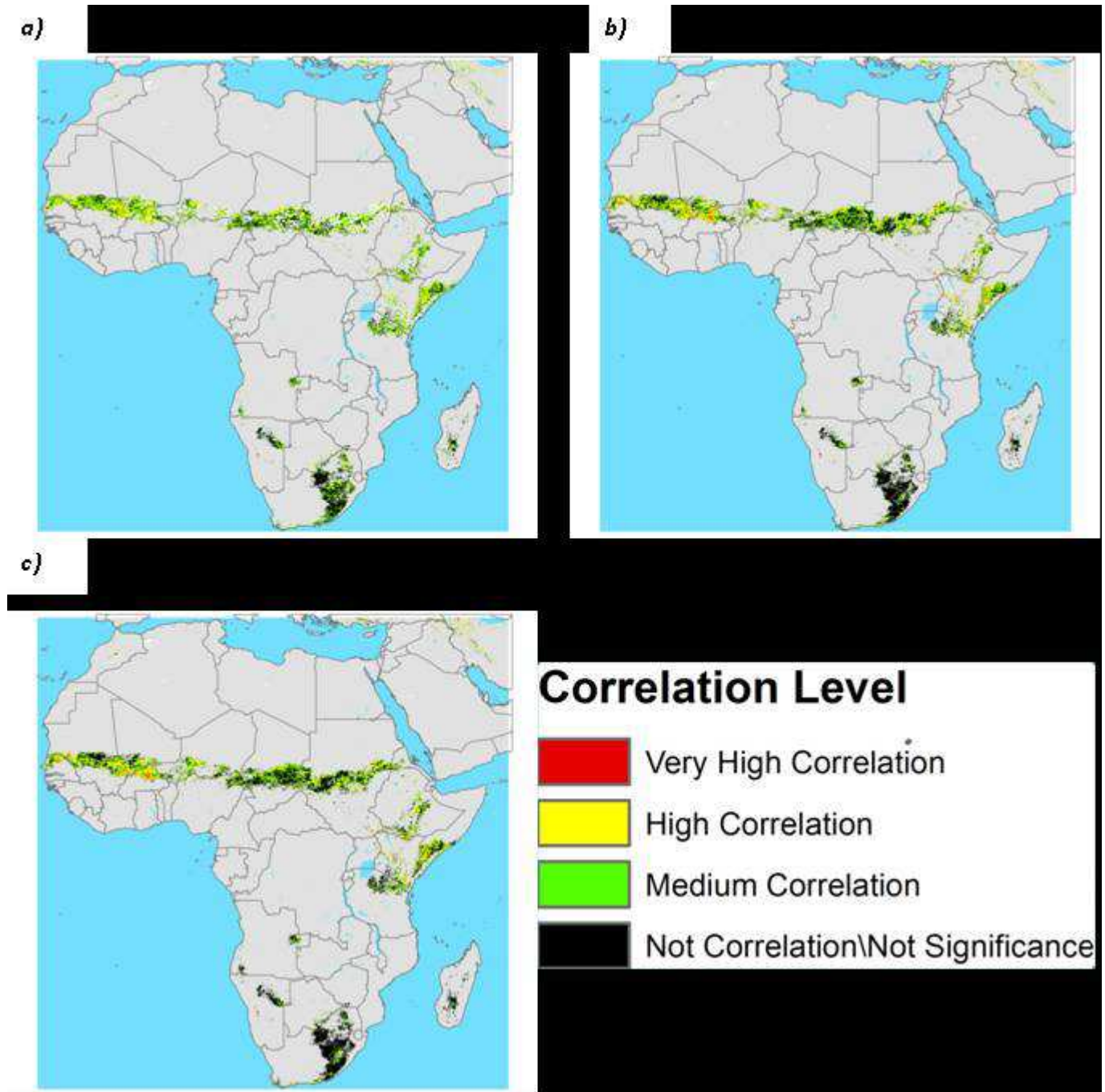


Figure 71. Maps showing the Maximum Correlation levels for the Amplitude (Amp) on a pixel basis for each cumulating intervals (a) 1 month, b) 3 months, c) 6 months) for the Grasslands vegetation land cover type (first growing season)

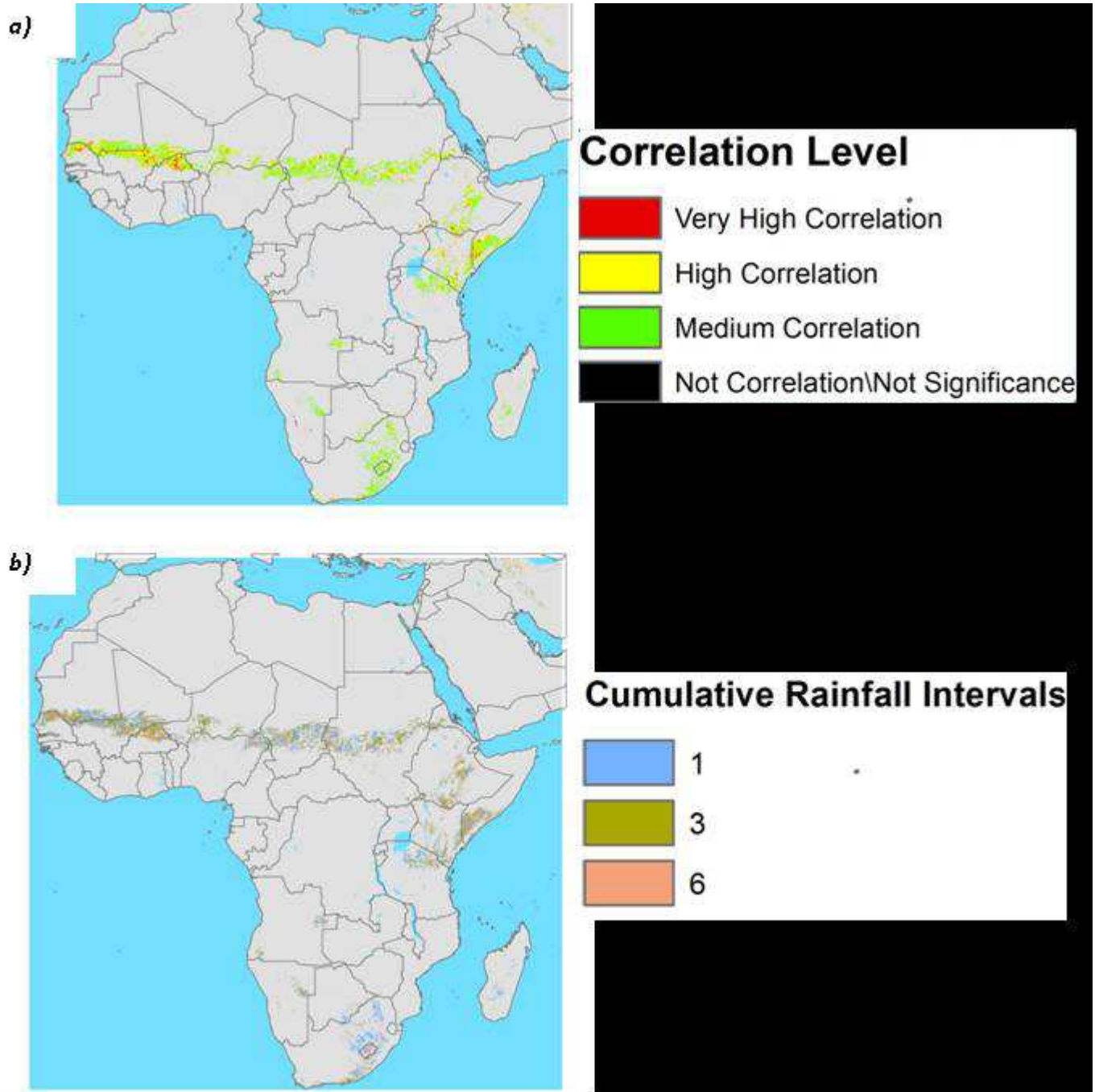


Figure 72. a) Maximum Absolute Correlation levels for the Amplitude (Amp) on a pixel basis for the Grasslands vegetation cover type for the first growing season, b) rainfall cumulating intervals corresponding to the absolute maximum correlation level for the Amplitude (Amp) on a pixel basis for the Grasslands vegetation cover type for the first growing season

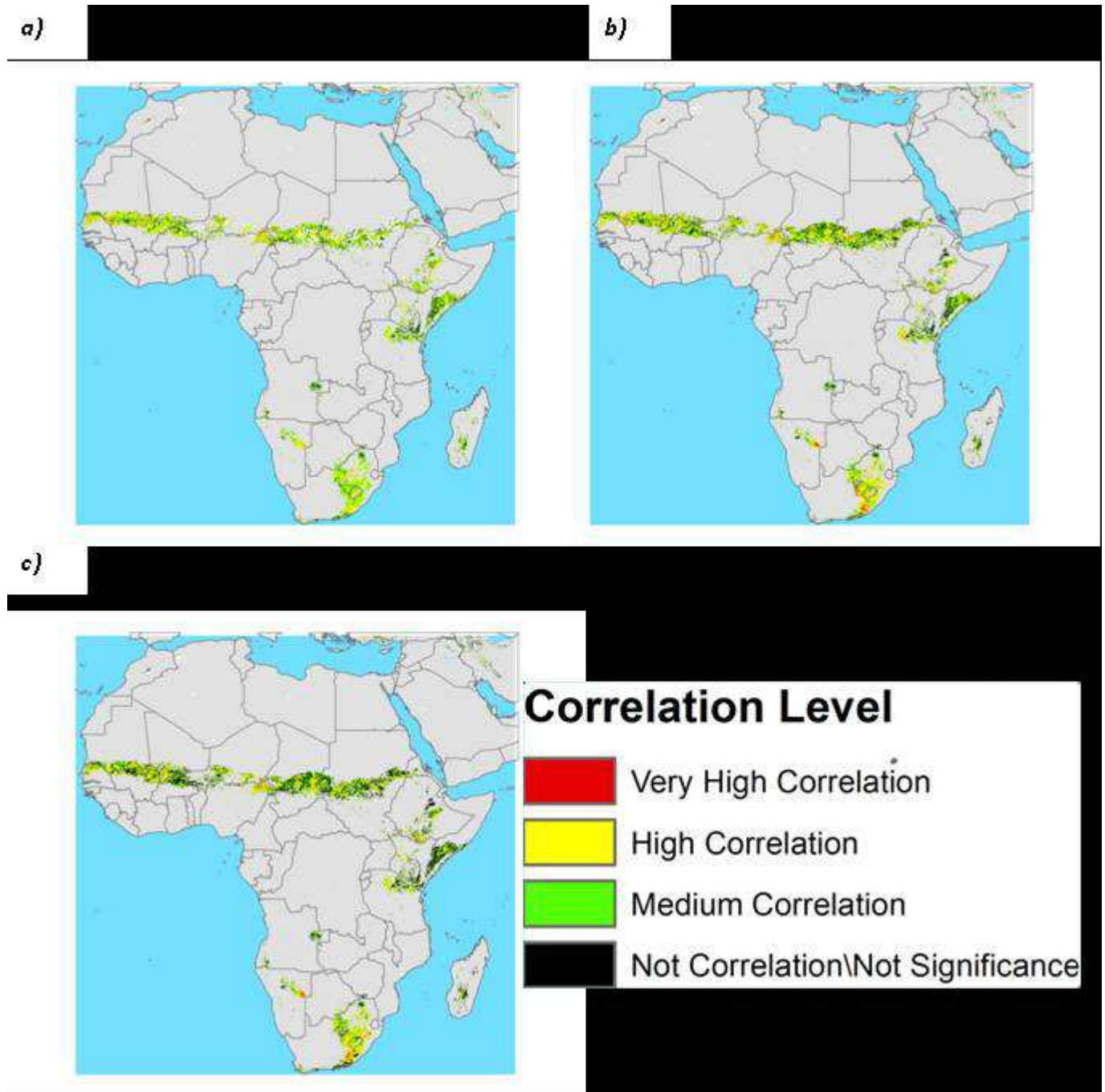


Figure 73. Maximum Correlation levels for the Length of the season (Len) on a pixel basis for each cumulative intervals for the Grasslands vegetation cover type for the first growing season a) 1 month, b) 3 months, c) 6 months.

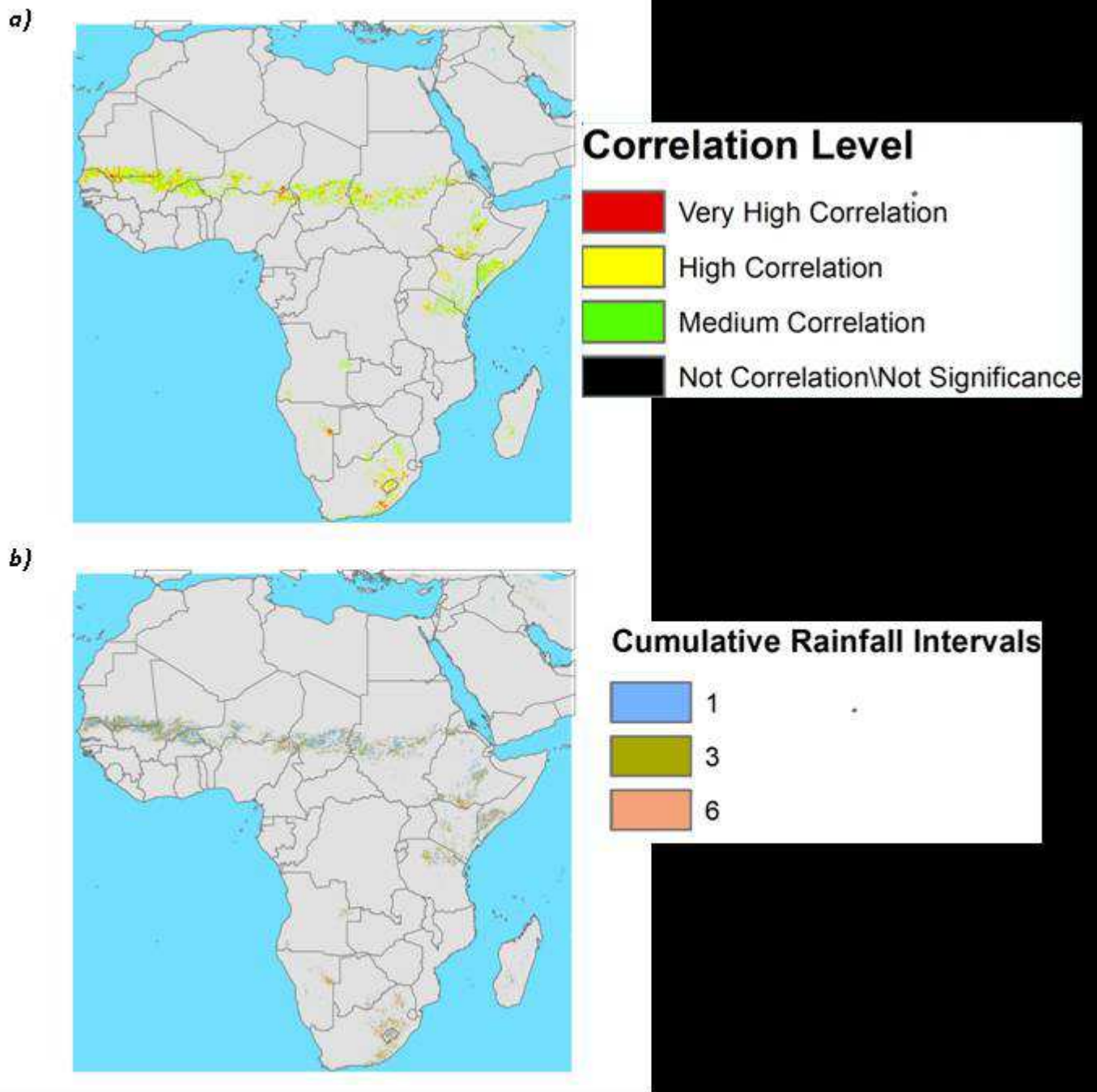
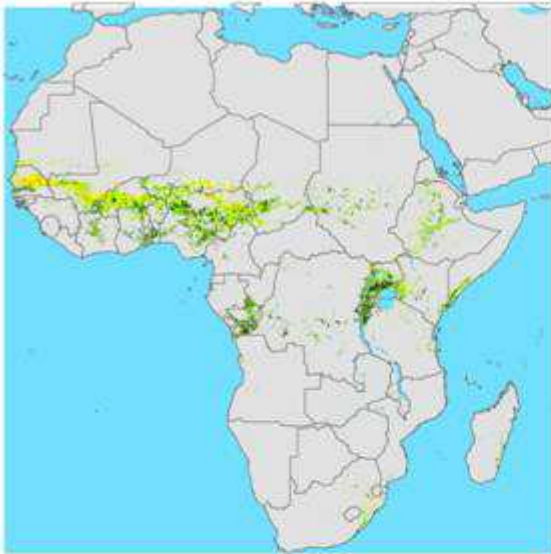
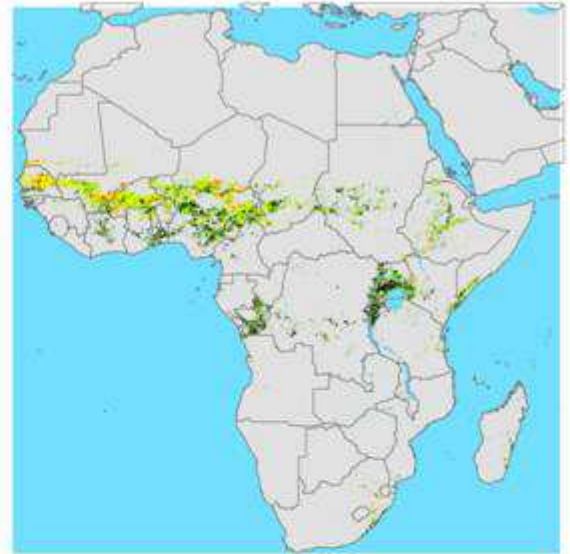


Figure 74. a) Maximum Absolute Correlation levels for the Length (Len) on a pixel basis for the Grasslands vegetation cover type for the first growing season, b) rainfall cumulating intervals corresponding to the absolute maximum correlation level for the Length (Len) on a pixel basis for the Grasslands vegetation cover type for the first growing season

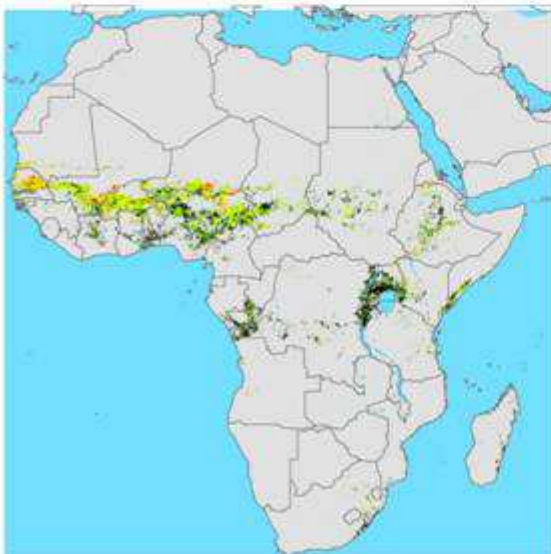
a)



b)



c)



Correlation Level





	Very High Correlation
	High Correlation
	Medium Correlation
	Not Correlation\Not Significance

Table 47. Maximum Correlation levels for the Seasonal Small Integral (Sml) on a pixel basis for each cumulative intervals for the Cropland/Natural vegetation mosaic cover type for the first growing season a) 1 month, b) 3 months, c) 6 months.

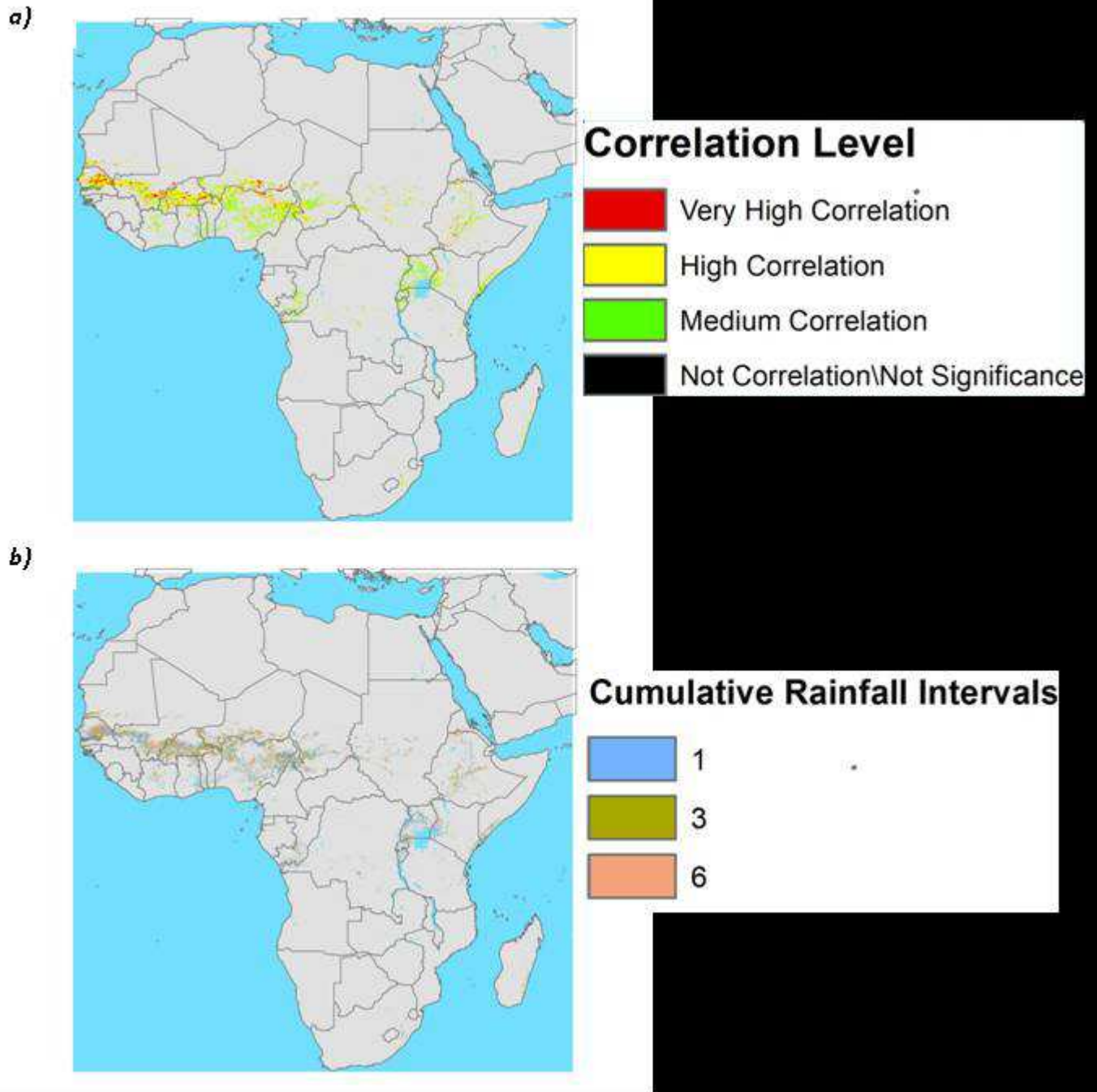


Table 48. a) Maximum Absolute Correlation levels for the Seasonal Small Integral (SMI) on a pixel basis for the Cropland/Natural vegetation mosaic cover type for the first growing season, b) rainfall cumulating intervals corresponding to the absolute maximum correlation level for the Seasonal Small Integral (SMI) on a pixel basis for the Cropland/Natural vegetation mosaic cover type for the first growing season

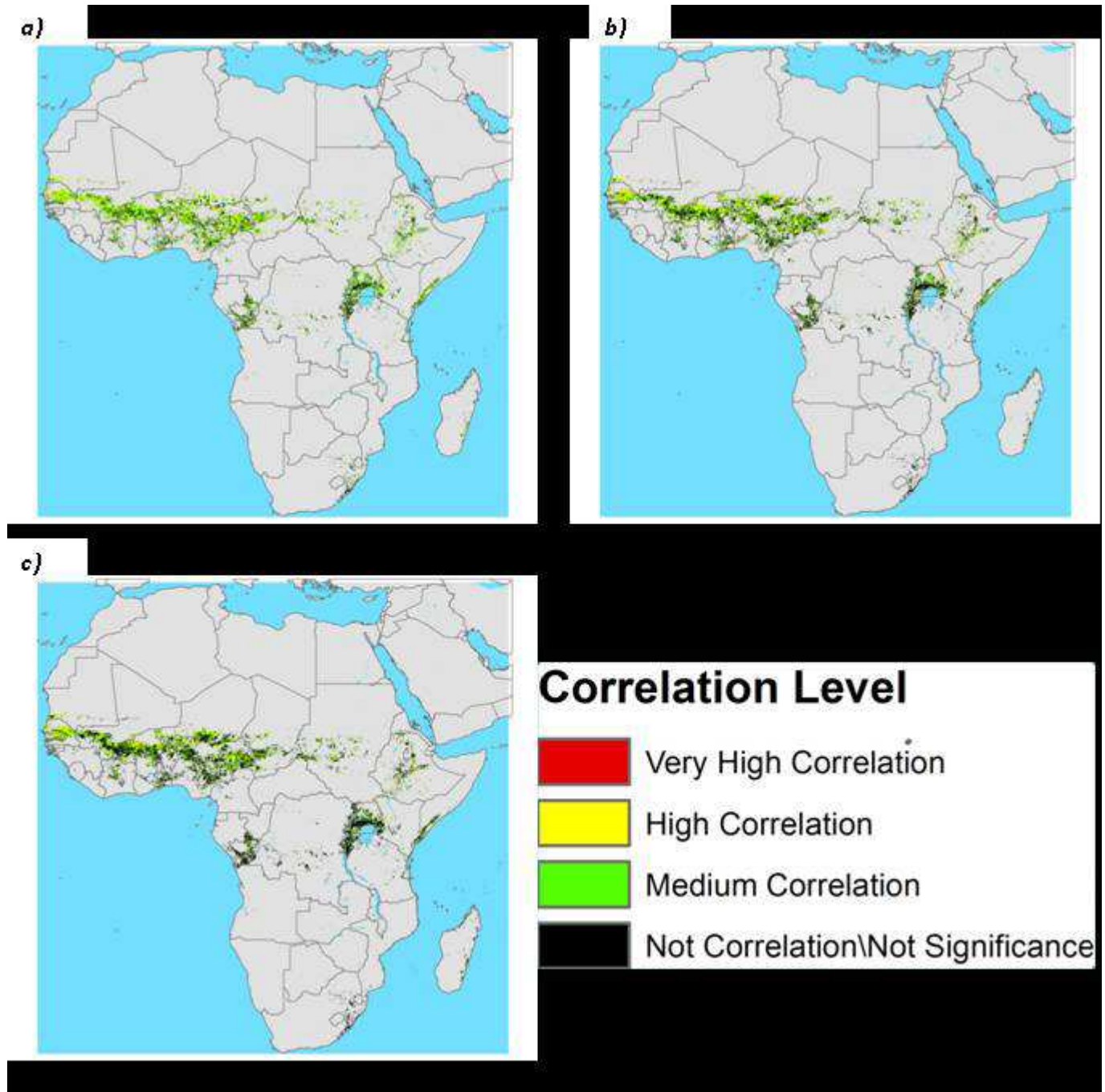


Figure 75. Maximum Correlation levels for the Amplitude (Len) on a pixel basis for each cumulative intervals for the Cropland/Natural vegetation mosaic cover type for the first growing season a) 1 month, b) 3 months, c) 6months.

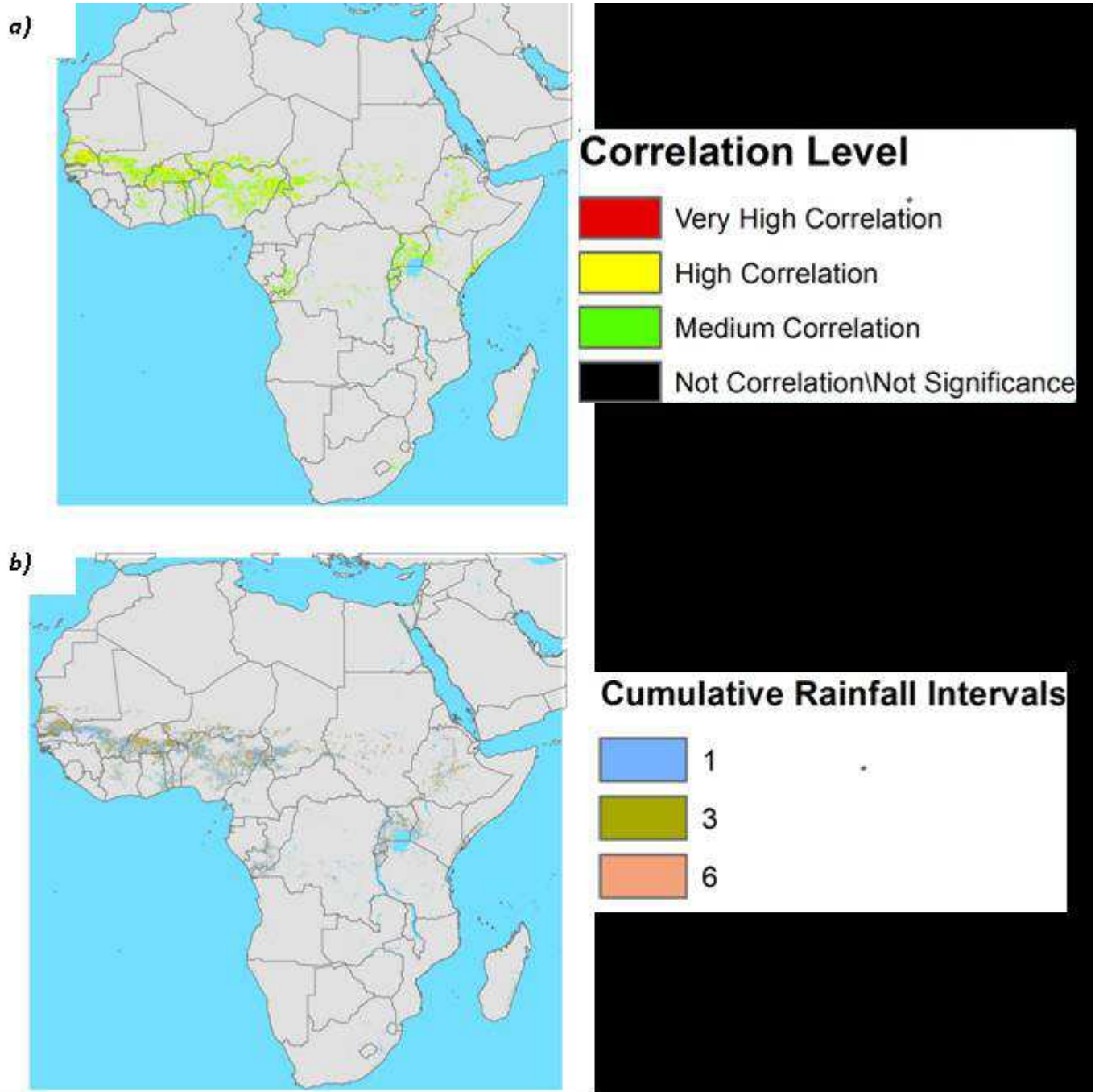


Figure 76. a) Maximum Absolute Correlation levels for the Amplitude (Amp) on a pixel basis for the Cropland/Natural vegetation mosaic cover type for the first growing season, b) rainfall cumulating intervals corresponding to the absolute maximum correlation level for the Amplitude (Amp) on a pixel basis for the Cropland/Natural vegetation mosaic cover type for the first growing season

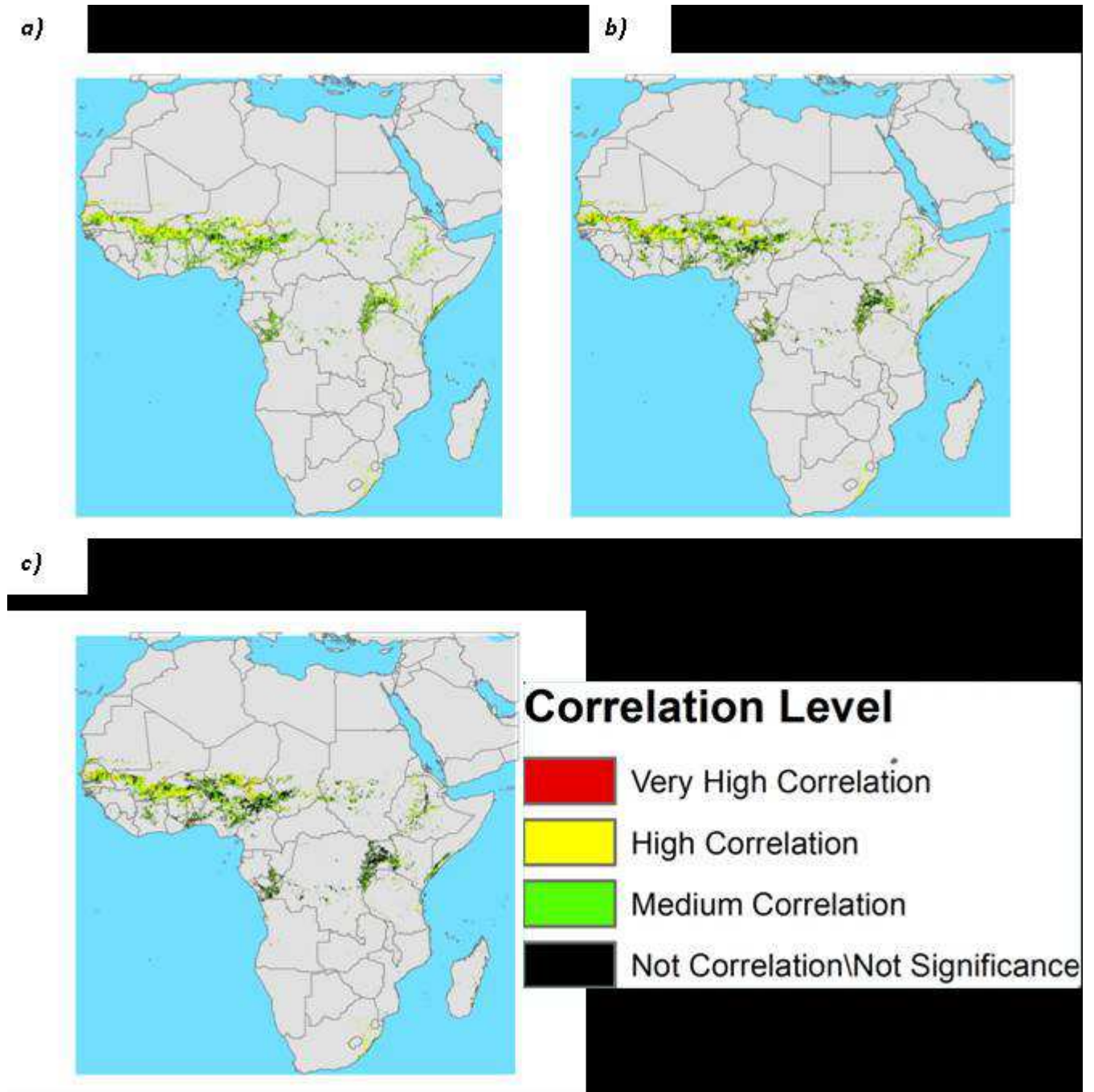


Figure 77. Maximum Correlation levels for the Length of the season (Len) on a pixel basis for each cumulative intervals for the Cropland/Natural vegetation mosaic cover type for the first growing season a) 1 month, b) 3 months, c) 6 months.

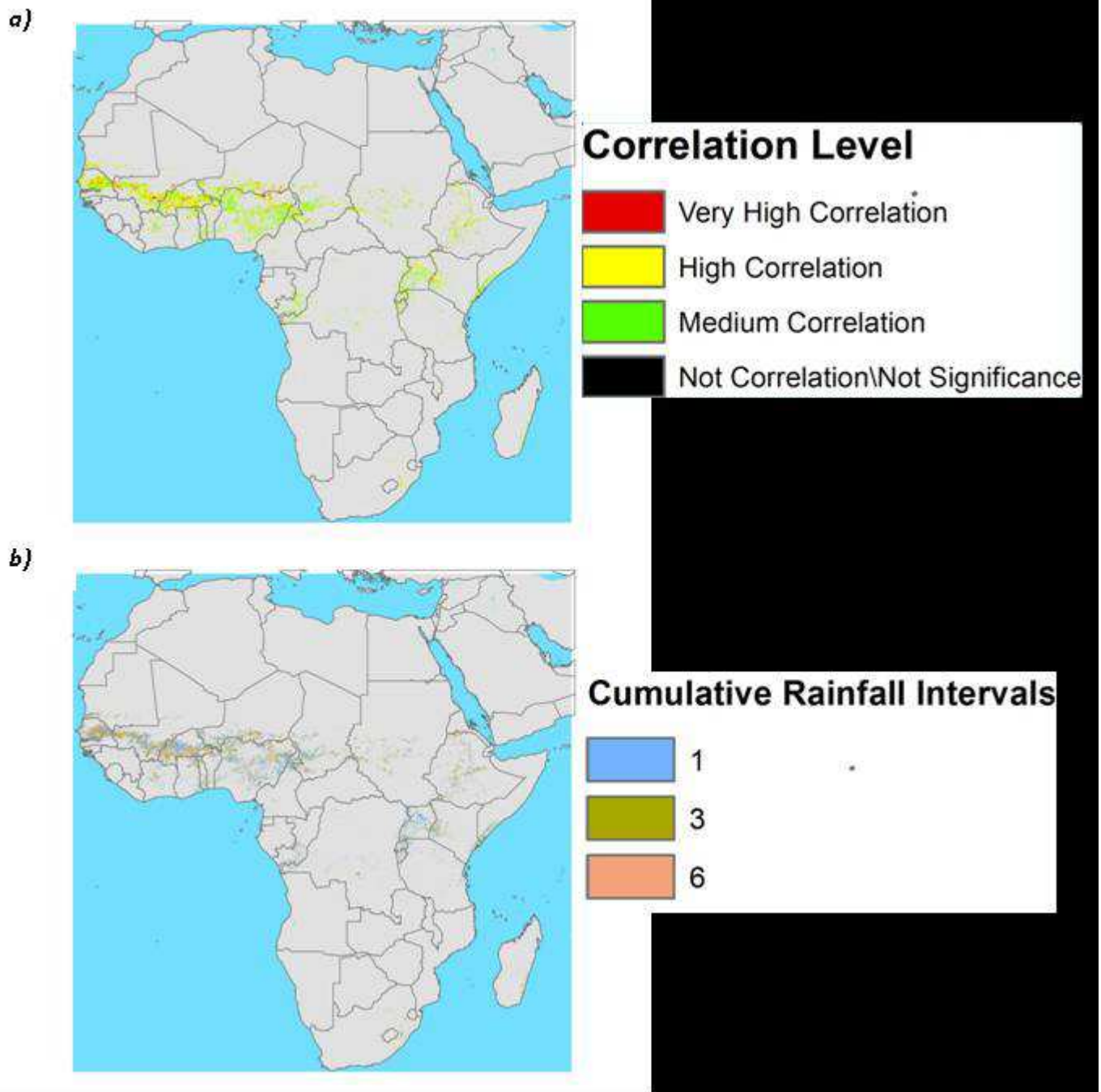


Figure 78. a) Maximum Absolute Correlation levels for the Length (Len) on a pixel basis for the Cropland/Natural vegetation mosaic cover type for the first growing season, b) rainfall cumulating intervals corresponding to the absolute maximum correlation level for the Length (Len) on a pixel basis for the Cropland/Natural vegetation mosaic cover type for the first growing season

8.3.2. Vulnerability Analysis

Open_Shrubland_Season2	Vulnerability Index		
Phenological Parameters	TRMM 1 Month	TRMM 3 Months	TRMM 6 Months
Amp	1,546	1,452	1,287
Base	0,930	0,902	0,805
Decr	1,282	1,121	0,911
Incr	1,357	1,096	0,914
Larg	1,412	1,363	1,215
Len	1,196	0,887	0,686
SMI	1,750	1,631	1,439

Table 49. Vulnerability Index for the phenological parameters using different rainfall cumulating intervals for the Open Shrubland land cover type and for the second growing season.

Woody_Savannas_Season1	Vulnerability Index		
Phenological Parameters	TRMM 1 Month	TRMM 3 Months	TRMM 6 Months
Amp	0,697	0,471	0,311
Base	1,107	0,976	0,755
Decr	0,833	0,559	0,360
Incr	1,119	0,827	0,630
Larg	0,844	0,658	0,482
Len	0,975	0,797	0,600
SMI	0,826	0,620	0,457

Table 50. Vulnerability Index for the phenological parameters using different rainfall cumulating intervals for the Woody Savannas land cover type and for the first growing season.

Woody_Savannas_Season2	Vulnerability Index		
Phenological Parameters	TRMM 1 Month	TRMM 3 Months	TRMM 6 Months
Amp	0,842	0,642	0,412
Base	0,817	0,648	0,506
Decr	0,866	0,601	0,359
Incr	0,937	0,568	0,367
Larg	0,674	0,588	0,400
Len	1,008	0,773	0,609
SMI	1,093	0,897	0,680

Table 51 Vulnerability Index for the phenological parameters using different rainfall cumulating intervals for the Woody Savannas land cover type and for the second growing season

Savannas_Season1	Vulnerability Index		
Phenological Parameters	TRMM 1 Month	TRMM 3 Months	TRMM 6 Months
Amp	0,761	0,516	0,366
Base	1,298	1,200	1,041
Decr	0,862	0,589	0,392
Incr	1,107	0,729	0,526
Larg	0,925	0,720	0,549
Len	1,111	0,989	0,853
SMI	0,991	0,792	0,654

Table 52. Vulnerability Index for the phenological parameters using different rainfall cumulating intervals for the Savannas land cover type and for the first growing season

Savannas_Season2	Vulnerability Index		
Phenological Parameters	TRMM 1 Month	TRMM 3 Months	TRMM 6 Months
Amp	1,114	0,847	0,463
Base	0,979	0,857	0,692
Decr	0,915	0,607	0,371
Incr	0,940	0,621	0,388
Larg	0,997	0,894	0,581
Len	1,265	1,099	0,779
SMI	1,454	1,290	0,923

Table 53. Vulnerability Index for the phenological parameters using different rainfall cumulating intervals for the Savannas land cover type and for the second growing season

Croplands_Season1	Vulnerability Index		
Phenological Parameters	TRMM 1 Month	TRMM 3 Months	TRMM 6 Months
Amp	0,839	0,736	0,588
Base	1,177	1,167	1,053
Decr	0,849	0,656	0,400
Incr	1,020	0,757	0,523
Larg	0,888	0,824	0,689
Len	1,229	1,185	1,000
SMI	1,236	1,219	1,058

Table 54. Vulnerability Index for the phenological parameters using different rainfall cumulating intervals for the Croplands land cover type and for the first growing season

Croplands_Season2	Vulnerability Index		
Phenological Parameters	TRMM 1 Month	TRMM 3 Months	TRMM 6 Months
Amp	0,925	0,762	0,526
Base	1,085	0,916	0,762
Decr	1,077	0,931	0,700
Incr	0,888	0,628	0,447
Larg	0,928	0,744	0,531
Len	0,695	0,675	0,548
SMI	0,985	0,794	0,650

Table 55. Vulnerability Index for the phenological parameters using different rainfall cumulating intervals for the Croplands land cover type and for the second growing season

Crop/Nat_Veg_Mos_Season2	Vulnerability Index		
Phenological Parameters	TRMM 1 Month	TRMM 3 Months	TRMM 6 Months
Amp	0,829	0,573	0,346
Base	0,921	0,813	0,648
Decr	0,925	0,546	0,338
Incr	0,895	0,504	0,305
Larg	0,835	0,695	0,536
Len	0,950	0,752	0,552
SMI	1,039	0,828	0,612

Table 56. Vulnerability Index for the phenological parameters using different rainfall cumulating intervals for the Cropland/Natural vegetation mosaic land cover type and for the first growing season

Grasslands_Season2	Vulnerability Index		
Phenological Parameters	TRMM 1 Month	TRMM 3 Months	TRMM 6 Months
Amp	1,492	1,448	1,255
Base	1,147	1,052	0,910
Decr	1,064	0,798	0,581
Incr	1,021	0,706	0,481
Larg	1,417	1,427	1,264
Len	1,548	1,508	1,332
SMI	1,979	2,069	1,870

Table 57. Vulnerability Index for the phenological parameters using different rainfall cumulating intervals for the Cropland/Natural vegetation mosaic land cover type and for the second growing season.